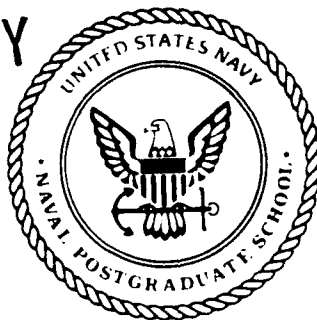# NAVAL POSTGRADUATE SCHOOL
Monterey, California

DTIC FILE COPY

DTIC
ELECTE
AUG 2 0 1990
S D
D

THESIS

STATISTICAL APPROACH TO
FAULT DETECTION OF GEARS

by

J. D. ROBINSON

DECEMBER 1989

Thesis Advisor: Y.S. Shin

Approved for public release; distribution is unlimited

90   32

REPORT DOCUMENTATION PAGE

Form Approved
OMB No 0704-0188

1a REPORT SECURITY CLASSIFICATION	1b RESTRICTIVE MARKINGS
UNCLASSIFIED	

2a SECURITY CLASSIFICATION AUTHORITY	3 DISTRIBUTION/AVAILABILITY OF REPORT
	Approved for public release;
2b DECLASSIFICATION/DOWNGRADING SCHEDULE	distribution is unlimited

4 PERFORMING ORGANIZATION REPORT NUMBER(S)	5 MONITORING ORGANIZATION REPORT NUMBER(S)

6a NAME OF PERFORMING ORGANIZATION	6b OFFICE SYMBOL (If applicable)	7a. NAME OF MONITORING ORGANIZATION
Naval Postgraduate School	Code 34	Naval Postgraduate School

6c. ADDRESS (City, State, and ZIP Code)	7b ADDRESS (City, State, and ZIP Code)
Monterey, CA 93943-5000	Monterey, CA 93943-5000

8a. NAME OF FUNDING/SPONSORING ORGANIZATION	8b OFFICE SYMBOL (If applicable)	9 PROCUREMENT INSTRUMENT IDENTIFICATION NUMBER

8c. ADDRESS (City, State, and ZIP Code)	10 SOURCE OF FUNDING NUMBERS			
	PROGRAM ELEMENT NO	PROJECT NO	TASK NO	WORK UNIT ACCESSION NO

11 TITLE (Include Security Classification)

STATISTICAL APPROACH TO FAULT DETECTION OF GEARS

12 PERSONAL AUTHOR(S)
Robinson, John D.

13a TYPE OF REPORT	13b TIME COVERED	14 DATE OF REPORT (Year, Month, Day)	15 PAGE COUNT
Master's Thesis	FROM _____ TO _____	December 1989	204

16 SUPPLEMENTARY NOTATION The views expressed in this thesis are those of the author and do not reflect the official policy or position of the Department of Defense or the U.S. Goverment

17	COSATI CODES		18 SUBJECT TERMS (Continue on reverse if necessary and identify by block number)
FIELD	GROUP	SUB-GROUP	Machinery vibration monitoring, Fault detection, Machinery condition monitoring, (Ch -

19 ABSTRACT (Continue on reverse if necessary and identify by block number)

The cost associated with machinery maintenance is a major portion of operating expenses. Vibration analysis, used as a method of monitoring the condition of machinery, provides a means to identify machinery faults before significant levels of damage occur. The results of research using statistical parameters of the vibration signal produced by machinery is presented. The statistical parameters investigated included the mean, mean square, variance, and coefficients of skewness and kurtosis. These values are compared with results of spectrum analysis techniques similar to methods used by the United States Navy in machinery programs. The investigation focuses on the use of band limited statistical parameters used as a fault detection technique that permits machinery operation to be catagorized as "satisfactory" or "unsatisfactory." Simple gardes Reynolds Trees, Statistical Analysis, gears.

20 DISTRIBUTION/AVAILABILITY OF ABSTRACT	21 ABSTRACT SECURITY CLASSIFICATION
☒ UNCLASSIFIED/UNLIMITED ☐ SAME AS RPT ☐ DTIC USERS	Unclassified

22a NAME OF RESPONSIBLE INDIVIDUAL	22b TELEPHONE (Include Area Code)	22c OFFICE SYMBOL
Y.S. Shin	(408) 646-2568	Code 69Sg

DD Form 1473, JUN 86   Previous editions are obsolete   SECURITY CLASSIFICATION OF THIS PAGE

STATISTICAL APPROACH TO FAULT DETECTION OF GEARS

by

J. D. Robinson
Lieutenant , United States Navy
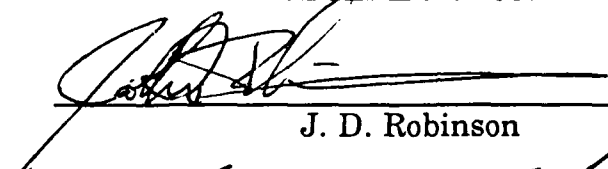B.S.E.E., United States Air Force Academy, 1981

Submitted in partial fulfillment of the
requirements for the degree of

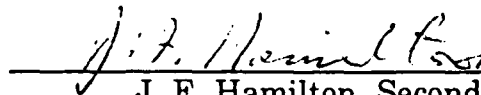**MASTER OF SCIENCE IN MECHANICAL ENGINEERING**

from the

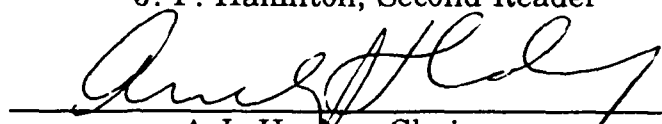**NAVAL POSTGRADUATE SCHOOL**
DECEMBER 1989

Author: _____

J. D. Robinson

Approved by: _____

Y.S. Shin, Thesis Advisor

_____

J. F. Hamilton, Second Reader

_____

A.J. Healey, Chairman,
Department of Mechanical Engineering

ii

ABSTRACT

The cost associated with machinery maintenance is a major portion of operating expenses. Vibration analysis, used as a method of monitoring the condition of machinery, provides a means to identify machinery faults before significant levels of damage occur. The results of research using statistical parameters of the vibration signal produced by machinery is presented. The statistical parameters investigated included the mean, mean square, variance, and coefficients of skewness and kurtosis. These values are compared with results of spectrum analysis techniques similar to methods used by the United States Navy in machinery monitoring programs. The investigation focuses on the use of band limited statistical parameters used as a fault detection technique that permits machinery operation to be categorized as "satisfactory" or "unsatisfactory."

Accesion For

NTIS CRA&I

DTIC TAB

Unannounced

Justification

By

Distribution /

Availability Codes

Dist   Avail and / or
            Special

A-1

TABLE OF CONTENTS

ACKNOWLEDGEMENT

I wish to express thanks to Professor Young Sik Shin and Professor James Hamilton for their guidance in completing this thesis. I would also like to thank Mr. Glenn Reid for his time and input on the various phases of the written document. Without their intellectual support, this work would not have been accomplished. Also greatly appreciated is the help and encouragement given by Mr. Mardo Blanco who was always cheerful and willing to lend a hand or just chat during the many hours of data collection and typing.

I. INTRODUCTION

The maintenance of machinery has long been recognized as a major portion of operating costs. Minor changes that result in improvements to maintenance programs have the potential to produce large cost savings. In addition, these changes can lead to increased safety, availability, and efficiency of the machinery. This thesis presents the results of research into alternative methods of fault detection using the vibration signal produced by machinery. Statistical parameters of the vibration waveform are utilized and the results compared with standard frequency spectrum analysis techniques, which is the method used by the US Navy's for vibration analysis. Utilizing a small gear train model, the statistical parameters of the vibration signal are examined from the context of a fault detection, vice diagnostics, process that can be used to quickly categorize the condition of machinery components as "good" or "bad."

A. MACHINERY MAINTENANCE PROGRAMS

Maintenance, simply stated, is the process of preventing or correcting a fault in a machine. Performing a complete overhaul on a pump, which includes replacement of bearings and wear rings and balance of the impellor, is obviously maintenance. However, simple tasks such as lubricating a bearing is also a form of maintenance, as is replenishing oil in a sump. These actions although quiet different in scope are both considered maintenance. Figure 1 illustrates a concept the reader should be familiar with. This figure depicts what is

1

commonly called, a 'bath-tub curve' or more formally a machinery failure rate curve.
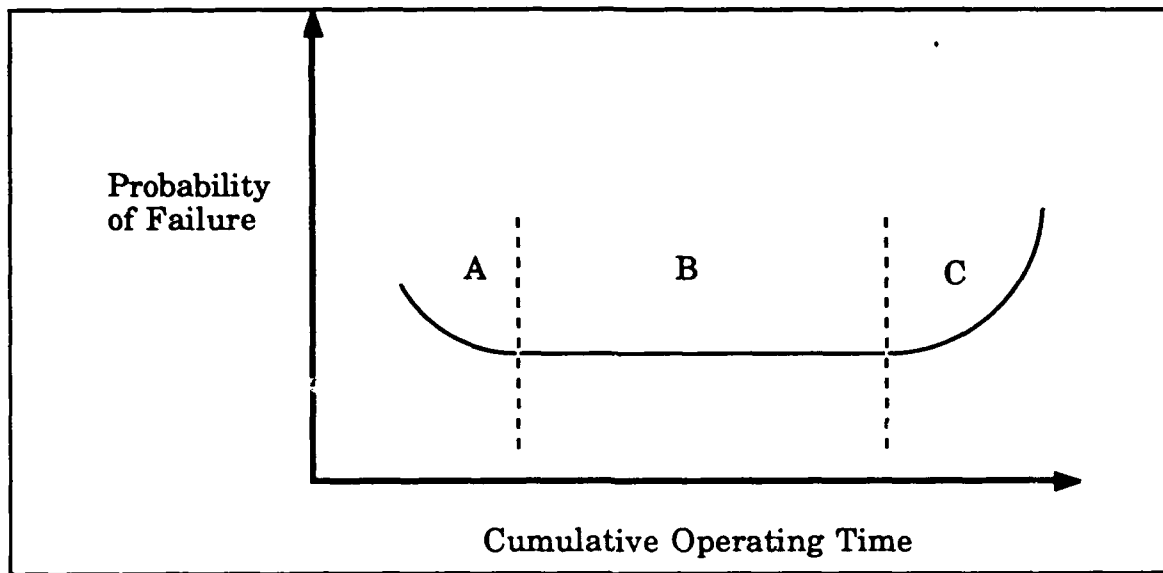
Figure 1. Failure rate curve for machinery.

This curve graphically depicts the failure process that machinery and machinery components experience during lifetime. The horizontal axis is a time scale representing cumulative operating time experienced by machinery. The vertical axis of the curve represents the probability of failure occurring to the machinery. The area on the left hand side of the curve, denoted by the letter A, indicates the probability of failure occurring to relatively new components. This portion of the curve is called the break-in period. The middle flat part of the curve, denoted by letter B, represents the normal useful life of a component. The right hand side of the curve, letter C, represents the increase in the probability of failure after the component has exceeded normal useful life. The use of this curve to describe the breakdown of machinery is very common in the literature on condition monitoring of machinery.

2

The failure rate curve of similar components may be quiet different depending on several factors. For example, a quality assurance program can remove components that might normally cause machinery to experience a short lifetime, this would produce a change in the left side of the curve. Similarly improper lubrication would decrease the width of the middle portion of the curve, and greatly increase the slope of the right hand side of the curve, indicating the component has a shorter useful life. Although calculation of this curve for individual machinery is rarely done, the concept provides an appreciation for the various maintenance programs that are in use and for the development of the concept of condition monitoring.

Machinery maintenance programs can be grouped into three broad categories; crisis maintenance, preventive maintenance, and predictive maintenance, [Ref. 1]. These programs are illustrated in Figure 2.
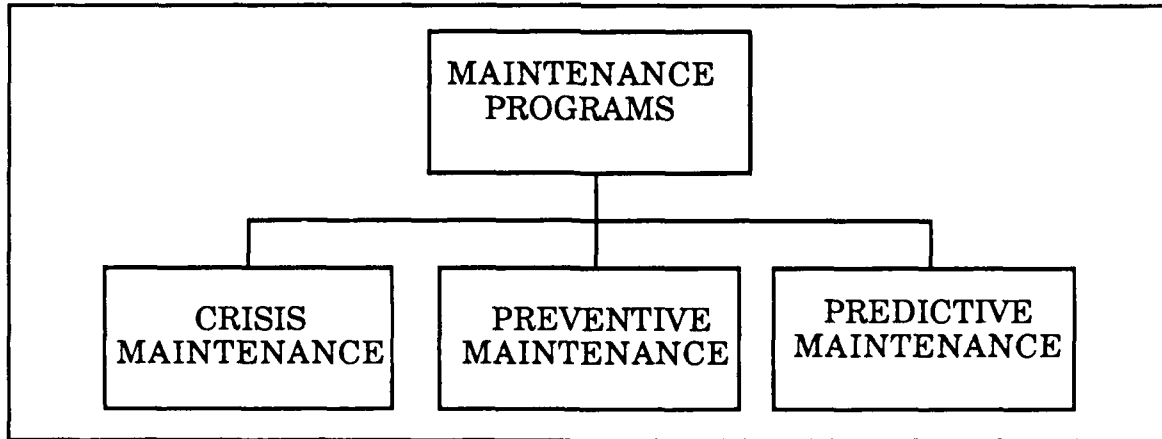
Figure 2. Machinery maintenance programs.

Although these programs will be discussed separately, in practice aspects of all three can be found in actual programs. This classification is a method to conveniently group the programs to describe methodology and present specific features particular to a single method.

3

Much of the information used in these descriptions was adapted from Reference [2].

1. Crisis Maintenance

A crisis maintenance program has no specific maintenance guidelines. Instead, the performance of maintenance actions is dependent on the observation and experience of machinery operators. The natural result of this type of system is machinery that degrades to a point where it is eventually unfit for service. Relating this process to the failure rate curve, the machinery has moved into area C on the curve. Changes to the program to reduce loss in readiness due to inopportune failure of equipment normally consists of overhauling machinery prior to failure. Little or no effort is made to establish the actual condition the machinery. It should be obvious, that this type of maintenance is inefficient and expensive. Additionally, permitting a machine to run until failure often results in additional components being unnecessarily damaged. Overhauling machinery without knowledge of the component status is wasteful of spare parts and the practice often leads to additional damage to machinery due to incorrect assembly after overhaul. Though this type of maintenance seems crude, it was routine practice for Naval ships and aircraft to undergo such maintenance. Reductions to budgets and increasingly complex and expensive machinery systems have provided motivation to implement more efficient maintenance strategies.

2. Preventive Maintenance

The next level of maintenance is preventive maintenance. In this system, specific maintenance is performed in accordance with a regular schedule. This approach to maintenance should be familiar to

all Naval personnel exposed to the Navy's preventive maintenance system (PMS) or the several variations on the concept. The scheduled 'checks' or maintenance actions have been developed from past experience, manufacturer's recommendations, and feedback from operators of the machinery. Relating this maintenance to the bath-tub curve, the goal is to perform simple maintenance, such as greasing, on machinery in order to extend the flat portion of the curve. Complex maintenance, such as overhaul, would ideally be performed after the machine has moved into the right hand portion of the curve. This would result in a longer useful life for the machinery.

The frequency of catastrophic failures and unexpected shutdowns is reduced with this type of program, however, no attempt to determine where on the curve the machine is operating is made. An underlying assumption in this type of program is that similar machines degrade in similar fashion, rate, and amount. The assigned maintenance intervals are based on statistically averaged measures that have generally proven acceptable. However, these intervals are optimal only for units which degrade exactly as the average unit of the class. This aspect of preventive maintenance programs is the result of attempting to avoid serious outages. The established intervals are conservative in nature and result in inefficient use of time, money, and effort servicing units which are performing above the average. Similarly, units that perform below average may fail prior to maintenance, and, just as in crisis maintenance programs, the failures can induce additional damage to other machinery components.

Another disadvantage of preventive maintenance arises when considering the emphasis on prevention of specific faults. By necessity,

5

the preventive maintenance schedule is designed to prevent faults that either occur frequently or that can have significant impact on the system should they occur. This produces a system unresponsive to faults not anticipated and in turn results in maintenance actions that attempt to correct the symptoms but not the problem itself. This results in a less cost effective program until specific actions that address the problem are implemented.

3. Predictive Maintenance

The final category of maintenance is predictive maintenance. In this program machinery faults are detected at an early stage of development and maintenance is performed at a level that supports readiness. Maintenance is performed only on components in which needed. Predictive maintenance attempts to perform maintenance on components at the start of the final stage of the failure rate curve. This minimizes the amount of maintenance performed on a specific piece of machinery, while maximizing the effectiveness of the maintenance that is performed. In this approach, many of the problems associated with the other schemes of maintenance are reduced. Unfortunately the techniques needed to accurately predict the condition of machinery have not been developed for all machinery. The development and use of techniques to determine the condition of a component is called condition monitoring.

B. CONDITION MONITORING

The techniques used in a predictive maintenance program to detect and diagnose a fault is called condition monitoring. It is important to note that the term condition monitoring is not universal in the

literature, but it is the most descriptive and least awkward of the many terms used. Goals for a condition monitoring program are:

- provide warning of trouble at earliest possible time
- reduce needless overhauls
- reduce maintenance actions
- reduce spare parts inventories

It is emphasized that condition monitoring cannot prevent failures from occurring, but unnecessary maintenance work and expense can be reduced with a properly designed system. The goals of condition monitoring are achieved by utilizing a system that:

- requires minimum capital investment
- is robust and trouble free
- capable of being used at lowest competent level

Reference [3] lists six technology groups used individually or in combination to achieve the goals of condition monitoring. These technological areas are aural monitoring, visual monitoring, operational variable monitoring, temperature monitoring, wear debris monitoring, and vibration monitoring.

These six areas can be grouped in a more logical manner, (Figure 3). The first four methods together can be described as traditional monitoring techniques. Wear debris monitoring is a somewhat abbreviated description for the type of monitoring actually performed, more descriptive is wear debris and lubricant monitoring. Vibration monitoring will be left as a category by itself. With these changes the methods of condition monitoring become traditional monitoring, vibration monitoring, and wear debris and lubricant monitoring.

```
                    ┌─────────────┐
                    │  CONDITION  │
                    │ MONITORING  │
                    │   METHODS   │
                    └──────┬──────┘
         ┌─────────────────┼─────────────────┐
  ┌──────┴──────┐   ┌──────┴──────┐   ┌──────┴──────┐
  │ TRADITIONAL │   │WEAR DEBRIS AND│  │  VIBRATION  │
  │ MONITORING  │   │  LUBRICANT   │   │ MONITORING  │
  │             │   │ MONITORING   │   │             │
  └─────────────┘   └─────────────┘   └─────────────┘
```
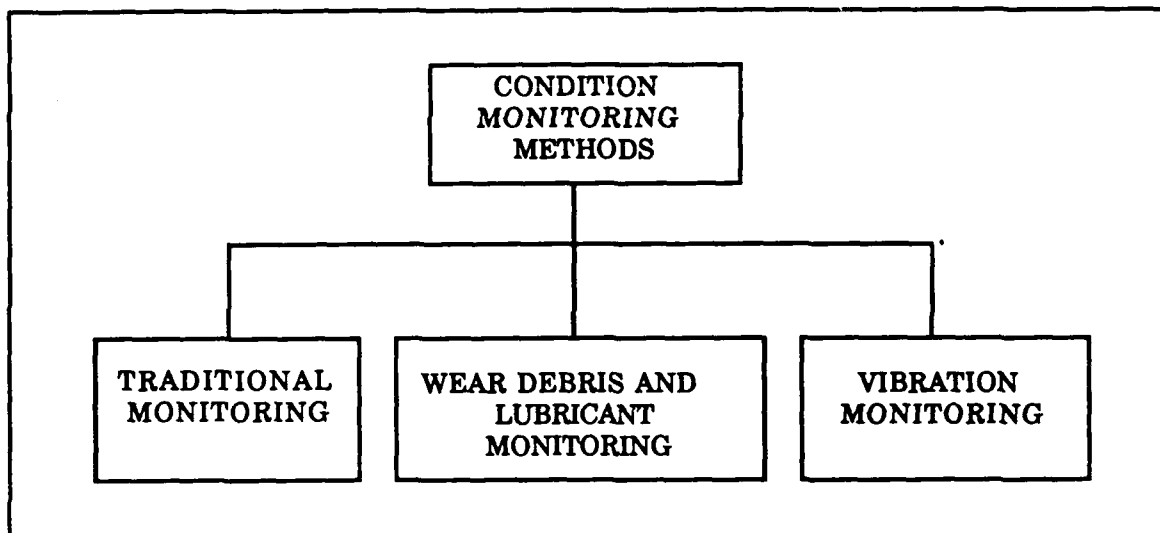
Figure 3. The methods of performing condition monitoring.

Wear debris and lubricant monitoring will be abbreviated as wear based monitoring for the remainder of this report. Traditional monitoring includes many of the methods that operators and maintenance personnel have used for years, in evaluating the condition of machinery. Temperature, pressure, level, and speed are all familiar parameters that fall under the traditional monitoring method. However, technology is providing new methods of monitoring machinery that lie within the boundaries of traditional monitoring; borescope, thermograph, acoustic monitoring, and infrared imaging are examples of just a few of the new methods being used to monitor machinery.

Wear based monitoring deals with the measurement and classification of the wear material produced during operation and the condition of lubricating or hydraulic oils in the machinery system. Often in the literature this monitoring is referred to as tribology.

Vibration monitoring uses the vibrations produced by machinery to evaluate the condition of machinery. Of the three condition monitoring methods, vibration monitoring is, by far, the most widely written about and used method in condition monitoring.

C. FAULT DETECTION AND DIAGNOSTICS

Use of the condition monitoring methods to monitor machinery can be described as a fault detection and diagnostics process. Figure 4 illustrates this process.
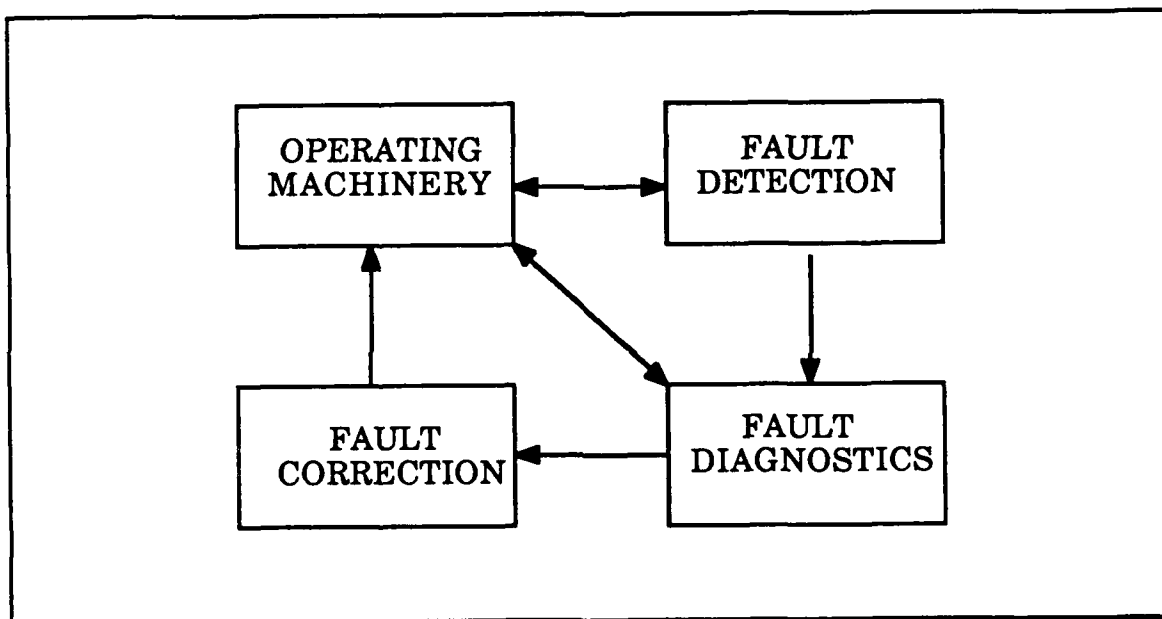
Figure 4. Fault detection and diagnostics process.

The upper left hand block represents operating machinery. The fault detection block represents a process used to detect a fault in the machine. This action may be as simple as the monitoring of operating parameters such as lube oil pressure or temperature, or it could be more elaborate using a combination of methods. The double arrow between the upper two blocks indicates that fault detection may lead to a

modification of the machinery's operating condition, such as shutting down the machinery if an extreme condition is detected.

An extreme condition would be considered as a situation that would result in the machinery being destroyed if no action is taken. Fault detection is considered the key step in the condition monitoring process. Detection of a fault as early as possible allows accurate diagnostics to be performed. One of the problem areas in the literature is the use of monitoring techniques as both detection and diagnostics processes. Use of these techniques in this manner is wasteful of time and data processing capabilities. More effective monitoring could be accomplished by developing detection techniques that are used to monitor the machine for a change in operating condition and then calling a more detailed diagnostic process when a change in state is detected. Reference [4] points out that the fault detection processes should detect a majority of faults as early as possible, give few false alarms, and provide sufficient information to enable a decision to be made as to when diagnostics is required. It is important to note that the detection process can be made much more effective by combining several monitoring methods and using the collected data in tandem. When a fault is detected the fault diagnosis process begins.

Fault diagnosis involves the process of trouble shooting the machinery to determine the cause of an alarm produced by the detection process. The diagnostic process may utilize data collected in fault detection, but this is not necessary. Normally the diagnostics process involves obtaining more data from the machine. This process has several steps:

- determine if a fault is valid or a false alarm
- determine the nature of the fault
- determine the severity of the fault
- determine the optimum method for correction

Once the fault has been identified, a determination is made as to whether the machine can be left in its current operating status. If it cannot remain operating a decision on how and when to repair the machine is made. Overhauling the machinery may be required, or a simple repair such as lubricating a component may be sufficient to keep the machinery operating at a level which does not affect the readiness of the unit. The lower left hand block of Figure 4 represents the action taken. When the decision on action is implemented, the machine is restored to an operating condition and the process continues. It is emphasized that maintenance actions do not have to be performed just because a fault is detected. Machinery components do experience wear and components reach an end of useful life. Design of a system that provides the information to, or makes the decision for, maintenance personnel on the severity of a fault and prediction of remaining life is the goal of a predictive maintenance program. In this investigation the use of statistical variables for fault detection is compared to use of traditional spectral analysis.

D. MONITORING GEARS

Gears permit the transfer of energy between two shafts. The process is important in that components of a system can be designed for maximum efficiency, with the gears acting as the interface between the components. Specific uses for gears are to change speeds in a

system, change direction of rotation, and transmission of power. Although the use of gears is simple to comprehend, it is difficult to understand what is happening to the gear while in operation. In the preface to the 1st edition of Gears by H.E. Merritt [Ref. 5], he writes:

> "There are many sources of printed information on gears. The trouble is that, so wide is the range of problems, and so disjointed their treatment in over-specialized contributions to the literature of the subject, that the serious student often has difficulty in seeing the wood for the trees."

He goes on to state:

> "Geometrical relationships apart, we still know very little about gears. The enormous strides which have been made in gear materials and finishing processes, reflected in remarkable developments in gear performance, are the work of the metallurgist and the designer and maker of tools, cutters and measuring instruments, and are the result of a process of evolution in which the physicist has so far played little part. As a result , the seeker after truth still gropes dimly in the fog which surrounds the facts of what happens to gear teeth under load, and to the oil which separates them. Until these facts emerge, recourse must be had to empirical methods."

Much has changed in the almost 50 years since this was written, but, the interaction that occurs between two gears is still not fully understood. The complex loading and dynamics that occur to gear teeth are being studied with a full arsenal of experimental and computational capabilities, but inroads into comprehending the process is slow, especially in the area of fault detection and diagnostics.

1. Types of Gears

Use of gears in the Navy is as varied as the equipment in the naval inventory. Used on submarines, surface ships, and aircraft, gear sets can range from tiny precision gears in time pieces, to massive

marine reduction gear used for propulsion in ships and submarines. The importance of each of these gear systems varies, damage to a gear in a ship's chronometer is of little importance in the digital age, whereas a fault to a helicopter's transmission gear box could result in an enormous cost in terms of human life or replacement of an aircraft.

Just as the equipment using gears varies, there are many different types of gears used in machinery. The most common types are:

- spur gears
- helical gears
- spiral gears
- bevel gears
- worm gears

Under each of these broad categories there are subcategories of gears. A discussion of the differences between the construction and uses of the different types of gears is beyond the scope of this paper, however References [5] and [6] should be more than sufficient in providing additional background.

2. Causes of Gear Noise

A gear system can be modeled as a collection of lumped masses, spring and damping elements. An excitation applied to the system will produce vibrations which are transmitted through the system and can be monitored on the gear casing. In an ideal system, the excitation force results from the contact occurring between the meshing teeth of the gear and pinion. The cause of this excitation force can be broken down into two broad, but not necessarily distinct categories, [Ref. 5-8]:

- Forces produced by loading applied to the gears

- Forces generated by discrepancies in the tooth

The excitation force caused by the first category can be produced by deformations of the gear teeth caused by transmitted load, forces due to rapid changes in speed, excitation of natural frequencies, and cracks on a tooth. The second cause for the excitation force takes into account :

- geometric faults due to design, manufacturing, or defects
- wear occurring to the gear
- misalignment of the gears

A general term used in the literature to describe the excitation force is transmission error (TE). Transmission error can be defined as the difference between the position that the output shaft of a gear drive would be if the gearbox were perfect and the actual position of the output shaft, [Ref. 6,7, and 9].

Starting with an estimated TE, the system response for various gear faults can be estimated using lumped element models. With these models a gear system design can be evaluated. However, for condition monitoring purposes the effect of an unknown TE is being investigated and the models are of limited use. Instead current practice is to use empirical methods to develop techniques for monitoring the condition of gears.

3. Basic Faults of Gears

When performing condition monitoring it is important to be familiar with basic gear faults that can lead to failure. Smith [Ref. 6] lists these faults as pitting, scuffing, root cracking, and wear. Pitting is a failure occurring to the surface of a gear. It is caused by high Hertzian

14

contact stresses and leads to a small area of the tooth being removed. For most operations pitting is not a serious problem.

Smith [Ref. 6] defines scoring as a form of scuffing that occurs from a lack of lubrication to the system. Scuffing occurs on the surface of a tooth when the lubricant film breaks down, a localized weld forms on the meshing surface, and damage occurs when the weld breaks as the surfaces separate. Both scuffing and scoring are considered serious problems.

Root cracking is also a serious problem, especially for high speed gears, such as those used in helicopter transmissions. In these applications gear technology is pushed to the limit. Root cracking occurs when fatigue cracks propagate through the gear tooth, resulting in a loss of strength for the individual tooth during mesh. This loss of strength eventually results in complete loss of the tooth or of a portion of the tooth.

Wear is the removal of metal from the surface of the gear tooth, and is a normal occurrence for a gear. Normal wear occurs in a uniform manner over the entire working surface of the tooth. Nonuniform wear, the result of misalignment, can weaken gear teeth and lead to premature failure of gear teeth.

A ranking of gear faults in order of seriousness would be:

- Root cracking
- Scoring
- Scuffing
- Non-uniform wear
- Pitting
- Uniform Wear

Each of these faults are described in detail by Smith [Ref. 6] and Merritt [Ref. 5]. Merritt provides additional detail and includes numerous photographs illustrating damage caused by these faults.

The detection and diagnostics of these faults using non-destructive testing based on characteristics of the machinery that can be monitored is the goal of condition monitoring. This investigation uses vibration monitoring to investigate the effect gear damage has on the vibration of a gear mesh and statistical properties of the vibration signal.

II. VIBRATION ANALYSIS TECHNIQUES

A FREQUENCY ANALYSIS

Smith [Ref. 6] notes that occasionally an oscilloscope can be used to examine the vibrations produced by machinery. Use of this method may result in detection of specific features in the signal, but the vibration signal is very random and additional electronic equipment and signal analysis techniques are normally required.

The most popular techniques for analyzing vibration signals is frequency analysis. Smith [Ref. 6] notes that frequency analysis is often referred to by an endless number of terms, including frequency analysis, wave analysis, Fourier analysis, Fast Fourier analysis, power spectrum analysis, spectral analysis, power density spectrum analysis, spectral density analysis, and many others. For all practical purposes the methods do the the same thing, present information that indicates the level of vibration at particular frequencies.

Reference [10] notes several reasons why frequency analysis of vibrations is the method most often used in condition monitoring programs:

- large reduction of data compared to time signal format
- data presented in easily understood format
- data characteristics easily extracted
- FFT algorithm widely available

This final reason is probably the primary reason for the popularity of frequency analysis. The availability of equipment and software with Fast Fourier Transform (FFT) algorithm has enabled frequency

analysis to be performed in the field. Unfortunately this popularity may have prevented other more promising techniques of vibration monitoring to be investigated and used.

1. Discussion of Frequency Analysis

In this research synchronously averaged power spectrums were used to monitor the effect of damage on the vibration produced by a pair of gears. The results from these measurements were evaluated using methods similar to those used in industry and the U.S. Navy.

The theory behind computation of the power spectrum using the Fast Fourier Transform can be found in texts dealing with random vibrations such as References [11-13]. Use of these techniques result in the time domain data produced by a vibration transducer transformed into a frequency domain representation. Figure 5 illustrates this process.
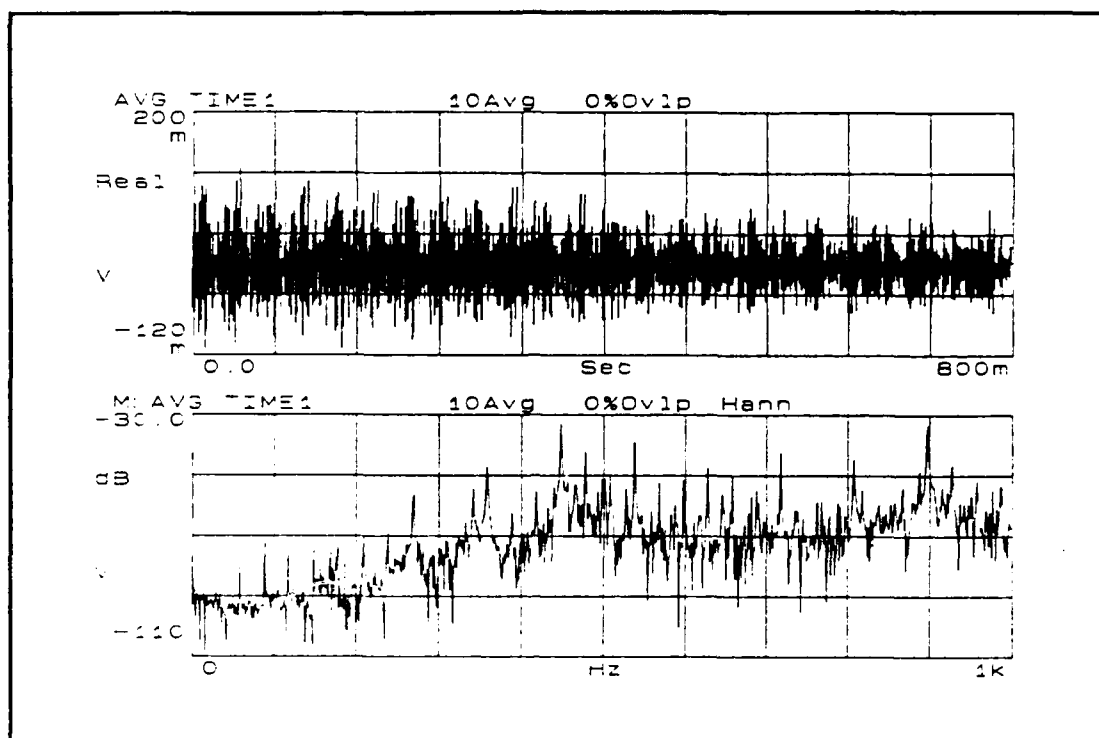
Figure 5. Time and frequency domain representations of a signal.

The upper portion of this figure depicts a vibration signal in the time domain. The lower portion of the figure depicts the same data after performing an FFT on it. The result is a representation of the signal in the frequency domain. With this process the frequency components that make up the time domain signal can be separated. In theory, evaluation of machinery condition can be made by analyzing the changes that occur to the frequency components of this spectra. This process is straight forward, but assumptions are made when taking these measurements. The major assumption is that the vibration signal is stationary. A stationary process is a process such that average values made from the process do not change over time. This implies that the machinery being monitored is at the same loading conditions as prior measurements and that the machinery is operating at a constant speed. For most machinery this assumption can be made.

19

Minor load variations and speed changes will not, generally, greatly affect the measurement.

One aspect of the frequency spectrum measurement performed in this investigation that is somewhat different from normal naval practice is the use of a technique called time synchronous averaging. In synchronous averaging, a trigger signal, called a keyphasor, is produced by the occurrence of a specific event. Such as the rotation of a shaft. This trigger is used to start the collection of a data record. With use of this technique vibrations not related to the event triggered on will tend to average out of the final frequency spectra. This results is a reduction of the background noise contamination and enhancement of frequency components related to the trigger signal. Figure 6 illustrates this effect.
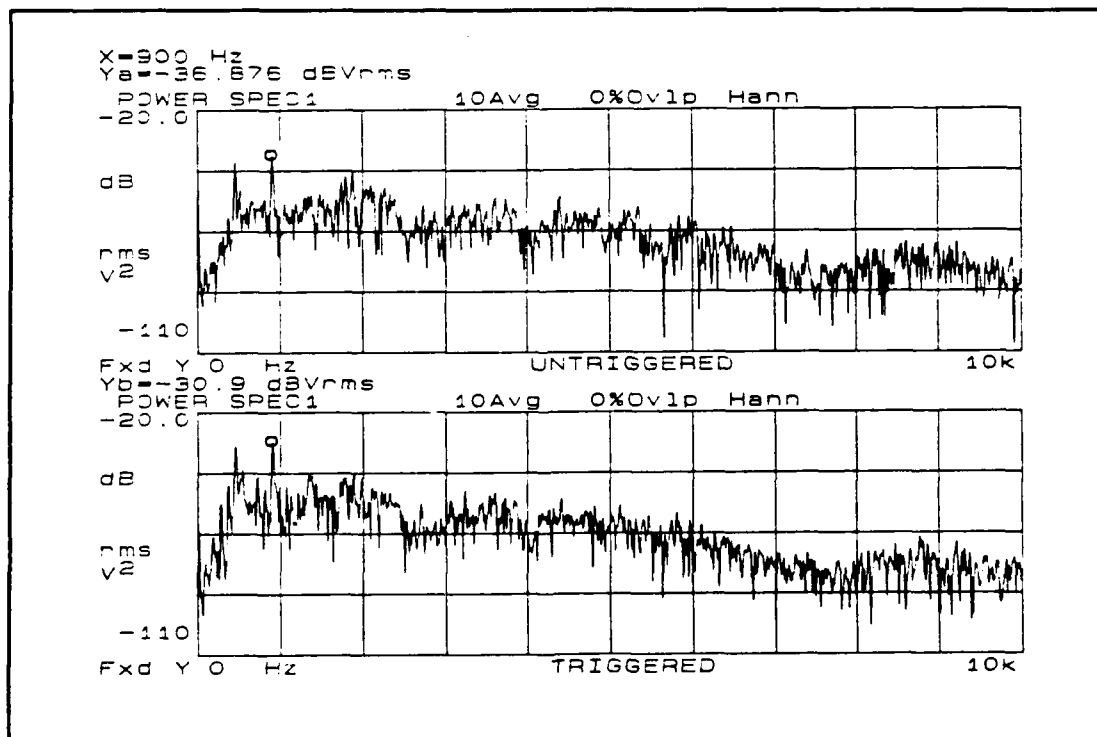
Figure 6. Reduction of noise contamination with keyphasor.

In this figure the upper spectrum was produced without use of a trigger, the lower figure was made with a trigger marking the revolution of a shaft. Both measurements were made over a frequency span of 0.0 to 10.0 KHz, and ten data records were averaged before plotting. In the lower figure the frequency components are clearer than in the untriggered spectrum and the background noise level, referred to as the "grass", is lower. Since the investigation was centered on the noise produced by a damaged gear, the use of a triggered spectrum was used in producing frequency spectrums used in this investigation.

The use of frequency spectrum can be grouped into three different ways for evaluation of the condition of machinery. These methods are:

- broad band or overall vibration levels
- narrow band frequency levels
- advanced methods.

The first two methods are very common in the literature and used extensively in the field. The third method is a broad category used to classify monitoring techniques that are proprietary, experimental, or so complex that wide spread use in the field does not seem probable.

The first two methods of analysis will be used in the analysis of the data collected in this research. Overall vibration level is a simple monitoring technique that measures the root mean square (rms) level of a vibration signal being monitored, much like a multi-meter measures an electrical voltage signal. In fact, these measuring devices are essentially performing a broad band measurement over the frequency band the device is capable of measuring. This method is

simple, easily adaptable to hand held devices, and produces data values which can be manipulated easily. This method of vibration monitoring was the primary monitoring method in most early vibration monitoring programs. Computation of a full frequency spectrum is not required when using this method, but already computed spectra can be used to calculate the overall rms level of the measurement by integrating the spectrum over the monitored frequency range.

Narrow band monitoring methods, which use the amplitude of individual frequency components, appear to have been used when the FFT became widely available. When this occurred it was found that monitoring the changes of individual frequency component permitted detection of damage and diagnosis of the probable causes of the damage to be made at the same time. The individual frequency components proved to be more sensitive to damage than the broad band measurements. Figure 6, presented earlier, is useful in illustrating how this method is used. In this spectrum several distinct tonals are very prominent, for example the cursor marks the 900 Hz frequency component. For the machine being monitored this frequency is the second harmonic of a gear mesh frequency, to the left of this frequency is the gear mesh frequency, approximately 900 Hz. In analysis of the frequency spectrum these frequency components can be related to dynamics events occurring within monitored machinery. In a monitoring program the individual frequencies are monitored for changes. Evaluating the changes in these frequencies and relating the change to a machinery's condition is generally gained through experience with similar machinery, and with manufacture guidelines. Reference [1] provides guidelines for setting alert levels on machinery

22

monitored in the Navy surface ship vibration monitoring program. For machinery with no other guidelines available, an alert crite on is indicated when a specific frequency component experiences a 6 dB increase from the previous measurement. Reference [14] is more specific, stating that a rise of 6-8 dB over a baseline measurement should be considered significant, while noting that a 20 dB increase should be considered serious.

These levels can be related to the fault detection and diagnostics process presented in Chapter I. The 6 dB rise would be equivalent to a fault being detected. The 20 dB rise can be thought of as a measure of damage, this level indicates to the operator that shutdown and repair of the machinery is needed. The use of operating frequencies of monitored machine can be considered as a diagnostic process that assists in locating the probable source of the fault producing the increase in vibration. Use of the 6 dB level for fault detection provides a means to classify the data from frequency spectra and to make comparisons with the statistical parameters calculated.

2. Vibrations Produced by Gears

The vibration monitored at the casing of a gearbox is produced by the transmission error between the gears in the mesh. The vibration travels from the mesh to the gear case where sensors can be attached for monitoring. In addition to the vibration produced by the gear mesh, other dynamic events occurring within the gearbox will be transmitted to the casing. The vibration signal monitored is made up of frequencies that can be related to the dynamic events occurring within the gearbox. The vibrations monitored at the casing can be thought of as being composed of five groups of frequencies.

- shaft revolution frequencies
- gear mesh frequencies
- ghost frequencies
- other frequencies
- natural or resonance frequencies

Shaft frequencies are produced by rotation of the shafts gears are mounted on. This frequency can be calculated using equation (1).

$$f_s = RPM/60 \quad Hz \tag{1}$$

where:

f_s is the computed shaft frequency in Hertz
RPM is the shaft speed of rotation in revolutions per minute

The shaft frequency can often be seen in a frequency spectrum as a distinct frequency component. Once the frequency of one shaft is calculated the frequency of the second shaft can be calculated using equation (2) which is a form of the gear law.

$$f_{s2} = (f_{s1} * t_{g1})/t_{g2} \quad Hz \tag{2}$$

where:

f_{s2} is the frequency of shaft number 2 in Hertz
f_{s1} is the frequency of shaft number one calculated from equation (1)
t_{g1} is the number of teeth on gear number 1
t_{g2} is the number of teeth on gear number 2

This equation can be used to determine the shaft speed throughout a multiple shaft gearbox. The gear mesh frequency is associated with the number of teeth on a gear of interest. It can be computed using equation (3).

$$f_g = t_g * f_s \quad Hz \qquad (3)$$

where:

    f_g is the gear mesh frequency in Hertz
    t_g is the number of teeth on the gear
    f_s is the shaft frequency of the shaft the gear is mounted on

Like the shaft frequencies, gear mesh frequencies can often be seen as distinctive spikes in a frequency spectrum. The gear mesh frequency will often have harmonics. These harmonics can be calculated as:

$$f_{gn} = f_g * n \quad Hz \qquad (4)$$

where:

    f_{gn} is the nth harmonic of the gear mesh frequency in hertz
    f_g is the gear mesh frequency in hertz
    n is the harmonic desired, n=2,3,4 . . .

Similar to the shaft frequency, the gear mesh frequency and harmonics can often be seen as distinctive spikes in the frequency spectra. Another feature that is associated with gear mesh frequencies is called sidebands. The sidebands can surround the gear mesh frequencies. The sideband frequencies are related to both shaft frequency and the gear mesh frequencies. Equation (5) can be used to calculate the frequencies of possible sidebands.

$$f_{sb} = f_g \pm (n * f_s) \quad Hz \qquad (5)$$

where:

    f_{sb} is the sideband frequencies in hertz
    f_g is the gear mesh frequency in hertz
    f_s is the shaft frequency in hertz
    n is the desired multiple of the sideband

The sideband components, when present, can have the appearance of surrounding the gear mesh frequency or making the gear mesh frequency wider.

Randall [Ref. 15] states that ghost components have the appearance of gear meshing frequencies when viewed in the frequency domain, but they appear at frequencies that do not correspond to the number of teeth on any gear in the system. Faults that produce these ghost components have origins in the manufacturing process of the gears and the mechanisms that create them come from defects on the gear cutting equipment. The amplitude of frequency components of the ghost frequency generated during operation do not vary with changing loads. As wear occurs to the gear teeth the ghost components will tend to decrease, [Ref. 15].

Other frequencies is a term to lump frequency components observed in the frequency spectra of gearboxes that are not related to the gear mesh. These frequencies can include frequencies produced by bearings, lubrication systems, couplings, and the gearbox prime mover. Braun [Ref. 10] states that as a vibration signal moves through a machinery's structure it is modified. This modification is due to the gear boxes natural frequencies. Braun goes on to indicate that the changes to the signal can be "quite drastic", and that the natural frequencies can "mask many excitation-induced characteristics." He concludes by noting that in condition monitoring, this characteristic is important, because of the effect it can have on other frequencies. There are several methods of determining the natural frequencies of a system. One method is by finding the transfer function of the monitored system. A simpler and more practical method that can be used for already

existing equipment is by monitoring a machine at different speeds and displaying the frequency spectrums in a cascade type plot, [Ref. 10]. Both these methods are discussed in more detail in Chapter IV.

B. EFFECT OF FAULTS ON GEAR FREQUENCIES

With a perfect set of gears operating at a constant speed the task of condition monitoring would be a very simple one. Frequency domain techniques would produce spectrums consisting of discrete frequency components and harmonics at each of the gear mesh frequencies. Condition monitoring could be accomplished using a form of trend monitoring with alarm conditions based on levels found using models or empirical data. Unfortunately the gears used in machinery are not perfect and the operating speeds are not constant. In addition, many of the basic types of faults that are found on gears produce vibrations that may obscure other more serious faults.

In Chapter I, the basic gear faults were presented, each of these faults will affect the frequencies produced by the gears by a form of modulation. This modulation will be either amplitude modulation or frequency modulation. In both cases the modulation results in sidebands around the basic gear mesh frequencies, and ghost components if present. As previously described the sidebands are offset from the basic gear mesh frequency by the shaft frequency. Figure 7 presents a frequency spectra that shows a gear mesh frequency surrounded by sidebands.
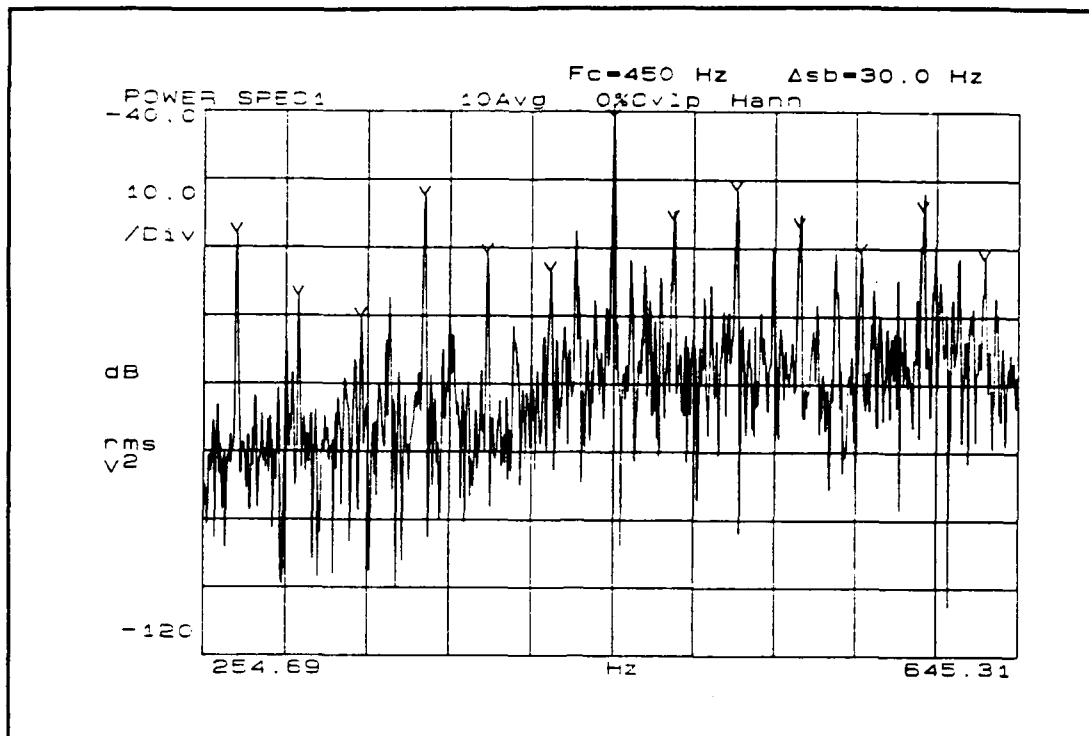
Figure 7. Gear mesh frequency surrounded by sidebands.

In this figure the gear mesh frequency occurs at 450.00 Hz. It is surrounded by sidebands at 9.0 Hz and 30.0 Hz, these sideband frequencies are related to the rotation speed the gears of the mesh are mounted on. Frequency modulation normally occurs from faults that effect the entire working surface of the gear, [Ref. 6 and 15]. Additionally, frequency modulation can be produced by changes in the speed of the gear, [Ref. 15]. Normally the amplitude of the gear mesh frequency component is not affected by this modulation. The sidebands produced by frequency modulation, also called phase modulation, cover a narrower frequency span than those produced by amplitude modulations and can be thought of as "smearing" the gear mesh frequency across a small frequency span, [Ref. 6].

Amplitude modulation is normally associated with single tooth damage, or localized damage, [Ref. 6, 8,and 15]. For minor surface

damage, Stewart [Ref. 8] indicates that amplitude modulation does not occur. He suggests that modulation occurs only when the loss of metal leads to a situation that may cause displacement of the tooth. The amplitude modulation from this single tooth fault will normally produce sidebands that are over a broad frequencv range but low and uniform in amplitude, [Ref. 15 and 16]. Figure 8, from Reference [15], illustrates the differences between the sideband patterns of a localized fault and a distributed fault.
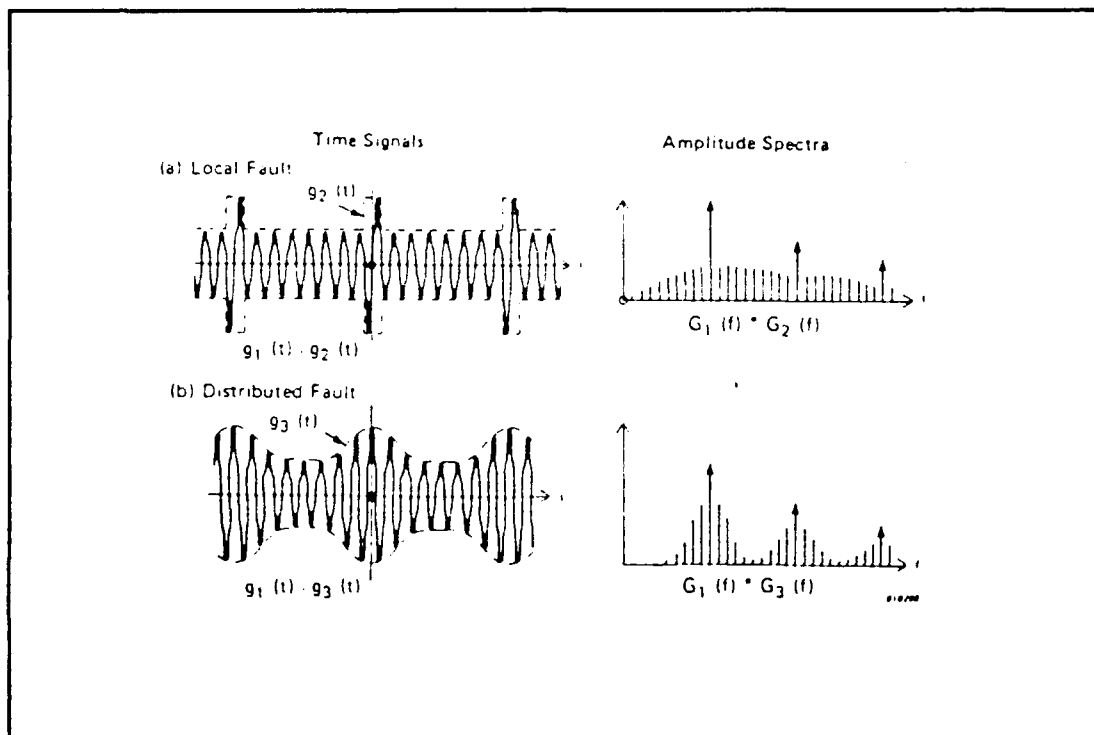

Figure 8. Sidebands for (a) localized and (b) distributed faults.

The upper portion of this figure (a) shows how a local fault, causes a series of impulses to appear in the time domain, which produce sidebands low and uniform in the frequency domain. The lower figure (b) shows a distributed fault that causes frequency modulation in the

time domain and non-uniform sidebands in the frequency domain. This gives the appearance of the gear mesh frequency being "smeared".

Another effect of modulation is the amplitude of the gear mesh frequency component can decrease as energy is transferred from the gear mesh frequencies to the sidebands. Smith [Ref. 1] points out that for very high modulation the amplitude of the sidebands may be larger than the gear mesh frequency they are associated. Stewart [Ref. 8] also notes that in addition to the modulation effects, localized faults can excite a systems natural frequencies.

If the frequency spectrum of either of these two types of modulations were looked at separately the type of modulation occurring might be distinguished. However, in practice the sidebands for an amplitude modulated signal may be at the same level as the background noise and be obscured, [Ref. 8] or both types of modulation may occur, as is common in gears. The modulation from one source may be out of phase with the modulation from another source producing sidebands that that are not be symmetrical, [Ref. 8]. Reference [17] presents another problem in that a gearboxes natural frequencies may significantly effect the sidebands produced by modulation. All these factors result in making it impossible to identify the type of fault by examining the effects of modulation, [Ref. 8]. This is a significant problem when using frequency analysis techniques to identify faults in geared systems.

C. STATISTICAL PARAMETER ANALYSIS

1. Concept of Fault Detection

From these discussions it can be seen that frequency analysis of gears can be quiet complicated. Much of the literature dealing with

gears indicates that simple frequency analysis of the gear mesh frequency components may simply not be sufficient to detect faults. Monitoring additional frequencies complicate matters through additional administrative requirements. More sophisticated monitoring techniques often require additional electronics, along with increased complexity and need for highly skilled maintenance technicians.

Attempts to automate these monitoring techniques invariably lead to the need for complex automated data processing systems which require large capital outlay and additional maintenance staff to support the processing equipment. For most organizations these problems make the advanced techniques an option that is not cost effective.

The real problem with these monitoring methods, in the author's opinion, is not the cost or the complexity, but the manner in which they are used. Most monitoring techniques attempt to perform both the detection and diagnostics process at the same time. On the surface this would not appear to be a disadvantage. The literature indicates that when frequency analysis was just starting to be used in industry, the collection of data was accomplished by hand with maintenance personnel going from machine to machine, collecting data on magnetic tape or by recording specific frequency data by hand from some type of portable FFT analyzer. The ability to combine the detection and diagnostics process for this type of monitoring was sensible because the time required to collect and analyze the data was already significant. This method of data collection can be thought of as a first generation monitoring system.

The rapid progress made in automatic data processing capabilities permitted a second generation of frequency analysis programs to be implemented on desk top computers and in simple automated programs. The cost of these systems permitted the monitoring of critical equipment only. This made the continued use of the dual detection/diagnostic techniques reasonable.

The rapid growth in computer capabilities has allowed new methods of manipulating the spectrums to be developed and for complex techniques to be developed to manipulate the vibration signals. Many of these third generation monitoring methods require large amounts of processing capabilities and/or large data storage capabilities. The major problem with these techniques is that they still are being used as a detection methods. This method of use requires the need for large processing capabilities dedicated solely for condition monitoring. It is unrealistic to expect a production plant or a Naval vessel to justify the costs of the computer equipment needed for these types of monitoring methods. So the newer techniques, some of which appear to be quiet effective, never really get widely used.

A more efficient monitoring program would consist of a detection system continuously monitoring a machine or system for faults and once a fault is detected diagnostics techniques would be called to pinpoint the problem. By having a simple, yet effective, detection system and a callable diagnostic routines condition monitoring systems could be incorporated into the computer control systems that are becoming standard in complex machinery. This permits effective monitoring without requiring massive dedicated computer systems. Simple detection techniques could also be incorporated into handheld

devices so that machinery could be quickly categorized as "satisfactory" or "unsatisfactory". The majority of the machinery would be screened as satisfactory, allowing the unsatisfactory machines to be monitored with a more advanced diagnostics technique.

This concept is not new, it has been the normal practice used in maintenance for many years. Machinery operators use traditional monitoring techniques such as pressure or temperature to detect problems, once a problem is detected, trouble shooting, or diagnostics, is performed to locate the problem. When the problem is located it is corrected. This is the process of fault detection and diagnostics discussed in Chapter I. A reliable method of fault detection is the reason the statistical parameters of a vibration signal are being investigated. The statistical parameters investigated are the mean, mean square, variance, and normalized third and fourth moments about the mean.

2. The Probability Density Function

Statistical parameter analysis is called "amplitude domain description of signal" by Braun, [Ref. 10]. This method of vibration monitoring has as its foundation the computation of the probability density function (p.d.f.) of the time domain vibration signal. Braun states: "In the limit, this p.d.f. describes the percentage of time for which the signal lies within a certain amplitude range." Figure 9 is a p.d.f. from a measured signal from a small machine.
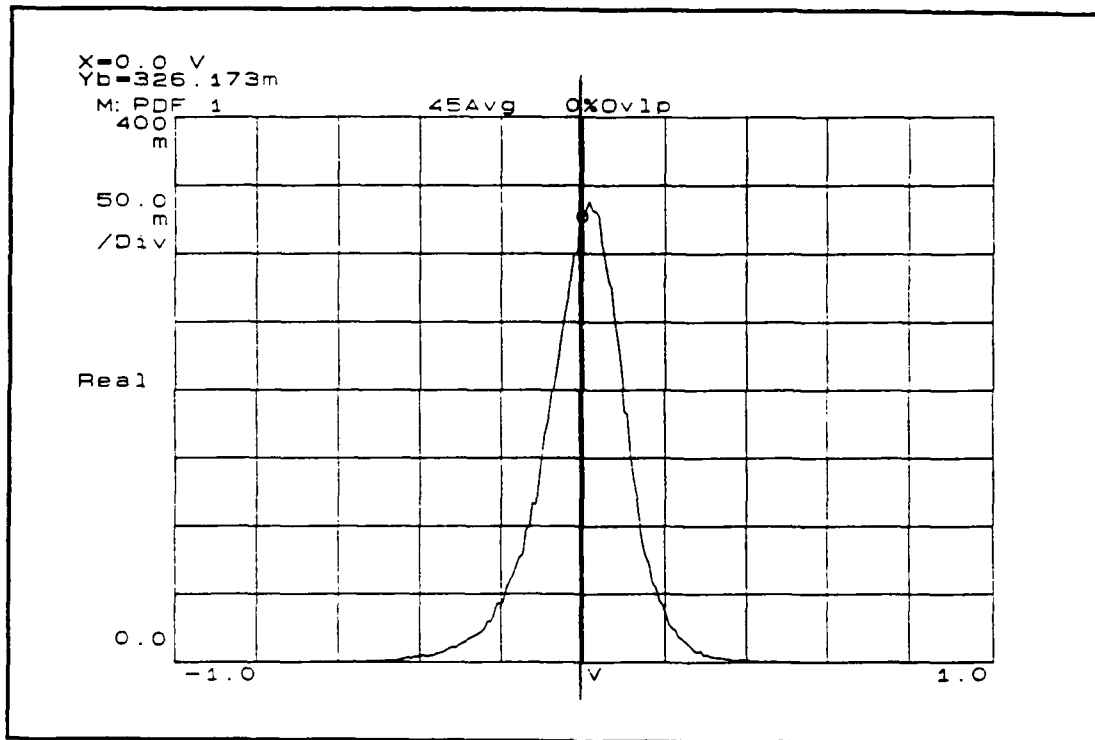
Figure 9. Probability density function for a small machine.

The use of the probability density function of a time signal has several features that make it an excellent candidate for use as a fault detection method in a condition monitoring program. First the p.d.f. is easily adaptable to measurement in an automatic monitoring program. In most automated monitoring programs the analog vibration signal is converted to a digital form prior to application of a FFT algorithm, this digital form can easily be converted to a probability density function. Second, Braun [Ref. 10] indicates that use of statistical parameters results in a large reduction of data after the p.d.f. is converted to statistical parameters. Use of these parameters results in the calculation of numerical values from the monitored time records. This can be compared with the eight hundred frequency levels found in a typical spectrum when recorded for stored. The third reason is the statistical parameters present information on the overall state of the

machinery. In a frequency spectrum the individual frequency components are indicative of specific events. This feature provides maintenance personnel with a means to evaluate the overall condition of the machinery and recognize when something is affecting the entire machine.

Braun [Ref. 10] indicates that the p.d.f. is insensitive to variations of a monitored vibration signal. The vibration signal produced by machinery changes with factors such as load, speed, lubrication, and temperature, but in general the overall shape of the probability density function does not seem to be greatly affected. For many types of machinery the probability density function takes the form of a normal distribution, similar to that seen for random noise.

3. Mean of the distribution

The mean of the probability density function is an indication of the point which divides the the p.d.f. into two equal areas. The vertical line placed on Figure 9 shows indicates the mean of the sample p.d.f., the readout in the upper left hand corner of the figure shows the value to be 0.0 V. The mean value for a monitored vibration signal is primarily of the dc component of the signal. Physically it can be thought of as the reference point about which vibration is taking place. When monitoring a frequency span that does not include the dc component of the signal would be expected to be near zero. Figure 10 can be used to understand the mean value.
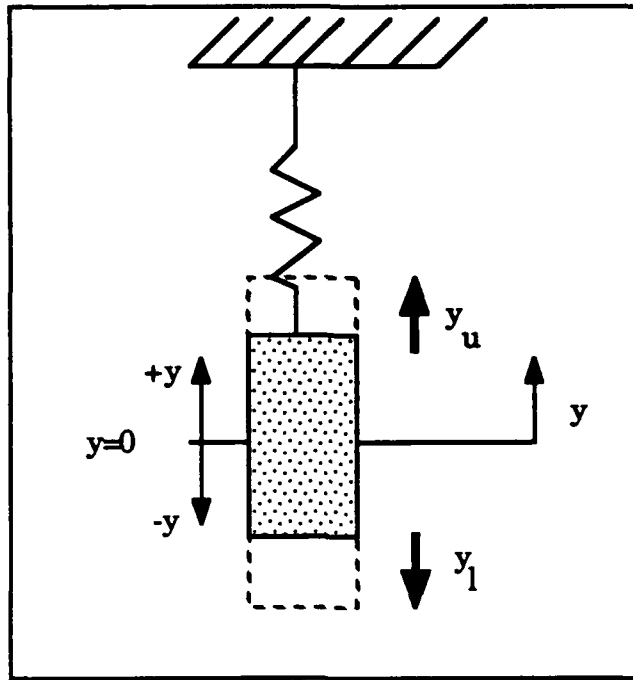
Figure 10. Free vibration with mean of zero.

Figure 10 illustrates a mass capable of free vibration. If $|y_u| = |y_l|$ and the at rest position of the mass is at y=0, than the mean of the movement is zero. When monitoring a machine the situation is slightly different, this is illustrated is Figure 11.

Figure 11. Vibration of a machine.

In this case the mounting of the machinery will restrict movement in the y direction, and may lead to a non-zero mean value.

36

The stiffness of the foundation and construction of the machine would have the effect of preventing a significant amount of movement, but the measurement of a small magnitude for the mean value is possible. Equations used for the computation of this and the remaining statistical parameters are presented in Chapter V.
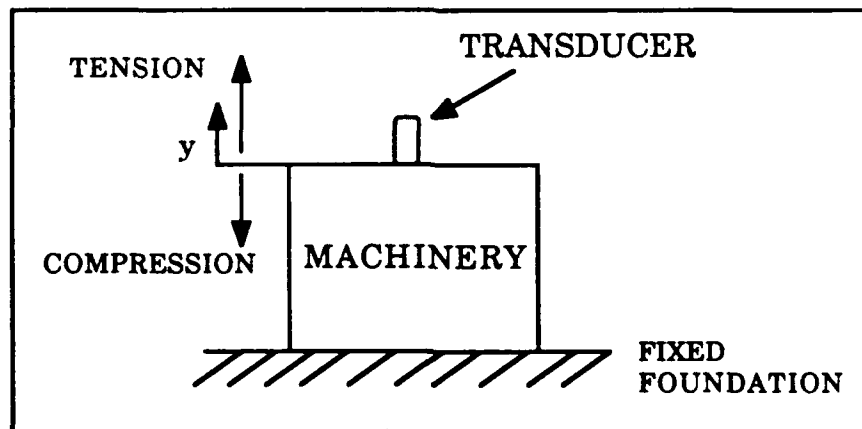
4. Mean Square Value and Variance

Earlier discussions in this chapter addressed the effect of distributed and localized faults on the frequency spectrum, these types of faults are expected to cause the p.d.f. to grow wider. The mean square value and the variance of the p.d.f. can be viewed as indicators of the scatter in the data represented by the p.d.f. The relationship between the variance and the mean square value will be discussed in Chapter V, but as damage occurs to the machinery the p.d.f. of the measured signal will change, Figure 12 illustrates the change after damage.
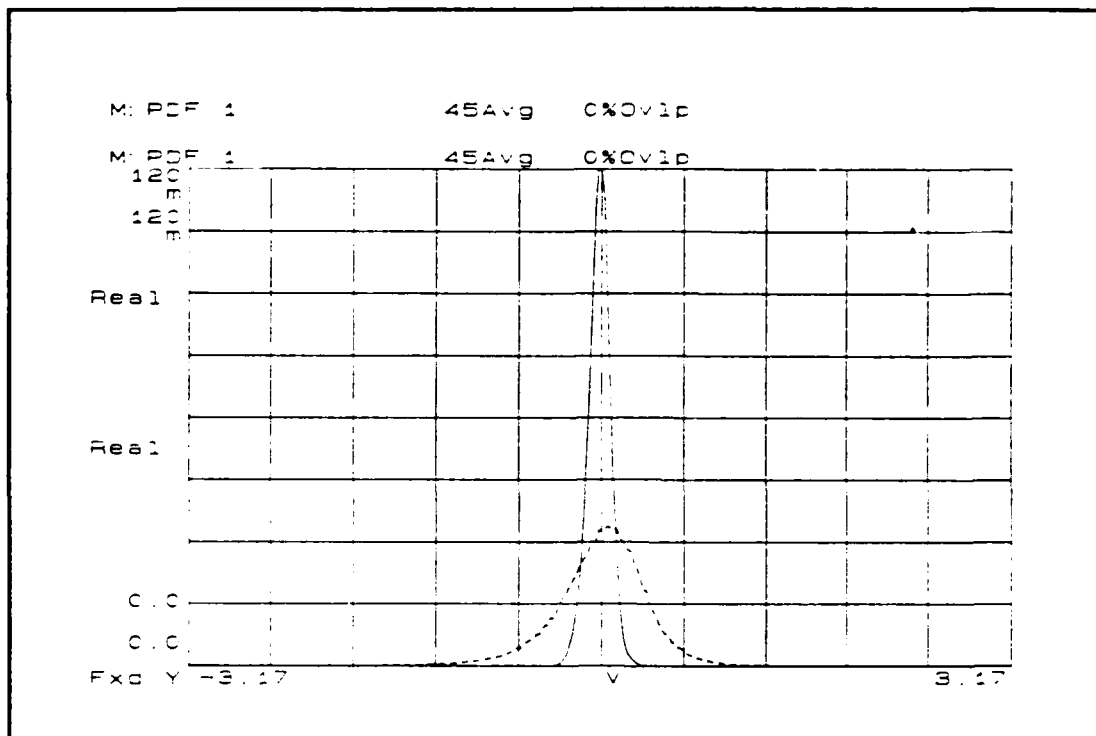
Figure 12. Effect of damage on the probability density function.

In the figure, the solid line is the p.d.f. of an undamaged machine. The dotted line is the p.d.f. of the same machine with damage. The damaged p.d.f. has a "fatter" appearance and a larger mean square value and variance. The "fatter" appearance is an indication that the data measured for the damaged machine is spread over a wider range of values.

It should be noted that the mean square value is the rms level of the vibration signal squared. The rms value of the vibration has traditionally been used as an indicator of the condition of the machinery.

5. Third Moment and Coefficient of Skewness

The third moment of the p.d.f. is an indication of the symmetry of the p.d.f. The coefficient of skewness is a normalized value of the

38

third moment about the mean, normalized using variance. Use of this parameter for machinery monitoring purposes was not found in the literature.

6. Fourth Moment and Coefficient of Kurtosis

The fourth moment is a measure of the activity that is occurring in the tails of the probability density function [Ref. 8 and 18] and can be thought of as an indicator of the flatness of the p.d.f. The fourth moment is normalized using the variance. Figure 12 can be used to understand kurtosis better. In the undamaged p.d.f. the distribution of measured values is very small, the area of the p.d.f. can be enclosed in a tall, narrow rectangular area. If a similar box was drawn around the damaged p.d.f. it would be wider and squatter, indicating a flatter appearance.

The use of the normalized coefficients of skewness and kurtosis allows the unchanging nature of the probability density function to be used. This means that even if the load on the machine or speed of the machine changes, the shape of the probability density function will remain essentially the same, and the normalized values should remain steady. When damage occurs to the machinery the p.d.f. changes, and the normalized values change allowing them to be used as a fault detection technique, [Ref. 8 and 18].

III. MODEL DESCRIPTION

For this research a small diagnostics model developed by Stamm [Ref. 2] was utilized to evaluate the changes in vibration resulting from damage to a set of gears. Use of this model allowed experimental vibration monitoring techniques to be tested and developed on simple machinery in an experimental setting. The diagnostic model was configured as in Figure 13.
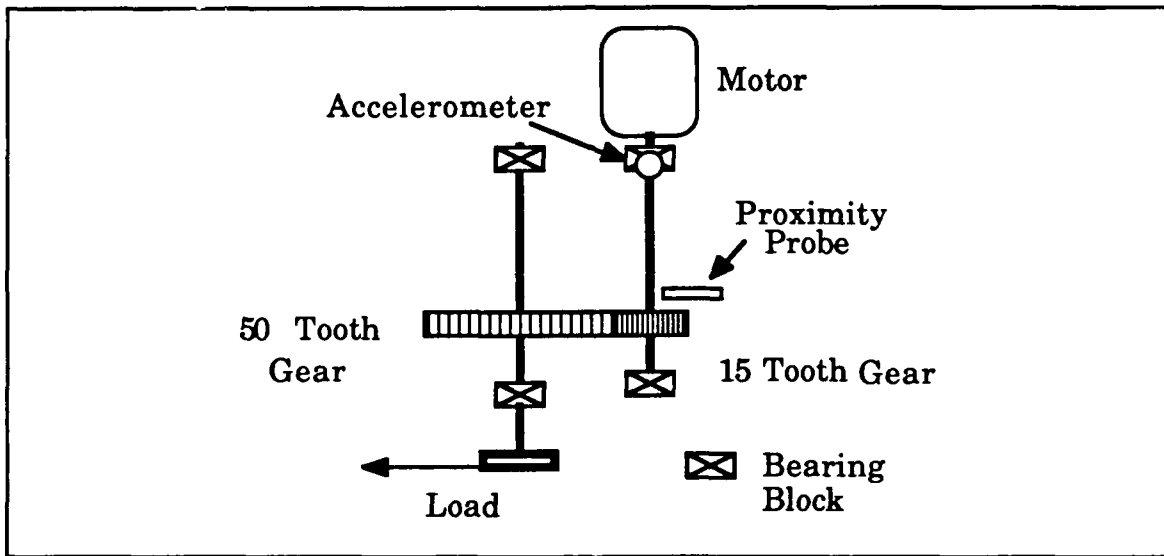
Figure 13. Diagnostics model used in investigation.

The model is configured as a simple speed reduction machine, consisting of two parallel shafts with gears mounted on the shafts. An electric motor provided drive for the system and a friction brake provided load. Instrumentation included a piezoelectric accelerometer to measure vibrations and a non-contacting proximity probe to measure speed and provide a keyphasor signal. Only a description of the configuration used in the research will be made, Reference 2 has

40

detailed descriptions of the design and construction of the diagnostics model.

A. DIAGNOSTICS MODEL

A Bodine Electric Company Type NSH-34, one fifteenth horsepower, variable speed, DC motor provided drive for the system. Motor speed was controlled with a Bodine model ASH-403, DC motor controller. All experiments were run at a speed of 30± .2 Hz (1800±12 RPM). The driving shaft of the diagnostics model was coupled to the motor output shaft using a short section reinforced rubber hose, force fit over the ends of the shafts. This method reduced the effect of small alignment inaccuracies, and also reduced motor related vibrations transmitted to the mechanical side of the diagnostics model. The coupling was sufficiently tight to transmit the torque of the motor without slippage.

The two shafts of the model were supported by bearing blocks fabricated from rectangular aluminum stock. Inside each of the blocks, ball bearings were mounted to permit free rotation of the shafts. Bearings were Fafnir model AS3K radial ball bearings, this is a light weight general purpose ball bearing. On each bearing block a small steel pad was mounted. The pads permitted transducers to be magnetically mounted on the bearing block in a manner similar to that used in the Navy's vibration monitoring program, [Ref. 19]. The pads were finish ground and affixed to the top of each bearing block by use of a cyanoacrylate ester compound (super glue). Reference [19] indicates that this method of attachment is the most favorable method of affixing

the pads. It should be noted that the glue became brittle after a period of about one year leading to the pads falling off the model.

Midway along the driving shaft a 15 tooth steel stock spur gear was placed. Opposite this gear on the driven shaft was a 50 tooth spur gear. The gears were mounted to the shafts by use of small set screws. The spur gears used had three eighths inch face width and a 14.5 degree pressure angle. Neither gear was hardened. Throughout this investigation the 15 tooth gear was the gear in which damage was applied. The contact ratio between the two gears was calculated as 1.90. This was calculated following the description provided by Smith in Reference [6]. Figure 14 is helpful in following the calculations.
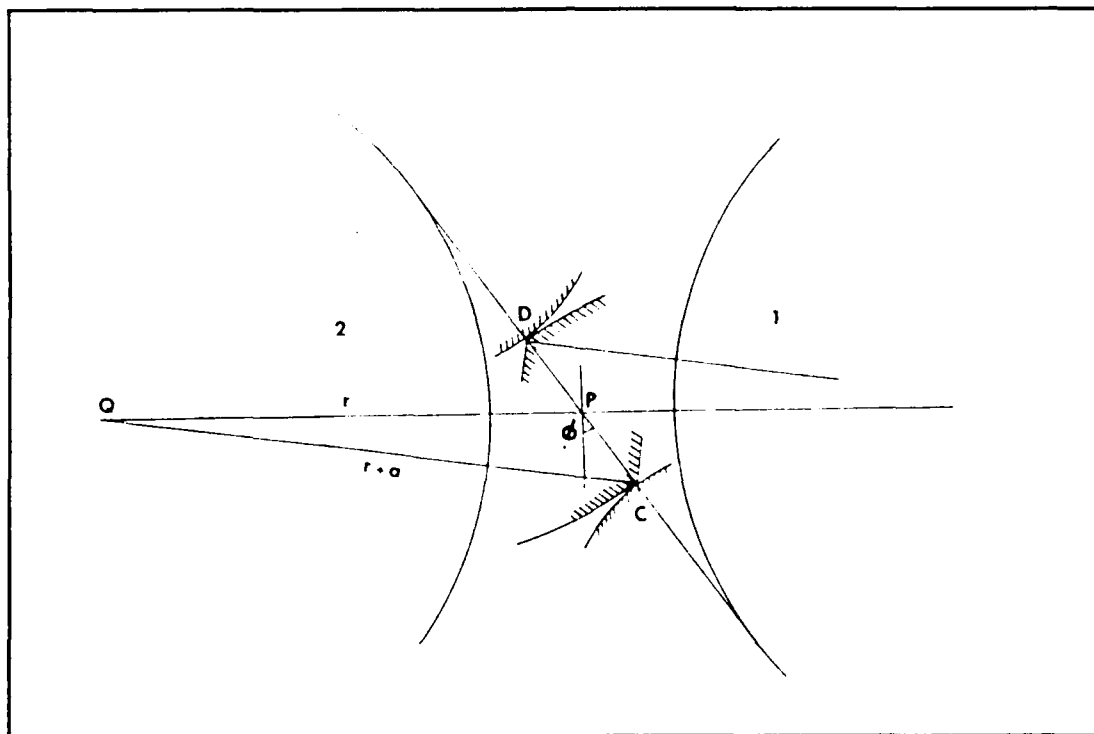

Figure 14. Calculating gear mesh contact ratio, [Reference 6].

In this figure the 50 tooth gear will be designated as gear one, and the 15 tooth gear will be designated as gear two. The contact ratio is

defined by Smith as "the average number of pairs of teeth in contact in a spur mesh . . . ." Contact ratio can be calculated using equation (6), from References [6 and 20].

$$M_c = L_{DC}/(p*\cos\phi) \qquad \text{unitless} \qquad (6)$$

where:

M_c is the contact ratio,
L_{DC} is the length between point A and B (see Figure 14),
p is the circular pitch,
ϕ is the gear pressure angle in degrees.

For the gears used in the model the catalogue specification provided the following:

diametral pitch P equal to 20 teeth/inch
pressure angle ϕ equal to 14.5°

Circular pitch p is calculated with equation (7):

$$p = \pi/P \qquad \text{inches} \qquad (7)$$

Circular pitch was calculated as p=0.1571 inches.

In Figure 14, r is the radius of the pitch circle of the gear, and r+a is the radius of the tip circle. Specifications for the gears used on the model give for the 15 tooth gear:

$$r_2 = 0.375 \text{ inches}$$

$$(r_2 + a_2) = 0.425 \text{ inches}$$

and for the 50 tooth gear:

$$r_1 = 1.25 \text{ inches}$$

$$(r_1 + a_1) = 1.50 \text{ inches}$$

The length L_{AB}, shown in Figure 14, can be written as:

43

$$L_{DC} = L_{DP} + L_{PC}$$

Using trigonometric relationships, Smith provides equations to calculate the lengths L_{PD} and L_{PC} [Ref. 6]):

$$L_{DP} = -r_1 \sin \phi + [(r_1 \sin \phi)^2 + (a_1^2 + 2a_1 r_1)]^{.5} \quad \text{inches}$$

$$L_{PC} = -r_2 \sin \phi + [(r_2 \sin \phi)^2 + (a_2^2 + 2a_2 r_2)]^{.5} \quad \text{inches}$$

Using these relationships:

$$L_{DP} = 0.162 \text{ inches}$$

$$L_{PC} = 0.127 \text{ inches}$$

and the length L_{AB} is:

$$L_{DC} = 0.289 \text{ inches}$$

All values needed for the calculation of M_C the contact ratio have been calculated:

$$M_C = 1.90$$

Load on the system was provided by friction drag. The friction drag was produced using a leather strap applied ᵗ ᵎ a disc mounted on the forward end of the driven shaft. This simple method provided a stable load on the machine without introducing an additional noise source. Monitoring of the load was accomplished by placing a Simpson model 303 multipurpose meter in series between the motor controller and the motor. The level of current drawn by the motor was used to ensure the load on the system was fairly stable. The motor current level was adjusted by adding or decreasing tension on the leather strap.

Components of the model were mounted on a three quarter inch Plexiglass foundation measuring 20 inches by 24 inches. A thin rubber mat was placed beneath the foundation to prevent it from sliding and to reduce vibration caused by operation of the model (rattling). The entire

model was placed upon a large marble table. The heavy structure prevented vibrations from other machinery in the work space to interfere with measurements of the diagnostics model.

Frequencies expected to be produced by the diagnostic model can be found using equations (1-9). Knowledge of the basic frequencies expected to be produced by any type of machine is very important prior to beginning machinery vibration analysis.

driving shaft speed: 30 Hz
driven shaft speed: 9 Hz
gear mesh frequency: 450 Hz
second harmonic of the gear mesh frequency: 900 Hz

The gear mesh related frequencies will be monitored in the frequency spectrums recorded during research.

B. TRANSDUCERS

Two transducers, an accelerometer and a non-contact proximity probe, were used to convert machinery motion into electrical signals for use in monitoring the condition of the diagnostics model.

1. Accelerometer

A PCB model 302A06 accelerometer was used to convert the vibration of the diagnostic model to electrical signals. Figure 15 is an illustration of the instrument from the support documentation.
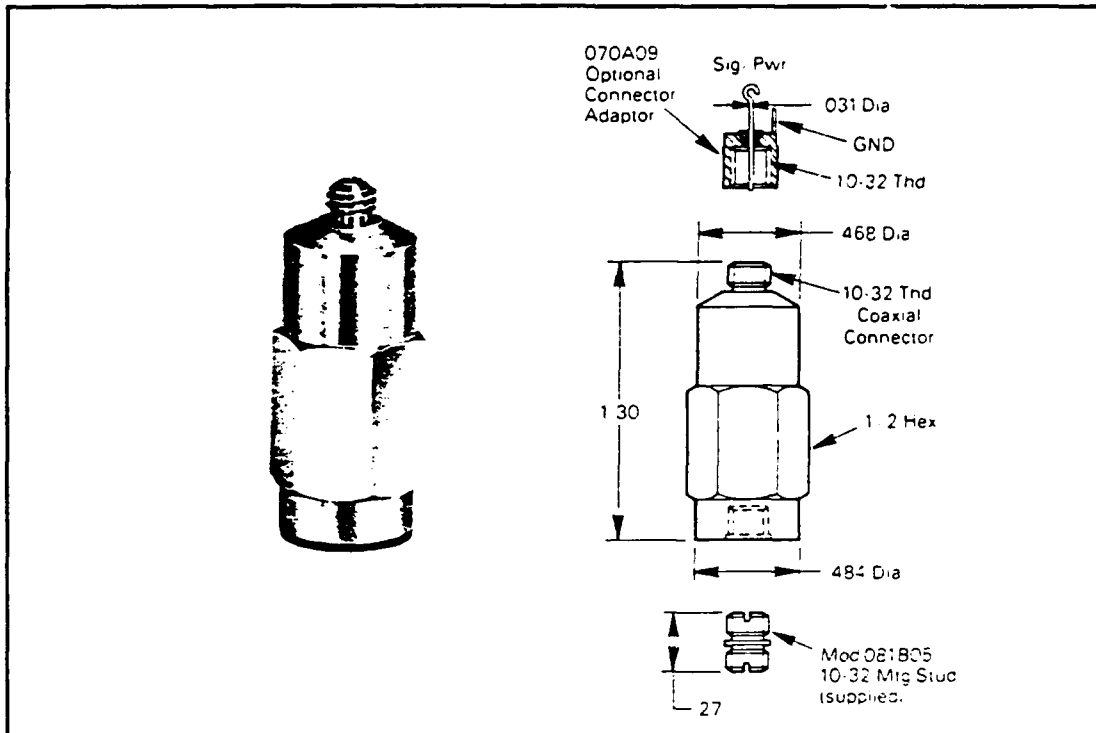
Figure 15. Model 302A06 accelerometer.

The 302A06 accelerometer is a precision instrument designed for measurement in industrial and field applications. It is a quartz based transducer, ground isolated with built-in amplifiers. The transducer is rated for a frequency range of 0.7 to 10,000 Hz with a voltage sensitivity of 10.00 mV/g with a resolution of .1 mV (.01g). It is important to note that the transducer is rated for with a lower frequency of 0.7 Hz, the instrument measures frequencies down to 0 Hz, but the measurements do not fall in the linear portion of the piezoelectric element, [Ref. 16]. The acceleration signal from the transducer was fed to a signal conditioner where it was amplified by a factor of x10. The specification sheet for this accelerometer is included in Appendix A. The instrument was mounted to the diagnostic model using a magnetic attraction base, PCB model 080A27, provided with the transducer. A thin coat of silicon grease was applied as a lubricant to all

interfaces of the transducer, mount, and diagnostics model. The use of the silicone grease enhances the transmission of high frequency vibrations from the diagnostics model to the transducer. The accelerometer was connected to a power supply/signal conditioner using a standard cable fitted with 10-32 micro plug connectors. The power supply/signal conditioner is described in Chapter IV.

2. Proximity Probe

A Kalman Measuring Systems model KD-2300-1SUM non-contacting proximity probe and signal conditioner was used to measure the speed of the diagnostics model and produce a keyphasor signal. The proximity probe was mounted on a portable stand, this method of mounting provided a method to monitor all shafts of the model with one set of equipment. During the research, the proximity probe was placed in position to monitor the rotation of the set screw of the 15 tooth gear. The principle of impedance variation caused by eddy currents produced in a metal target is utilized by the proximity probe to produce an electrical signal. As the set screw moves into and out of the face area of the probe the electrical signal produced can be used to measure the speed of the model. Figure 16 illustrates the trigger signal produced by this transducer.
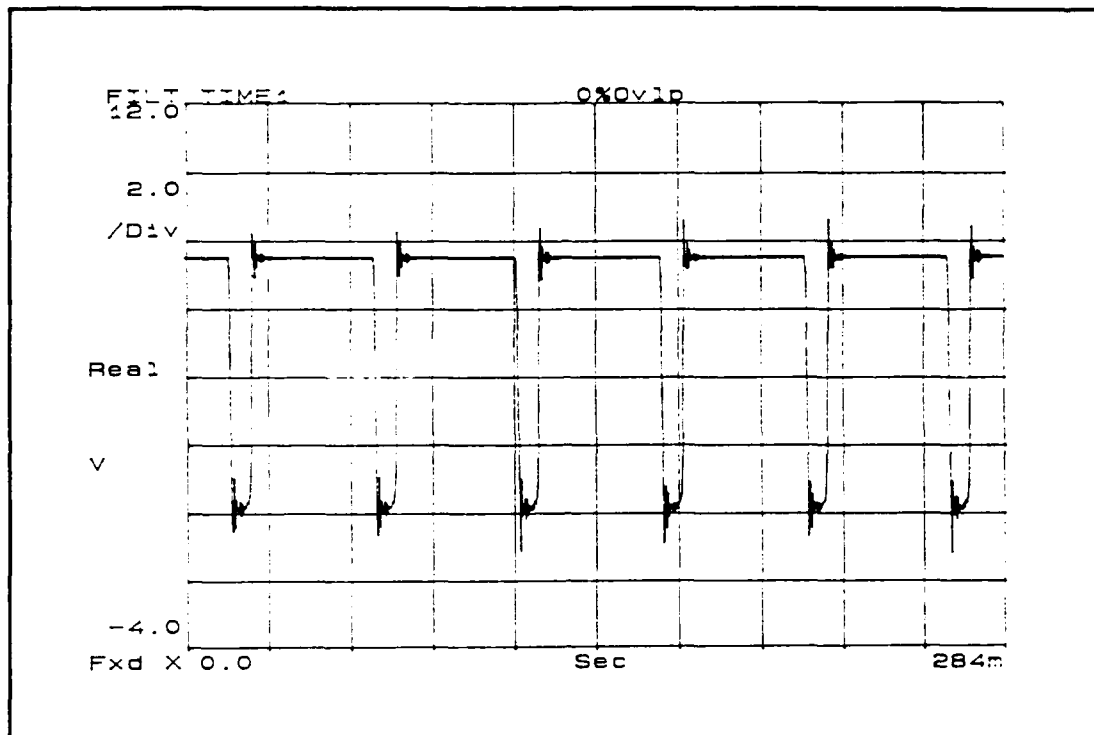
Figure 16. Trigger signal from proximity probe.

This signal is a square wave and triggering can be accomplished on either the leading or trailing edge. The system is capable of measuring frequencies up to 50 KHz, well beyond the speed capabilities of the diagnostics model.

48

IV. TEST EQUIPMENT

In this investigation the vibration signal produced by the diagnostics model was analyzed in two different methods, traditional frequency analyses and with statistical parameters. Electronic test equipment used to collect, analyze and present the data is illustrated in Figure 17.
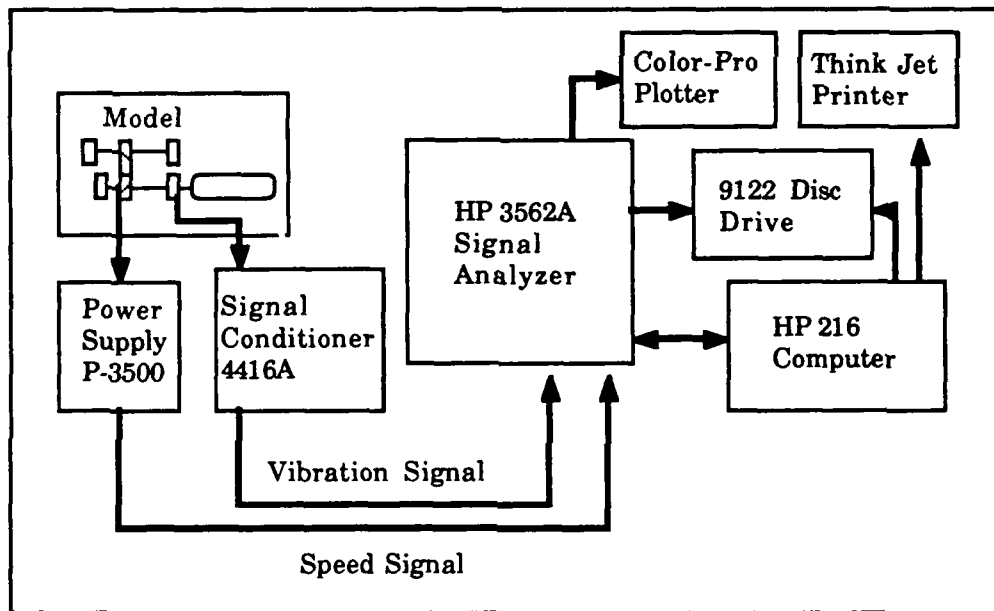

Figure 17. Electronic test equipment used in research.

The key component of this measurement system is the HP3562A Dynamic Signal Analyzer (DSA). The HP3562A is a two channel instrument that allows a multitude of signal analysis techniques to be performed. In this investigation the DSA was used to collect data from the vibration signal and from this data compute the spectrums and p.d.f of the signal produced by the accelerometer mounted on the diagnostics model. Data operations such as filtering, processing, display, storage, and output were controlled using functions incorporated in the DSA. In

49

addition the DSA is an HP-IB compatible system able to be controlled by an external table top computer. This capability proved to be very useful in the computation of statistical parameters from the probability density function.

Using the HP-IB bus, the DSA was controlled by a HP 216 series 9000 computer. The HP216 is a table top computer that uses the Hewlett Packard Basic language. Basic language programs were used to facilitate the collection and computation of the statistical variables described in Chapter II. Appendix B provides a listing of one of the programs used in the collection and analysis of the statistical values. The use of the HP216 as a system controller was essential, as the number of steps required to be performed in the computation of the various statistical values made hand calculations on the DSA virtually impossible. Once the values of the various statistical parameters were calculated the HP 216 was used to store the data and manipulate it to normalize the third and fourth moments. The HP 216 was not used in the collection or analysis of the spectrum measurements, although it is possible to completely automate the entire data collection and manipulation process.

Additional equipment used for storage and presentation of data included a HP Think Jet printer. The printer, controlled by the HP 216 computer, was used to print the statistical values of the measured signal. A HP Color Pro plotter was used to produce plots of the frequency spectrum and probability density functions, and a HP 9122 Dual Disc Drive was used to store plots and programs on 3.5 inch microdiscs.

A. MODEL TESTING

In preparation for model testing, several initial tests were conducted to verify the performance of the measurement equipment and investigate specific characteristics of the diagnostic model. Three tests were conducted; the first to investigate the resonant frequency of the transducer mount. The second, to determine natural frequencies of the diagnostics model. The final test, to verify operation of the speed measurement and keyphasor electronics.

1. Transducer Resonance Frequency Test

In this research the accelerometer utilized to measure vibrations was mounted to the diagnostics machine utilizing a magnetic mount. The ideal method of monitoring would be permanently mount the transducer to the model. However, a portable method of mounting was desired to enable the transducers to be used in future research. A magnetic mount was chosen over stud mounting in order to approximate the method used by the Navy in the existing vibration monitoring programs. The use of a magnetic mounting base affects the resonance frequency of the transducer, [Ref. 19]. The PCB 302A06 specifications indicates that the resonant frequency of the mounted accelerometer is 30 kHz. Use of the magnetic mount has the potential to lower this resonance frequency into the frequency range of 0-10 kHz. The frequency range used in the research. An impact hammer test was conducted in order determine the transducers resonance frequency. Figure 18 is a simple illustration of the equipment used.
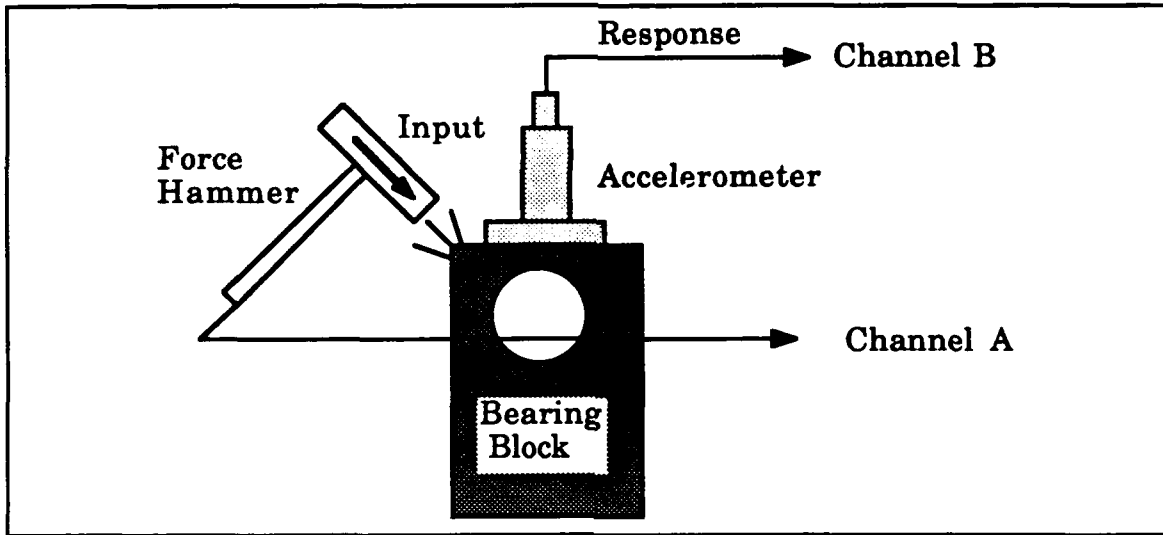
Figure 18. Equipment used to conduct the impact test.

The structure of interest is excited by striking it with an instrumented hammer near the location where the polished metal pads were mounted. The hammer has a force transducer attached and this signal is fed to one channel of a two channel analyzer. The excitations of the structure are monitored with an accelerometer which feds to a second channel on the analyzer. With these two signals the transfer function of the structure can be measured, [Ref. 16]. Figure 19 shows the programming of the HP3562A for the measurement.

```
                  Linear  Resolution

MEASURE:    CHAN 1                  CHAN 2
            Freq Resp               Freq Resp

WINDOW:     CHAN 1                  CHAN 2
            Uniform                 Uniform

AVERAGE:    TYPE       # AVGS       OVERLAP    TIME AVG
            Stable        51        0%         Off

FREQ:       CENTER                  SPAN       BW
            6.26 kHz                12.5kHz    15.6 Hz

            REC LGTH   Δt
            64.0mS     62.5µS

TRIGGER:    TYPE       LEVEL        SLOPE      PREVIEW
            Chan 1     35.0mVpk     Pos        Off

INPUT:      RANGE      ENG UNITS    COUPLING   DELAY
    CH 1    892mVpk    9.48mV/EU    AC (Flt)   0.0 S
    CH 2    795mVpk    10.1mV/EU    AC (Flt)   0.0 S

SOURCE:     TYPE                    LEVEL      OFFSET
            Off                     0.0 Vpk    0.0 Vpk
```

Figure 19. HP3562A state for impact test.

The transfer function calculated by the HP3562A enables the effect of the magnetic mounts resonant frequency to be examined. Figure 20 presents the transfer function of the impact hammer measurement.
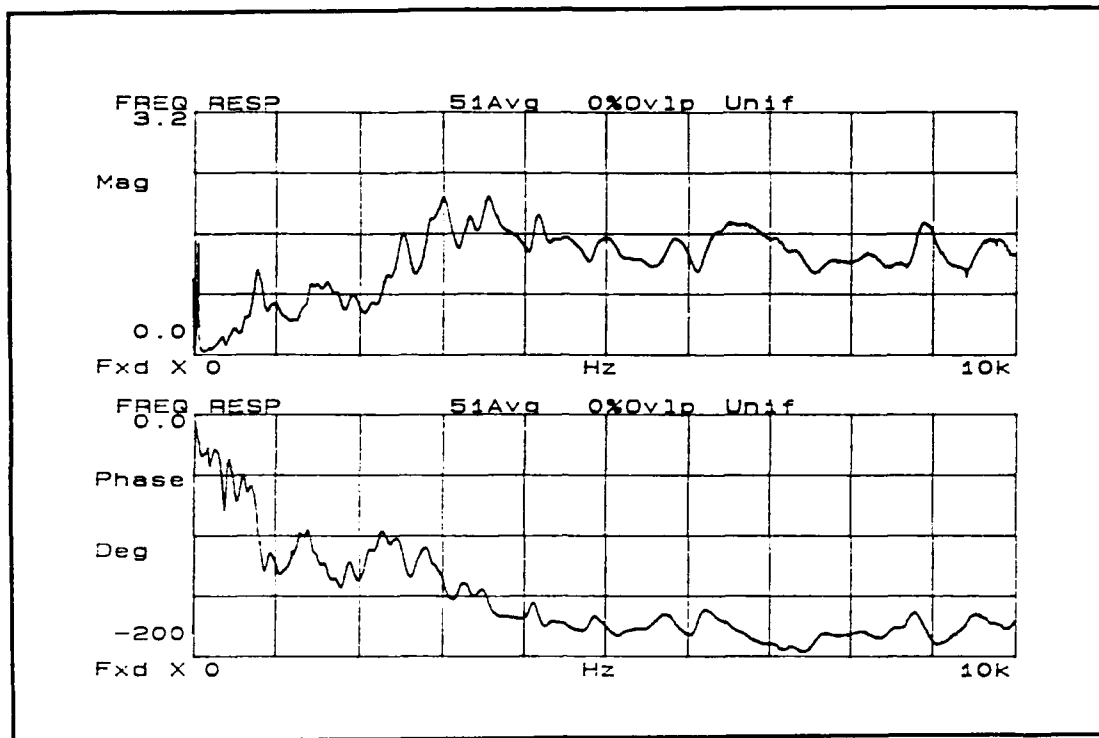
Figure 20. Transfer function measurement from impact test.

The plot traces shown in Figure 21 are the amplitude and phase representations of the measured transfer function. Reference [11] states that a resonance frequency can be identified by a rapid shift in the phase measurement of 180° and a corresponding peak in the magnitude portion of the trace. Neither are seen in this measurement, it does not appear that a resonance frequency lies in the area of interest.

Coherence is a measure of how well the data sample matches the data set and is used as an indication of the noise contamination of the measurement. It is a ratio that has a value from zero to one, and for this test a value above 0.8 was considered acceptable. Figure 21 indicates that the coherence, for this measurement, was acceptable across the frequency span of interest, 0.0 to 10.0 kHz. The drop in coherence after 9.0 kHz is due to the useful range of the impact

54

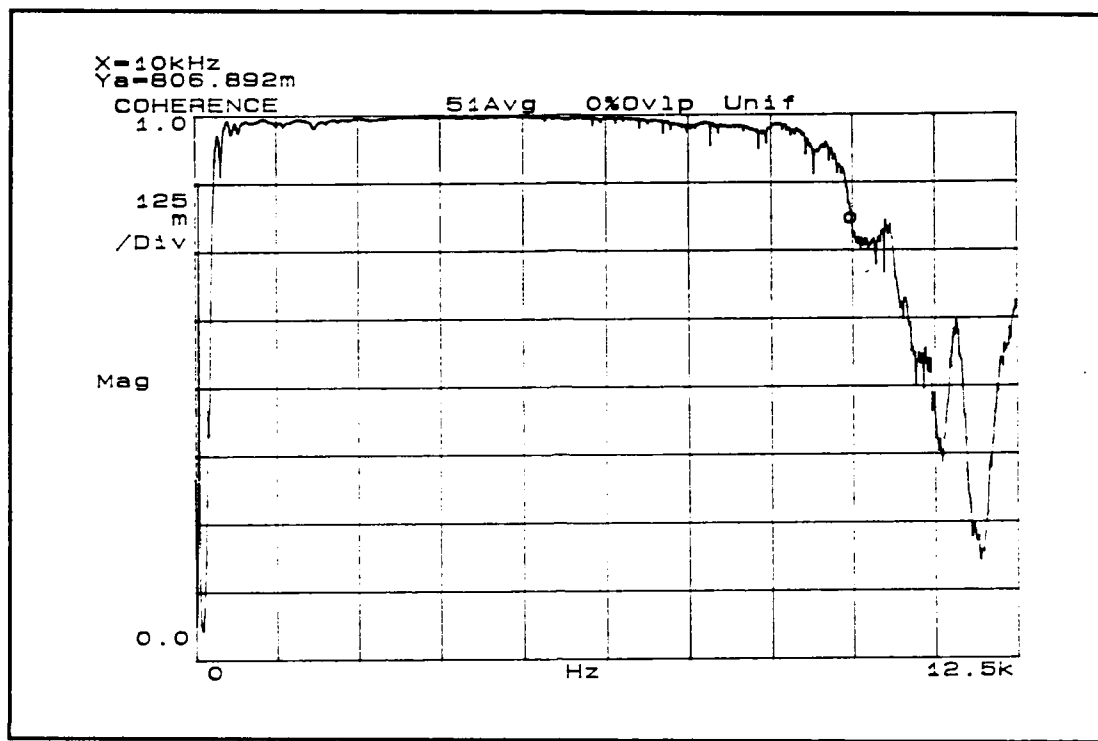hammer being exceeded, but the coherence of the data is still greater than 0.8.

X=10kHz
Ya=806.892m
COHERENCE   51Avg   0%Ovlp Unif

Figure 21. Coherence measurement of the impact tests.

2. Diagnostics Model Natural Frequency.

In Chapter II the effect of a systems natural frequencies on the vibrations produced by machinery was discussed. These natural frequencies can cause misinterpretation of measured spectrums. For example a piece of machinery may naturally experience small changes in speed. The amplitude of specific frequency components tend to increase with an increase in machine speed, and decrease as speed reduces as they are related to the speed of the system. Such as the gear mesh frequency being a multiple of a shaft frequency. For machinery with small variations in speed, experience with the machinery enables the maintenance personnel to establish a "feel" for the variation that

occurs in a monitored frequency. A natural frequency that falls within the range of machinery drift can cause the amplitude of a monitored frequency to experience a dramatic increase, or decrease, in level and can be misinterpreted as a fault occurring. In this investigation the speed of the diagnostic model was allowed to vary slightly so investigation of the models natural frequencies was made.

In the laboratory, determination of a machinery's natural frequencies could be accomplished by measurement of the transfer function of the system using methods similar to those used in determination of the transducers natural frequency. However, in the field use of this method on existing machinery is impractical. An alternative method can be found in Reference [21]. This method utilizes different operating speeds to determine the structural natural frequencies. This requires the machinery to be variable in speed or for measurements to be made during start up or shutdown. Using this method, a series of spectrums are made over a range of operating speeds. The natural frequencies of the machinery are determined by comparing the spectrums. A natural frequency can be identified by a small frequency band that changes amplitude as speed of the machinery changes, but does not change frequency. Spectral events that grow with increasing speed but also move along the frequency scale can be associated with dynamics of operation.

The HP3561A single channel analyzer has the ability to simultaneously display successive frequency spectrums to ease analysis. The equipment set-up illustrated in Figure 17, was used for this process except a HP3561A was substituted for the HP3562A. The HP3561A was configured to measure an untriggered spectrums over several

56

different frequency spans. Three different frequency spans (1.0 Hz to 1 kHz, 1.0 to 4.125 kHz, and 4 to 10 kHz) were examined to provide sufficient resolution over the entire frequency range used in the investigation.

During the runs the diagnostics model was started at a speed of approximately 15 Hz (900 RPM) and the spectrum of the output from the accelerometer measured. The model was then operated at progressively faster speeds until 15 separate spectrums were measured. Figure 22 presents the spectrums measured from 1.0 Hz to 1.0 kHz.
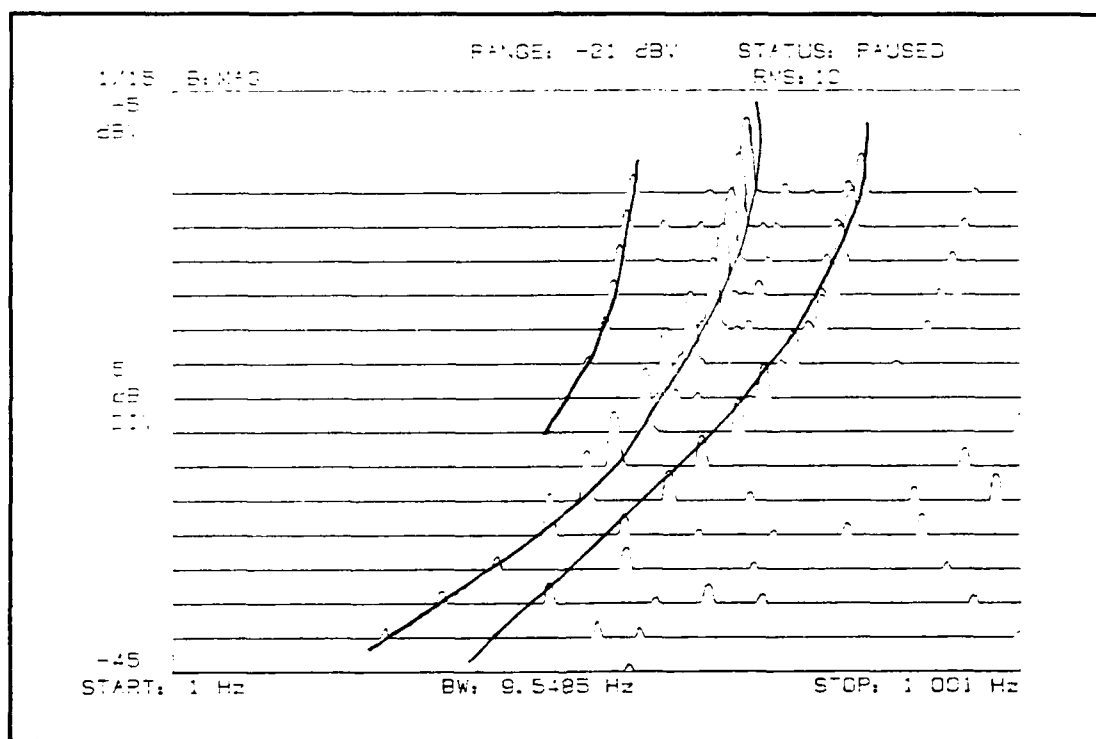

Figure 22. Spectrums for frequency span 1 Hz to 1.0 kHz.

This trace appears much smoother than the previous spectra illustrated in this report, due to the larger bin width of the HP3561A. On this trace lines have been added to show how this type of plot can be used to follow a changing frequency. This trace illustrates the

relationship between speed of the model and other frequencies. This trace only has spectral events related to speed of the machinery. Figure 23 is the spectrums from the frequency range of 1.0 kHz to 4.125 kHz.
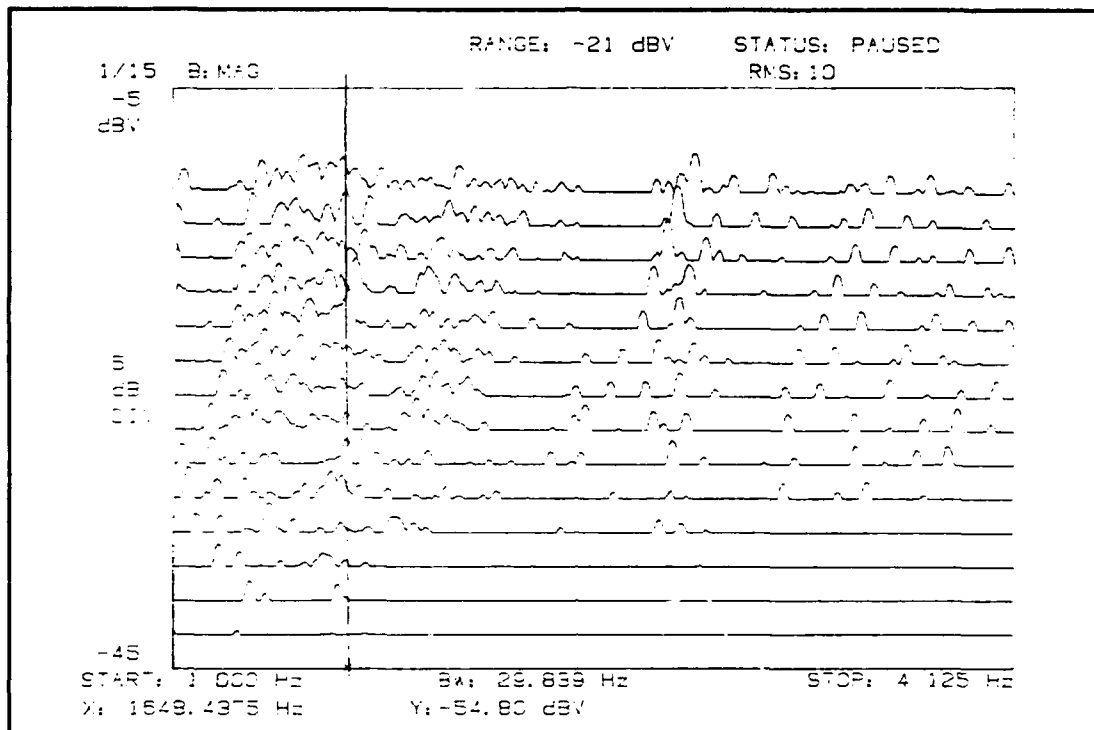

Figure 23. Spectrums for frequency span 1.0 kHz to 4.125 kHz.

In this figure several ridges associated with the dynamics of the machine can be seen. The most predominant one, occurring on the left side of the plot is associated with the gear mesh frequency which increases as the speed of the model is increased. At 1648.4 Hz, marked by the perpendicular line on the plot, there appears to be a natural frequency. The effect of this frequency can be seen in sixth trace measured as a large hump near 1648 Hz. Examination of the spectrums reveals that at this frequency speed related components increase dramatically as they move through and excite this natural frequency. No other natural frequency is apparent from this series of

measurements. A final series of measurements were made over the
frequency span of 4.0 to 10.0 kHz. The resulting plot is presented in
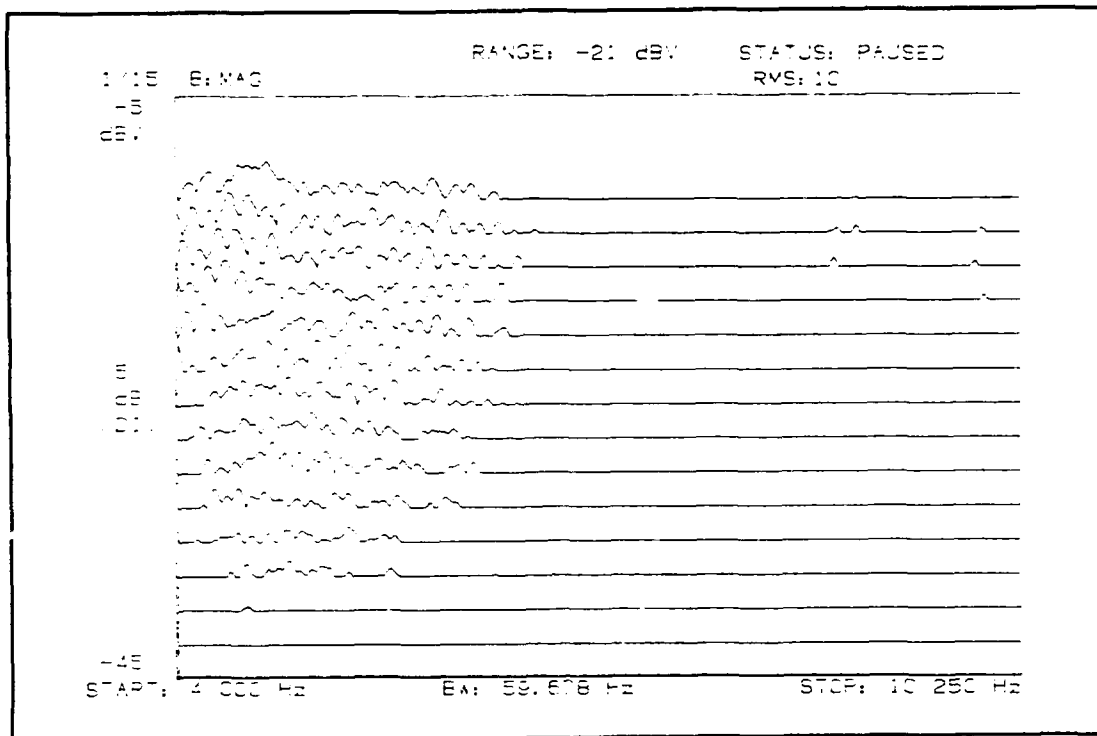Figure 24.

Figure 24. Spectrums for frequency span 4.0 to 10.0 kHz.

This series of measurements is very cluttered on the left side of
the graph, but no natural frequencies stand out. So the only natural
frequency of the model located was near 1648 Hz. This frequency
should not interfere with the individual frequencies to be monitored in
this research.

3. Tachometer tests

Verification of proper operation of the proximity probe was
accomplished using the test stand shown in Figure 25. This test stand
was formed using an existing test fixture used to measure the damping
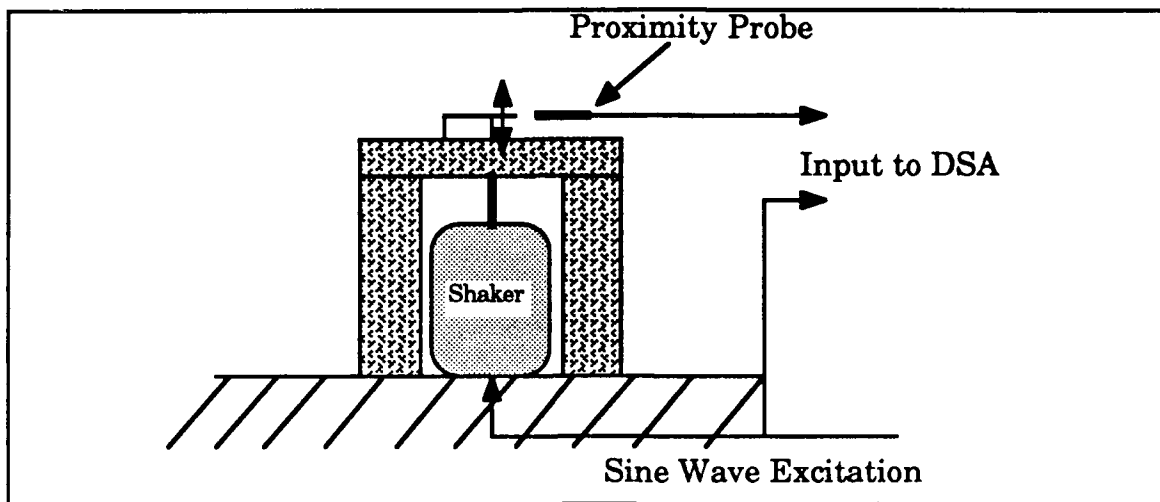characteristics of thin beams.

Figure 25. Test equipment to verify proximity probe accuracy.

The shaker was excited using a sine wave input generated by the HP3562A signal analyzer. The sine wave causes the shaker to move the clamping device mounted on top of the fixture at the same rate as the input signal. The proximity probe was mounted such that the edge of the clamping device moved in front of the face of the probe. This movement in front of the proximity probe produces a signal that is monitored by the HP3562A. This signal is then compared to the input signal. Figure 26 is the programmed configuration of the HP3562A for this measurement.

```
                    Linear Resolution
MEASURE:  CHAN 1                   CHAN 2
          Freq Resp                Freq Resp

WINDOW:   CHAN 1                   CHAN 2
          Hanning                  Hanning

AVERAGE:  TYPE        # AVGS       OVERLAP    TIME AVG
          Avg Off         10       0%         Off

FREQ:     CENTER                   SPAN       BW
          50 Hz                    100 Hz     187mHz

          REC LGTH    At
          8.0 S       3.91mS

TRIGGER:  TYPE        LEVEL        SLOPE      PREVIEW
          Freerun     0.0 Vpk      Pos        Off

INPUT:    RANGE       ENG UNITS    COUPLING   DELAY
   CH 1   AutoRng↑    1.0 V/EU     DC (Flt)   0.0 S
   CH 2   AutoRng↑    1.0 V/EU     DC (Flt)   0.0 S

SOURCE:   TYPE        FREQ         LEVEL      OFFSET
          Fxd Sin     15.0 Hz      0.0 Vpk    0.0 Vpk
```

Figure 26.   HP3562A setting used in measurements.

To verify the proximity probes operation over a range of operating speeds, several different frequencies were used as input to the system. Frequencies of 15, 20, 30, 40, and 60 Hertz were used as input. Figure 27 presents the result of the 20 Hz measurement.
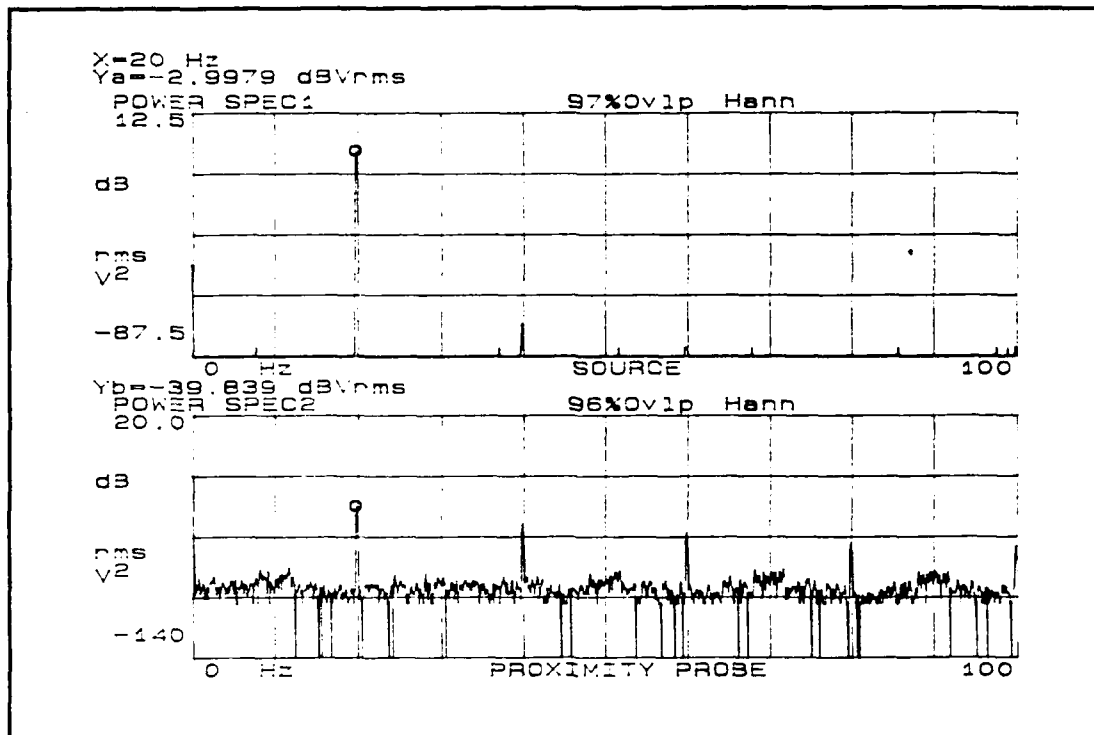
Figure 27. Comparison of input signal and measured output signal.

The frequency spectrums for the input signal is presented in the upper portion of the trace, the output signal from the proximity probe is the lower portion. The small frequency 'spikes' in the output spectrum are due to the square wave signal produced by the probe, and are harmonics of the base frequency. This square wave appearance was presented earlier in Figure 16. The fundamental, the frequency of interest, is always the largest of these components. Analysis of the traces showed the proximity probe accurately measured the speed of the clamping device, and that the proximity probe can be used as an accurate tachometer to measure the speed of the diagnostics model. The spectrums of the other input frequencies were much the same as the 20 Hz results and will not be presented.

V. MEASUREMENT PROCEDURES

This research was the second investigation dealing with machinery vibration monitoring that had been accomplished at the school. Because of this the investigation was also interested in establishing a baseline knowledge on techniques and experimental procedures.

A. DAMAGE PROCESS

For this research two new 15 tooth pinions were damaged to investigate the changes occurring to the vibration of the gears. In each case the damage to the pinion was limited to a single tooth to provide an aspect of control on the experiments. Two different types of damage were investigated:

- damage to tooth wear surface
- gouging of the tooth

The statistical parameters calculated from the resulting machinery vibrations were examined for responsiveness to the damage.

For the experiments the diagnostic model was operated with a new pinion for approximately eight hours to wear in the new pinion. After this wear in period the black finish on the pinion had been removed leaving a shiny uniform wear area on each tooth. Data was collected on the worn gear and used as baseline data for comparison to subsequent damage. Due to the small size of the pinion and the difficulty of damaging a single tooth while the pinion was installed in the model, the pinion was removed, damaged and re-installed. Prior investigations

63

revealed that this procedure introduced little change in the characteristics of the diagnostics model. During the experiments, the pinion was damaged several times, the details of the specific damage applied is discussed in Chapters VI and VII along with analysis of the measured data. Each level of damage applied to the pinion is designated by a letter, starting with A and proceeding through the alphabet. This method provides a convenient shorthand method of labeling damage without prejudgment of the severity of the damage. After each level of damage, the diagnostics model was operated for a period of approximately one and a half hours, during which the data used in the investigation was collected.

B. FREQUENCY SPECTRA MEASUREMENTS

In Chapter II frequency analysis techniques for condition monitoring were described. Subsequent chapters have presented information relating to the HP3562A signal analyzer, measurement methods and the use of frequency spectrums. In this research broad band and narrow band vibration levels and statistical parameters are discussed for each of the pinions damaged.

Frequency spectrums were measured over two spans 0.0 to 1.0 kHz and 0.0 to 10.0 kHz using a keyphasor signal as a trigger. Frequency spec. measured used the acceleration of the monitored vibration signal. Figure 28 presents typical programing for a HP3562A spectrum measurement.

```
                  Linear  Resolution

MEASURE:  CHAN 1                   CHAN 2
          Power Spec               Off

WINDOW:   CHAN 1                   CHAN 2
          Hanning                 Hanning

AVERAGE:  TYPE        # AVGS       OVERLAP    TIME AVG
          Stable          10       0%         On

FREQ:     CENTER                   SPAN       BW
          5 kHz                    10.0kHz    18.7 Hz

          REC LGTH    Δt
          80.0mS      39.1μS

TRIGGER:  TYPE        LEVEL        SLOPE      PREVIEW
          External    6.0 Vpk      Neg        Off

INPUT:    RANGE       ENG UNITS    COUPLING   DELAY
   CH 1   AutoRng↑    1.0 V/EU     AC (Flt)   0.0 S
   CH 2   AutoRng     1.0 V/EU     AC (Flt)   0.0 S

SOURCE:   TYPE                     LEVEL      OFFSET
          Rndm Noise               0.0 Vpk    0.0 Vpk
```

Figure 28. State for measuring triggered spectra.

Presentation of frequency spectra in a written document is somewhat difficult. Flipping between pages is not conducive to the flow of the document and it is difficult to point out specific characteristics of spectra. To avoid this problem yet still utilize the data available in frequency spectra, a compromise was made. In this report, amplitude from frequency spectra will be presented in graphs in a manner that reflects the changes occurring as the pinion was damaged. The values to be used in the graphs are calculated using equation (8)

$$dB_C = dB_M - dB_U \qquad (8)$$

where

dB_C is the change in amplitude used for plots
dB_M is the measured amplitude of interest
dB_U is the baseline amplitude of interest

65

Equation (8) produces a baseline measurement of 0.0 dB. An example will make the process clear. A baseline measurement for a specific frequency was (-86.329 dB), a measurement taken after damage was (-80.983) dB. Using equation (8)

$$dB_c = -80.983 - (-86.329) = 5.346$$

This method minimizes confusion that arises when working with negative dB levels. The practice appears to be standard in vibration monitoring literature.

This research uses two methods of utilizing the measured frequency spectrums. Band levels will be calculated from the 0.0 to 10.0 kHz and the 0.0 to 1.0 kHz measurements by integration of the measured frequency spectra. Integration results in an broadband level of vibration that is useful as an indicator of the affect damage has on the entire vibration signal.

The second method of utilizing the measured frequency spectra is to track changes that occur to individual frequencies. Three frequencies will be monitored; the driving shaft frequency (30 Hz), the gear mesh frequency (450 Hz), and the second harmonic of the gear mesh frequency (900 Hz). Originally sidebands surrounding the gear mesh frequencies were to be trended, but these frequencies were very difficult to use and the data provided little information.

C. COMPUTATION OF STATISTICAL VALUES

The HP3562A is a versatile instrument, that when controlled by a table-top computer can be used to measure and manipulate data in a manner that would be impossible to complete by hand. After measurement of the acceleration of the machines vibration signal, the

built in math capabilities of the instrument were used to calculate the mean, mean square, and variance, as well as the third and fourth moments about the mean. A sample calculation of these quantities will be demonstrated using a random noise signal as input to the analyzer. The random noise signal has an amplitude of 1.0 volt peak to peak, Figure 29 shows a typical signal used in this example.
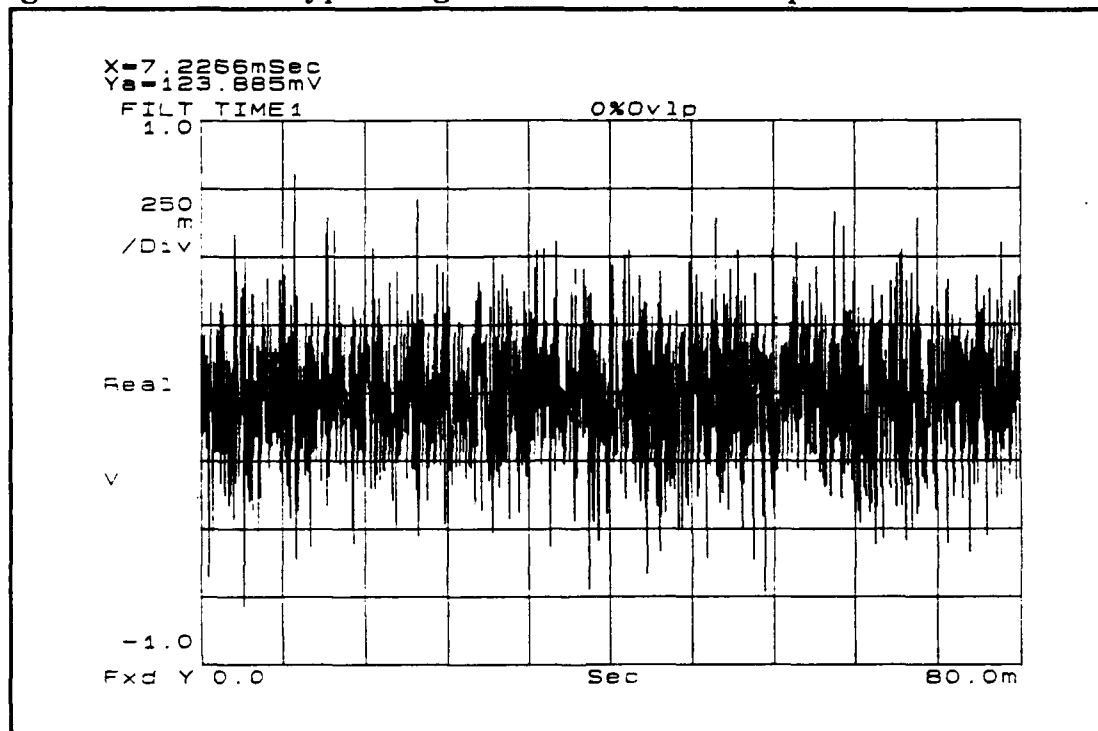

Figure 29. Random noise input.

1. Histogram Measurement

The HP3562A was programmed as shown in Figure 30. This configuration results in the analyzer calculating the distribution of measured amplitudes, which is called a histogram.

```
                Linear Resolution

MEASURE:   CHAN 1                    CHAN 2
           Histogram                 Off

WINDOW:    CHAN 1                    CHAN 2
           Hanning                  Hanning

AVERAGE:   TYPE        # AVGS       OVERLAP   TIME AVG
           Stable          45       0%        Off

FREQ:      CENTER                    SPAN      BW
           5 kHz                    10.0kHz   18.7 Hz

           REC LGTH    Δt
           80.0mS      39.1μS

TRIGGER:   TYPE        LEVEL        SLOPE     PREVIEW
           Freerun     0.0 Vpk      Pos       Off

INPUT:     RANGE       ENG UNITS    COUPLING  DELAY
   CH 1    AutoRng     1.0 V/EU     DC (Gnd)  0.0 S
   CH 2    AutoRng↑    1.0 V/EU     DC (Flt)  0.0 S

SOURCE:    TYPE                      LEVEL     OFFSET
           Rndm Noise               0.0 Vpk   0.0 Vpk
```

Figure 30. Typical state used in measurement of statistical values.

The HP3562A samples the signal at either 1024 or 2048 individual points/record depending on the programmed frequency range. Measurements that start at dc (0.0 Hz) contain 2048 points, while measurements starting at any other frequency are sampled 1024 times in each record. Forty five measurements of the random input signal were made for the histogram shown in Figure 31.
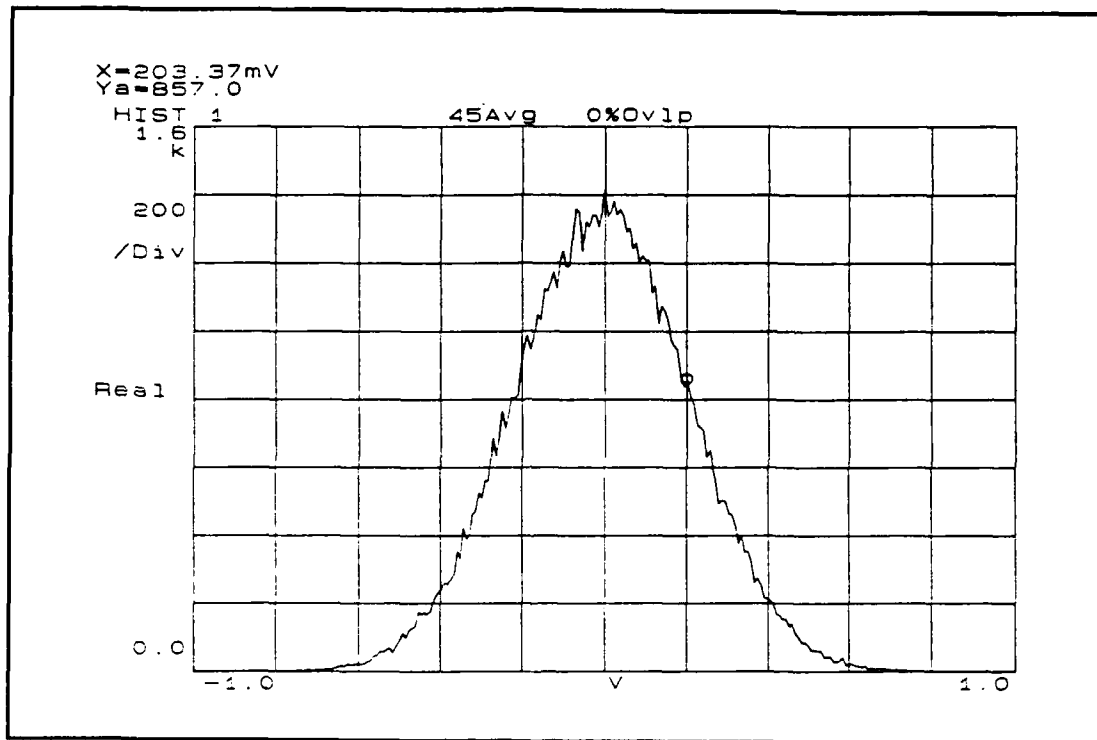
Figure 31. Histogram of the input signal.

The x-axis of the histogram represents the span of amplitudes measured in the input signal. The y-axis indicates the number of times a specific amplitude was measured. For example, in Figure 31 the cursor indicates that the amplitude 203.37×10^{-3} V was measured 857 times, the readout of the cursor location is located in the upper left corner of the plot.

2. Calculation of the Probability Density Function

The HP3562A calculates the probability density function, denoted p(x), by normalizing the histogram, [Ref. 22]. The probability density function is calculated using equation (9).

$$p(x) = \frac{n_x}{Nr(\Delta V)}$$

(9)

69

where

  n_x is the number of times the amplitude x was measured

  N is the number of points in the measured record, 2048 or 1024

  r is the number of records in the measurement

  ΔV is the difference between each amplitude measurements

Figure 32 is the probability distribution function of the histogram shown in Figure 31.
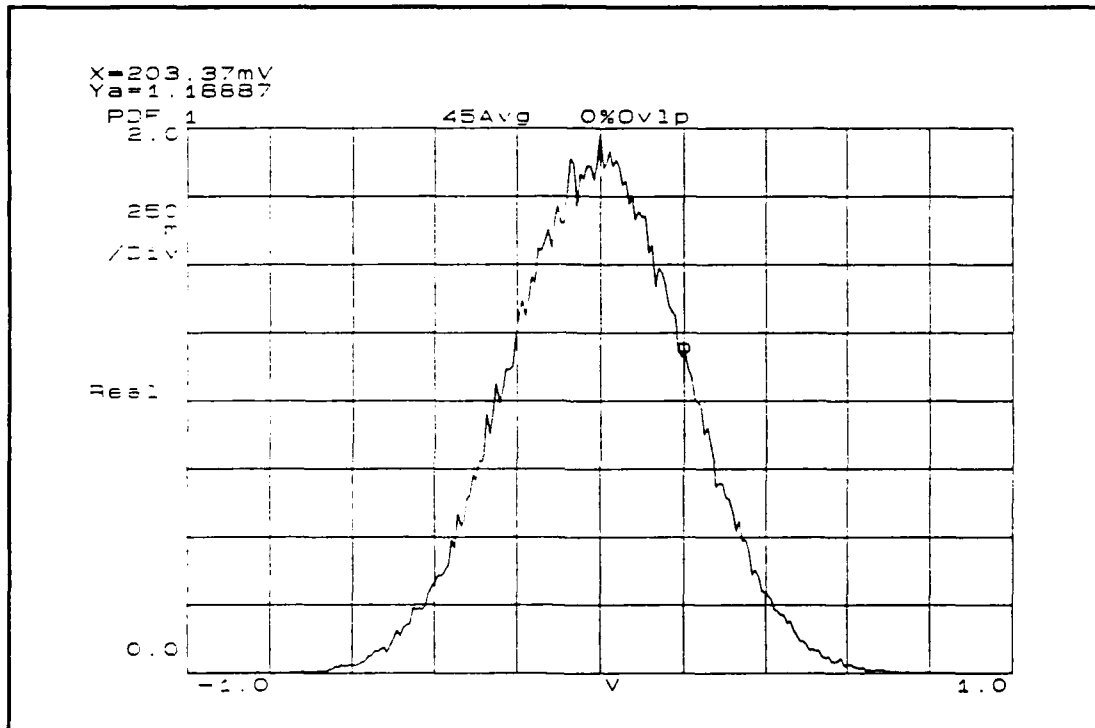
Figure 32. Probability density function of the input signal.

For the example signal the amplitude of 203.37×10^{-3} V was measured 857 times n_x , N is the number of points in each record, 2048 points, r is the number of records measured, 45 records, ΔV for the measurement is 7.82×10^{-3} V. These values result in a p(x) of 1.189. The cursor in Figure 32 indicates a value of 1.18887 calculated by the HP3562A , the difference is due to round off in the hand calculations.

The HP3562A's capabilities to perform math manipulations can be used to calculate desired statistical values of the p.d.f. The use of these capabilities requires the user to "visually" or graphically follow calculations of desired values. This visual calculation process will be presented using the probability density function shown in Figure 32.

Note in Figure 32 that the y axis of this plot is not the probability of occurrence for a specific amplitude. Reference [22] states that "the probability of an input signal falling between two points (measured amplitudes) is equal to the integral of the curve between those points." Earlier figures depicting the p.d.f. for machinery were produced by multiplying a constant equal to the ΔV of the measurement. This step is not required for the calculations of the statistical parameters.

3. Calculation of the Mean

The mean value x of a probability density function is calculated by:

$$\bar{x} = \int_{-\infty}^{+\infty} x p(x) dx \tag{10}$$

where

  p(x) is the probability density function
  x is an integration variable

The resulting value has the units of volts. Equation (10) requires a function x=y for multiplication with the probability density function, p(x). The HP3562A math functions can be used to produce that function. The process starts by dividing the probability density function by itself to produce a value of one, i.e.:

$$\frac{p(x)}{p(x)} = 1$$

Figure 33 is the resulting trace displayed on the HP3562A.
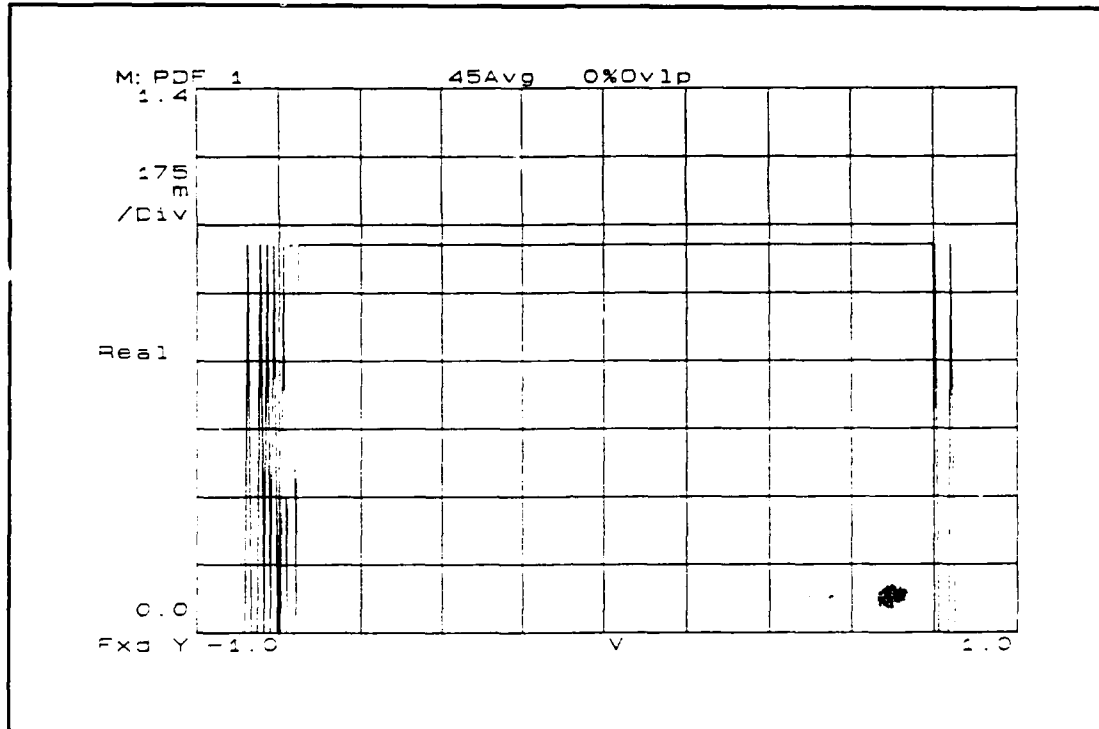
Figure 33. Probability density function divided by itself.

This function can be integrated to produce a straight line:

$$y = x + c$$

Where c is a constant that offsets the line from the origin. Figure 34 displays the resulting trace after the integration.
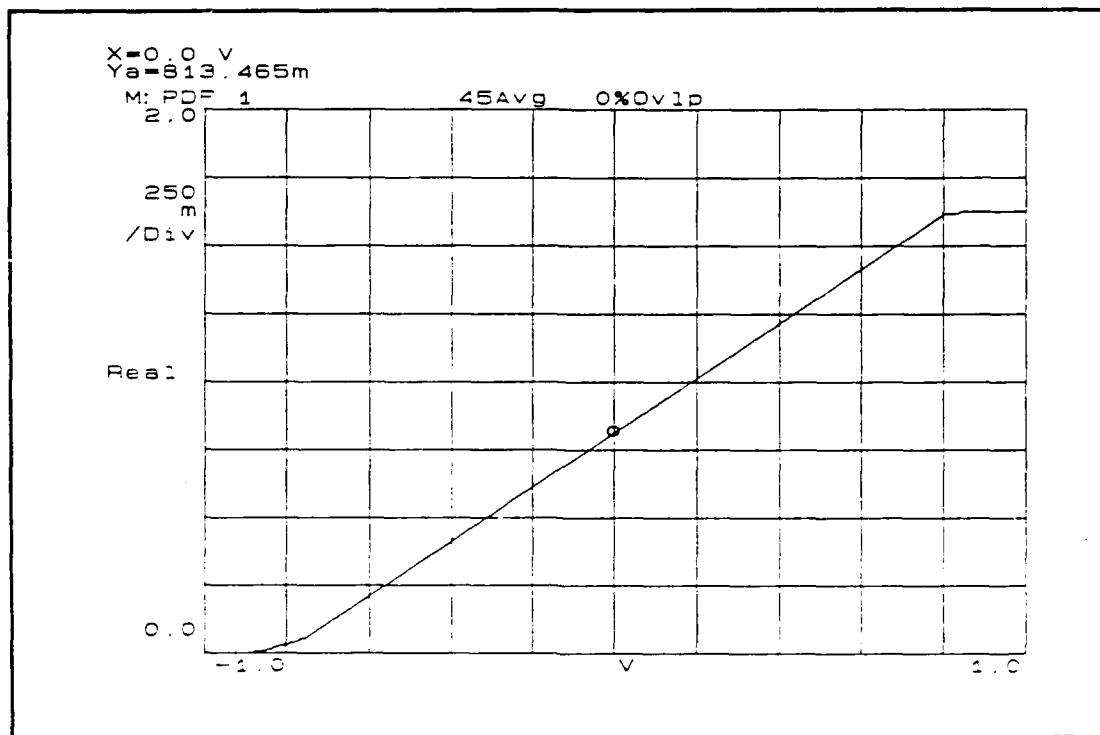
Figure 34. Result of integration.

The cursor has been placed at x=0 to illustrate that offset by a constant of 813.465×10^{-3}. This value is subtracted from the trace producing the function:

$$y=x$$

Figure 35 shows the results of this subtraction.
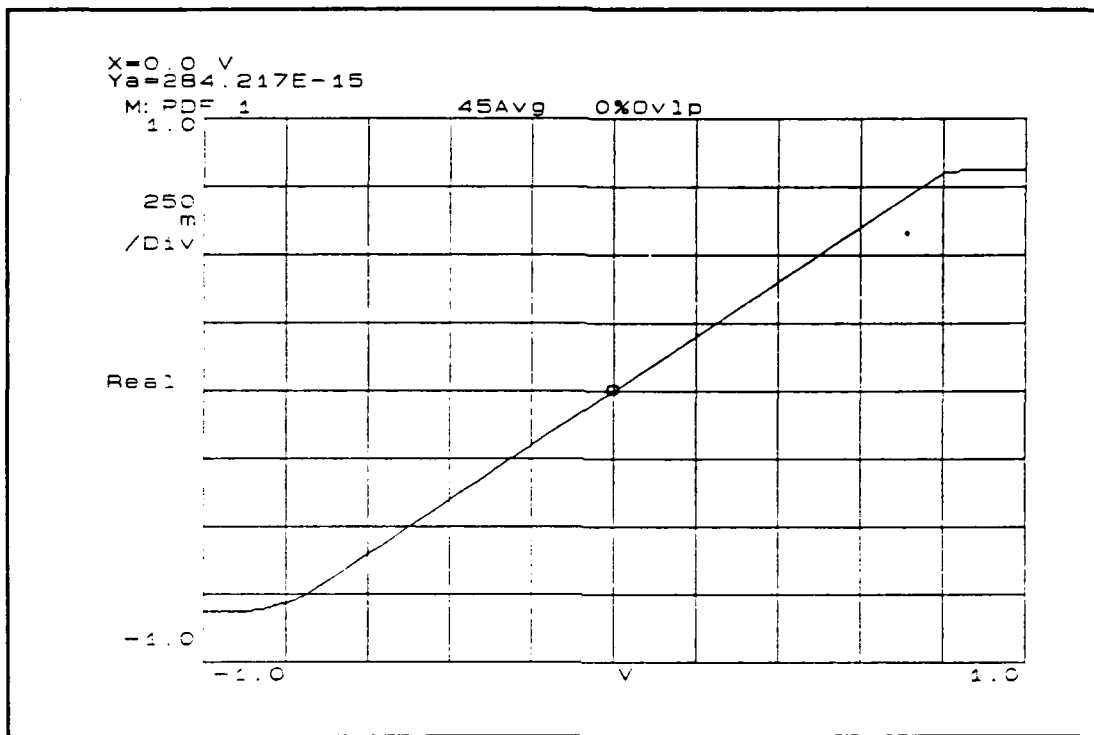
Figure 35. The function y=x.

There is still a slight offset of approximately 10^{-12} shown in Figure 35, but the value is considered negligible. This trace is used as the x=y function required in equation (10). The probability density function is multiplied by this function, Figure 36 depicts the results.
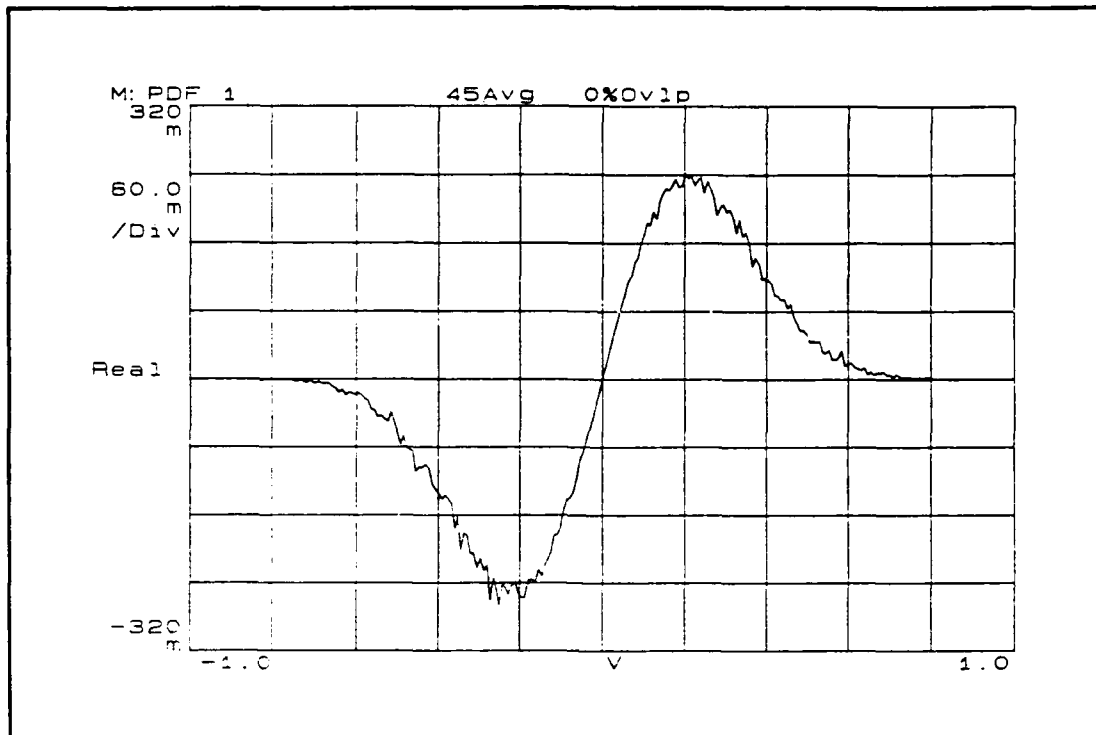
Figure 36. Result of multiplication between p.d.f. and x.

The integration of this product results in the trace shown in Figure 37 and the final value (at the cursor) is the mean value, other values on the curve are of little use as they represent iterative values of the integration process.
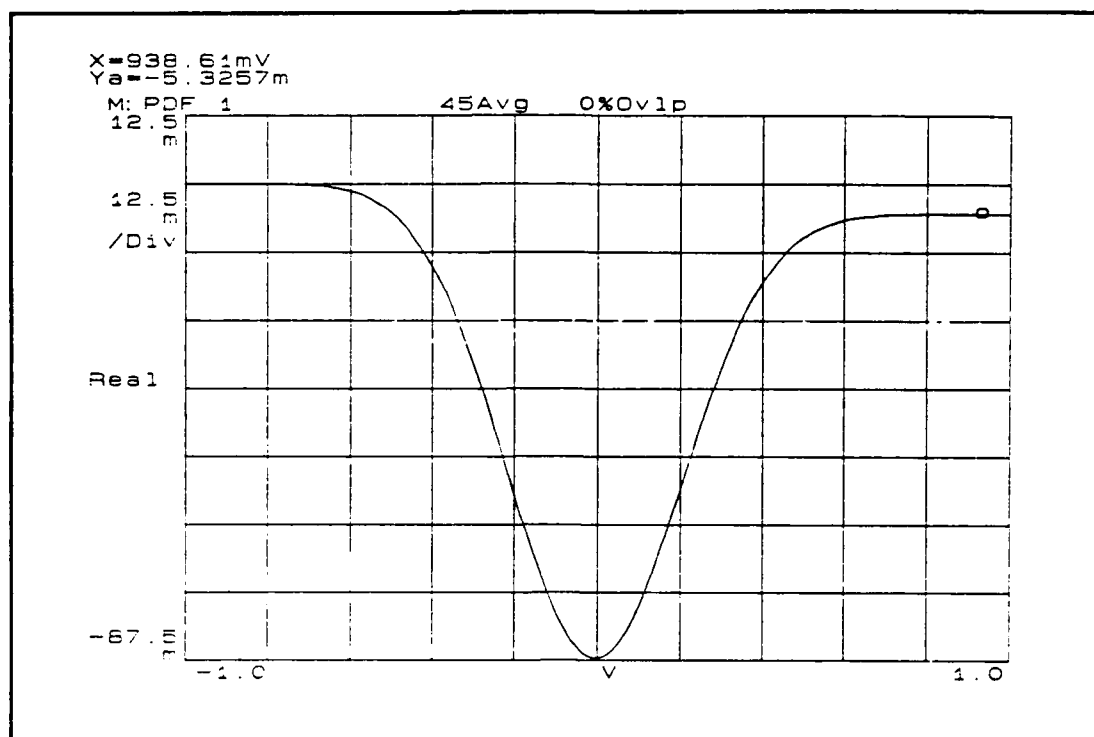
Figure 37. Mean value of the input signal.

The cursor indicates a mean value of the signal to be -5.3257 mV. For a random signal with no offset the mean should be zero, the measured value represents either a slight dc offset in the signal generator, or could be the result of the number of averages used in the measurement. In either case it is representative of the signal expected to be measured from the diagnostics model.

Procedures similar to these are used to calculate the mean square value, the variance, and the third and fourth moments about the mean. Step by step illustration of the calculation for these quantities will not be attempted, however, the process used in calculating each statistical value and a trace with the cursor placed at the final calculation will be presented. The sequence of calculating the remaining parameters is essentially the same as that used in calculation of the mean.

4. Calculation of the Mean Square Value

The mean square value Ψ^2, also called the second moment of the probability density function, is defined as:

$$\Psi^2 = \int_{-\infty}^{+\infty} x^2 p(x)dx$$

(11)

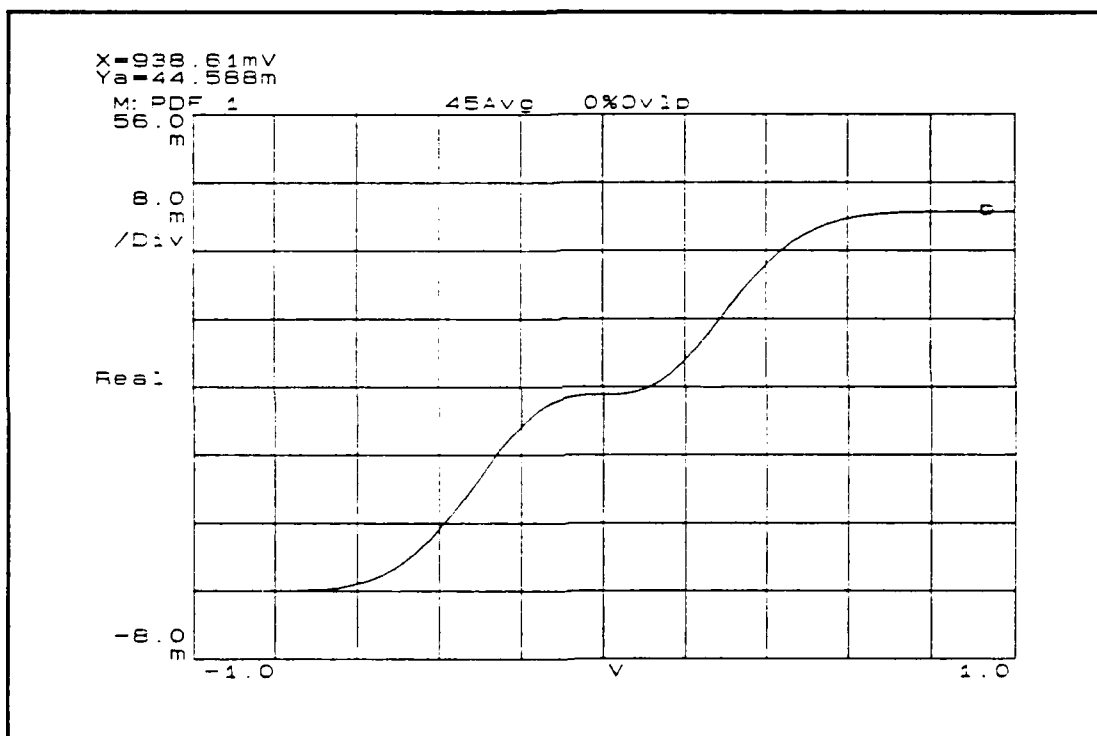The units of the parameter is volts squared. Calculations using this formula results in the trace shown in Figure 38.

Figure 38. Mean square value of the example signal.

The cursor indicates that the mean square value for the example signal is equal to .044588 V^2.

5. Calculation of Variance

The variance σ^2 of the probability density function can be defined as:

$$\sigma^2 = \int_{-\infty}^{+\infty} (x - \bar{x})^2 p(x) dx \tag{12}$$

Units of the variance are volts squared. With some algebraic manipulation equation (12) reduces to:

$$\sigma^2 = \Psi^2 - (\bar{x})^2 \tag{13}$$

The variance is sometimes referred to as the second moment of the probability density function about the mean. For signals with a mean equal to zero, the variance is equal to the mean square value. Figure 39 shows the results of the calculation of the variance using equation (12).
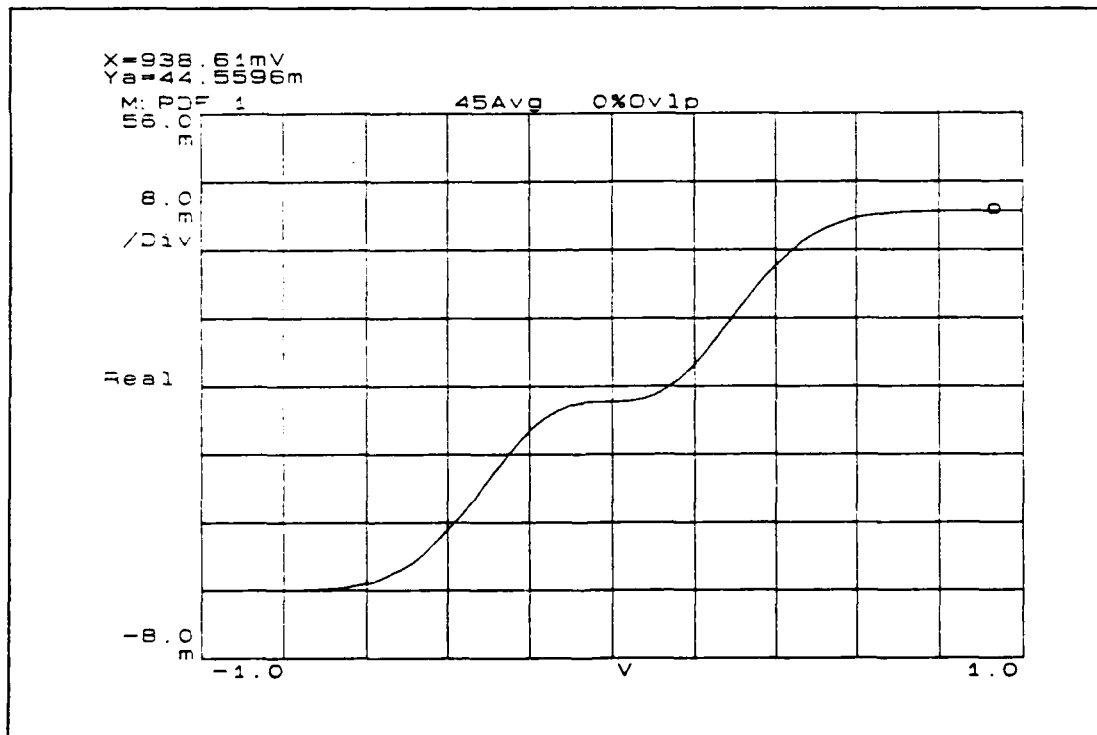

Figure 39. Variance of the input signal.

The the cursor indicates the variance of the signal is 44.5596x10^{-3} V^2. Use of equation (13) with the mean and mean square values computed in previous sections results in a variance of 44.5596x10^{-3} V^2. Calculation of the variance using equation (13), is faster than use of equation (12) and is the method used for this research.

After analysis of the data was completed it was found that very little difference occurred between the mean square value and the variance. This is due to the very small mean value measured from the vibration signal. Therefore only the results of the mean square measurements is presented in this report.

6. Calculation of the Third Moment and Skewness

The third moment of the probability density function about the mean (M$_3$) is computed by:

$$M_3 = \int_{-\infty}^{+\infty} (x - \bar{x})^3 p(x) dx$$

(14)

Units for this parameter are volts cubed. This moment can be normalized using the variance of the measured signal

$$\alpha_3 = \frac{M_3}{(\sigma^2)^{1.5}} \quad (\text{unitless})$$

(15)

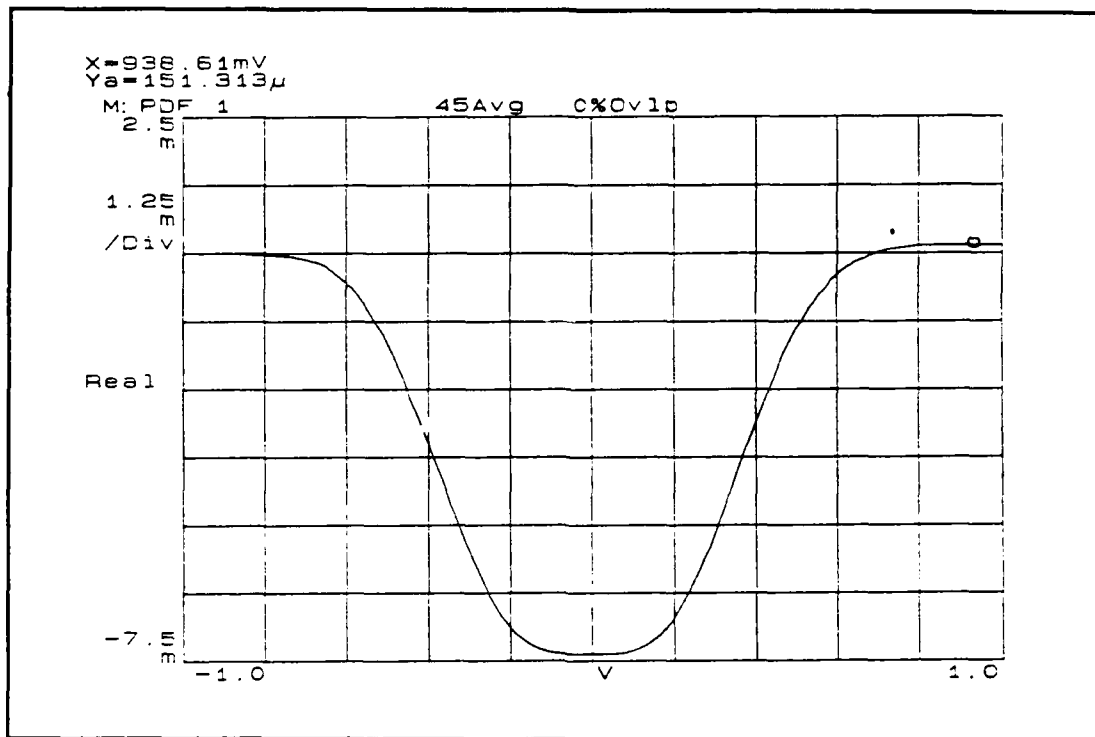and is called the coefficient of skewness, or skewness. Figure 40 illustrates the result after use of equation (14).

79

Figure 40. Third moment about the mean.

The cursor indicates the value of the third moment as 151.313×10^{-6} V^3, using the variance of 44.5596×10^{-3} V^2, and equation (15) results in a skewness of .016 . The skewness of a probability density function is an indicator of the symmetry of the probability density function about a vertical axis placed at the mean. Small values of skewness would indicate that the probability density function is very symmetric, while larger values of skewness indicates that the probability density function has shifted. Use of skewness for monitoring purposes was not found in the literature, making it difficult to classify whether the measured value of .016 is typical for a random noise signal.

7. Calculation of the Fourth Moment and Kurtosis

The fourth moment of the probability density function about the mean (M_4) is calculated

$$M_4 = \int_{-\infty}^{+\infty} (x - \bar{x})^4 p(x)\,dx$$

(16)

Units for the fourth moment are volts to the fourth power. This value can be normalized using:

$$K = \frac{M_4}{(\sigma^2)^2} \qquad \text{(unitless)}$$

(17)

The normalized value is called the coefficient of kurtosis, or kurtosis. Figure 41 illustrates the results from the example signal.

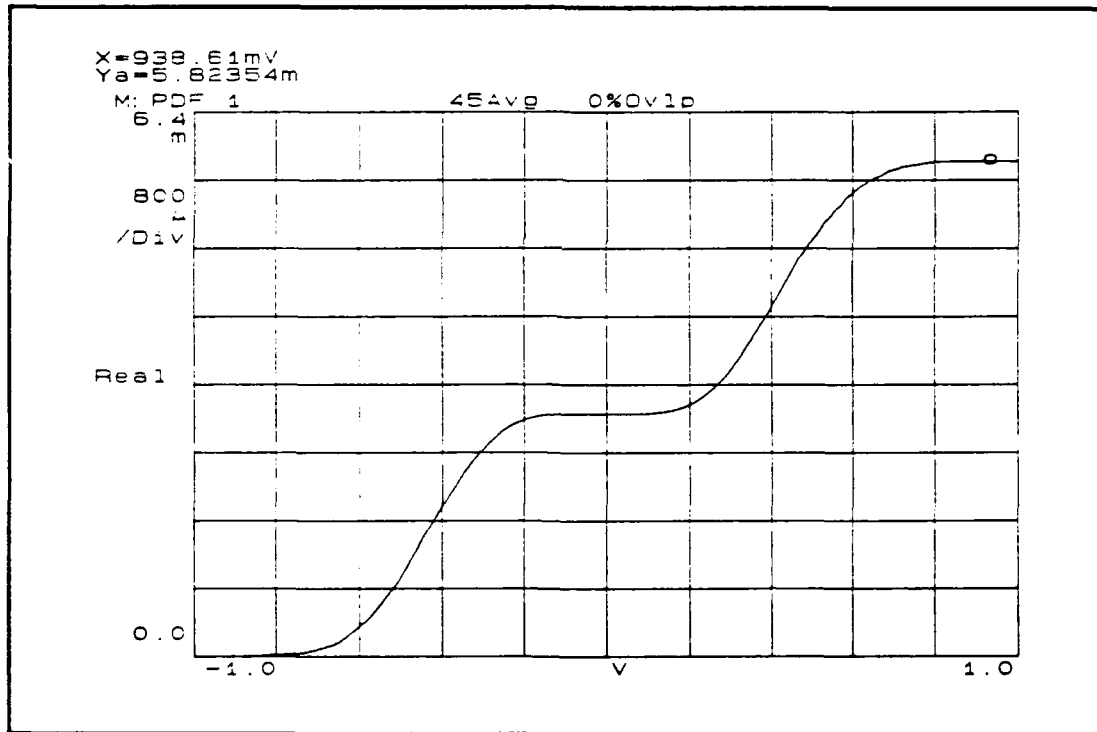**Figure 41. Fourth moment about the mean.**

The measured value of 5.8235×10^{-3} V^4, marked with the cursor, is normalized using equation (17) to a value of 2.933. The kurtosis value for a Gaussian distribution is 3.00 [Ref. 10], so the calculated value is

81

reasonable. Braun [Ref. 10] indicates that damage often causes a "typical" response in the monitored time signal. Isolated peaks occur in the time signal, and as damage increases the frequency of these peaks will increase. The peaks caused by the initial damage would be seen in the probability density function as an increase in the ends (or tails) of the probability density function. This increase in tails of the probability density function causes an increase in the fourth moment and in turn an increase in level of the kurtosis.

The methods of calculating the statistical parameters described in this section were incorporated in HP Basic programs that were run on the HP216 computer. A sample program is included in Appendix B.

VI. ANALYSIS OF PINION ONE

A. DESCRIPTION OF DAMAGE

Pinion one was utilized to investigate the vibration change resulting from damage to the wear area or face of a tooth. Six different levels of damage, denoted by the letters A thru F, were made to pinion one. The terminology used to describe areas of the gear is shown in Figure 42, from Reference [20].
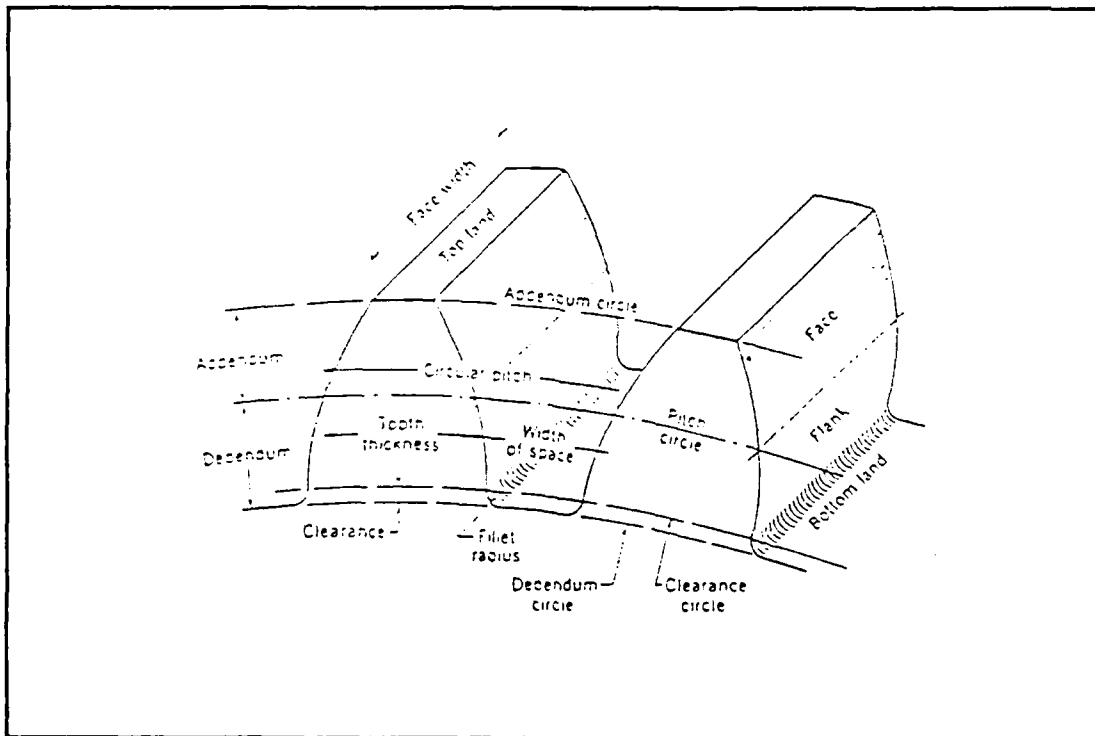

Figure 42. Gear terminology.

1. Damage Level A

For this level, damage was introduced to the pinion by one pass of a file across the tooth face, resulting in light scratch marks on the

tooth. Very little metal was removed from the tooth. Figure 43 illustrates the damage.
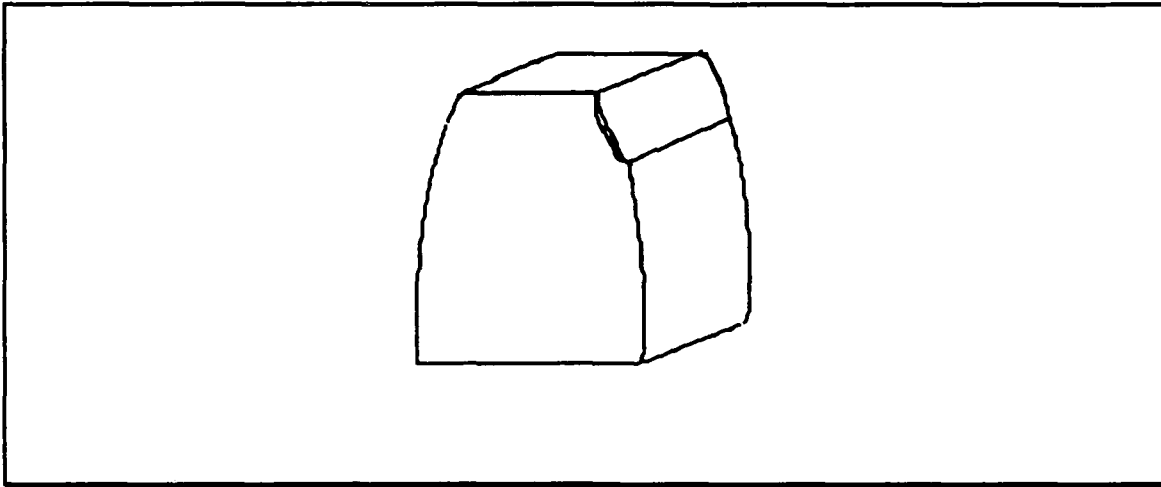
Figure 43. Damage level A.

Little change to the profile of the tooth was apparent from this damage. Upon start-up no difference in the output noise of the model was heard. After completion of the run the tooth was examined and it was noted that the file marks seen on the tooth had been worn away during operation, leaving a flat shiny surface.

2. Damage Level B

Damage applied in this run consisted of filing the tooth in a manner similar to that of damage level A, but additional material was removed from the face. Figure 44 illustrates the damage to the pinion tooth.
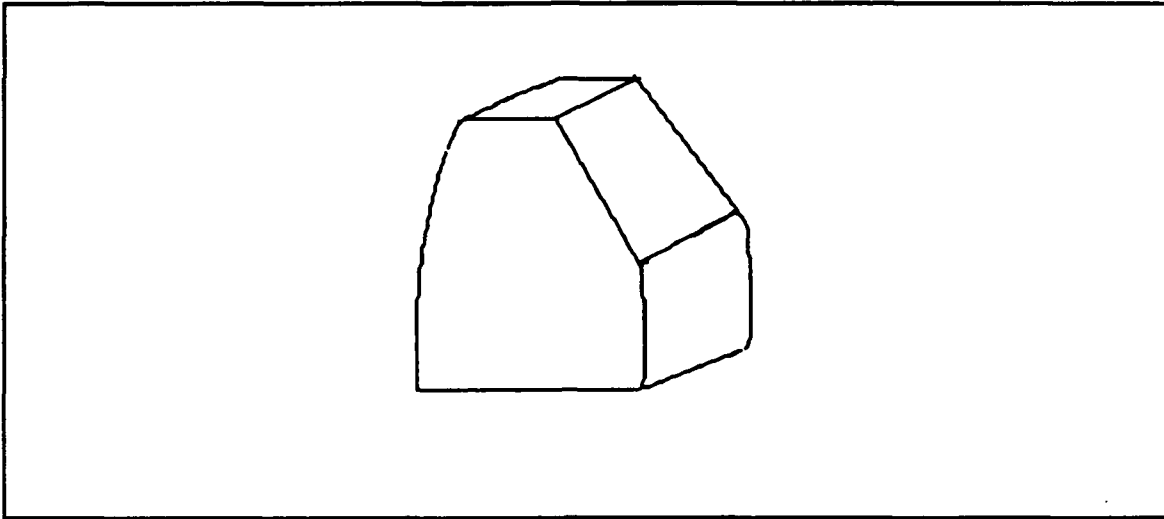
Figure 44. Damage level B.

The material removed resulted in a visual change in the profile of the tooth, so that it no longer had an involute shape. After the gear was installed and the model started, a noticeable rise in the level of audible noise was heard.

3. Damage Level C

Damage level C had a significant amount of material removed from the face of the tooth. The damage is represented in Figure 45.
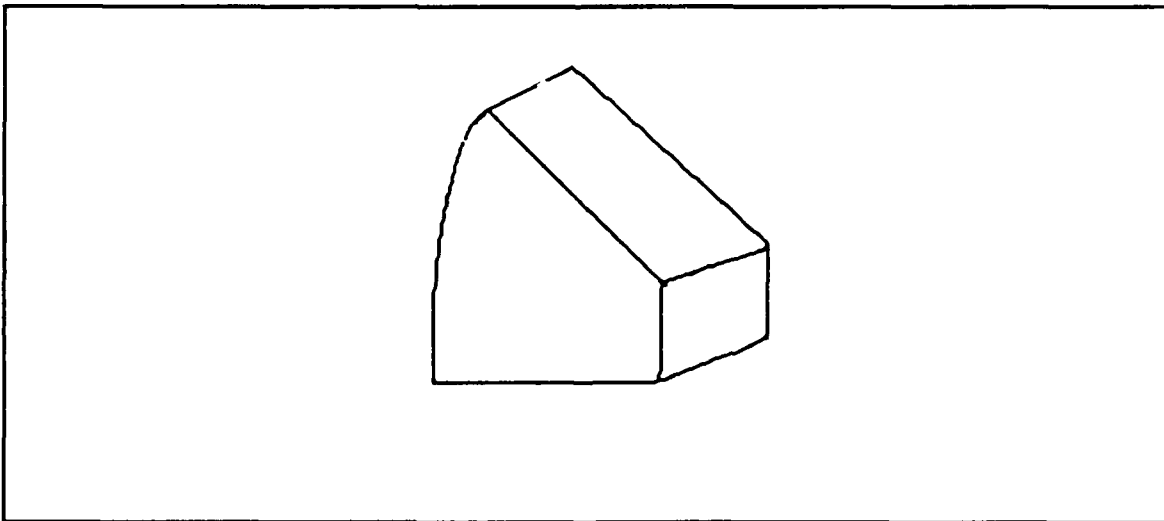

Figure 45. Damage level C.

This damage produced a significant change in the profile of the tooth, the leading edge of the face was completely removed leaving a flat area across the face of the tooth, only the lower portion of the face still held the involute shape. When the diagnostics model was started a higher pitch in the audible noise could be heard.

4. Damage Level D

Damage for this run was made by removing a small amount of material from what was at this point the trailing edge of the tooth. The damage is shown in Figure 46.
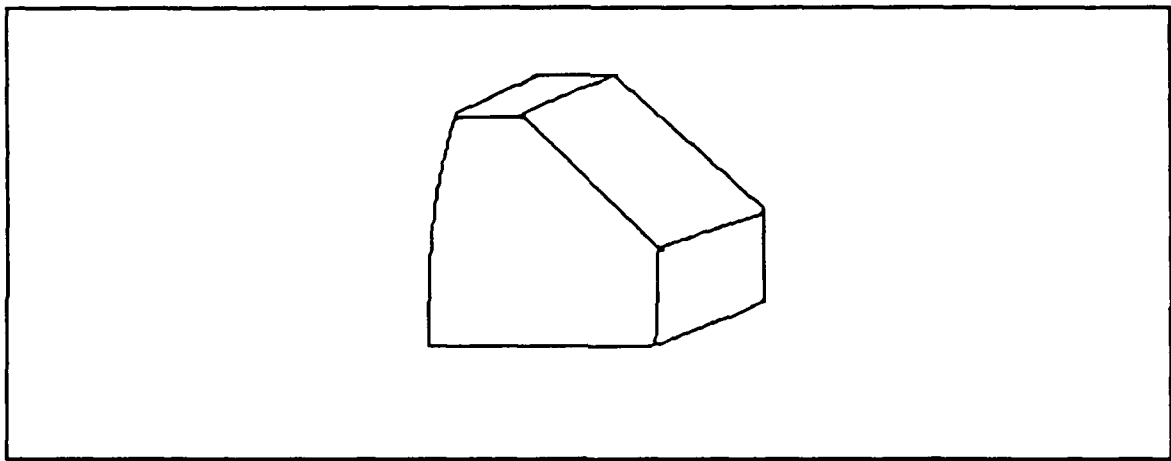

Figure 46. Damage level D.

The damage resulted in a flat area parallel to the original top land area of the tooth. Only a small amount of material was removed and the length, length being a circular arc, of the 'new' top land was no more than a quarter of the original thickness of the top land. After restarting the machinery noticeable clicking was heard, when timed it corresponded to the shaft rotation speed of approximately 30 Hz.

5. Damage Level E

Damage at this level consisted of removing additional material from the face of the damaged tooth. This damage is represented in Figure 47.
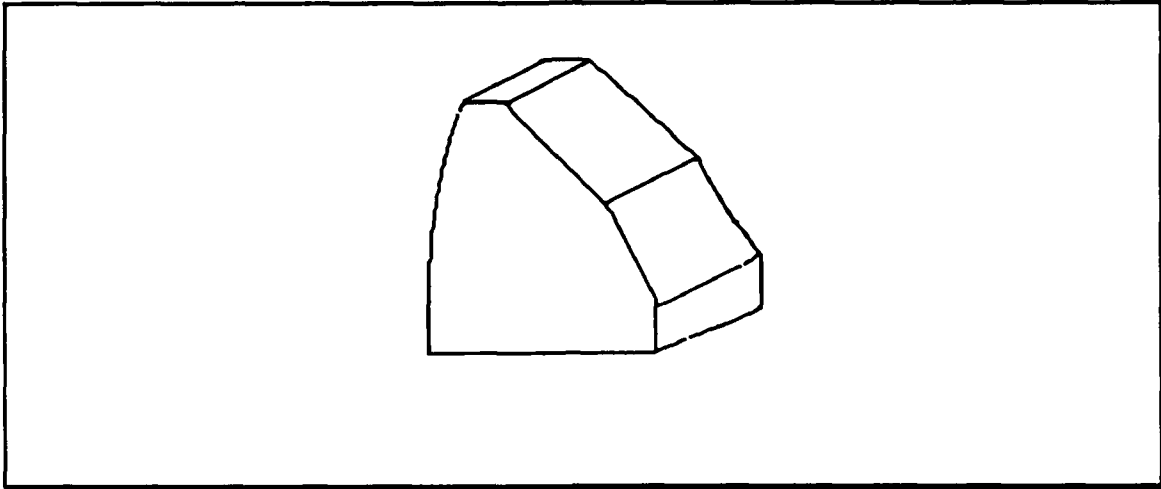

Figure 47. Damage level E.

The file was applied at a slightly different angle from the damage area produced earlier, the new damage resulted in removal of the remaining involute area at the bottom of the wear face of the tooth. The result was that the face area of the tooth was no longer a flat surface, but the intersection of two flat surfaces. At the start of operation, the clicking was louder than heard in damage level D, however, during operation the noise decreased noticeably.

6. Damage Level F

Final damage to the pinion consisted of removal of material from the face of the damaged tooth. Figure 48 depicts the damage.
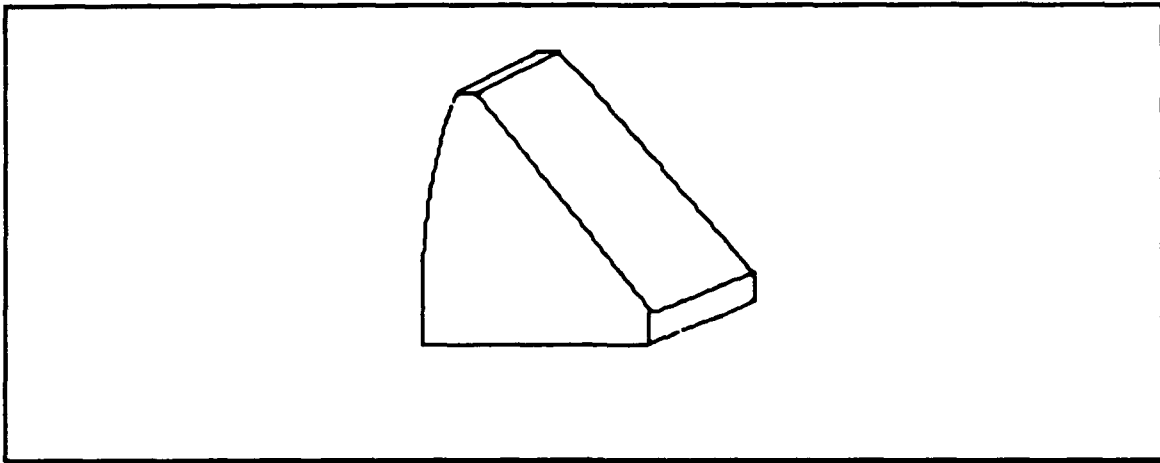
Figure 48. Damage level F.

Filing across the area previously damage, resulted in a reduction of the flat area at the tip of the tooth and establishing a uniform flat area on the face of the tooth. No noticeable change in the audible noise occurred after re-starting the model.

B. FREQUENCY SPECTRA ANALYSIS

During the investigation 25 different frequency spectra were recorded, nine of these spectra covered a frequency range of 0.0 to 10.0 kHz, and the remaining 16 spectra covered a frequency range of 0.0 to 1.0 kHz. Using these frequency spans, analysis of broad band rms level were completed. Additionally, analysis of the several narrow band tonal was performed using the data from the 0.0 to 1.0 kHz measurements. Tonals monitored were the driving shaft frequency (30 Hz), the gear mesh frequency (450 Hz), and the second harmonic of the gear mesh frequency (900 Hz), bin width for the 0.0 to 1.0 kHz measurement was 1.87 Hz.

1. Analysis of 0.0 to 10.0 kHz Broad Band Level

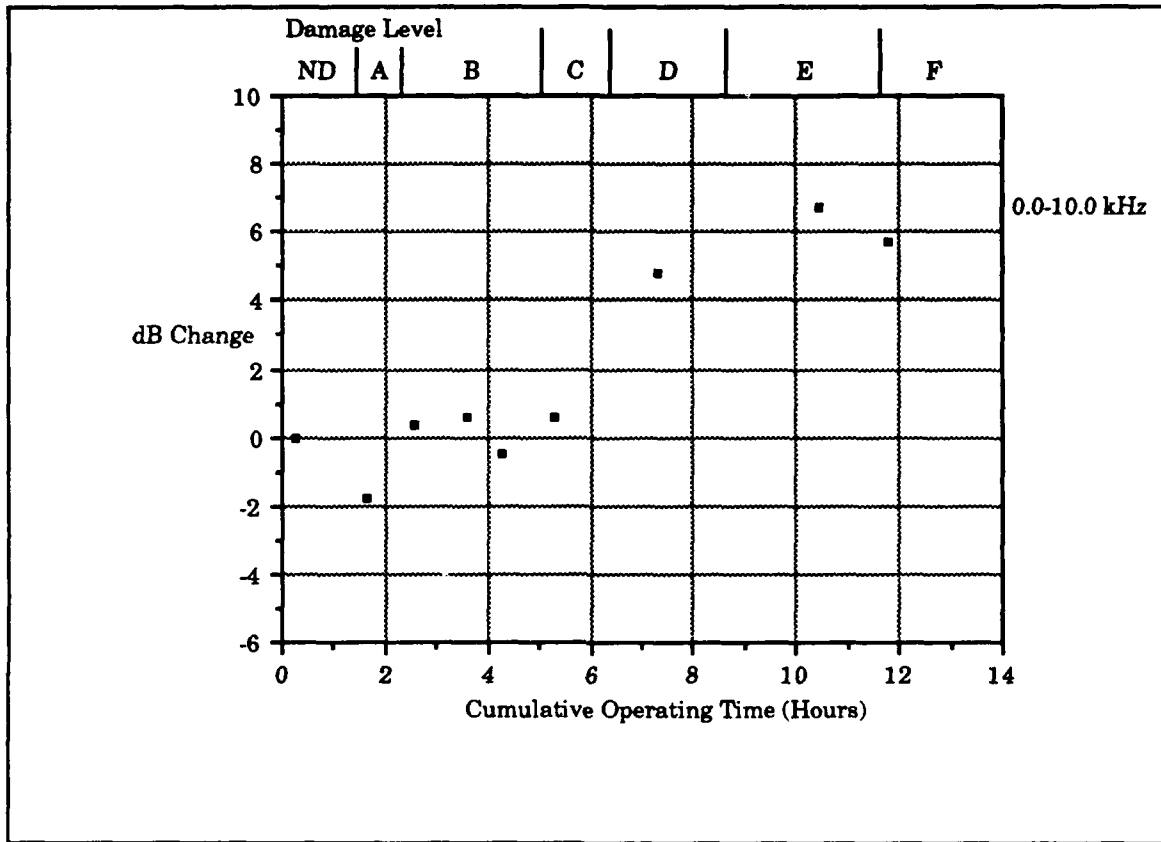The broad band vibration levels from the 0.0 to 10.0 kHz measurements are presented in Figure 49.

Figure 49. 0.0 to 10.0 kHz Broad Band Levels.

The horizontal axis in this graph represents the cumulative operating time of the diagnostics model. Time taken to introduce damage to the pinion and warm-up time for the machinery is not included in this measurement. The vertical axis represents the change in amplitude of the measured data. This method of presenting data will be standard for the remainder of this report.

Figure 49 indicates a steady increase in the broad band vibration level of the diagnostics model, with a slight decrease in level near the

89

conclusion of the run. A 6 dB change in the level of measurements occurs during damage level E. This change is considered detection of a fault. No serious change in level (20 dB rise) is seen in this data.

2. Analysis of 0.0 to 1.0 kHz Broad Band Level

The broad band vibration level from the 0.0 to 1.0 kHz measurements is presented in Figure 50, this graph clearly shows the model experiencing an increase in vibration levels during early stages of the experiment.
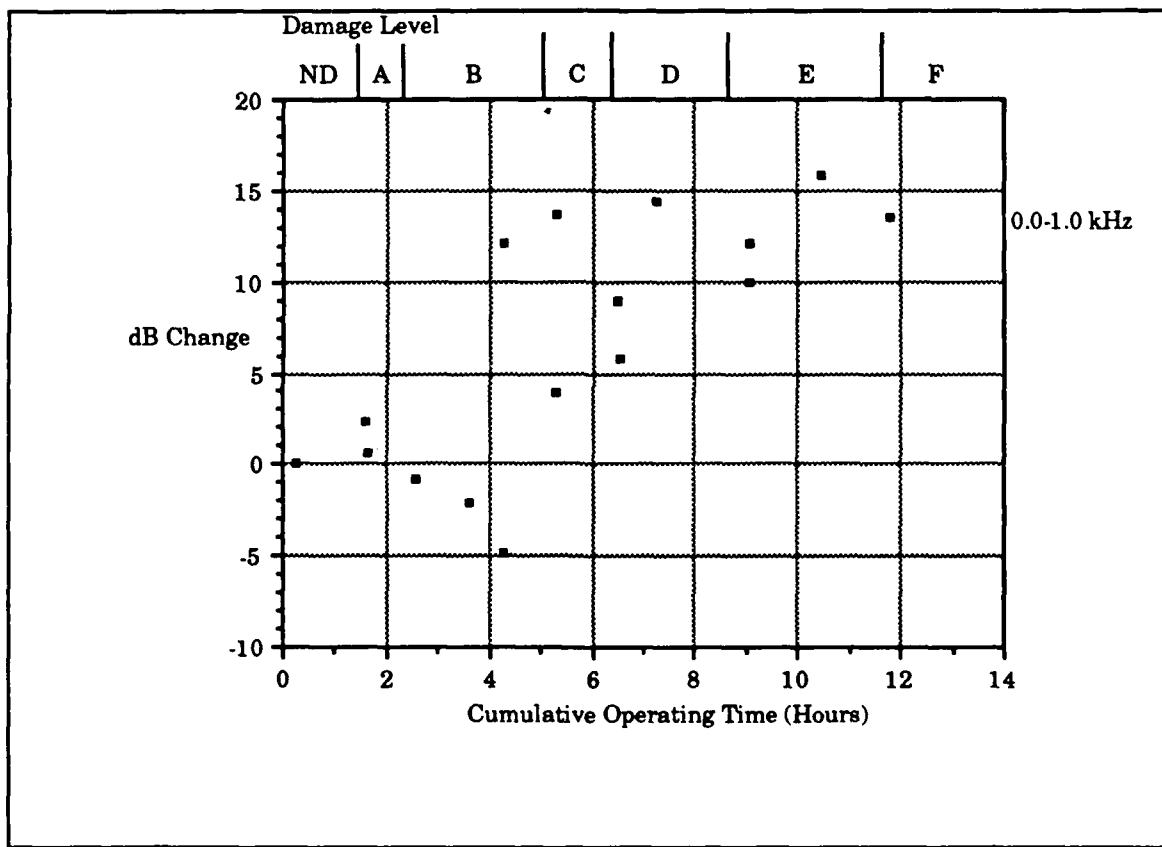

Figure 50. Narrow Band RMS Levels.

During damage level B a 6 dB increase has occurs and is considered as a fault being detected. After this rise the level continues to slowly increase. Another aspect of the graph to note is the 20 dB change

from the lowest measured levels to the highest level measured. Although this is not a serious change in accordance to the definition made in Chapter II , it is probably a cause for concern.

It is interesting to compare the results of this measurement to the results of the broader frequency measurements shown of Figure 49. One of the criticisms, found in the literature, of the use of broad frequency spans is that the method has a tendency to be very slow in responding to damage occurring. This work shows the narrow band measurement of 0.0 to 1.0 kHz reacted to the damage much earlier than the broader frequency measurement of 0.0 to 10.0 kHz. This appears to support the criticism seen in the literature.

3. Analysis of Operating Speed Frequency

The operating speed of the model was maintained at approximately 30 Hz. Using the 0.0 to 1.0 kHz measurement the change in amplitude of this component is shown in Figure 51.
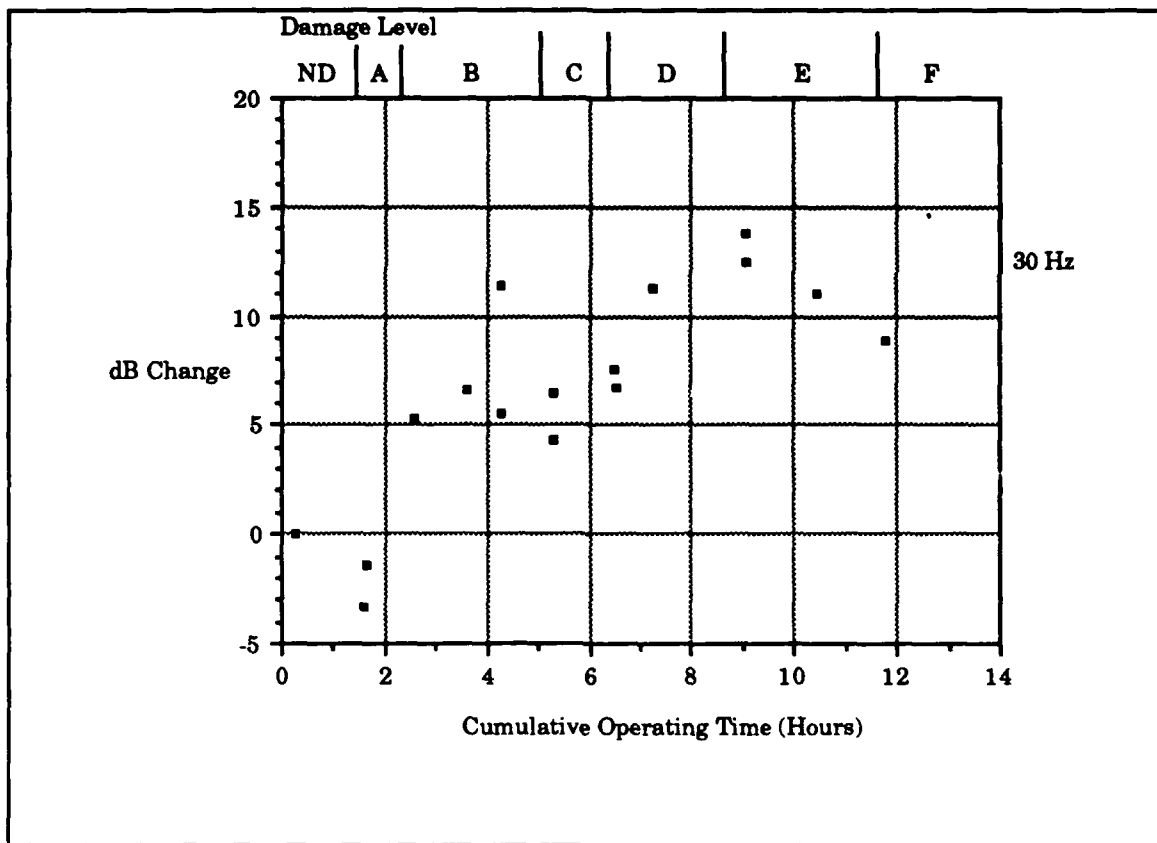
Figure 51. Amplitude of operating speed frequency.

Figure 51 indicates an increase in the amplitude during the experiment, with a slight decrease in level occurring at the end of the run. A 6 dB increase from the baseline measurement occurs fairly early in the test during damage level B, this level indicates a fault detected. The amplitude continues to rise until it has doubled during level E. A 20 dB increase, indication of a serious problem, does not occur.

A decrease in amplitude is near the end of the run, the decrease in level is curious because the pinion had experienced additional damage at the start of damage level F. This decrease in level is probably not due to fluctuations in the individual component, the levels were observed to vary by no more than about ±2.5 dB. During the damage

level E run, it was noted the audible noise produced by the diagnostic model seemed to decrease in level. Additional data was collected and the decrease in amplitude correlates to the decrease in audible noise level.

The 0.0 to 1.0 kHz broad band level, Figure 50, also shows this decrease. After the completion of damage level F, examination of the gear mesh revealed that the damaged tooth made contact only at the base of the tooth. The upper portion of the tooth had been damaged to such an extent it no longer made contact when the shafts were turned by hand. Apparently during operation, the tooth following the damaged tooth took a portion of the load the damaged tooth would normally have carried had it not been damage. The contact ratio of the gears, 1.90, makes this possible. Loss of contact may have occurred during damage level E, this indicates that the damage applied during damag^ level F of little significance.

Another interesting aspect of this graph is the decrease in vibration level that occurred in damage level A, this may be caused by the small amount of material removed from the gear making the gear mesh operate somewhat quieter. This situation appears to have been eliminated during damage level B.

4. Analysis of Gear Mesh Frequencies

a. Gear Mesh Frequency

Figure 52 depicts the changes in amplitude of the gear mesh frequency component, approximately 450 Hz.
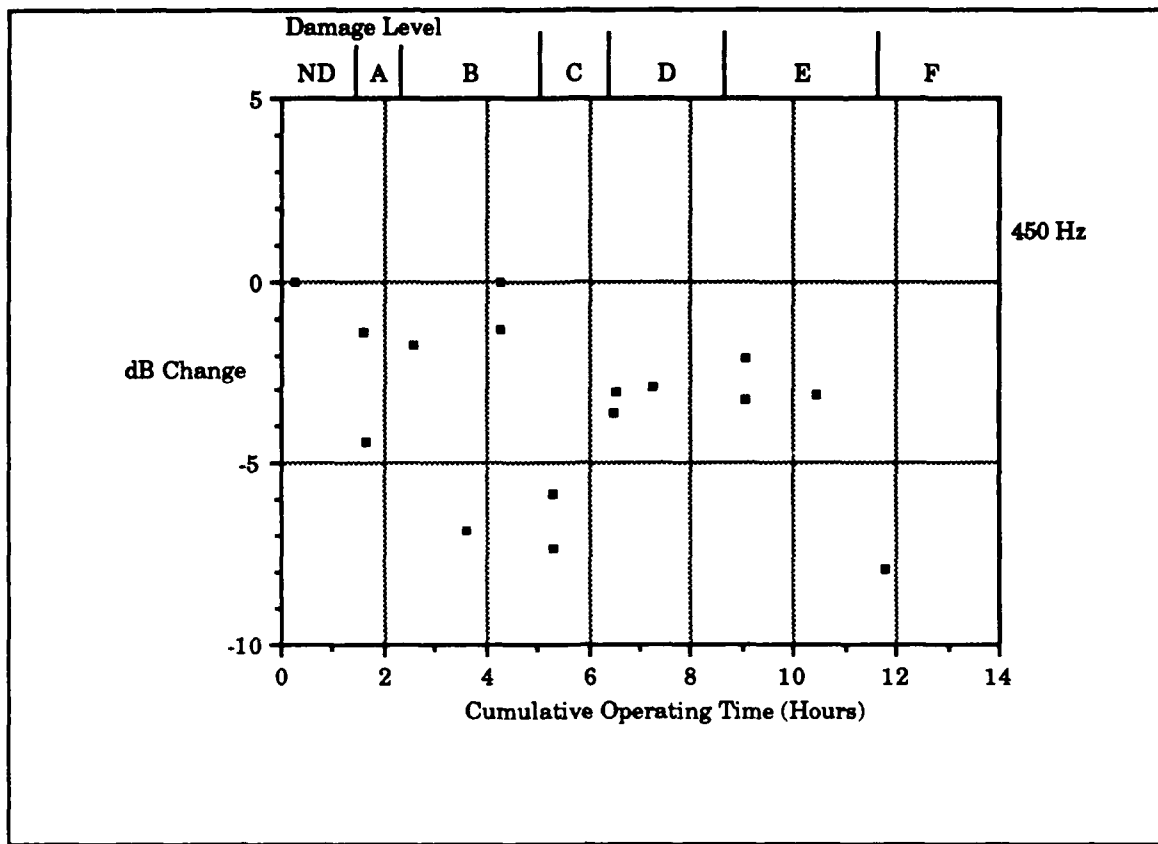
Figure 52. Amplitude of the gear mesh frequency.

The data in this plot indicates little overall change in the amplitude of the gear mesh frequency. The data has much more scatter than seen in the data from the 30 Hz tonal, Figure 51. Since no clear increase was seen no fault detection criteria was met.

b   *Analysis of Second Harmonic of the Gear Mesh Frequency*

Figure 53 depicts the change in amplitude of the second harmonic of the gear mesh frequency at approximately 900 Hz.
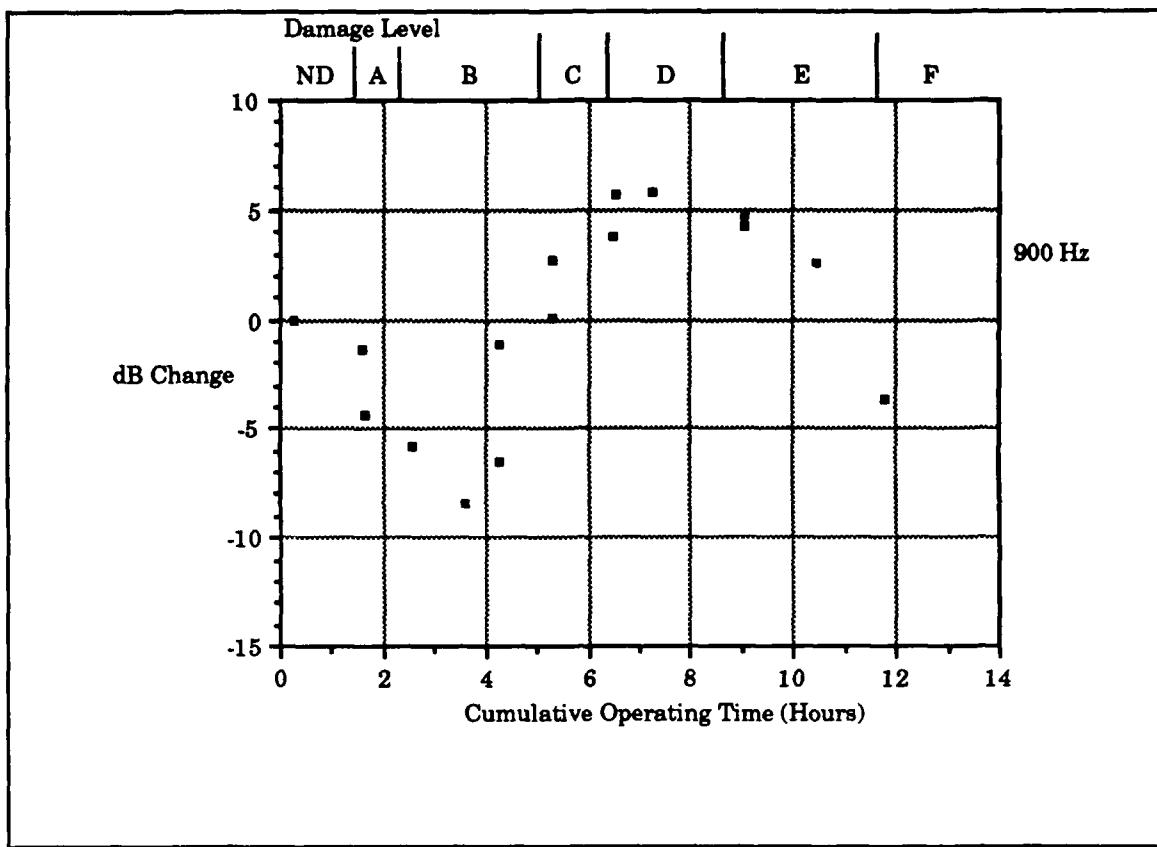
94

Figure 53. Amplitude of second harmonic of the gear mesh.

This plot shows a decrease in amplitude during the early damage levels, followed by a steady increase through the middle part of the experiment, at damage level C the amplitude starts the rise and in damage level D the measured amplitude rises to 6 dB over the baseline measurement. Indicating detection of a fault. Near the end of the run the plot shows a decrease, this corresponds to the decrease in audible noise noted during the operation of the gear. One aspect that stands out is the tightness of the data, contrast this to the data seen in Figure 52, the gear mesh frequency.

5. Conclusions From Spectra Analysis

The use of frequency spectra for fault detection had mixed results. The broad band analysis indicated faults during damage levels D and E. The measured data showed good response as the gear was damaged.

Analysis of individual frequencies showed that the 30 Hz tonal, driven shaft rotation speed, to be very responsive to damage. The response of the shaft rotation speed tonal is probably due to the damage of only one tooth. In "real" machinery the gear mesh components of the spectra would normally be used to monitor for problems.

The gear mesh frequencies were not as responsive, and only the second harmonic of the gear mesh frequency was of use in detection of to the pinion. The second harmonic indicated a fault during damage level D, the general poor response of these components is indicative of the complex nature of the response of gear vibration to damage. The specific gear mesh frequencies were of little use in fault detection, but the sidebands surrounding the mesh frequencies showed so much activity that using then for trending was practically impossible.

C. STATISTICAL PARAMETER ANALYSIS

Figure 55 is a 0.0 to 10.0 kHz frequency spectrum from an undamaged gear, that will be used to establish terminology used in the analysis of the statistical parameters.
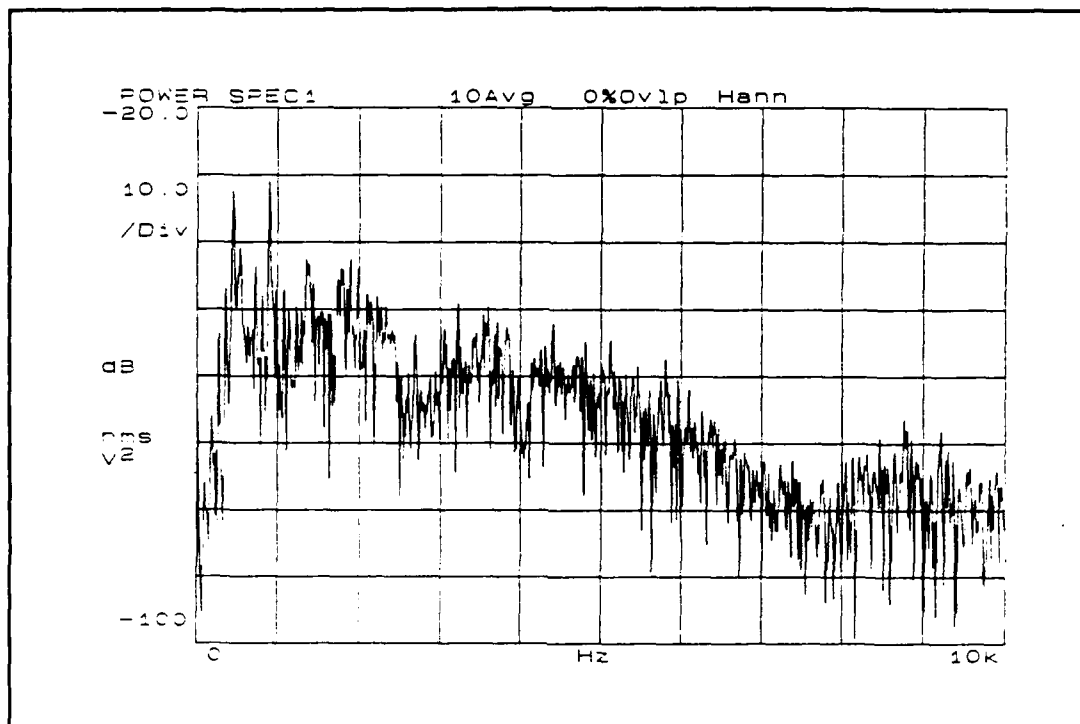
Figure 54. Undamaged gear spectra.

The activity in this spectrum can be broken into two fairly distinct regions. The first region spans a frequency range of approximately 0.0 to 4.0 kHz and contains tonals related to machinery operation, this frequency span will be referred to as a low frequency span. The remaining portion of the monitored range, from 4.0 to 10.0 kHz, will be referred to as high frequency span. Both these terms will be used analysis of the measured statistical parameters.

In defining the scope of this investigation, two goals were set. The first was to investigate the success of detecting faults using statistical parameters in different frequency spans. The second goal was to investigate a gear monitoring scheme based on monitoring the gear mesh frequency, gear mesh harmonics and sidebands surrounding the harmonics.

The statistical parameters of six different frequency spans were examined during the experiment involving pinion one. Spans examined were 0.0 to 10.0 kHz, .270 to 1.53 kHz, 1.62 to 2.88 kHz, 2.97 to 4.23 kHz, 4.32 to 5.58 kHz, and 5 and 10 kHz. The middle four frequency bands were coincide with harmonics of the gear mesh and six sidebands to either side of the harmonics.

For example, the frequency band of .270 to 1.53 kHz includes the gear mesh frequency (450 Hz) minus six sidebands of the operating speed (6x30=180 Hz), resulting in a lower frequency limit of .270 kHz. The upper frequency limit corresponds to the third harmonic (1.35 kHz) plus six sidebands for an upper limit of 1.53 kHz. The frequency span of 1.62 to 2.88 kHz is related to the fourth through sixth gear mesh harmonics, the span 2.97 to 4.23 kHz to harmonics seven through nine, and 4.32 to 5.58 kHz to harmonics ten through twelve. The six frequency spans selected for the investigation cover the measurable frequency span of 0.0 to 10.0 kHz. Figure 55 illustrates .
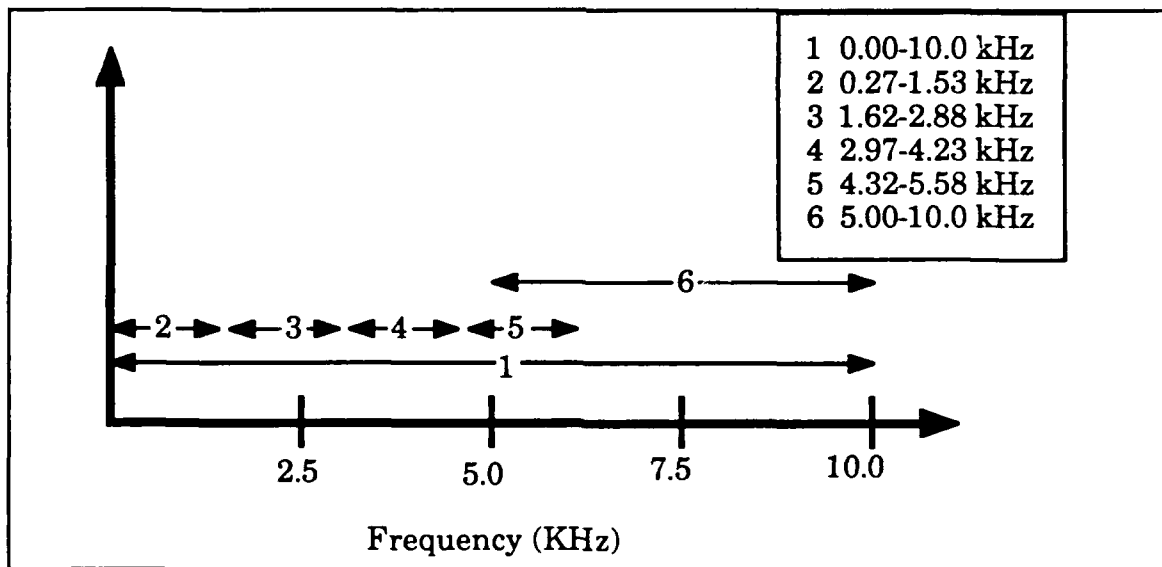

Figure 55. Coverage of frequency span in experiment.

The four "small" frequency spans are the same width and will be useful for comparing the effect of frequency change on the measured parameters. The frequency span 0.0 to 10.0 kHz covers the entire span of interest and the frequency span 5.0 to 10.0 kHz covers the frequencies not covered by the smaller spans.

The data from the two wide frequency spans should not, technically, be used for comparison with the data collected from the four small spans because of the difference in sampling rate. Direct comparisons will be avoided in the analysis, but at times comparisons may be necessary, when this occurs the difference in sampling rates should be kept in mind.

In the literature little information relating changes in the statistical parameters to damage was found. The exception is the mean square levels which can be converted to dB and compared using the earlier fault detection levels. It was desired to keep the levels of all parameters in volts, the 6 dB change is equivalent to a four fold increase using the units of volts squared. As discussed in Chapter V, the kurtosis level for a Gaussian random distribution is 3.0, deviation from this value could be considered as indication of a fault, but this may be to sensitive for monitoring purposes.

The machinery used in the investigation was subject to load changes, speed changes and influence from the operating environment. Experimental procedures attempted to keep the influence from these factors a minimum, but they do occur and introduce error into the measurement process. Without an understanding of the amount of error introduced the analysis of the statistical parameters will be suspect, to quantify the effect of the uncontrollable factors the

99

diagnostics model was operated for approximately eight hours in an undamaged condition, the frequency spans described earlier were monitored and the statistical parameters of the machinery measured. With this data the spread in measured values was established. Table 1 presents the standard deviation seen in the measurements of the undamaged machine. Deviation for the skewness for frequency spans other than 0.0 to 10.0 kHz were not computed, the reason for this is explained later in this chapter.

TABLE 1. STEADY STATE DEVIATION OF PARAMETERS.

Frequency Span	Standard Deviation			
	Mean (v)	Mean Square (v**2)	Skewness	Kurtosis
0.0-10.0 kHz	.0013	.000660	.055	.228
0.27-1.53 kHz	.0010	.000085	------	.072
1.62-2.88 kHz	.0009	.000082	------	.077
2.97-4.23 kHz	.0010	.000047	------	.062
4.32-5.58 kHz	.0008	.000037	------	.082
5.00-10.0 kHz	.0006	.000046	------	.390

Since guidance on fault detection levels is not available from the literature, the data in Table 1 is useful in determining when a change in measured parameters is significant. For fault detection purposes the level for the mean square value will remain a four fold change from the baseline measurement, for the other parameters a change in level by four standard deviations will be considered significant and indicative of a fault detection. For example the standard deviation for the skewness of the 0.0 to 10.0 kHz frequency span is .055, four times this level is .220, (4 x .055), so a change of .220 from the baseline level will be considered a fault detected.

1. Analysis of the Mean

In the analysis of the mean value several plots show the mean value as a negative value, discussions will focus on the change of magnitude when this occurs.

a. *Frequency Span 0 .0 to 10 0 kHz.*

Figure 56 illustrates the mean values measured over the frequency span of 0.0 to 10.0 kHz. This plot shows a steady increase in magnitude as damage to the pinion occurs.
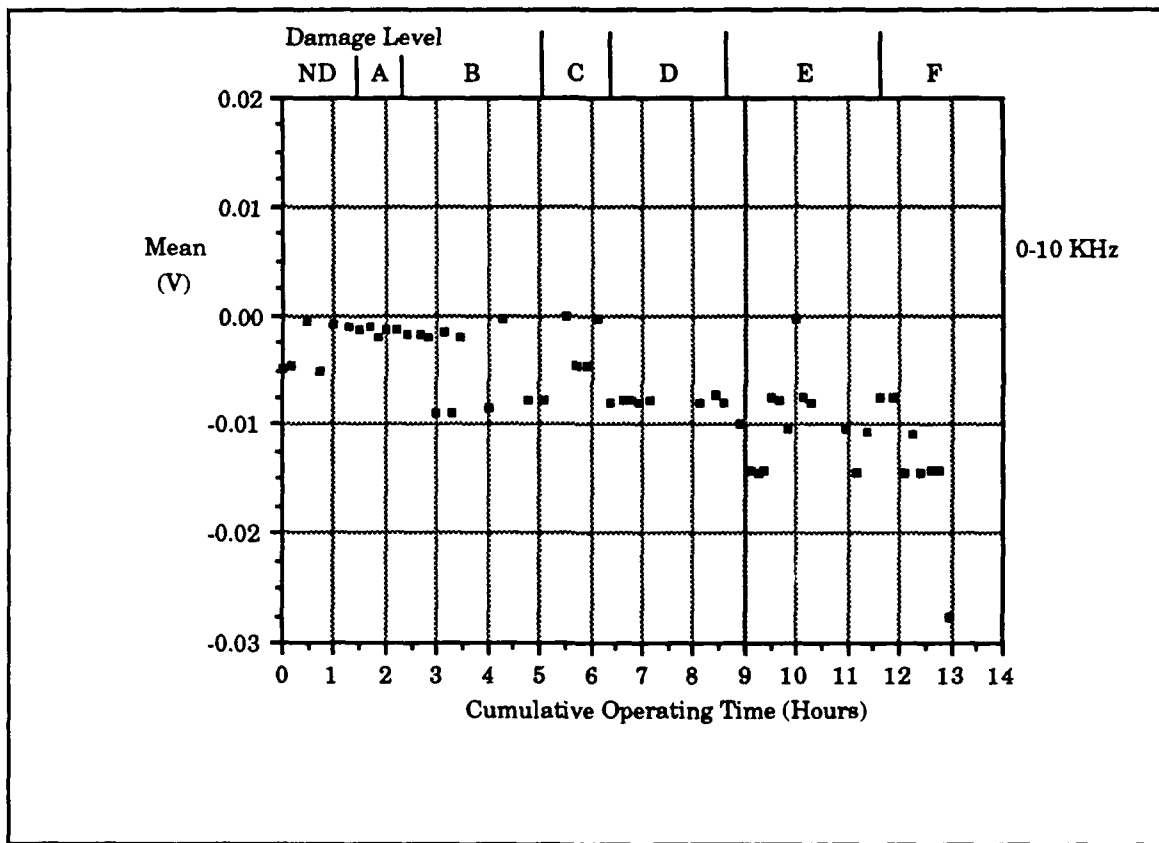

Figure 56. Mean Value of 0.0 to 10.0 kHz frequency span.

At the start of the experiment the data is fairly stable near 0.000V. Using the data from Table 1 fault detection would occur at .±0.005V. The baseline level is maintained through damage level A. In

101

damage level B the data becomes less steady, shifting between the baseline level and a level near -0.009, and although the fault detection criteria is met the magnitude does not remain above -0.005V until damage level D, at which a steady value near -0.01 V occurs. It is interesting to note that this level is very near the extreme level recorded during damage level B. The data maintains this level, although much more scattered, until the final series measurements where it again appears to increase in magnitude.

b   Frequency Span of .27 to 1.53 kHz

Figure 57 illustrates the data measured in the frequency span 0.27-1.53 kHz. This data includes the first three harmonics of the gear mesh frequency.
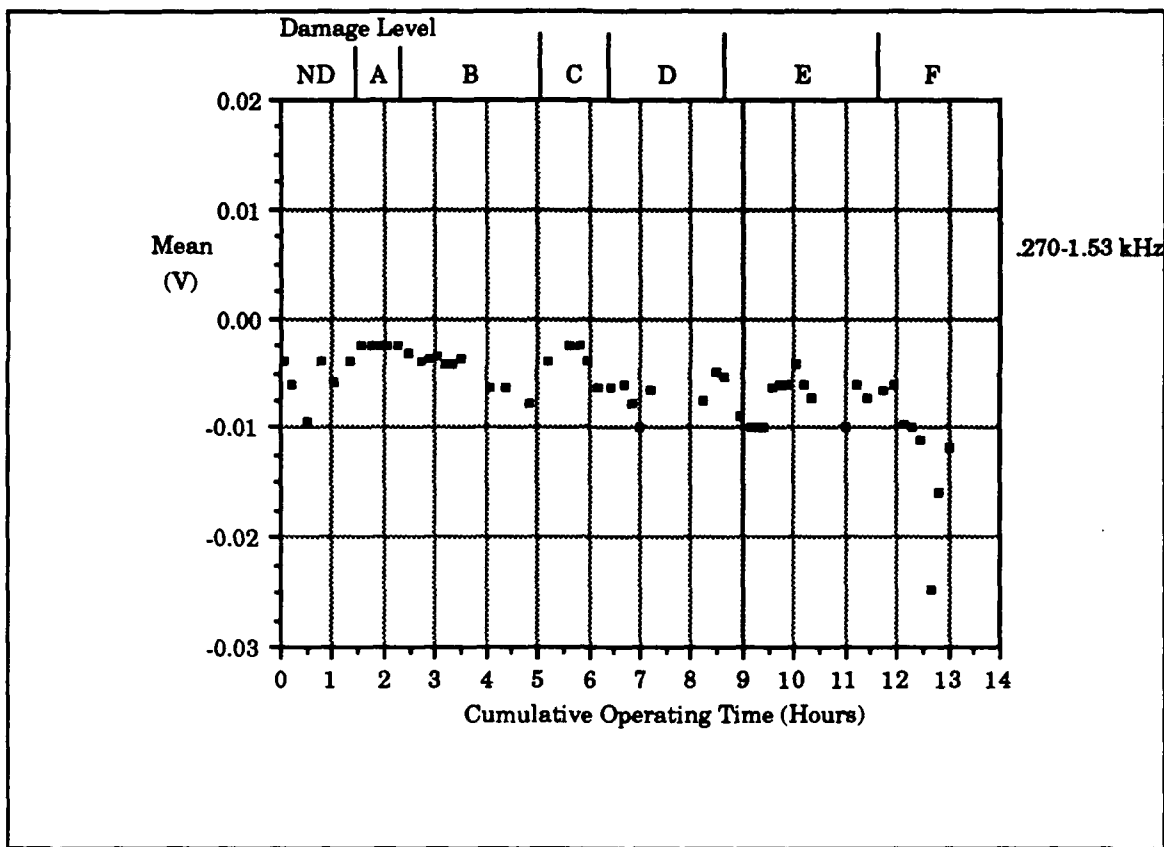
Figure 57. Mean of .27 to 1.53 kHz frequency span.

This data is very flat with a gradual increase in magnitude as damage is made to the pinion. The baseline level for this set of data is near -0.005 V, fault detection would occur at -0.001V or -0.009V. This level does not occur until damage level F.

c. *Frequency Span of 1.62 to 2.88 kHz*

The data included in this measurement includes the fourth through sixth harmonics of the gear mesh frequency. Figure 58 presents the results of the measured data from this frequency range.
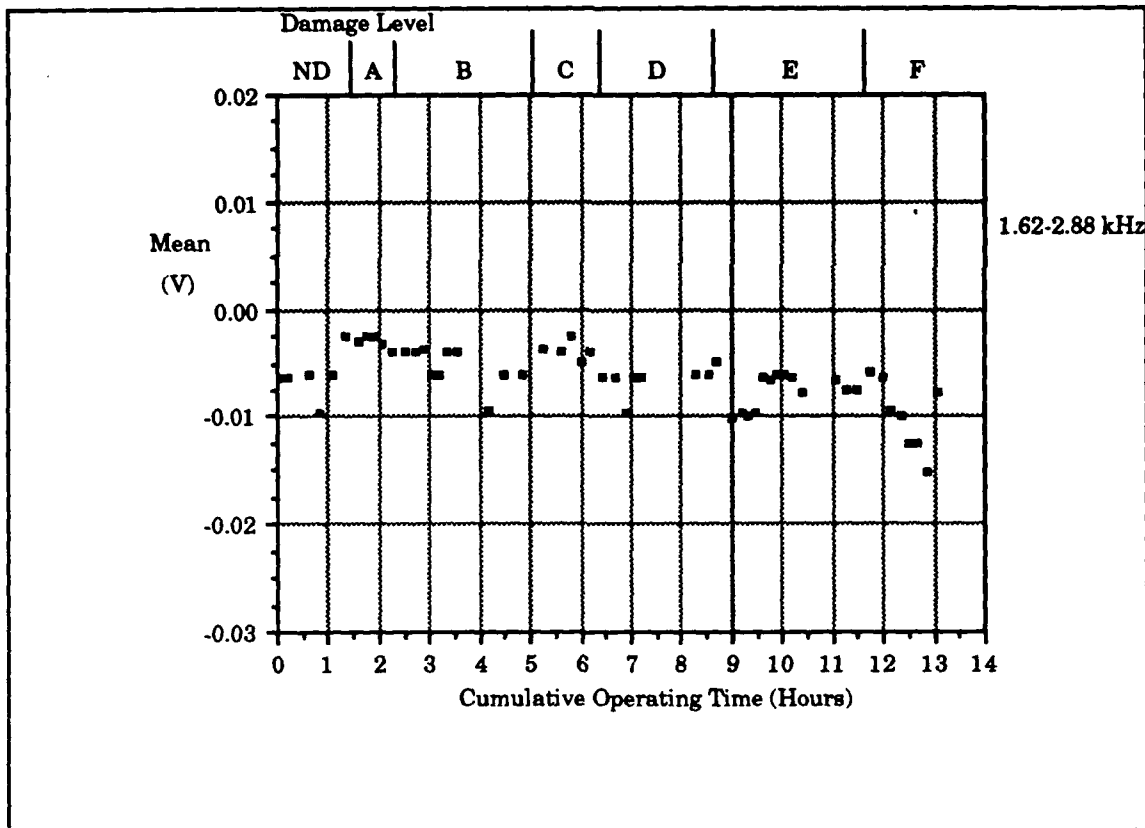
Figure 58. Mean of 1.62 to 2.88 kHz frequency span.

This data has the same trend seen in the Figure 57, the range of the data is fairly flat with a steady increase towards the end of the run. Baseline level is near -0.005V placing fault detection at a level near -0.001V or -0.009V. Fault detection occurs during damage level F, and although a rapid change in level occurs during damage level A, it is not steady and eventually decreases to a level near the baseline level.

d Frequency Span of 2.97-4.23 kHz

The data measured in this frequency band is shown in Figure 59. This span includes the gear mesh harmonics seven through nine.
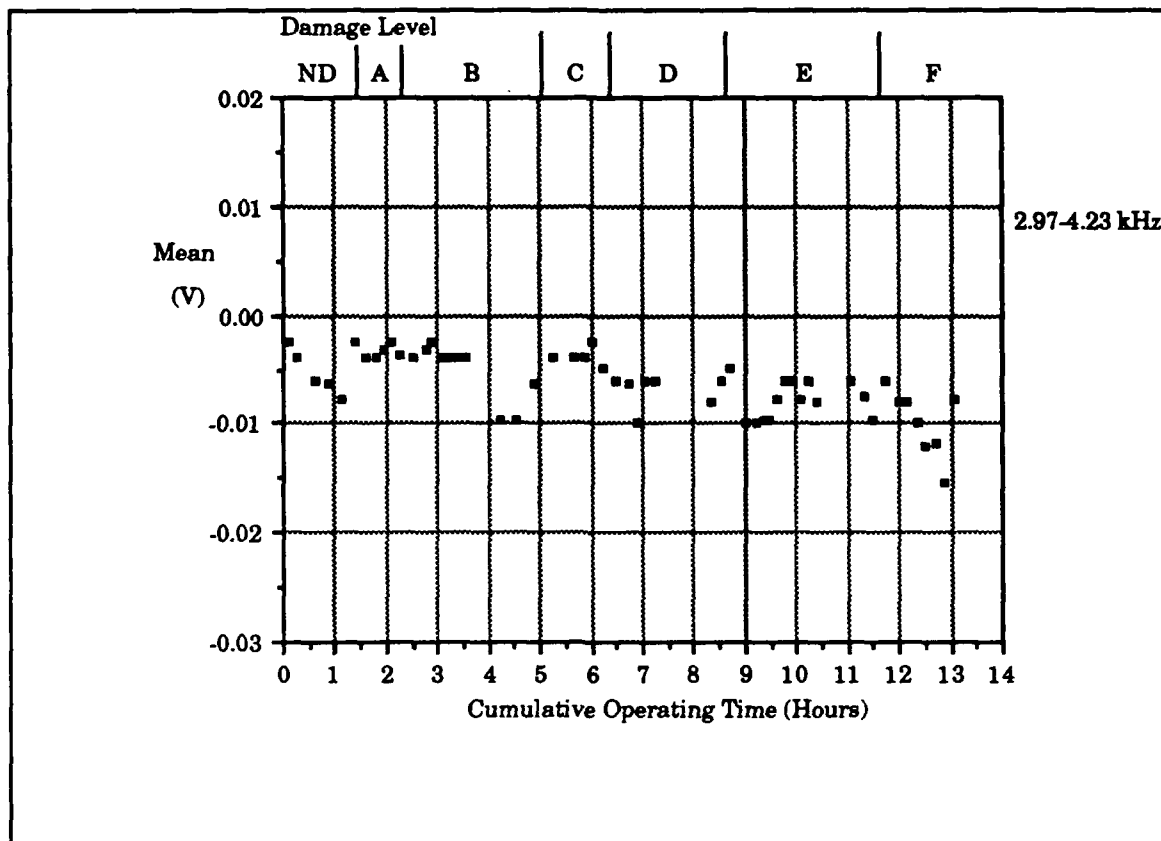
104

Figure 59. Mean of 2.97 to 4.23 kHz frequency span.

This data has much the same appearance as seen in the previous two frequency spans, except that at times the recorded data has an oscillatory appearance. This results in several measurements are significantly different from the baseline level, but the a fault is not detected until late in the run during damage level F. In damage level F the data rapidly increases in magnitude similar to the plots examined previously to a level where a fault is considered detected.

e. Frequency Span of 4.32-5.58 kHz

This data measured for this frequency span is shown in Figure 60. The frequency span used in this measurement includes harmonics of the gear mesh frequency nine through twelve.
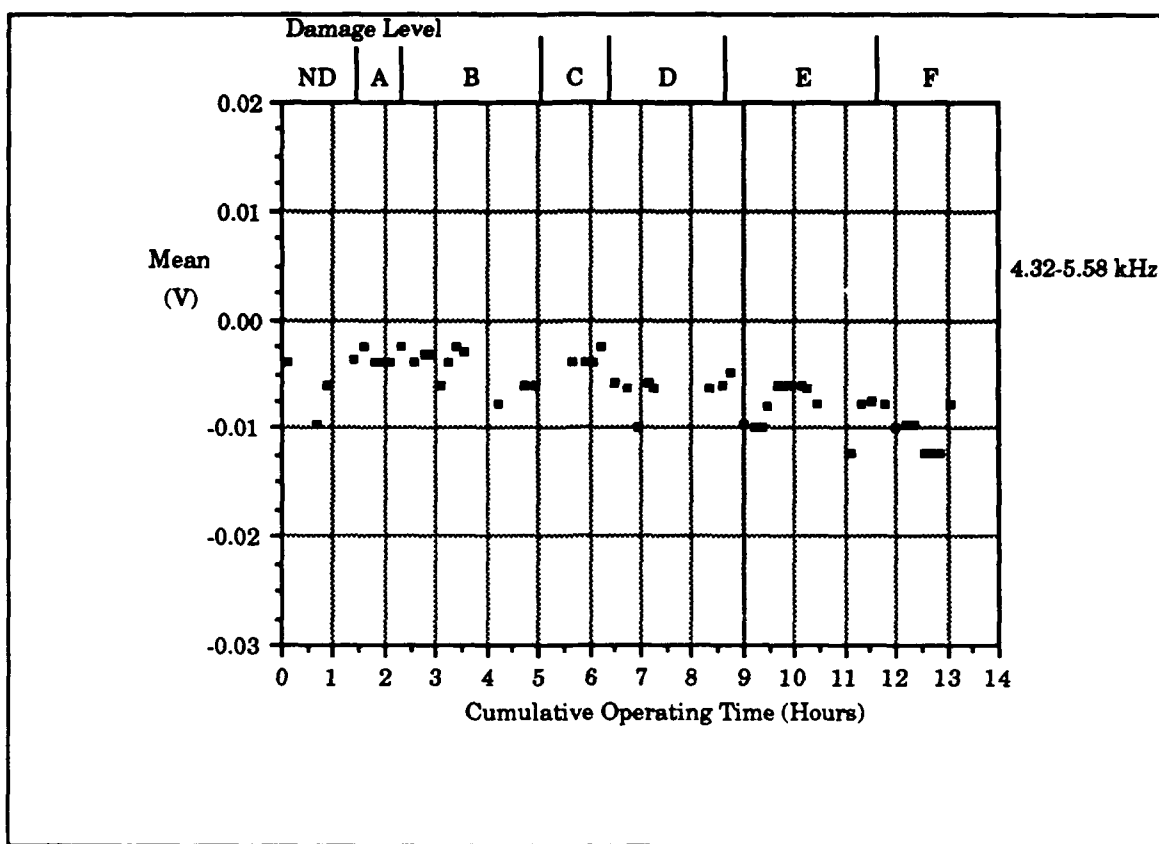
105

Figure 60. Mean of 4.32 to 5.58 kHz frequency span.

The graph shows an increase in magnitude much like that seen in the 2.97 to 4.23 kHz data, Figure 59. The smooth rise in magnitude and the scatter in the data does not allow detection of a fault to be made until late in the experiment.

f   Frequency Span of 5.0 to 10.0 kHz

The data measured in this measurement is illustrated in Figure 61. This range of frequencies, for the most part includes the frequency span outside those used in the previous frequencies.
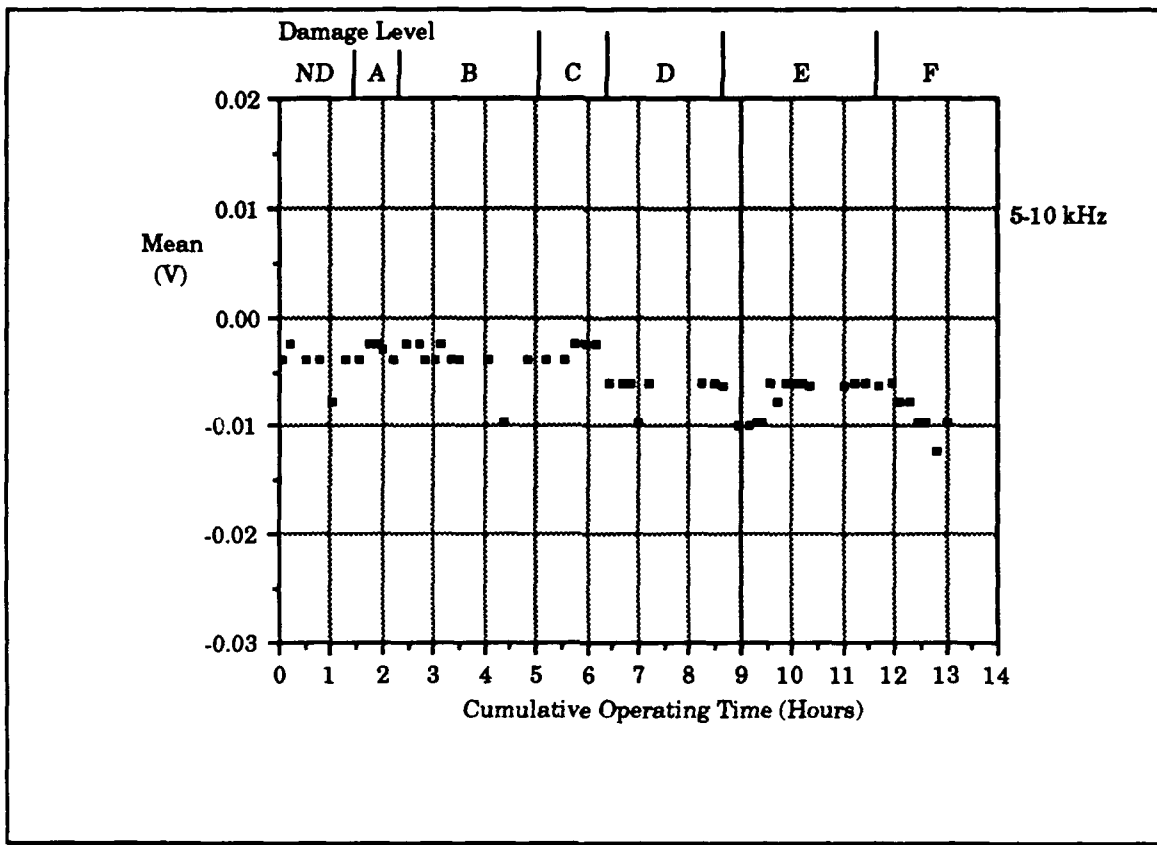
106

Figure 61. Mean of 5.0 to 10.0 kHz frequency span.

This graph is very interesting. It clearly shows two distinct levels of mean values. One level runs from the undamaged region through damage level C. After damage level C the mean grows slightly in magnitude and remains fairly steady until the final measurements.

Although the change in level is distinct, the magnitude of the change is fairly small and detection of a fault is not able to be made until the trend in the data can be recognized. This cannot be done until late in the experiment.

Several other aspects of this graph are noteworthy. The first is the stability of the data. The data has little of the scatter seen in the earlier plots. Another interesting characteristic of this graph is seen in

107

the data measured in during the level E run. At the start of this level, the <u>magnitude</u> of the mean value starts off at a high level, as the run continues this magnitude decreases to the "steady" level. During damage level E a decrease in the audible level of the gear noise was heard, this decrease in level appears to be reflected in this data. Inspection of the previous graphs reveals this phenomena in several of the other graphs of the mean value, but not as pronounced.

g. Conclusions From the Analysis of the Mean

The mean values calculated from the vibration signal were not responsive to early stages of damage. The earliest a fault was detected was damage level D using the 0.0 to 10.0 kHz frequency span. Results from other frequency spans indicated faults during the late stages of the experiment. These frequency spans had data which showed quite a bit of scatter making fault detection difficult. The small magnitude of the data was expected, being typical for the parameter measured.

2. Analysis of Mean Square Value

As discussed in Chapter V there is very little difference between the results of the mean square value and variance calculations, as such only the mean square value will be examined. Detection of a fault will be indicated from an increase of four times the baseline measurement.

a. Analysis of 0.0 to 10.0 kHz Mean Square Value

Figure 62 shows the mean square value recorded for the frequency span of 0.0 to 10.0 kHz. This broad band measurement shows an increase in level after damage level A.
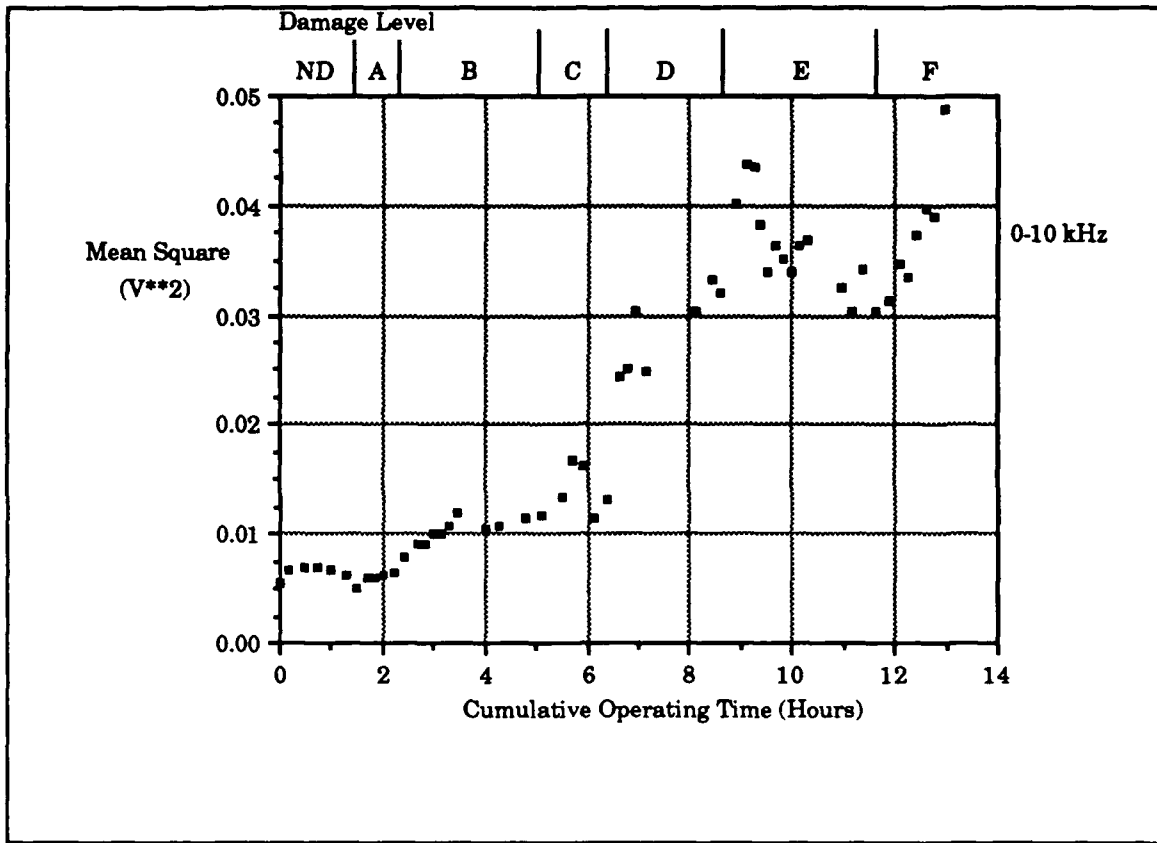
Figure 62. Mean square value for 0.0 to 10.0 kHz frequency span.

The mean square value in the early stages of this run is steady, showing only a small change in level through damage level A. In damage level B a rapid increase in level is seen, but the mean square value appears to have stabilized near the end of this damage level. In damage level C the measured values become less stable, and continues to rise through damage level D. An increase four times the baseline levels occurs in damage level D indicating fault detection. In damage level E an interesting response occurs. At the beginning of this damage level the mean square value has increased dramatically, but as operation continues the level drops to a fairly stable level. This same phenomena appears in damage level F, but the run is stopped before the

109

value has stabilized. Using the data from Table 1, it can be seen that this change in level is probably not due to normal operation.

This plot can be compared to the results of the broad band level plotted in Figure 49. The two plots are very similar in appearance, with fault detection occurring at same time in the experiment. The number of data points measured in the statistical approach makes analysis of the damage much simpler, but the measurements made in the spectral analysis portion of the experiment produced an accurate portrayal of the changes occurring to the machine.

b Analysis of 0.27 to 1.53 kHz Mean Square Value

Figure 63 presents the mean square value calculated from the 0.27 to 1.53 kHz frequency span. This span includes the first thru third harmonics of the gear mesh frequency. This data, although measured over a different span width, has a very similar appearance to the 0.0 to 10.0 kHz measurements, with the exception of a smaller amplitude, also similar is the appearance of the large change in amplitude during damage levels E and F. Fault detection occurs during damage level D.
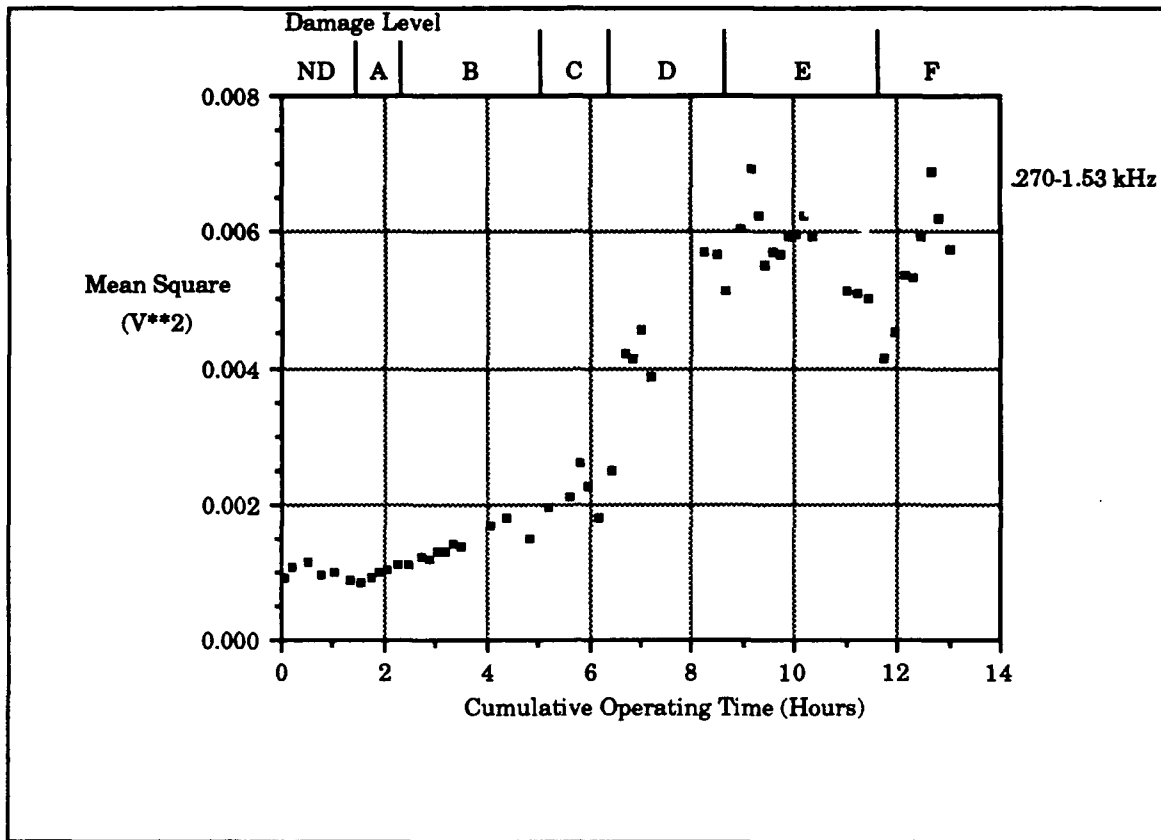
Figure 63. Mean square value for 0.27 to 1.53 kHz frequency span.

One aspect of this plot which is different from the previous measurement is the linear nature of the data in damage level A through C. This data is very indicative of an increasing damage. This characteristic of the data may be related to the greater sensitivity of the rms level at lower frequencies that was discussed when analyzing the the frequency spectra made for this experiment.

c. *Analysis of 1.62 to 2.88 kHz Mean Square Value*

The frequency span of 1.62 to 2.88 kHz is related to the fourth thru sixth harmonics of the gear mesh frequency. Figure 64 illustrates the data recorded for this span. The overall pattern of the data is very similar to that seen in the frequency span of 0.27 to 1.53

111

kHz, Figure 63. In this plot detection of a fault occurs during damage level D.
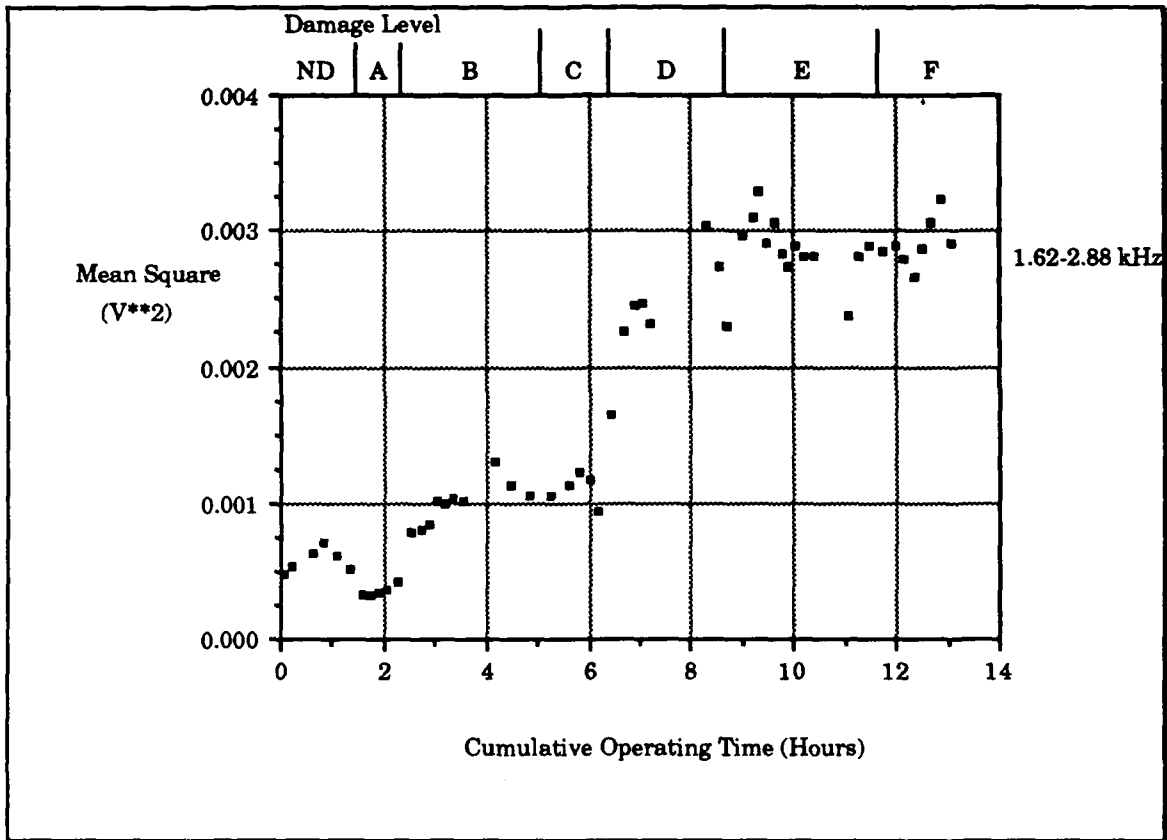

Figure 64. Mean square value for 1.62 to 2.88 kHz frequency span.

Besides the magnitude of the measurements, two significant differences are seen between this plot and Figure 63, first the trend of the data in the early part of Figure 64 is much less linear than the data seen of Figure 63. The data in damage levels A and B is fairly linear but the response seen in damage level C is rather flat after an initial rise. The second difference in the two plots is the much less distinctive nature of the spikes in damage levels E and F in the plot of Figure 64. The rise and fall of the data is still seen, but the relative change in amplitudes is much less than that seen in the lower frequency measurements.

112

d   Analysis of 2.97 to 4.23 kHz Mean Square Value

Figure 65 presents the results of the mean square value measured over the frequency span 2.97 to 4.23 kHz. This frequency span is related to the seventh thru ninth harmonics of the gear mesh frequency.
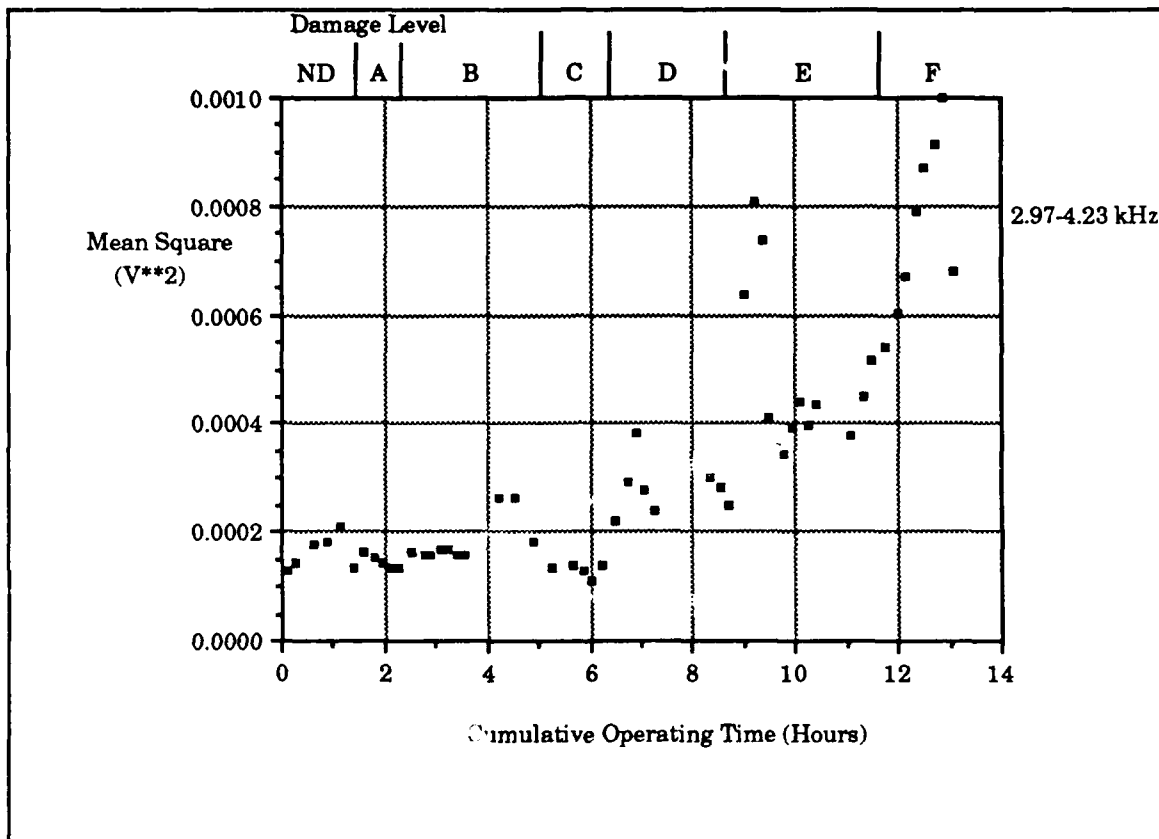

Figure 65. Mean square value for 2.97 to 4.23 kHz frequency span.

In the early damage levels of this data a significant change from the patterns of Figures 63 and 64 can be seen. the increase in amplitude is much flatter, and fault detection does not occur until damage level E. The spikes in damage level E and F are very prominent in this trace, and the relative level of these spikes is much larger that that seen in the earlier measurements.

e. Analysis of 4.32 to 5.58 kHz Mean Square Value

The mean square value measurement over the frequency span 4.32 to 5.58 kHz frequency span is presented in Figure 66. The data shows a pattern very similar to that seen in the frequency span of 2.97 to 4.23 kHz (Figure 65).
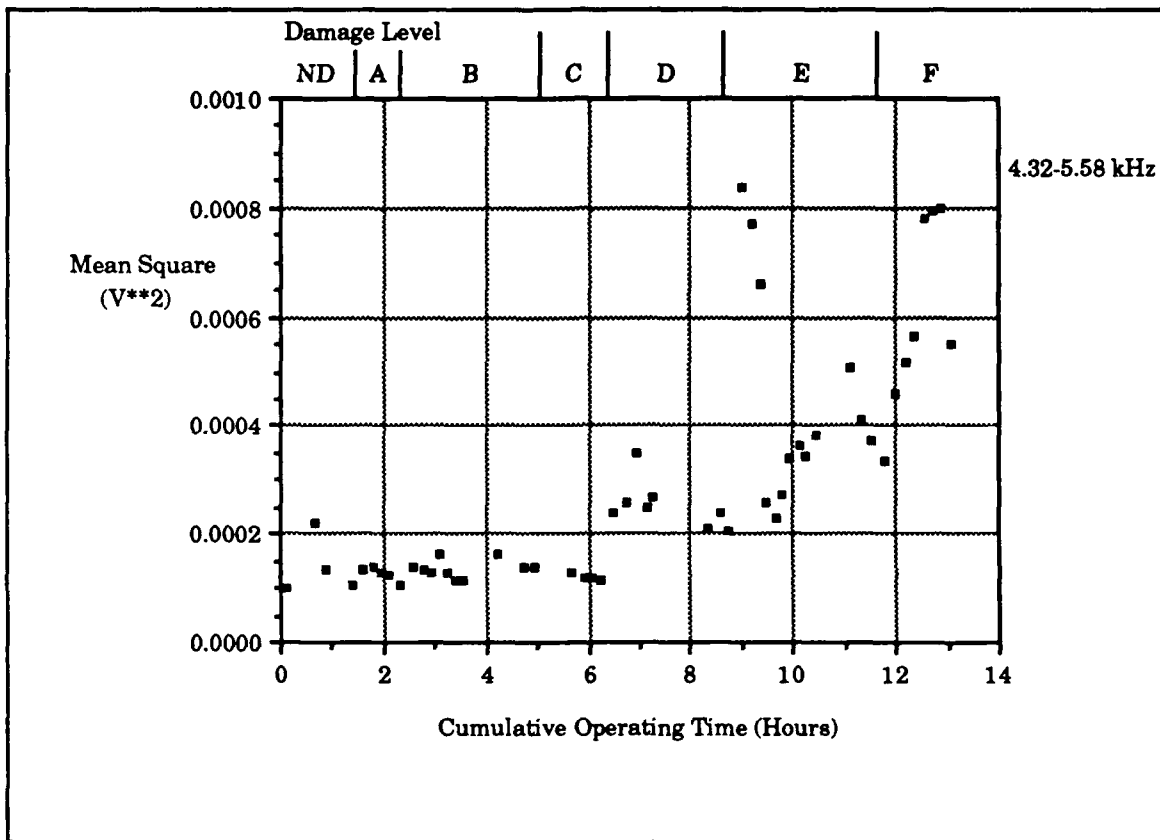

Figure 66. Mean square value for 4.32 to 5.58 kHz frequency span.

Like the previous frequency span fault detection occurs during damage level E, and the prominence of the spikes in levels E and F can be seen. The "flattening" of the data continues, in the 0.27 to 1.53 kHz data (Figure 63) a linear aspect of the data was noted. In the data of the 4.32 to 5.58 kHz span (Figure 66) the data measured in the early portion of the run is practically horizontal.

114

f. Analysis of 5.0 to 10.0 kHz Mean Square Value

The data measured for the frequency span 5.0 to 10.0 kHz is presented in Figure 67. This figure shows a very flat appearance as was noted in the previous series of data.
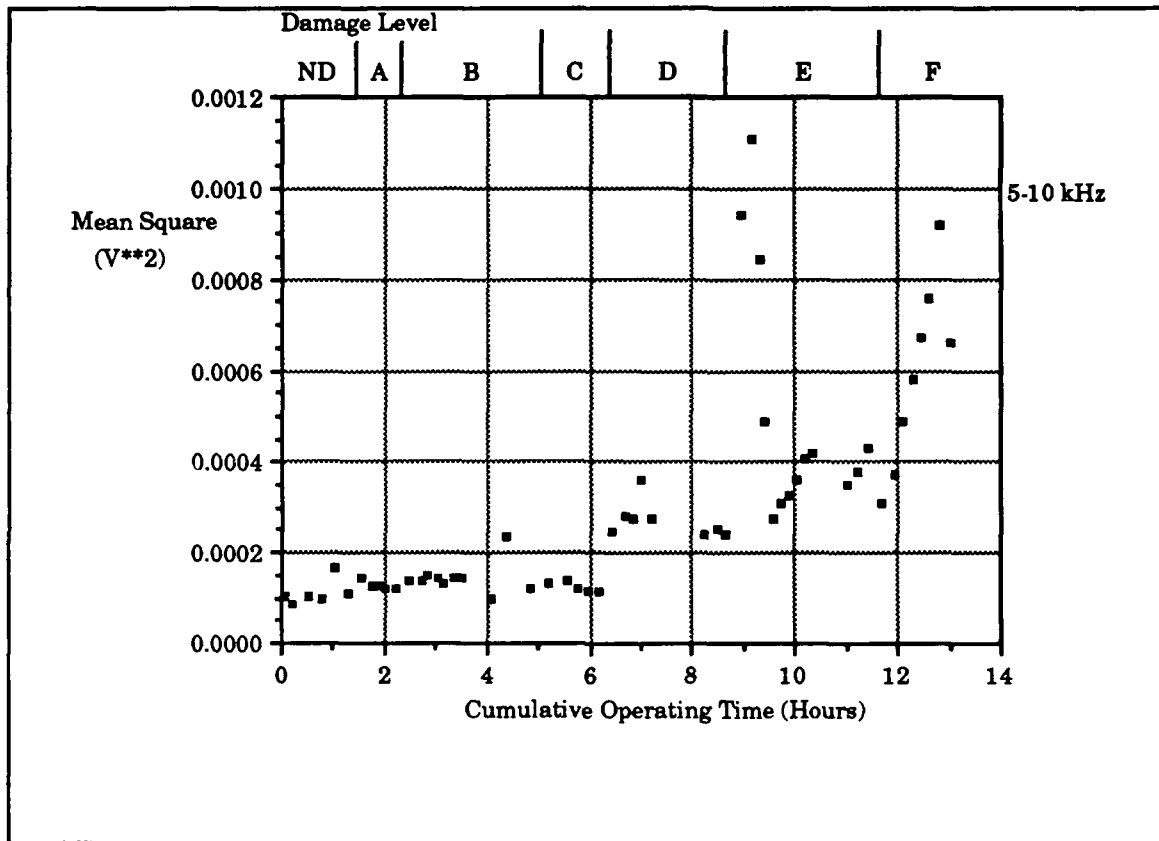

Figure 67. Mean square value for 5.0 to 10.0 kHz frequency span.

Fault detection parameters are satisfied during damage level E. Just as was seen in previous data sets, the prominent spikes can be seen in damage levels E and F. The prominence of these features is highlighted by the flattening of the measured data. This aspect is very noticeable in this frequency range.

115

g. Conclusions to Analysis of Mean Square Value

Fault detection using the mean square value was a level four times the baseline measurement. The mean square value of the different frequency spans measured for pinion one had fault detection occurring during damage level D or E.

Distinctive changes in the mean square value could be seen across the range of frequency spans, but in general the lower frequency measurements reacted to damage applied to the pinion early in the investigation. Also seen in the measurements of the mean square value was distinctive spikes in damage levels E and F. These spikes appear to occur after damage was applied and then decrease in magnitude as operation of the gears occurred. The decrease in level may be attributed to the wear process occurring in the gear mesh reducing the effect of the damage.

The response of the mean square value to the pinion damage made in this part of the investigation appeared to be related to the frequency span of the monitored data. Figure 68 illustrates the trend observed for this series of measurements.
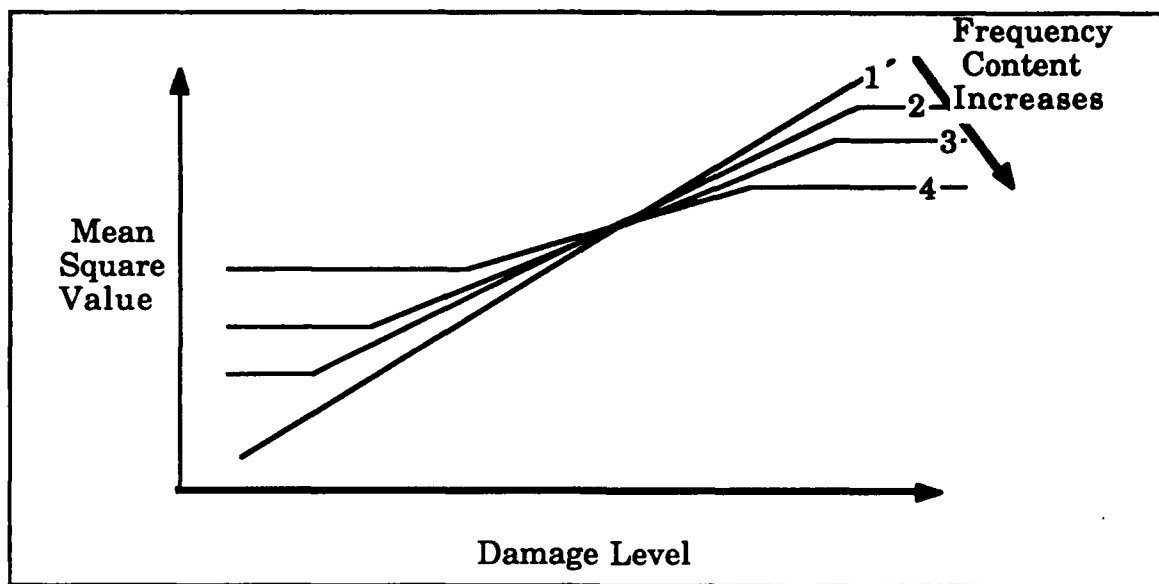
Figure 68. Trend of mean square value with frequency span.

The figure shows an ideal version of the data in damage levels A through D. In measurements with low frequencies monitored the response has characteristics similar to that depicted in the figure as line 1. As the frequency content of the monitored span increases the resulting data pattern become flatter, this is shown in lines 2 thru 5.

This phenomena can be explained by examining the broad band frequency spectra of the pinion. Figure 69 shows an undamaged and damaged measurement from pinion one. The damaged trace was made during damage level F.
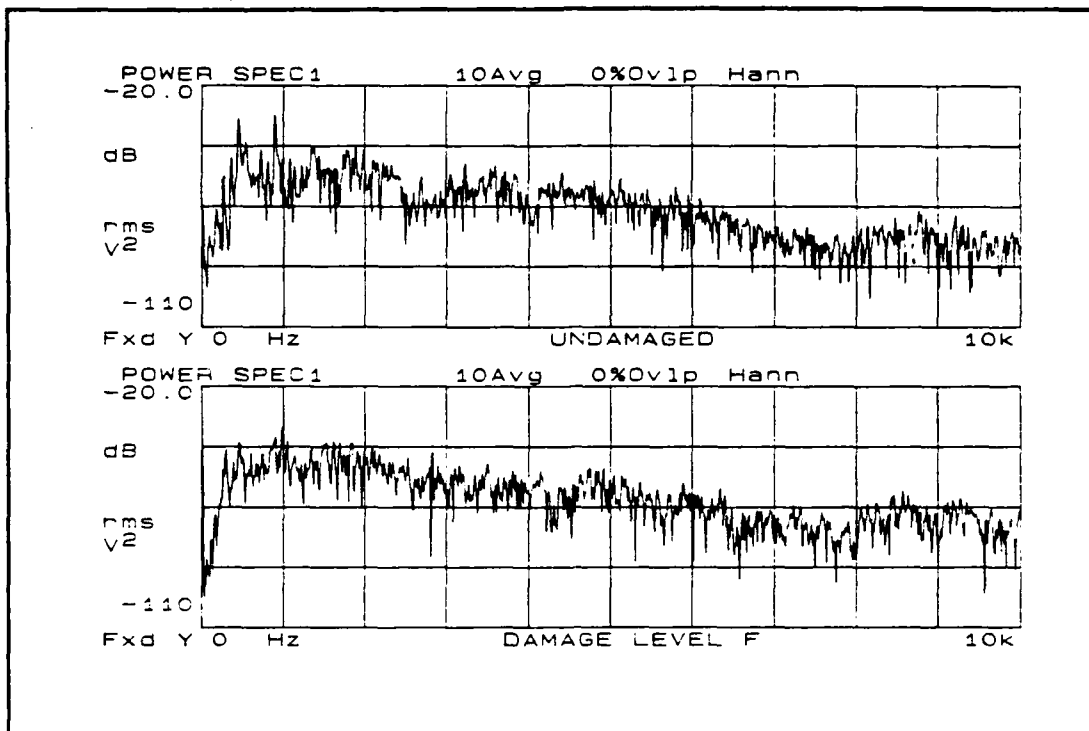
Figure 69. Comparison of frequency spectrums.

Comparing these traces in the frequencies below 3.0 kHz shows that more change has occurred than has in the higher frequencies. The higher frequency do increase, but the measured mean square values would produce data that changes much slower when compared to the level that would be measured from the lower frequencies.

3. Analysis of Skewness

The use of the coefficient of skewness for fault detection was ineffective for all but one of the frequency spans monitored, in the ineffective spans the skewness was very random with no clear pattern. The lone exception was the frequency span of 0.0 to 10.0 kHz. This is shown in Figure 70.
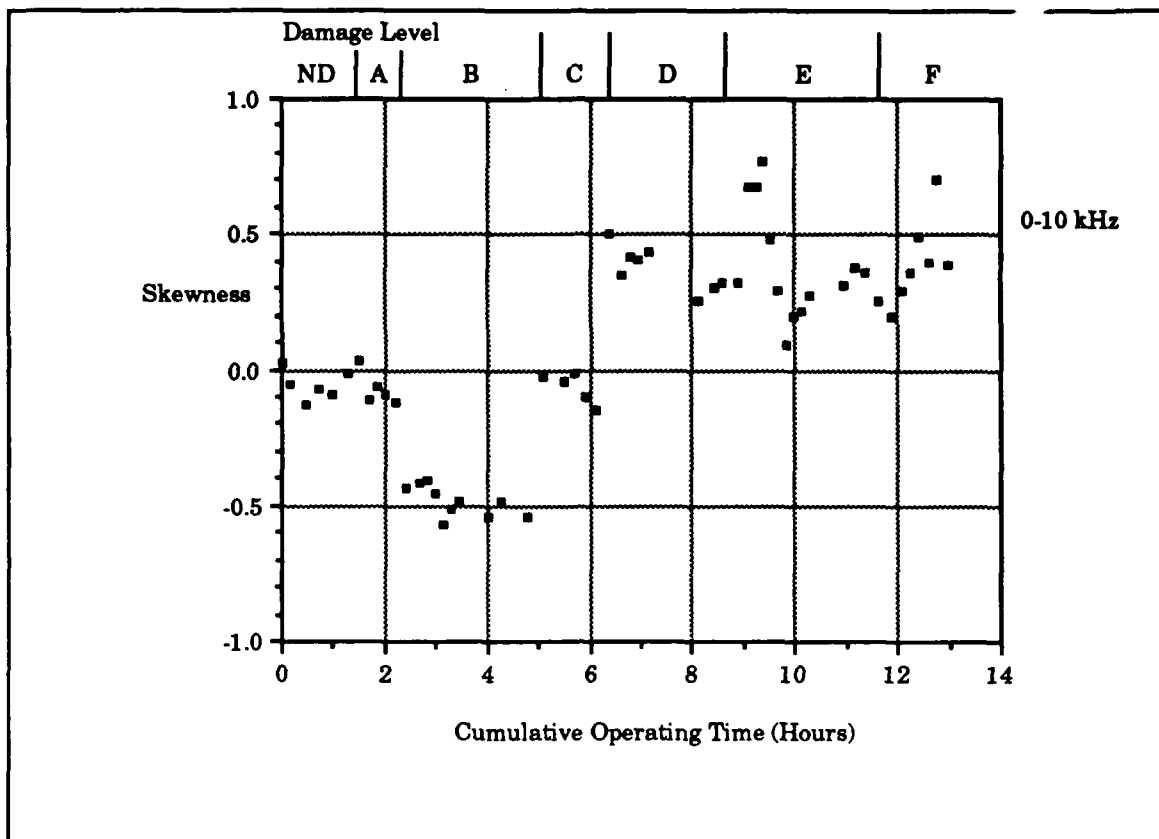
118

Figure 70. Skewness for 0.0 to 10.0 kHz frequency span.

This figure shows the skewness changing as damage was made to the gear, the reason for this change is not clear. With a baseline level at approximately -0.1, fault detection would occur at 0.12 or -0.32. This level is clearly reached during damage level B, the skewness returns to a level near the baseline during damage level C, but suddenly changes magnitude after damage level D. This large positive magnitude is maintained, though with much scatter, through the remaining experiment.

The responsiveness of the skewness parameter was not expected, and the changes in the level appear to be related to the damage made to the tooth. Damage made during damage levels A and

119

B were similar in nature in the sense that the same area of the tooth was damaged, little damage was made to the tooth during damage level A and very little change in the skewness value was seen. When damage level B was made the skewness became very negative with a obvious change in magnitude. In damage level C a large amount of material was removed from the tooth in a manner different from damage levels A and B. The response of the skewness shifted rapidly back to a level near the baseline level. Damage level D resulted in a clicking sound being produced by the gears that was heard for the remainder of the experiment, and the level shifted to a very positive level where it remained for the remainder of the experiment.

Figure 71 thru 75 present the data measured over the remaining frequency spans investigated for this pinion.
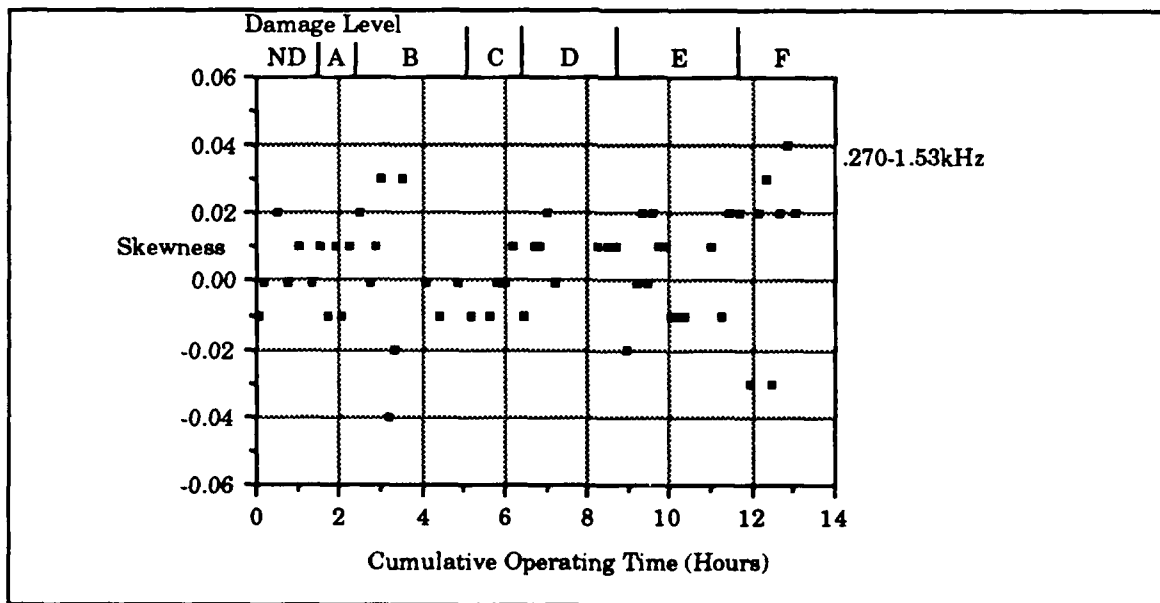

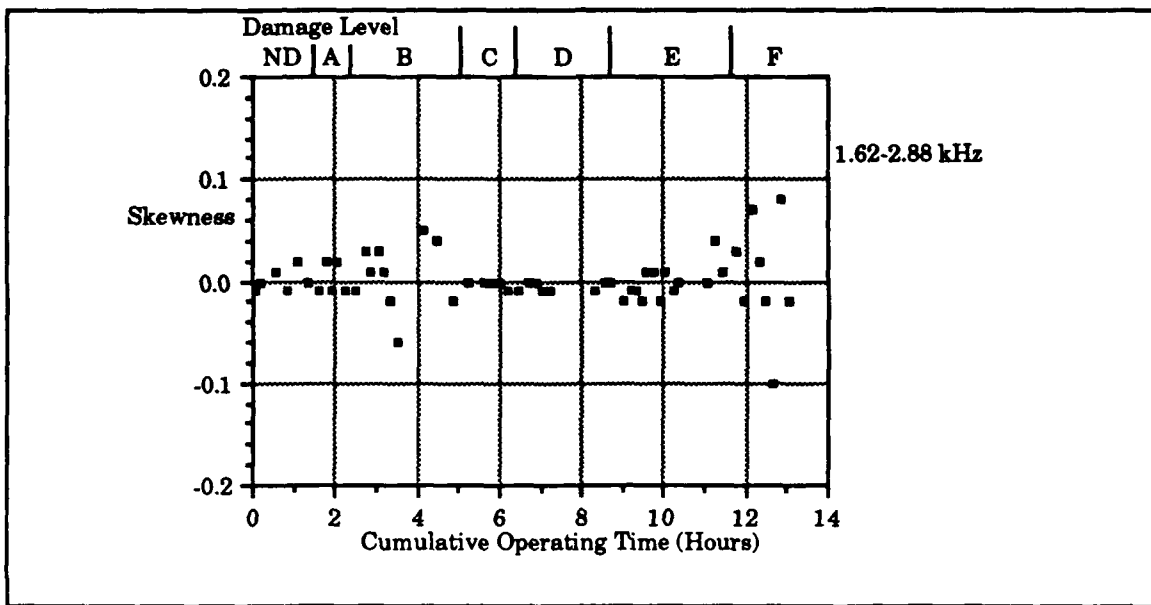Figure 71. Skewness for 0.27 to 1.53 kHz frequency span.

Figure 72. Skewness for 1.62 to 2.88 kHz frequency span.
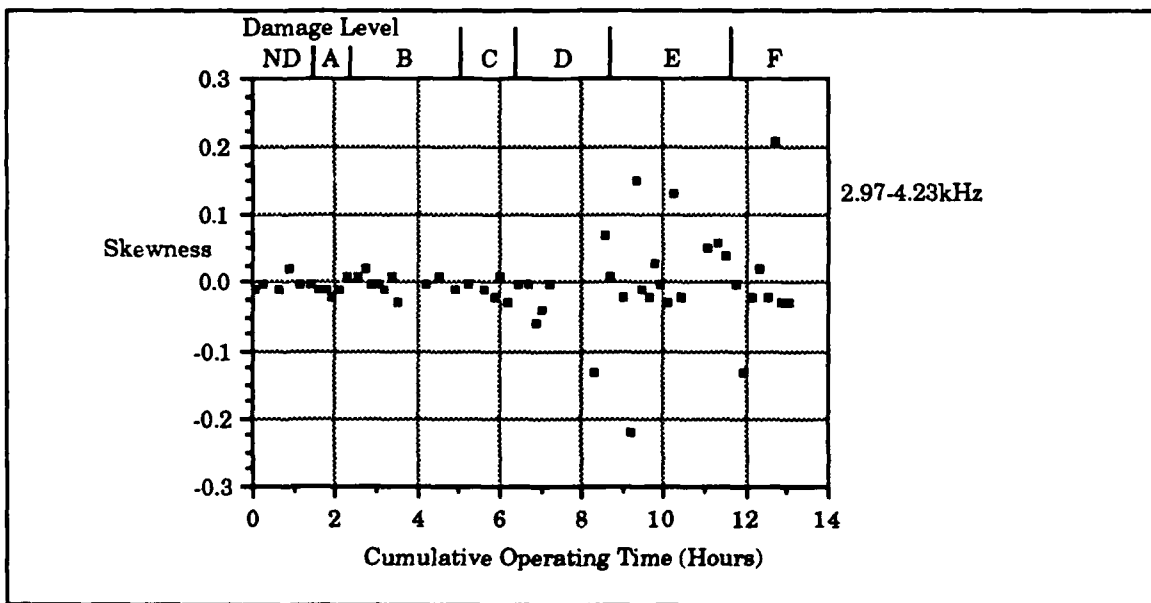
Figure 73. Skewness for 2.97 to 4.23 kHz frequency span.
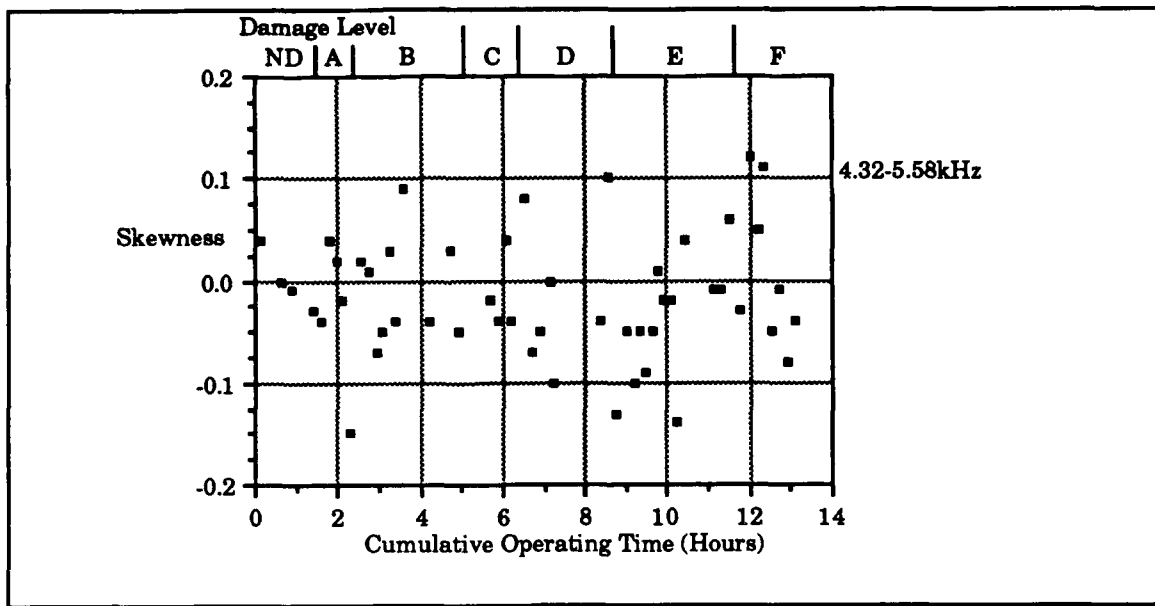
121

Figure 74. Skewness for 4.32 to 5.58 kHz frequency span.
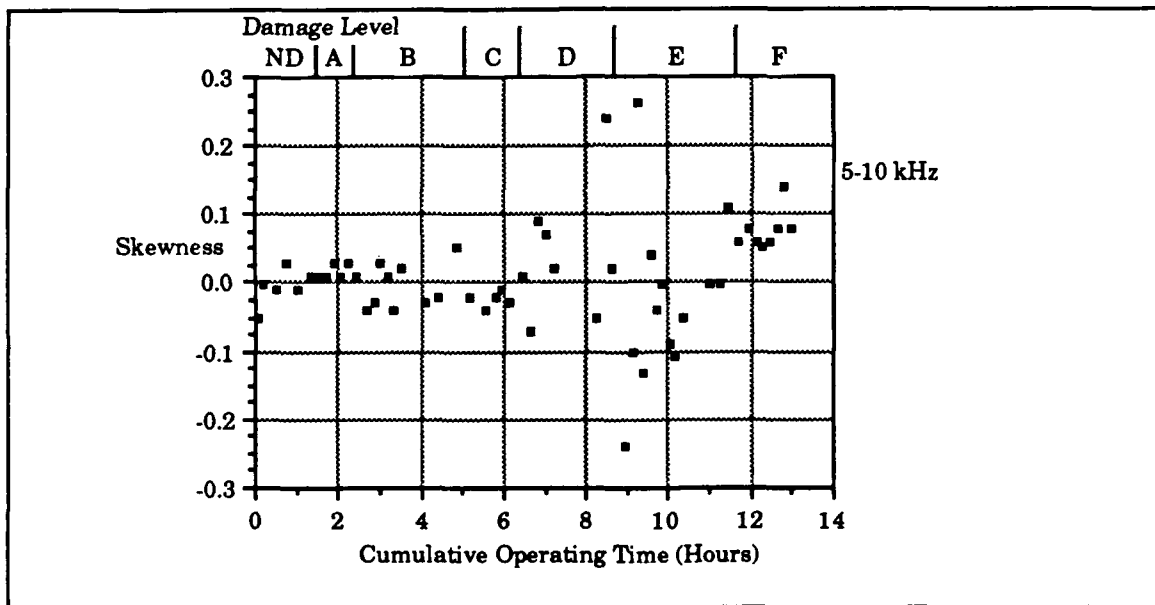

Figure 75. Skewness for 5.0 to 10.0 kHz frequency span.

4. Analysis of Kurtosis Levels

Kurtosis is the fourth moment of the probability density function normalized by the variance. The value of kurtosis for a Gaussian signal is 3.00. In theory the Kurtosis value will increase as impulsive events

122

occurs in the measured signal, this increase in the kurtosis level should be indicative of impulsive faults occurring in the monitored system.

a   Analysis of 0-10 kHz Frequency Bands

This measurement was made over the frequency span of 0.0 to 10.0 kHz. Figure 76 illustrates the data collected.
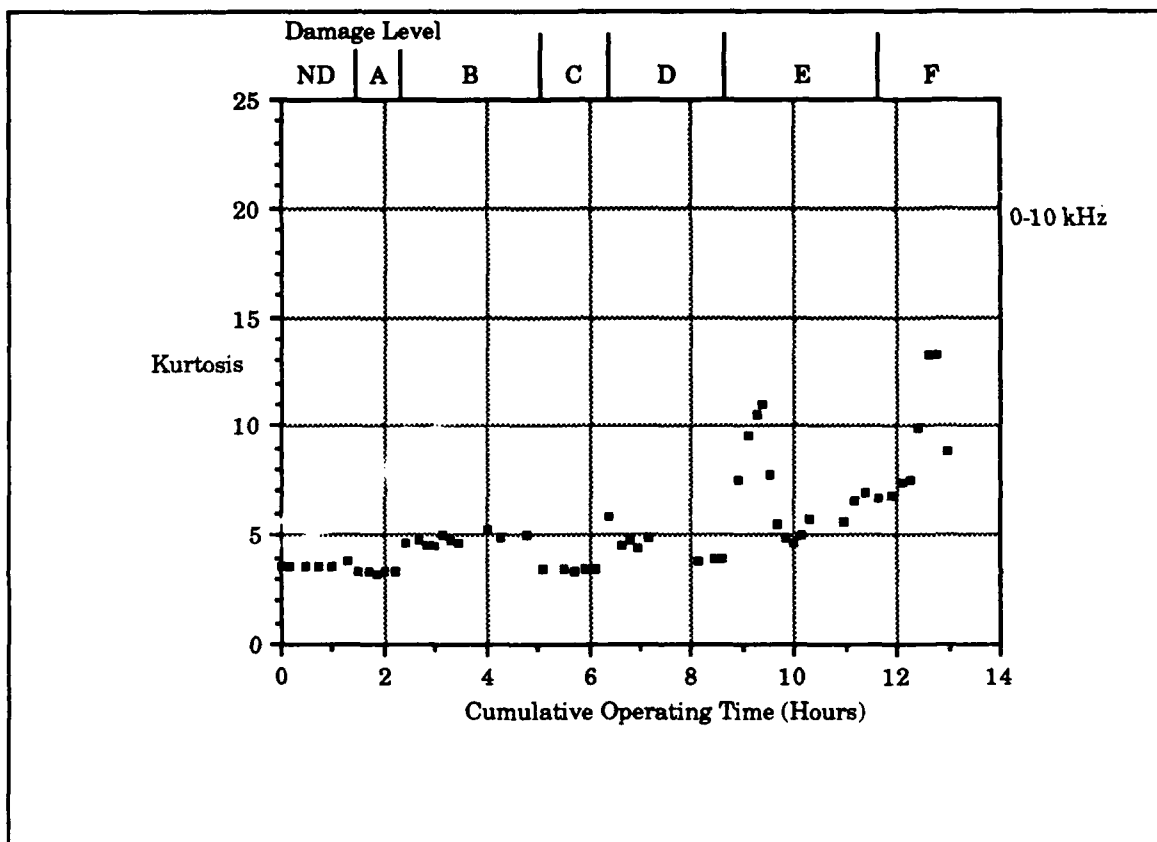
Figure 76. Kurtosis of 0.0 to 10.0 kHz frequency span.

In this graph an increase of the kurtosis value can be seen throughout the run. The baseline level is slightly greater than 3.0, and the fault detection level occurs at a magnitude near 5.0. A steady kurtosis value of 5.0 is reached during damage level B, and indicates a fault detected. During damage level C the kurtosis level drops back to a level near the baseline. In damage level D the kurtosis level again

jumps to a level above 5.0, but by the completion of the damage level collection has again fallen to a level below 5.0, it was during this damage level that a distinctive clicking was heard from the diagnostics model. Once damage level E occurs the kurtosis value does not fall below five again. The early stages of this run has some characteristics that bear closer investigation. Figure 77 is an expanded version of Figure 76, for this graph only damages levels through D are shown.
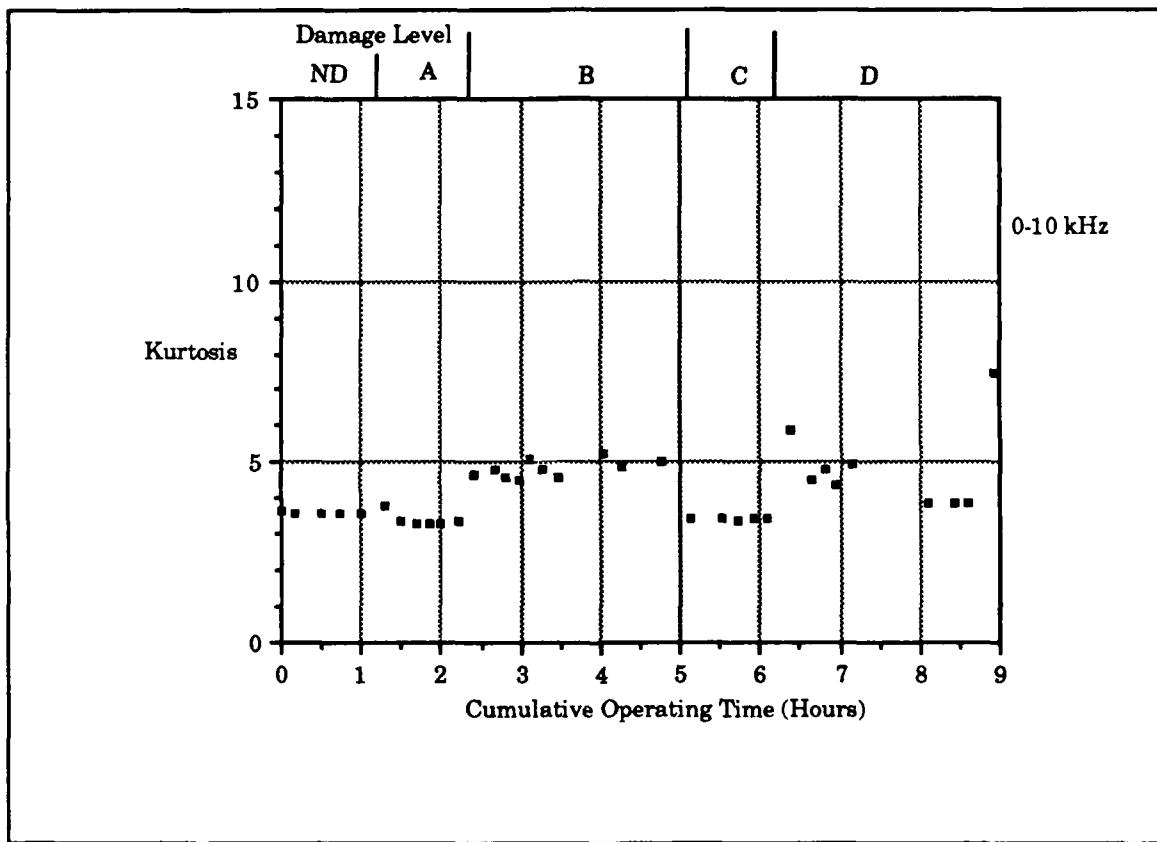

Figure 77. Expanded plot of 0.0 to 10 .0 kHz kurtosis value.

In this curve the kurtosis level of the measured data distinctly changes as damaged was made on the pinion. In the undamaged portion of the graph, the kurtosis level is very steady at a value of about 3.6. This value is slightly higher than that expected (3.0)

but in view of the change in magnitude of the kurtosis value that occurs in this data this difference does not appear to be significant. When a small amount of metal was removed in damage level A the kurtosis value fell to a value closer to 3.0 than the baseline value. This aspect is interesting and suggests a slight improvement in the condition of the gear over the baseline measurements. Once the kurtosis level has reached this new level it remains steady until damage level B, during damage level B the kurtosis rises to a value near 5.0. This level seems stable, but when damage level C is applied the level quickly drops back to a level comparable to the original measurements. Just after damage level D was made the kurtosis level jumped to a level above 5.0, as operation of the model continued at this damage level, the kurtosis level decreased to a level slightly higher than 3.0. This phenomena can be shown in more detail in Figure 78, which is an expansion of the damage levels D through F for this frequency span.
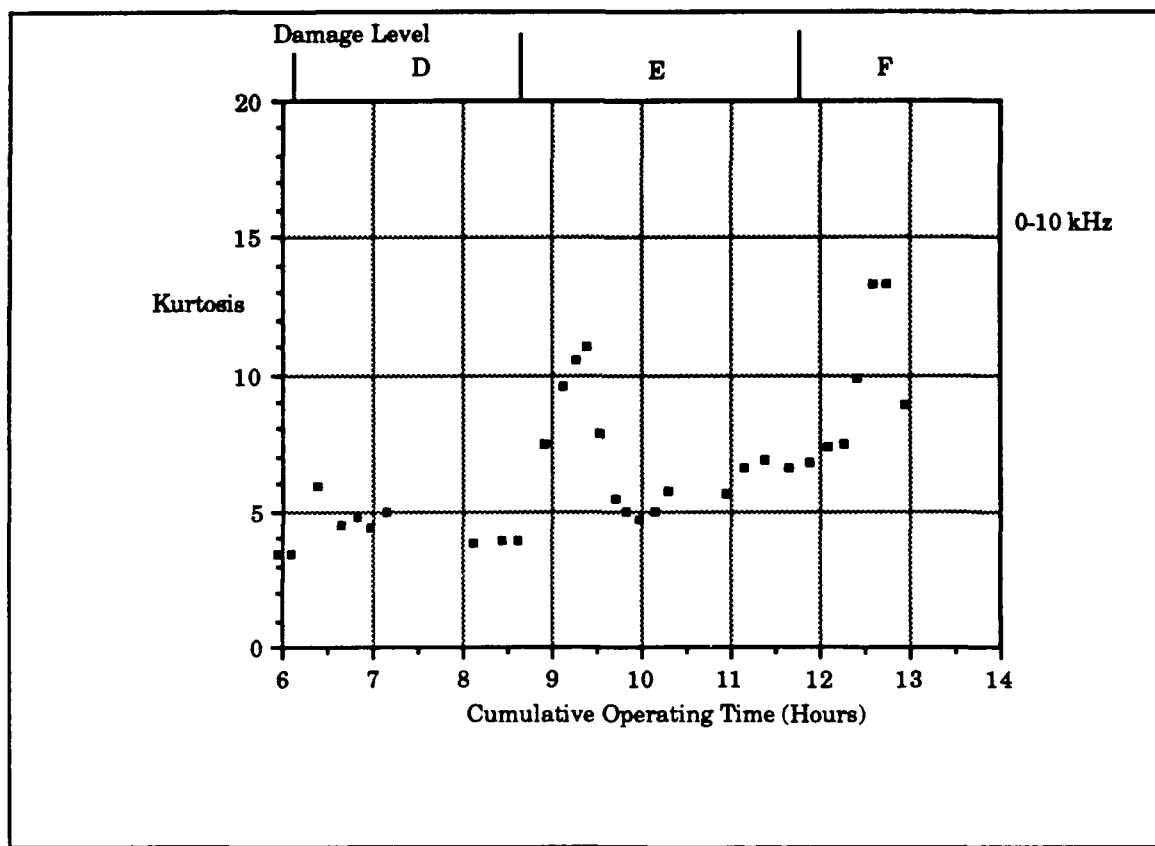
Figure 78. Damage levels D-E for the 0.0 to 10.0 kHz kurtosis.

In this plot the change in the kurtosis level between damage levels D and E is quiet distinct. A similar change in the data between damage levels E and F occurs, but the increase in level does not occur immediately after restarting the machine. Figure 79 is the data from the 0.0 to 10.0 kHz mean square value for the time time period. Comparison between the two figures is useful in illustrating the relationship between the mean square value and the kurtosis level.

126
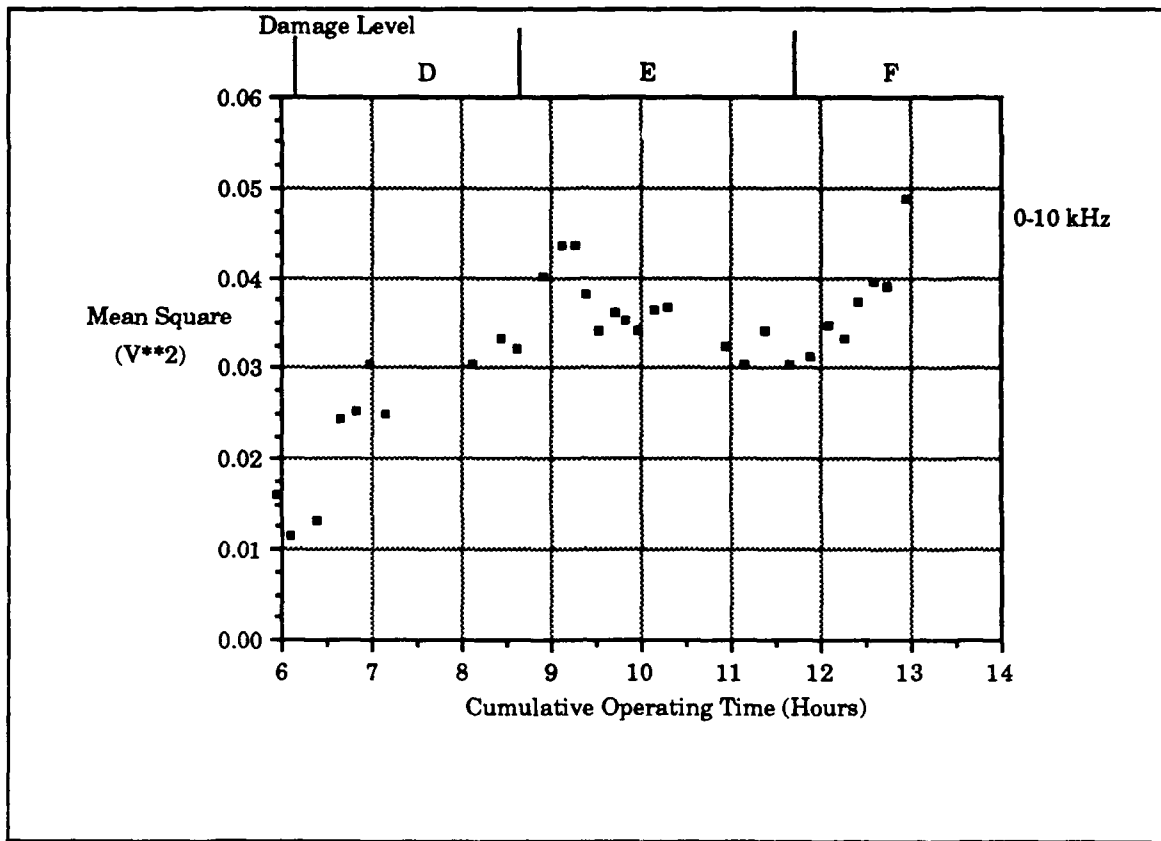
Figure 79. Expanded 0.0 to 10.0 kHz mean square measurement.

During damage level E the mean square value has increases. Figure 78 shows the kurtosis also starting to rise. This indicates the damage made on the tooth had a significant effect on both the magnitude of the vibration level, indicated by the increase in the mean square value, and on the impulsiveness of the signal, shown as a rise of the kurtosis level. As operation continued the mean square value decreased, this decrease in level had the effect of allowing the kurtosis level to increase. The mean square continues to decrease and the kurtosis level increases up to a point and it also begins to decrease. One possible explanation for this situation is that it indicates some type of wear process occurring. Large gross areas of damage would be the first

127

to be affected by wear and removal of these areas would lower the mean square value. Impulsive faults could be indicative of slapping damage that would decrease as the gears operate an either grind down these areas or blunt them by a hammering action. At this point in the experiment the tooth has been significantly damage and full contact is not occurring during mesh, hence the clicking heard during operation.

In damage level F less data was recorded but a similar process seems to be occurring,there is difference though, in damage level F both the mean square value and the kurtosis level rise and decrease at the same time. The response seen in this plot will also be seen in the other frequency spans monitored.

b *Analysis of .270 to 1.53 kHz Kurtosis Level*

Figure 80 presents the Kurtosis levels for the frequency span 0.27 to 1.53 kHz, this span includes the first through third harmonics of the gear mesh frequency. The resulting graph is very similar in appearance to the 0.0 to 10.0 kHz measurement of Figure 76. The similarity is in appearance only, as the magnitude of the kurtosis level is much smaller in this measurement.

128
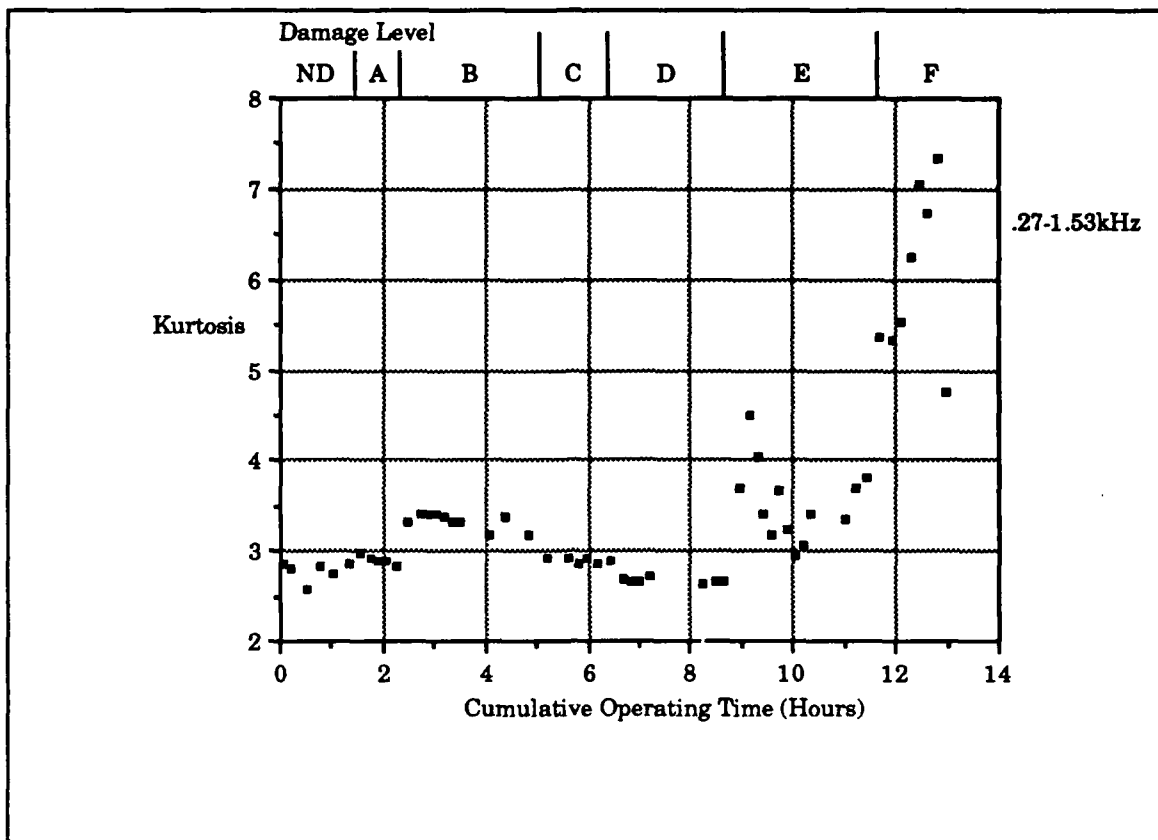
Figure 80. Kurtosis of 0.27 to 1.53 kHz frequency span.

Another difference is seen in the undamaged area of the graph, the measured kurtosis level is near 2.75 and does not rise to a level greater 3.0 until damage level B. An explanation for this low level of kurtosis appears to be due to the low frequencies monitored in this span. The measured span filters out the higher frequencies of the monitored signal, and would result in a baseline level less than 3.00.

An increase in level is seen at the start of damage level B, and although the magnitude of the change is small it is larger than four standard deviations from the baseline level, a level near 3.1 is sufficient for detection. A decrease in kurtosis is seen at the end of damage level B and continues to drop through through damage level D.

Rapid increases in the kurtosis level are seen during damage levels E and F, the magnitude of the increases is near 4.5 for damage level E and 7.5 for damage level F.

c. Analysis of 1.62 to 2.88 kHz Kurtosis Level

The kurtosis level from the frequency span 1.62 to 2.88 kHz is shown in Figure 81. This frequency span is related to the fourth through sixth harmonics of the gear mesh frequency. The overall pattern of this data is significantly different from the patterns seen in the previous frequency span.
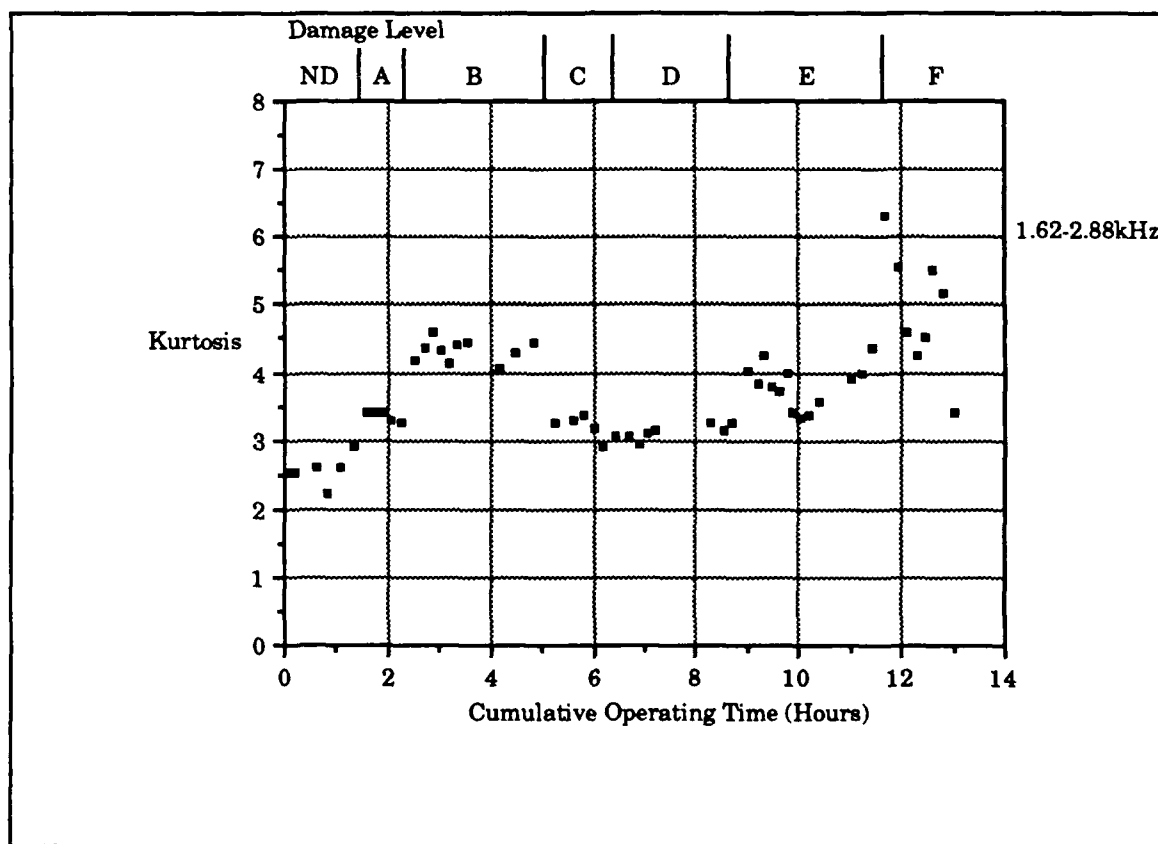

Figure 81. Kurtosis for 1.62 to 2.88 kHz frequency span.

The initial kurtosis values (approximately 2.5) are lower than the level seen in the frequency span 0.27 to 1.53 kHz, and the data

changes much more rapidly in this frequency span. Fault detection, based on a level four standard deviations above the baseline level, occurs during damage level A. From a level near 4.5 the kurtosis level in damage level B falls to a level near 3.0, this phenomenon was seen in each of the previous two frequency spans, and appears to be related to the rapid increase in the mean square value measured during this damage level. The rise in the mean square value, without a corresponding increase in the fourth moment causes a decrease in the kurtosis level. The spikes seen in the previous two frequency spans are seen in this graph, but they are not as distinct in this measurement.

d Analysis of 2.97 to 4.23 kHz Kurtosis Level

The frequency span of 2.97 to 4.23 kHz is related to the gear mesh harmonics seven through nine, a plot of the calculated kurtosis values is presented in Figure 82. This figure shows a very distinctive rise in kurtosis level after damage level C.
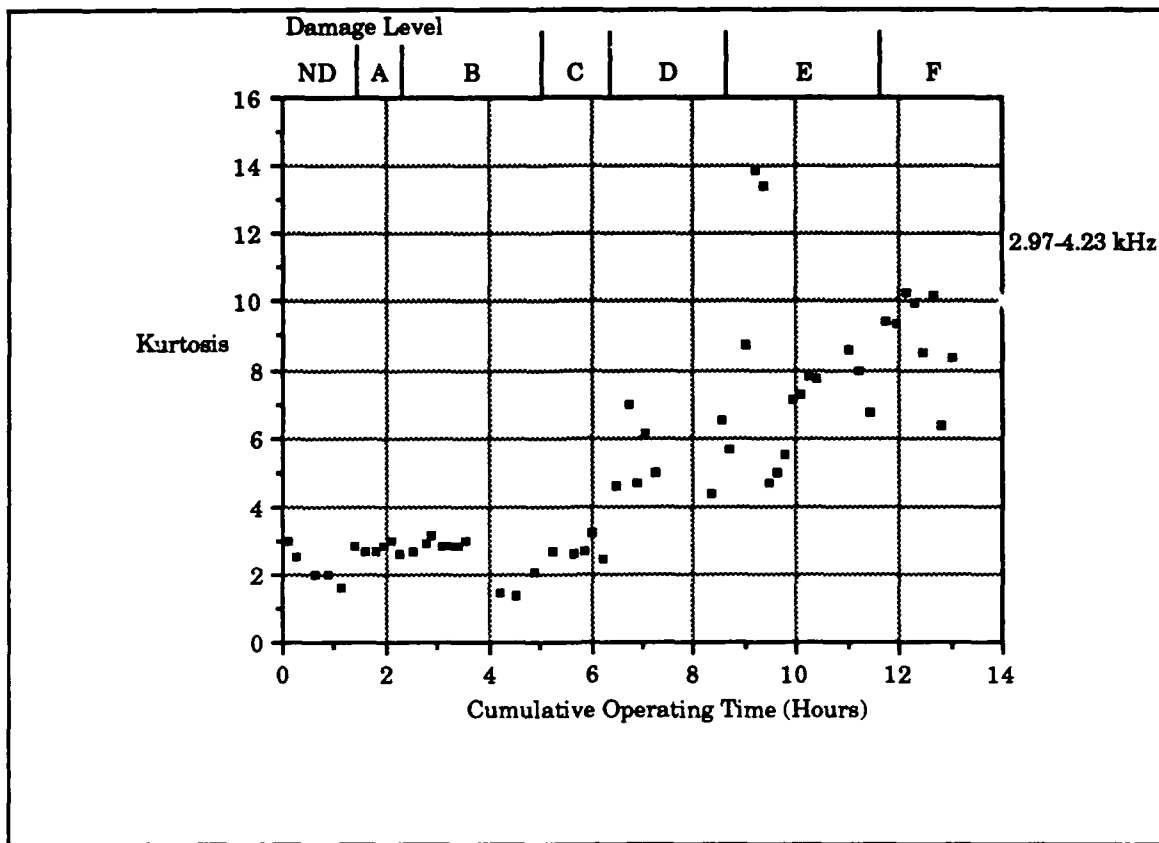
Figure 82. Kurtosis for 2.97 to 4.23 kHz frequency span.

Early stages of the run are difficult to analyze due to a lack of a steady baseline level. The baseline level appears to near 2.0. A rise in level appears to occur in damage level B, but the rise is not as distinct as the earlier frequency spans. One aspect of this data is the very large increase in level that occurs after the start of damage level D. This large of a rise was not seen previously. The spike in the kurtosis level during level E can be seen quiet clearly in this plot, while the spike in damage level F seen in previous frequency spans in not as distinctive in this span.

132

e. Analysis of 4.32 to 5.58 kHz Kurtosis Level

Figure 83 presents the kurtosis levels calculated from the frequency span 4.32 to 5.58 kHz, which correlates to the tenth through twelfth harmonics of the gear mesh frequency. The overall trend of the plot is a steady rise similar to that seen in the 2.97 to 4.23 kHz span, but with magnitudes much larger. Additionally more scatter is seen in the plot, this aspect can also be seen in the data from Table 1.
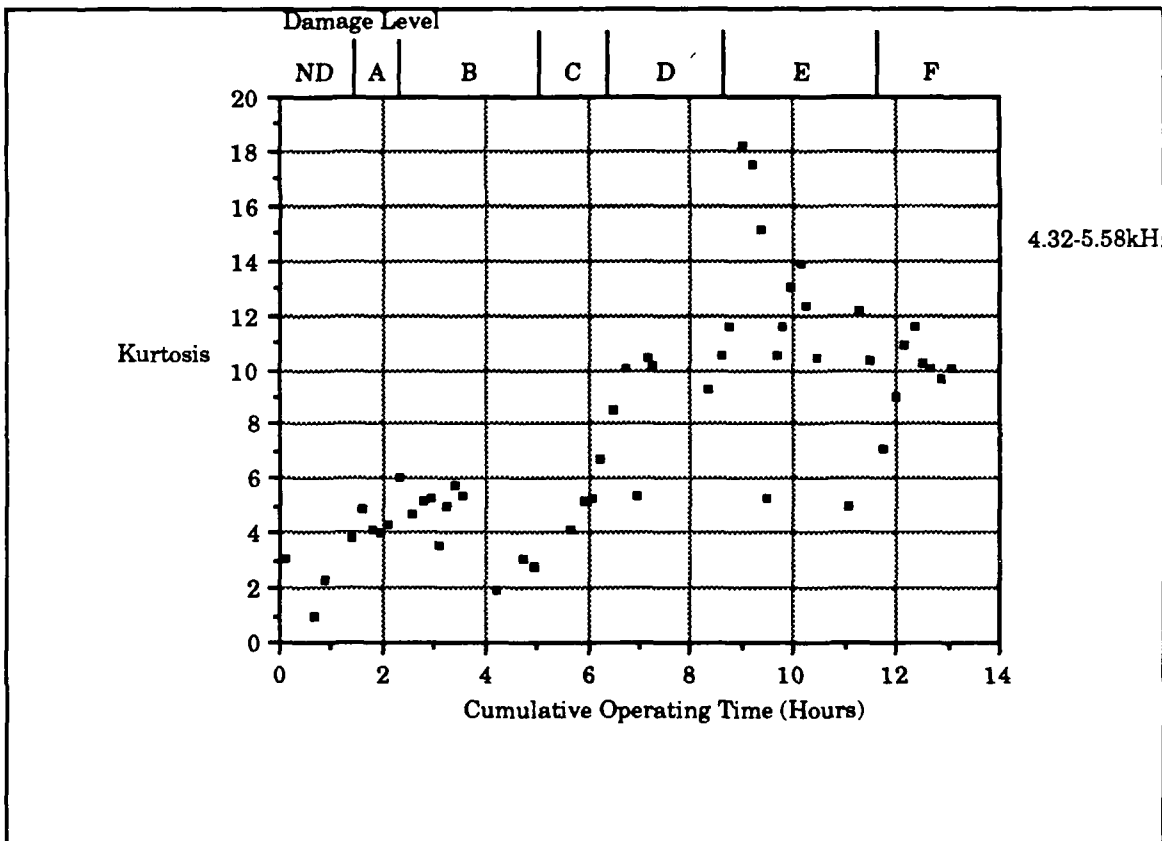
Figure 83. Kurtosis for 4.32 to 5.58 kHz frequency span.

The change of kurtosis in damage level A is the most significant of the frequency spans measured, but that the kurtosis level at the end of damage level B drops significantly. The measured mean square value for this damage level was fairly constant, see Figure 66, so

133

this would indicate that the impulsive characteristics of the monitored vibration signal was decreasing. This decrease could be the result of some type of wear process occurring to the gear. The spike in damage level E is very distinctive in this plot, showing a significant reduction in level as it falls to a "steady" level, the spike seen previously in damage level F is not distinctive.

f Analysis of 5.0 to 10.0 kHz Kurtosis Level

The kurtosis values for this frequency range are presented in Figure 84. The data is very responsive to the damage occurring after damage level C.

Figure 84. Kurtosis for 5.0 to 10.0 kHz frequency span.

134

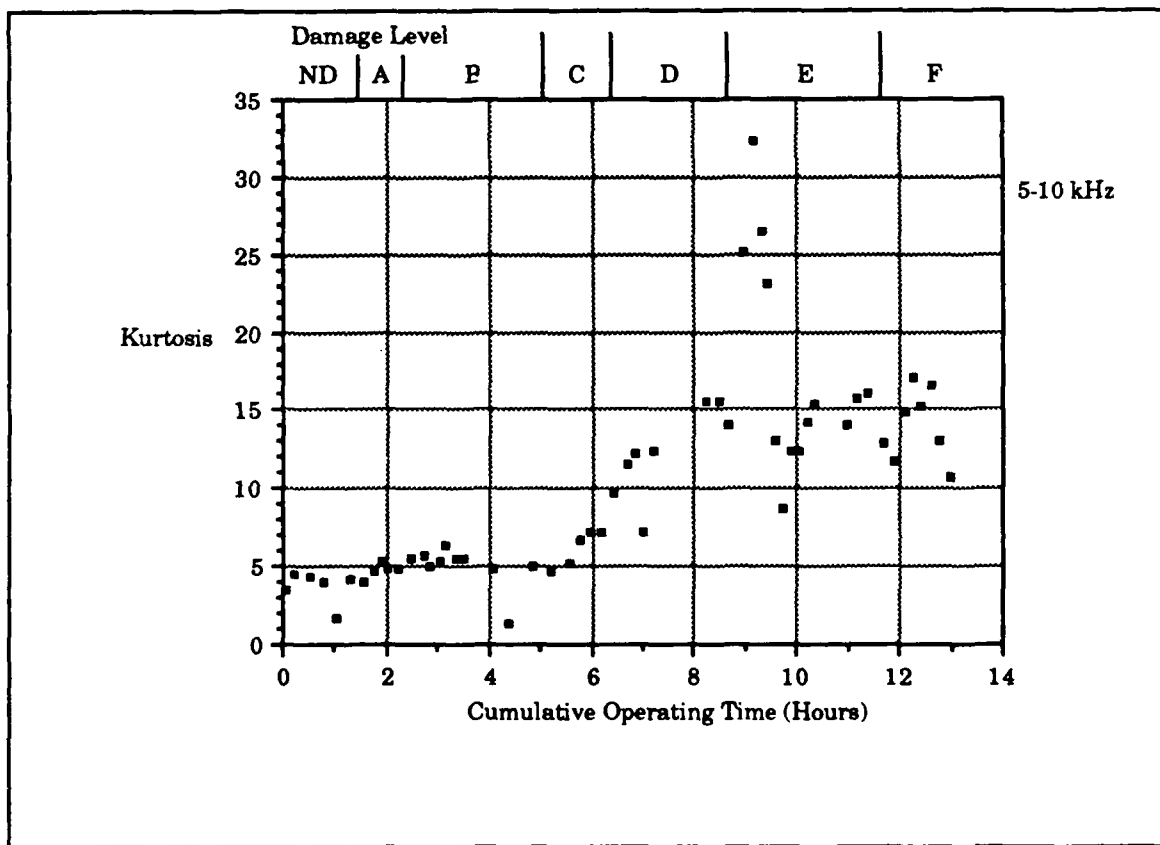The baseline level for this measurement starts at a level slightly higher than 3.0 (actual value 3.58) and fluctuates up to a level near 4.0. Using the baseline level of 4.0 fault detection occurs during damage level B at a level near 6.0. After damage level C the increase in kurtosis level becomes quiet dramatic.

Several aspects of this graph were noted. At the beginning of damage level E, the now familiar, rapid rise and decrease in kurtosis level can be seen, but the spike during damage level F is not seen at all in this data. Another aspect of this data is the magnitude of the kurtosis level at the conclusion of the run. After the decrease in level at the beginning of damage level E, the remaining data can be interpreted in two ways, first the kurtosis level appears to steady at a level near the final data measurements of approximately 10.5. The second method has the data oscillating near a level of 14.0. In either case this is the highest magnitude observed for the final kurtosis level in this experiment.

The response of the data from this frequency span appears to support an earlier statement that the frequency spans act like a filter for the impulsiveness in the measured signal, in this high frequency measurement the baseline level of kurtosis is higher than that expected for a random signal. The large magnitude of the data measured when the gear was damaged indicates the higher frequencies were more "impulsive" in nature than the data from the lower frequency measurements.

D. CONCLUSIONS

The statistical parameters calculated from the vibrations of pinion one were very interesting. In general the statistical parameters detected faults as well as that of the frequency spectrum.

The mean value was responsive to damage, but because of the small magnitude of the measurements use of the parameter for fault detection was difficult.

The mean square value was effective in the detection of faults after damage level D. Also, the mean square value appeared to be dependant on the frequency span used in the measurement. Lower frequency measurements appeared to be more responsive to damage than higher frequency measurements.

Skewness was very effective in detecting damage in the 0.0 to 10.0 kHz frequency span, but was of little use in all other spans monitored.

Kurtosis was very good at detecting damage, with detection occurring very early in the experiment. Like the mean square value the kurtosis measurements appeared to be dependent on the frequency used in the measurements. For this experiment the higher frequency measurements appeared more responsive to damage.

Tying the frequency spans monitored to specific harmonics of the gear mesh did not appear to have any effect on the data measured. The nature of the frequencies monitored, high or low, seemed to effect the data much more than the attempt to tie the spans to the dynamics of the gear mesh.

VII. ANALYSIS OF PINION TWO

A. DESCRIPTION OF DAMAGE.

In this portion of the research the effect of damage to the edge of a tooth was examined. Terminology used to describe the gear is shown in Figure 42. A single tooth on a 15 tooth pinion was damaged in the top land area of the tooth. The tooth was damaged four times, with the damage levels labeled as damage levels A through D, damage was introduced by striking a cold chisel applied to the tooth.

A new 15 tooth gear was prepared for use by running the diagnostics model for an eight hour period until the black finish on the gear had been worn off and a shiny wear pattern was produced on the tooth. After this break in period data collection begin.

At the start of the experiment the model was run with an undamaged gear to collect baseline data. This run lasted approximately two hours and forty minutes. This baseline data permitted an analysis to be made on the affect subsequent damage had upon the vibration of diagnostics model. The data collected during the period of no damage will be labeled "ND" on graphs in this section of the report.

1. Damage Level A

Upon completion of the initial undamaged run, the diagnostics model was stopped and damage introduced to the gear. Damage was applied by a blow to a cold chisel on the top land area of one tooth. The damage was applied to the same tooth throughout the experiment. This

the gear mesh. Figure 85 is a representation of the tooth damage. Figures 85 through 88 are adapted from Reference [20].
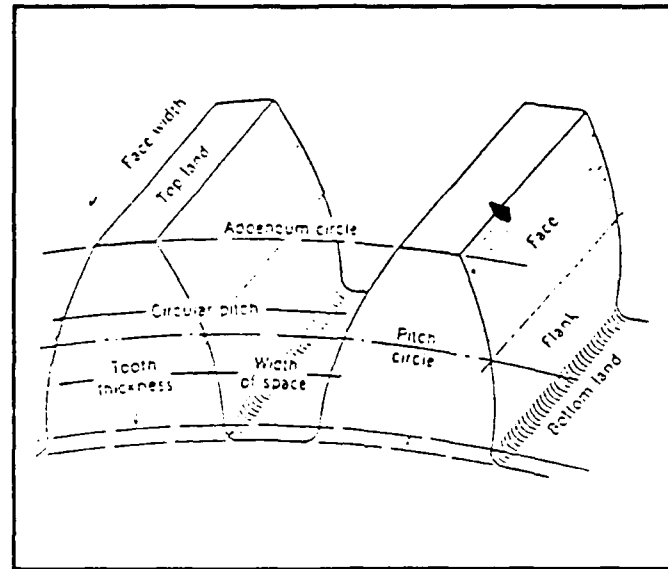
Figure 85. Damage level A.

This damage resulted in a small notch on the topland area near the wear face of the tooth, but only slight damage to the face of the tooth. This damage to the gear will be referred to as damage level A. The diagnostic model was restarted and ran for approximately two hours and 50 minutes while data was collected. After restarting the model a noticeable clicking sound could be heard coming from the gears. This clicking corresponded to the driving shaft speed, approximately 30 Hz.

2. Damage Level B

After damage level A, the model was stopped and additional damage applied, Figure 86 illustrates the the damage applied in damage level B.
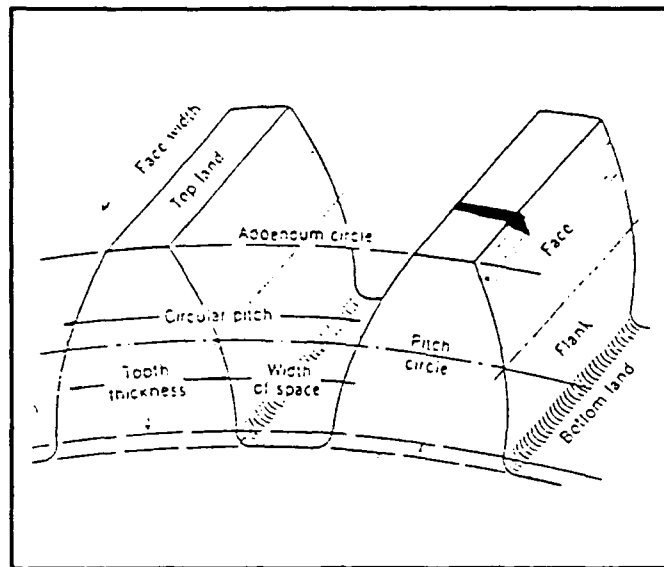
Figure 86. Damage level B.

This additional damage to the gear was applied in the same area as before, the major portion of the damage resulted in a large notch in the face of the tooth. A mound of damaged metal was formed around the 'wound'. The model was run for approximately 2 hours and 30 minutes with this damage. A noticeable increase in the level of the clicking could be heard coming from the operating gear after this damage.

3. Damage Level C

The damage applied during this level of damage was introduced by striking the cold chisel in the notch produced by earlier damage. This damage is shown in Figure 87.
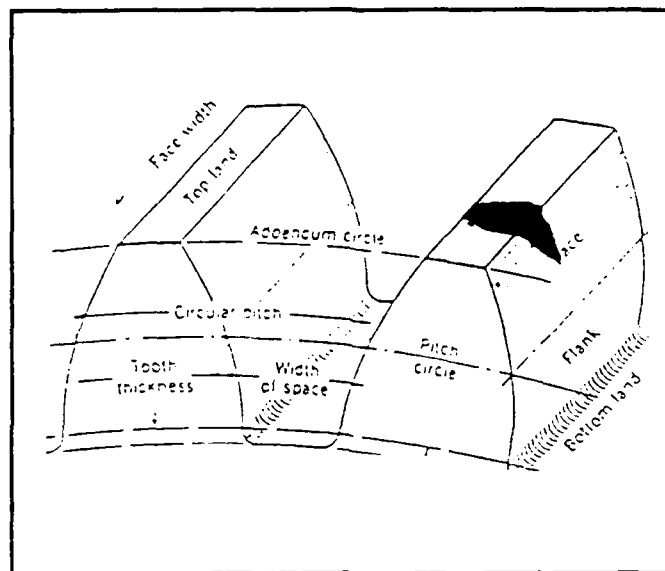
Figure 87. Damage level C.

The damage from this blow was wider and crossed the entire top land area of the tooth. The diagnostic model was run in this condition for approximately 2 hours and 20 minutes, after restarting the diagnostic model *no noticeable increase in the audible level of the noise* was heard.

4. Damage Level D

The final damage to the gear was produced by applying the cold chisel on the top land at an angle, but in the same notch as the original damage. This damage is referred to as damage level D. Figure 88 depicts the damage made to the gear.
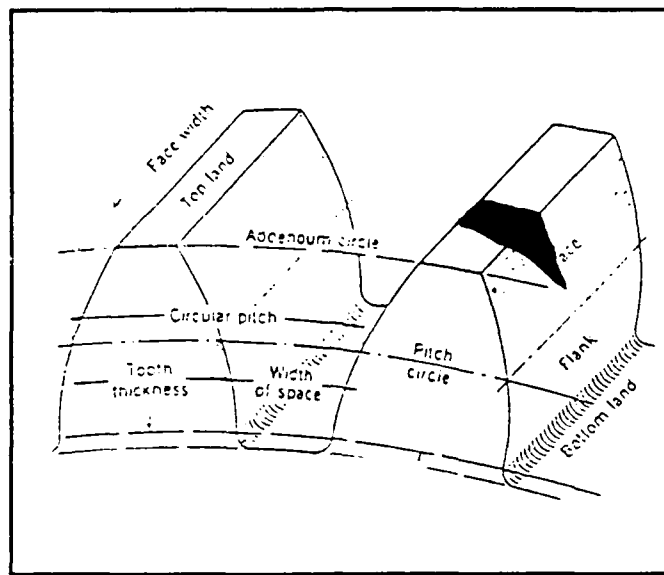
Figure 88. Damage level D.

This damage produced metal with a jagged appearance on the face of the tooth. The diagnostic model was run for 3 hours in this condition, a very noticeable (and annoying) increase in audible noise was produced by this damage.

A final comment is warranted prior to analyzing the results of the data collected. Each time the tooth was damaged an area of raised metal was produced around the notch directly on the wear area of the tooth. At the end of each run the damaged gear was examined, this examination revealed that in each case, the area raised by damage was found to have been smoothed, presumably by the natural sliding action occurring during gear mesh. This action can be looked at as the gears having an ability to 'heal' themselves.

B. RESULTS FROM SPECTRAL ANALYSIS

The damage applied to the pinion during this experiment only consisted of damage applied to a small portion of the wear area of the

tooth. During the investigation 15 different frequency spectra were measured. Five of these spectra covered a frequency range of 0.0-10.0 kHz, with the remaining spectra covering a frequency range of 0.0-1.0 kHz.

With this data, analysis of the broad band level for the two series of spectra was made, along with analysis of narrow band frequency components from the span of 0.0 to 1.0 kHz. Frequency components examined were the driving shaft frequency (30 Hz), the gear mesh frequency (450 Hz), and the second harmonic of the gear mesh (900 Hz).

1. Analysis of 0.0 to 10.0 kHz Broad Band Levels

The broad band levels from the frequency span 0.0 to 10.0 kHz are presented in Figure 89, the measurements present an opportunity to examine the overall vibration level the diagnostics model experienced during the experiment, in general these spectra do not sufficient frequency resolution to permit analysis of the lower frequency components that are produced by the diagnostic model.
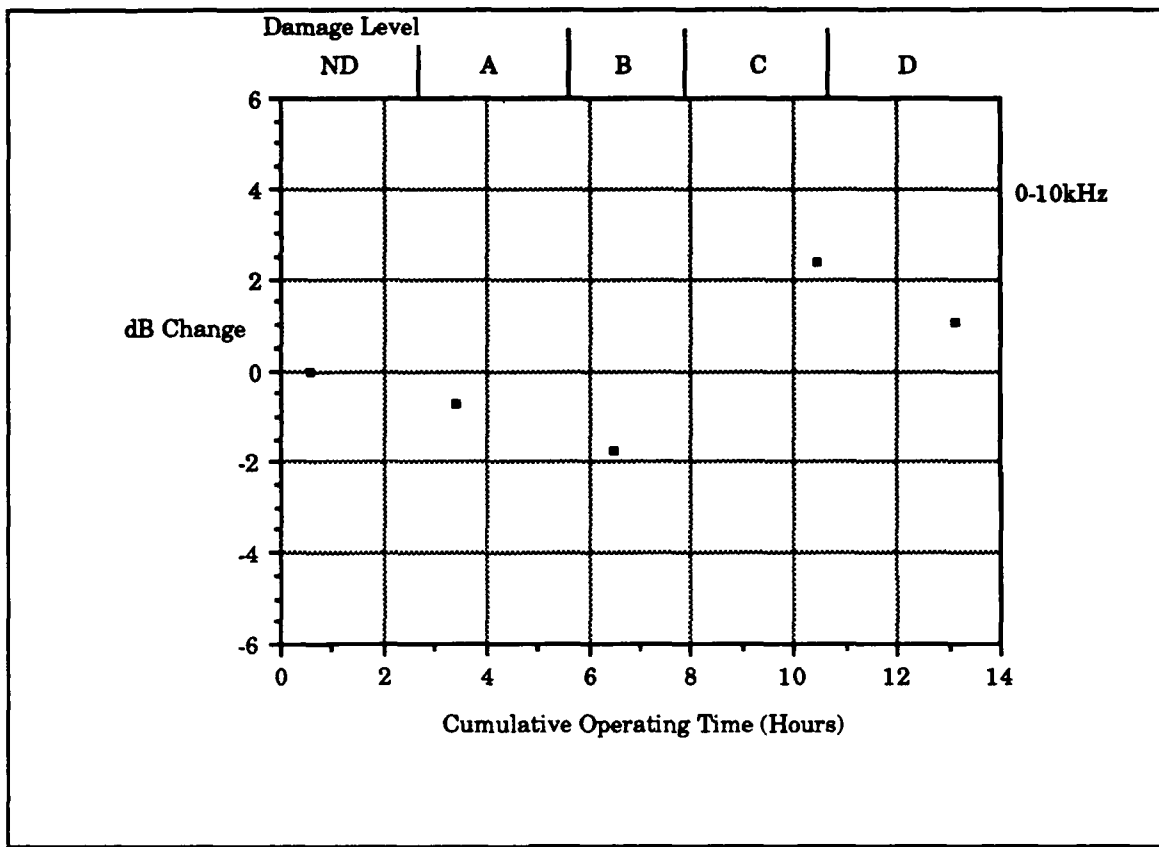
Figure 89. Broad band levels for 0.0 to 10.0 kHz span.

This plot indicates a steady level of vibration, with a slight increase in level occurring during the later portion of the run. A 6 dB increase over the baseline level is not seen in these measurements. Use of the information would not indicate a fault being detected in the machinery.

2. Analysis of 0.0 to 1.0 kHz Broad Band Level

The overall vibration level computed from the recorded narrow band power spectrum measurements is presented in Figure 90. This graph, like the 0.0 to 10.0 kHz measurement, indicates a steady level with little change occurring as damage was made to the pinion.
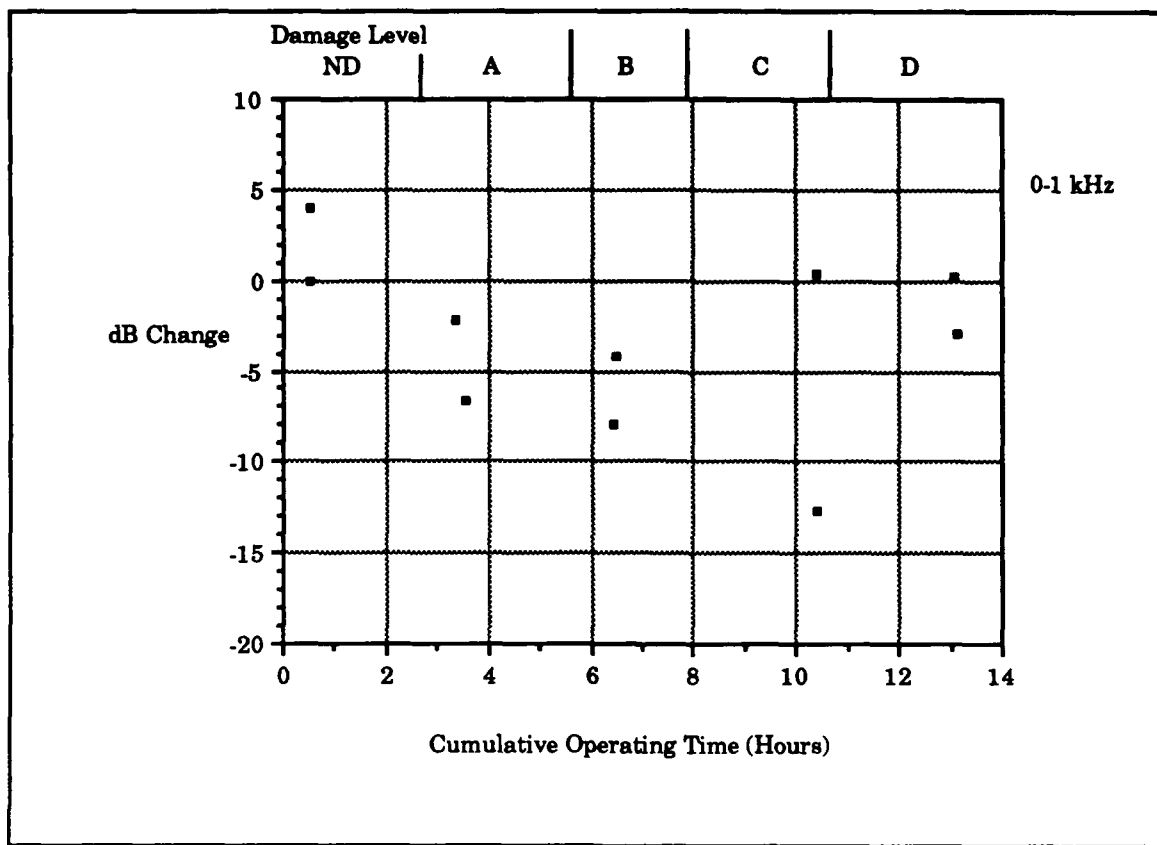
Figure 90. Broad band levels for 0.0 to 1.0 kHz span.

This data does not indicate a fault was detected, a decrease in level is seen in the measurements, with the final data returning to baseline levels. Neither broad band level appeared sensitive to the damage applied to the pinion.

3. Analysis of Operating Speed Frequency

Figure 91 depicts the change in the amplitude of the frequency component corresponding to the driving shaft operating speed, approximately 30 Hz.

144
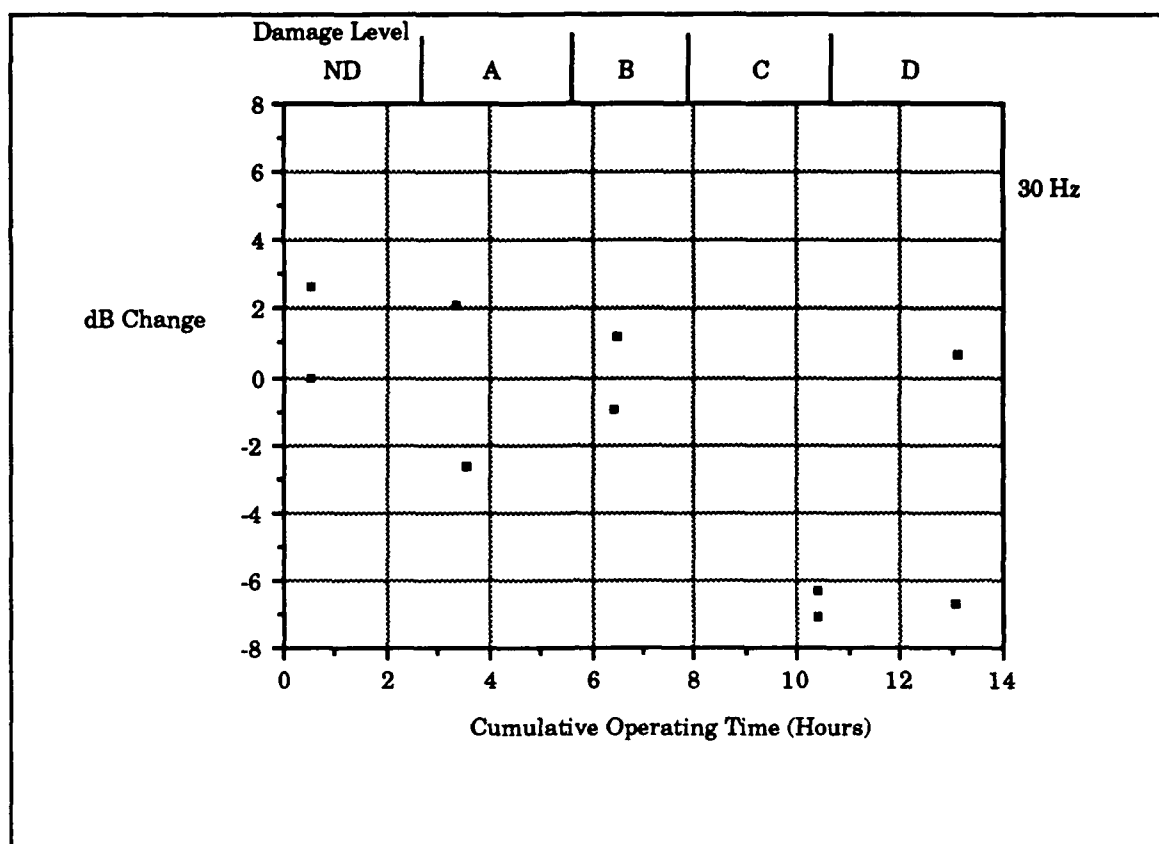
Figure 91. Amplitude of operating speed frequency.

The data presented in Figure 91 in similar to the data seen of Figure 90. The vibration level stays steady in the initial stages of damage and then drops during damage level C. In damage level D the level climbs back to baseline l͏ ͏ls. A 6 dB increase from the baseline vibration does not occur, so detection of a fault is not indicated. There is a 6 dB change in vibration in the measurements in damage level C and one of the measurements in damage level D, this change could be a cause of concern, but additional measurements would be needed before a fault could be determined.

4. Analysis of the Gear Mesh Frequencies

a. *Gear Mesh Frequency*

Figure 92 illustrates the changes in amplitude of the gear mesh frequency component, 450 Hz. This figure indicates a drop in the vibration level of the component.
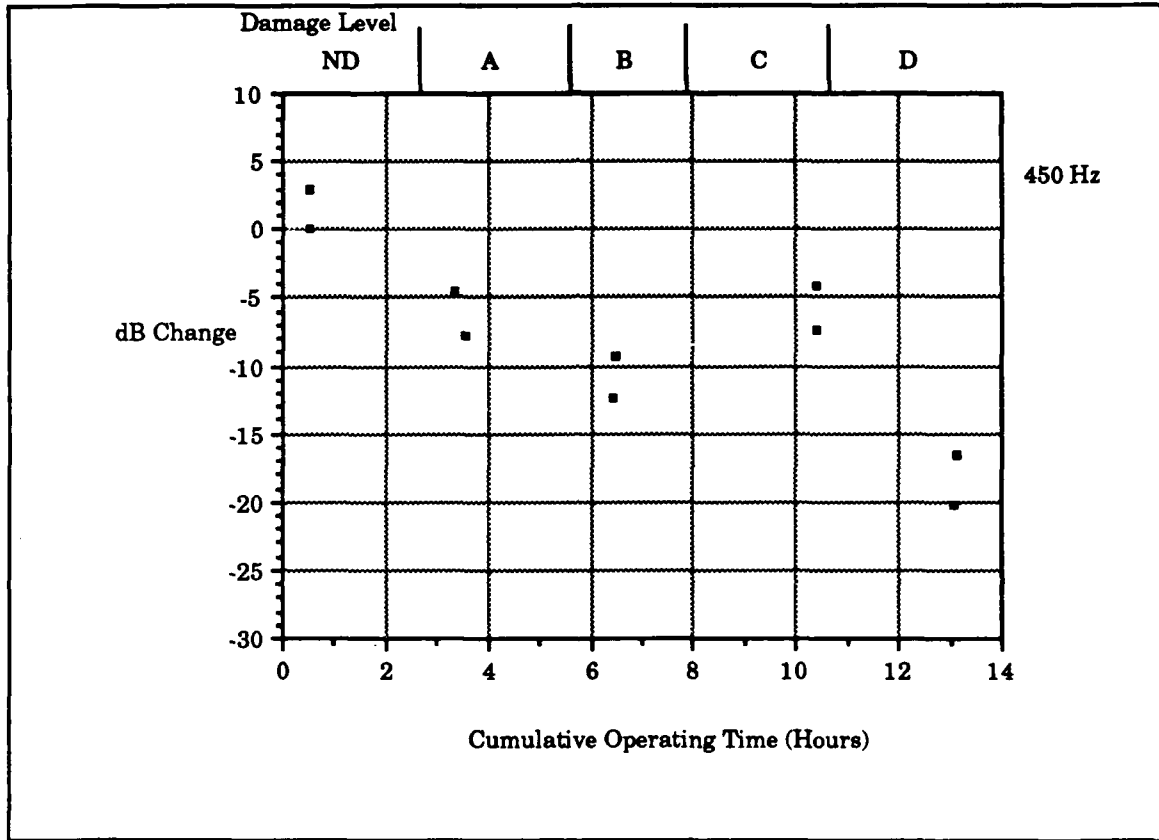
Figure 92. Amplitude of the gear mesh frequency.

In damage level A a 5-7 dB drop occurs from the baseline measurement, this decreased level remains fairly constant through damage level C, but during damage level D a significant drop of about 10 dB occurs. Because of the drop in level no fault is considered to be detected.

b Analysis of Second Harmonic of the Gear Mesh Frequency

Figure 93 presents the measured amplitudes of the second harmonic of the gear mesh frequency. This frequency was measured at approximately 900 Hz.
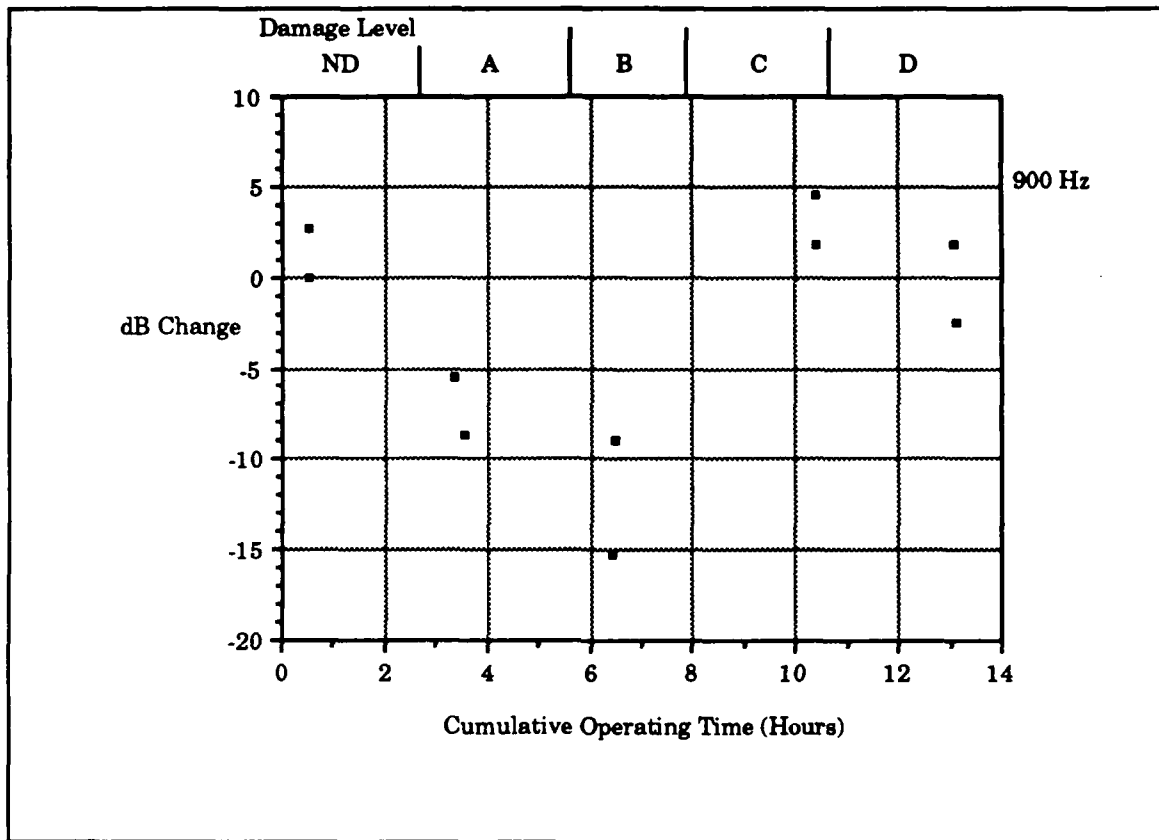
Figure 93. Second harmonic of the gear mesh frequency.

Like the other frequency components investigated, this plot does not indicate detection of a fault. The vibration level of the component decreases sharply in the early levels of damage (A and B), and increases after damage level C to a level 3-4 dB higher than the baseline level. This slight rise appears to decrease to a level near the baseline though after damage level D. The sharp drop in level from the

baseline measurement might be a cause for alarm, but the subsequent return to baseline levels indicates that the concern was not justified.

5. Conclusions from Analysis of Frequency Spectra

The use of frequency analysis techniques for the damage applied to pinion two were ineffective in detecting damage to the pinion, neither broad band vibration levels or individual frequency components indicated an increase in vibration level throughout the experiment. The lack of response of the gear mesh frequencies can possibly be explained by the effect a local defect has in producing sidebands around the gear mesh components. This effect was discussed in Chapter 1 and the effect was shown in Figure 8. The local defect produces sidebands around the gear mesh frequency and harmonics, and in some cases as the sidebands increase the level of the gear mesh harmonics will actually decrease, this appears to be the situation in this case. Figure 94 presents two high resolution, called zoom, measurements made of the gear mesh frequency component.

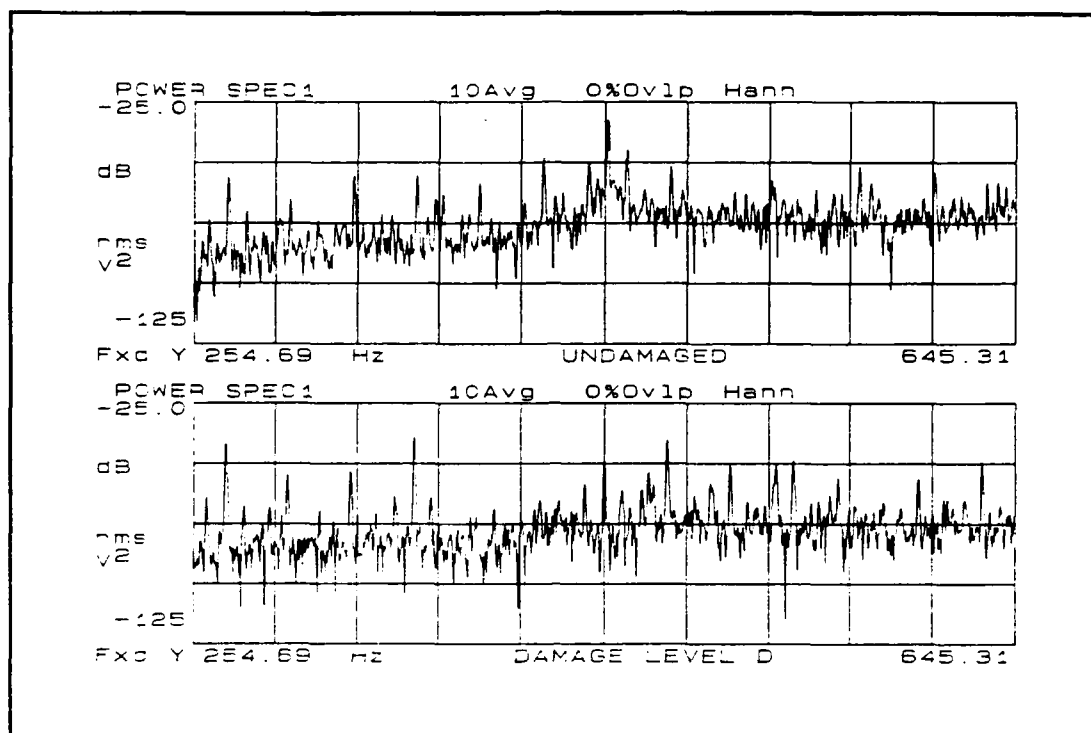**Figure 94. Zoom measurements of gear mesh frequency.**

The upper spectrum is a measurement made during the undamaged portion of the run, the lower spectrum was made during damage level D. The cursor marks the gear mesh frequency. In the lower trace the sidebands surrounding the gear mesh component have increased. Figure 95 is a similar set of measurements made around the second harmonic of the gear mesh frequency.

149
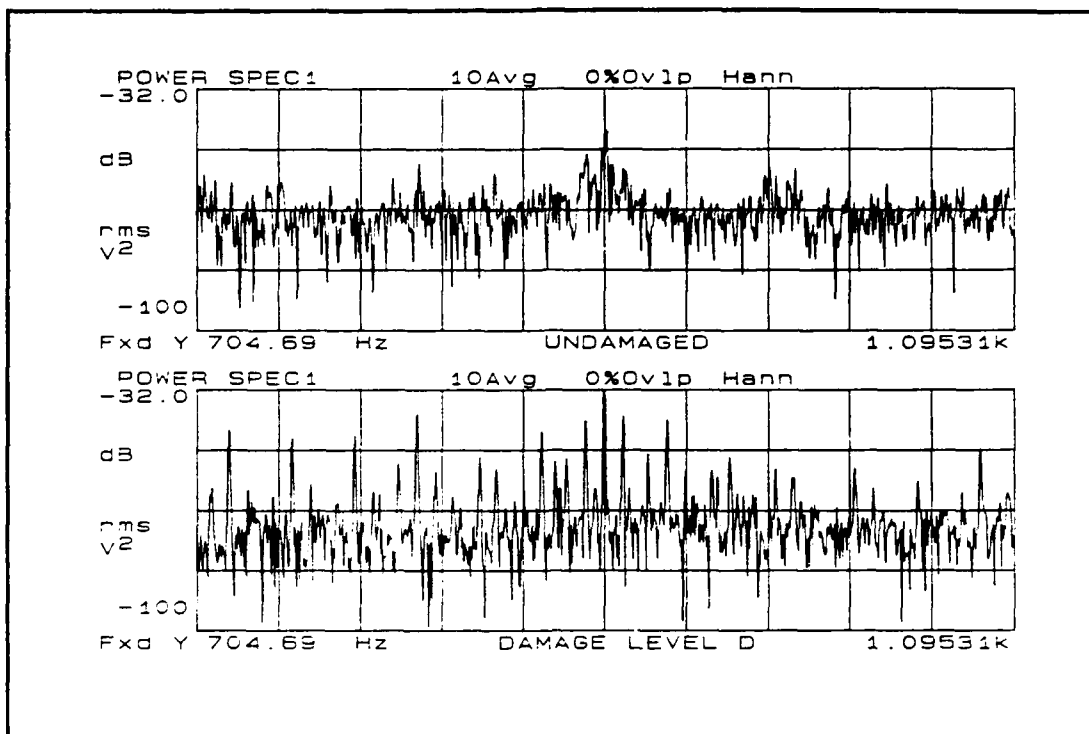
Figure 95. Zoom measurement around the second harmonic.

The upper trace is the harmonic of the gear undamaged,, the lower trace is a measurement made during damage level B. The spectrums show the same situation described for the gear mesh frequency. The sidebands of the damaged state have significantly increased, while the specific gear related component has decreased. The sidebands seen in these measurements are related to the driving shaft frequency (30 Hz), the driven shaft frequency (9 Hz), and a third frequency which may be related to a tooth indexing frequency. The monitoring of each of these sidebands though not impossible is difficult and requires a significant amount of time and/or computer programming. This situation makes the monitoring of gears extremely difficult.

The lack of response of the driving shaft frequency component is somewhat confusing. A noticeable clicking sound corresponding to the

150

shaft rotation speed was heard from the gears during damage level A. Subsequent damage lead to an increase in the audible level. Why this was not reflected in the amplitudes of the frequency spectra is unknown.

C. ANALYSIS OF STATISTICAL PARAMETERS

The statistical parameters of six different frequency spans were examined during this experiment. The frequency spans monitored were the same as those used in the analysis of pinion one, the spans were 0.0 to 10.0 kHz, 0.27 to 1.53 kHz, 1.62 to 2.88 kHz, 2.97 to 4.23 kHz, 4.32 to 5.58 kHz, and 5.0 to 10.00 kHz. The choice of the frequency spans coincided with harmonics of the gear mesh, however the earlier results showed little correlation between the specific harmonics and the results, no further mention of the harmonics will be made during the analysis of pinion two.

Fault detection criteria for the parameters monitored were discussed in Chapter VI, for the mean, skewness and kurtosis the criteria is based on the data from Table 1, a change in level equivalent to four stand deviations is used to indicate a fault, for the mean square value a four fold increase from the baseline level is required.

1. Analysis of the Mean Value Measurements

a *Frequency Span of 0.0 to 10.0 kHz Span*

Figure 96 presents the mean value measured over the frequency span of 0.0 to 10.0 kHz, this graph of the data shows a curve in which the magnitude of the mean value does not show a clear trend.

151
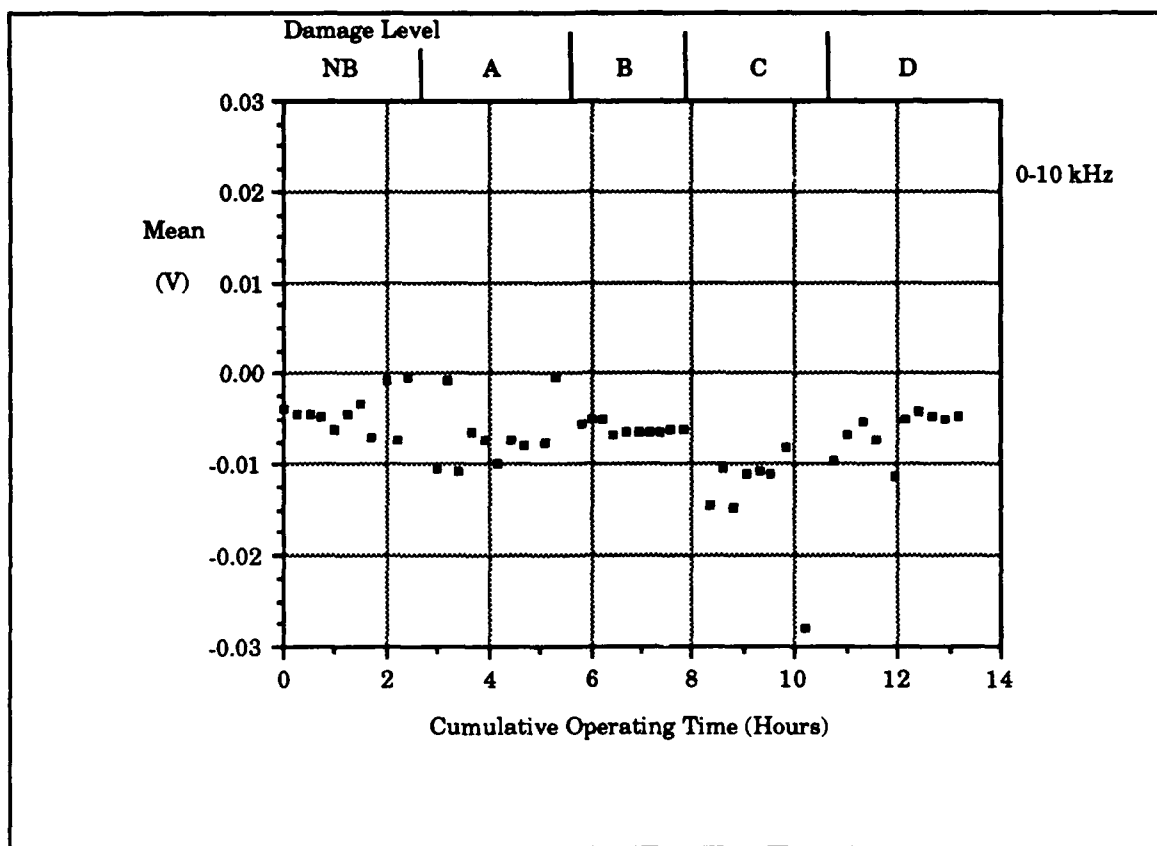
Figure 96. Mean value of 0.0 to 10.0 kHz frequency span.

The baseline magnitude is 0.005 volts, although it is not steady. A magnitude of 0.01 V is reached during damage level A, but returns to a lower level after continued operation. In damage level C the magnitude reaches 0.01V a second time, but returns to a lower level. The final series of data indicates that the level has stabilized at a value near the baseline measurements. The small change seen in this and other mean value measurements makes use of this parameter difficult to detect faults.

152

b *Frequency Span 0.27 to 1.53 kHz*

Figure 97 illustrates the data measured in the frequency span of 0.27 to 1.53 kHz. The data shows a general increase in the magnitude of the measured mean level.
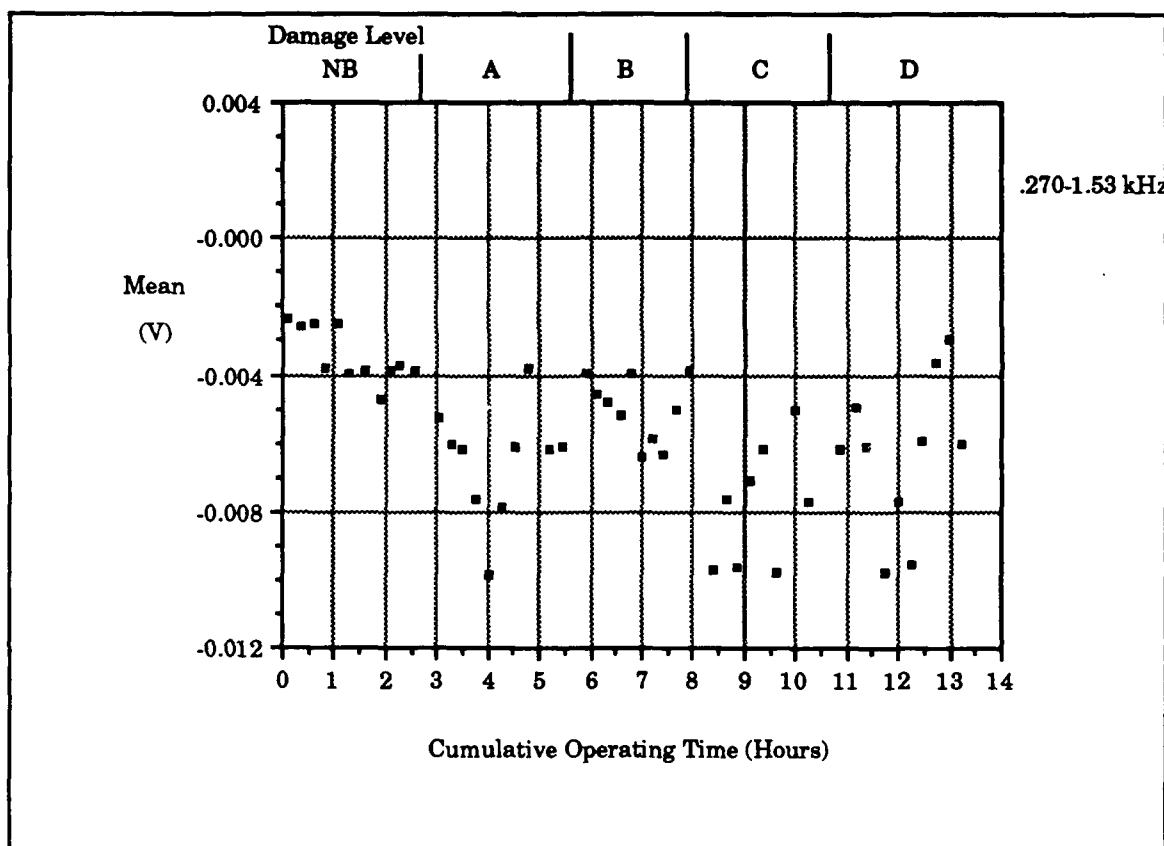
Figure 97. Mean value of 0.27 to 1.53 kHz frequency span.

The base line level for this measurement is estimated at 0.004 volts. Detection of a fault is difficult due to the scatter seen in the data.

c *Frequency Span of 1.62 to 2.88 kHz*

This data calculated from this measurement is presented in Figure 98. This plot is very flat in appearance with no significant change in level.
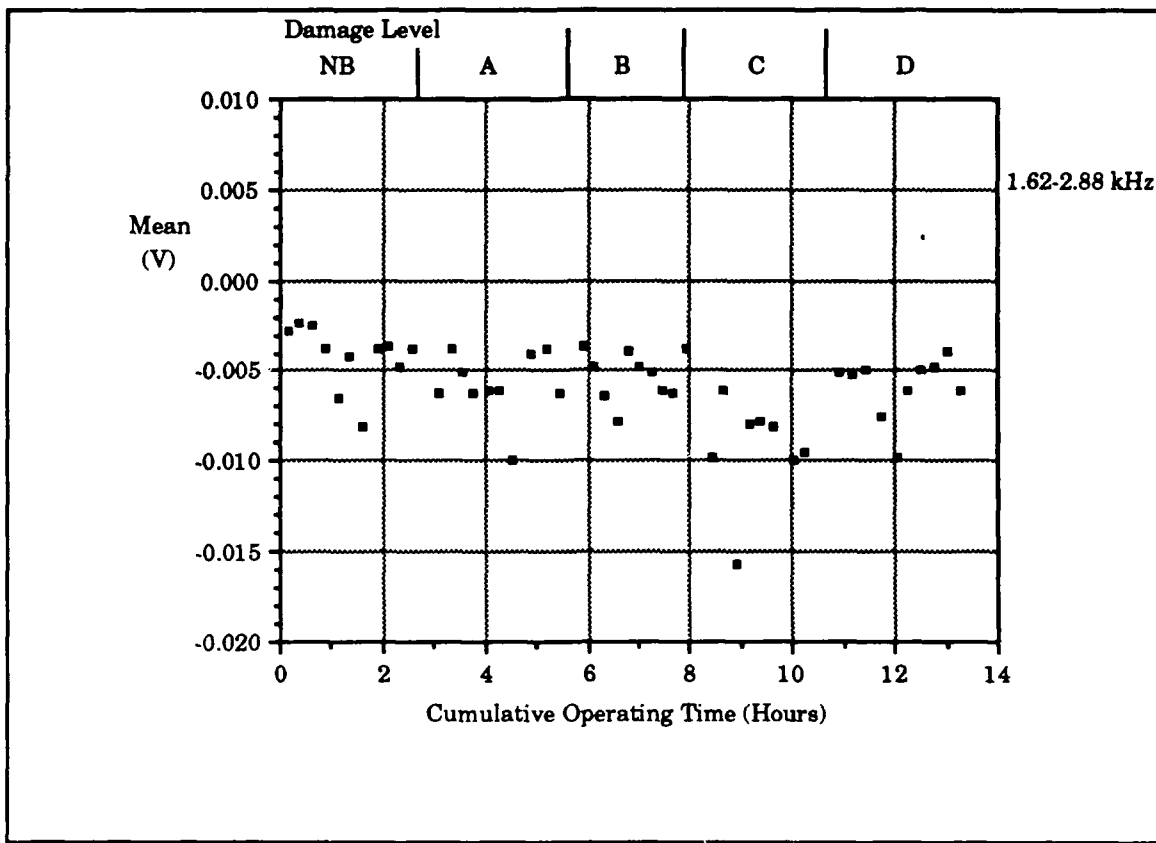
Figure 98. Mean value of 1.62 to 2.88 kHz frequency span.

Like the previous measurement the baseline magnitude of the measurement is near 0.0045 volts. A significant change in this level seems to occur during damage level C, but the level returns to a lower magnitude later in the experiment. Once again this plot shows data with quite a bit of scatter.

d Conclusions

The remaining frequency spans measured have similar results to those discussed, and analysis of each plot will not be made, however the remaining plots are provide in Appendix C for review.

The results from the measurement of the mean value of this pinion has results similar to that seen from pinion one. The

154

measurement over the span of 0.0 to 10.0 kHz proved to be the most effective in detecting a fault, other spans were plagued by a significant amount of scatter in the data.

2. Analysis of the Mean Square Value

The unresponsiveness of the statistical mean to the damage applied to the pinion was also seen in the measurement of the mean square value. In this experiment no frequency span met the fault detection criteria of a four fold increase over the baseline level, the cause for this appears to be the type of damage applied to the gears.

The broad band levels of the 0.0 to 10.0 kHz frequency spectra were a good indication of the results found when analyzing the mean square values. Figure 99 is the data collected from the 0.0 to 10.0 kHz frequency span. This measurement can be compared with the broad band measurement made from the frequency spectra shown in Figure 89.
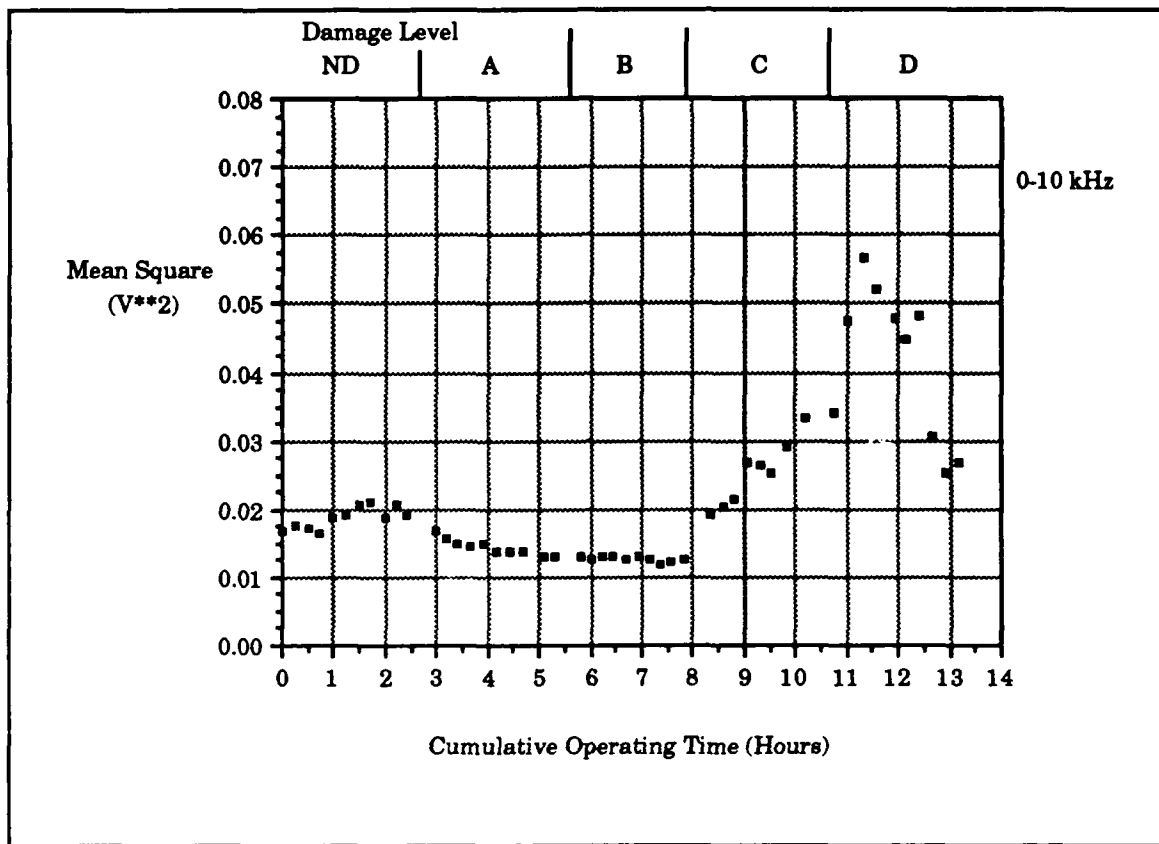
Figure 99. Mean square value for 0.0 to 10.0 kHz frequency span.

A comparison of Figures 89 and 99 reveals the frequency spectra measurements, with very little data, was very accurate in presenting the changes occurring to the gear.

The trend of the mean square value seen in pinion one measurements were also seen in the measurements of pinion two damage., frequency spans with low frequency content were responsive to pinion damage, but as the frequency content of the measurements increased the data showed less response to the damage. Figure 100 presents the results of the low frequency span 0.27 to 1.53 kHz.
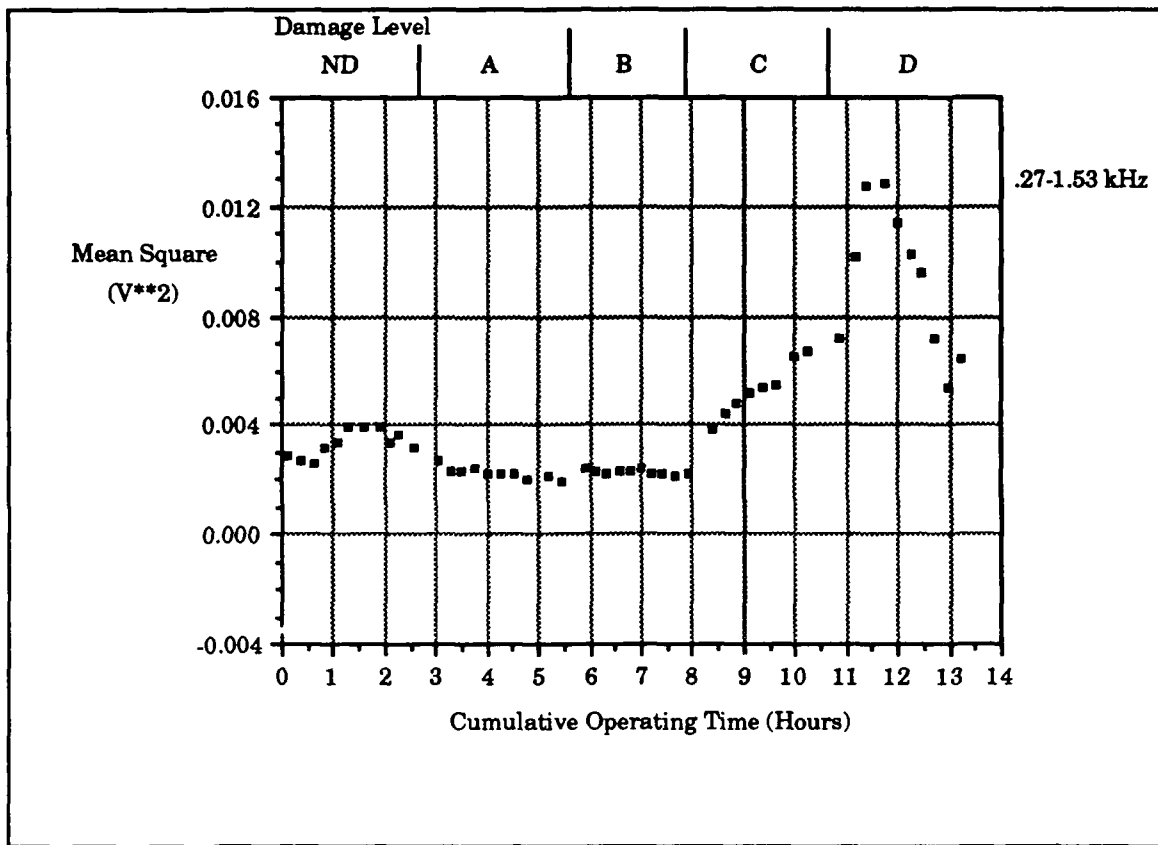
Figure 100. Mean square value of 0.27 to 1.53 kHz frequency span.

This graph shows a clear response to the damage applied on the pinion during damage levels C and D. During damage level D, as operation of the gears continued the level of the mean square value decreased indicating that some process might be reducing the effect of the damage to the gear.

Figure 101 presents the data collected over the frequency span of 2.97 to 4.23 kHz. This frequency span is made up of higher frequencies and reflects a flatter appearance.
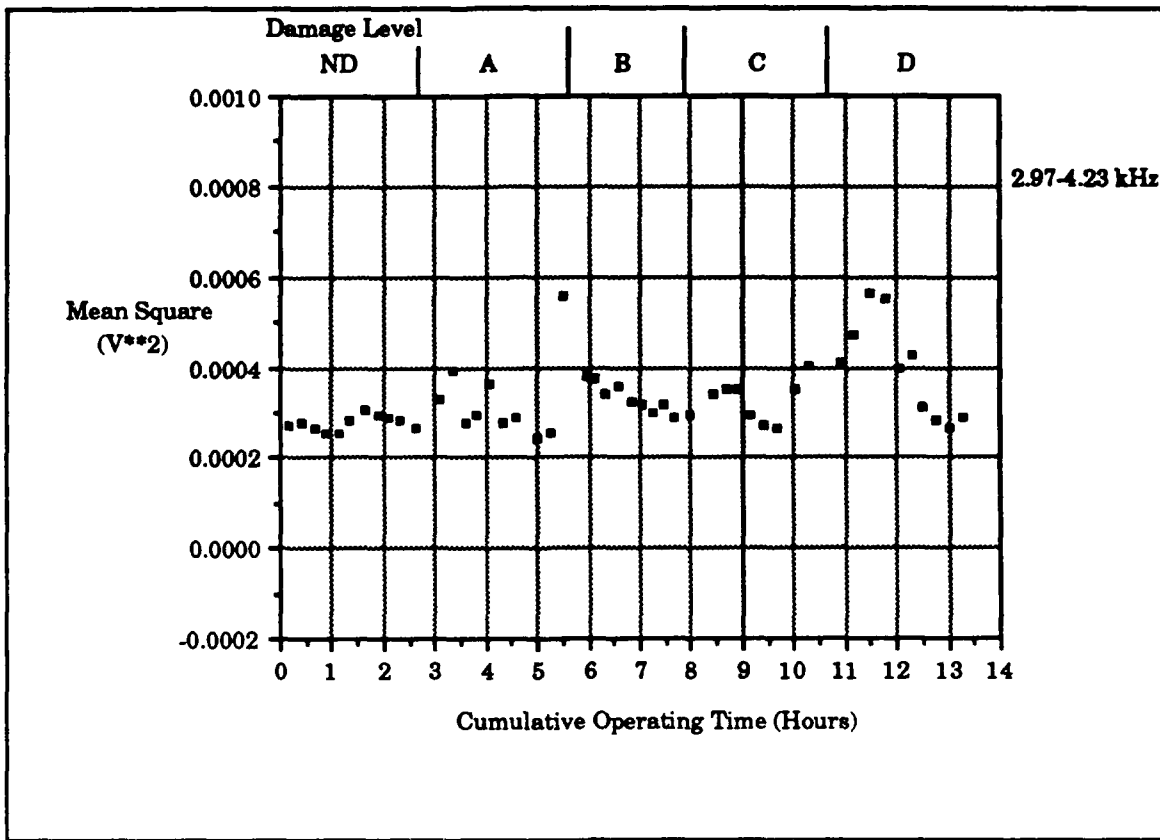
Figure 101. Mean square value of 2.97 to 4.23 kHz frequency span.

The increase in level during damage level C and D is still seen in this graph, but the relative change in level from the baseline measurement is not as large as the change that occurred in the 0.27 to 1.53 kHz span, (Figure 100).

Figure 102 represents the data collected in the frequency span 5.0 to 10.0 kHz frequency span. This graph shows the flattening of the response.
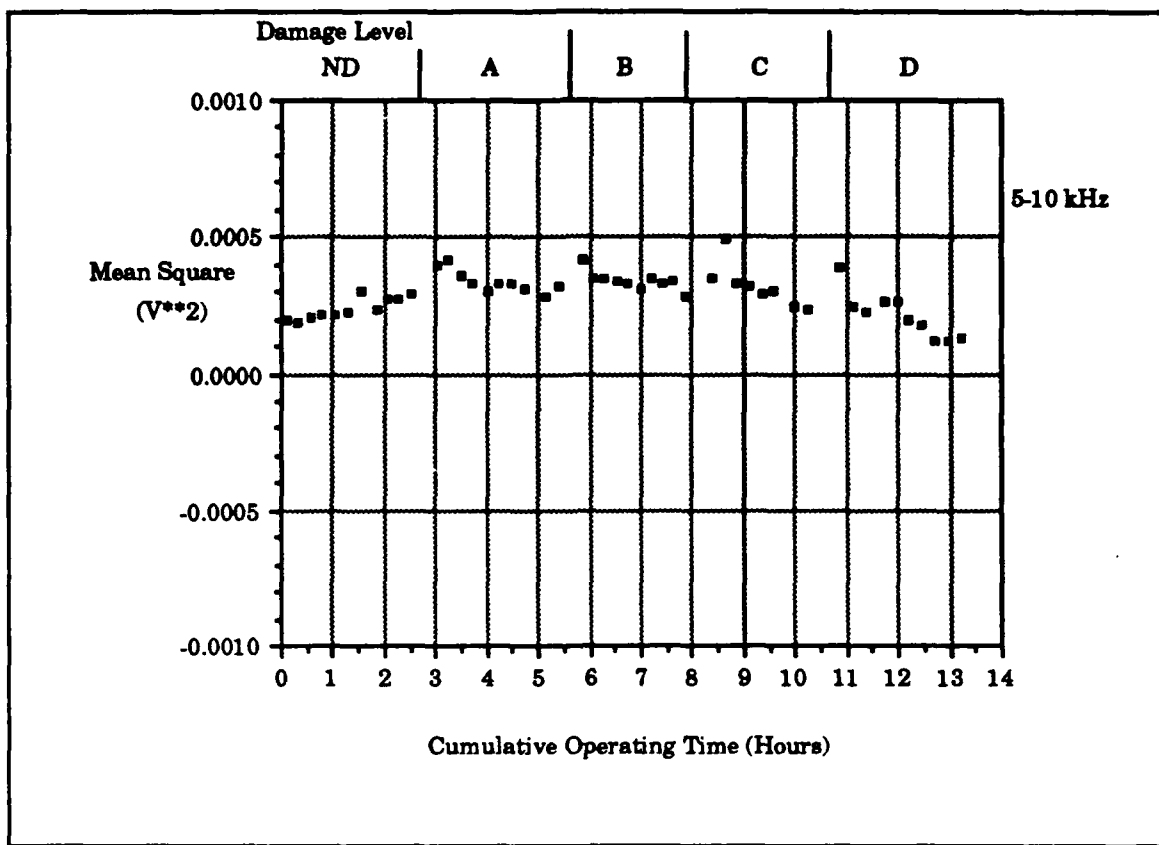
Figure 102. Mean square value of 5.0 to 10.0 kHz frequency span.

The rise in level seen during damage levels C and D in the lower frequency spans have been reduced to single rises in the data that quickly returns to the baseline levels. The increase in frequency content has made the data less useful for detection of damage using the criteria established for this investigation. It is interesting to note that in both Figures 101 and 102 at the start of both damage levels A and B an increase in the mean square was recorded. This level was not large enough to indicate a fault, but did occur after damage was made. These changes are not obvious in the measurements containing lower frequency components, (Figures 99 and 100). Similar results are seen in some the high frequency spans of pinion one. The high frequency spans

159

have a very small mean square value, when a small amount of damage occurs it may be able to be detected much earlier in the high frequency measurements because a small change has the capability of producing a significant change in the measured value. This aspect could prove useful in an automatic monitoring system after the parameters response to damage is more fully understood.

The remaining plots of the mean square data monitored are similar to the results presented and have been assembled in Appendix C. No additional information was gained from the data covering a larger frequency span than originally used.

3. Analysis of the Coefficient of Skewness

The response of the skewness parameter for this experiment was similar to that seen in the analysis of pinion one. The skewness measured with the frequency span 0.0 to 10.0 kHz is shown in Figure 103.
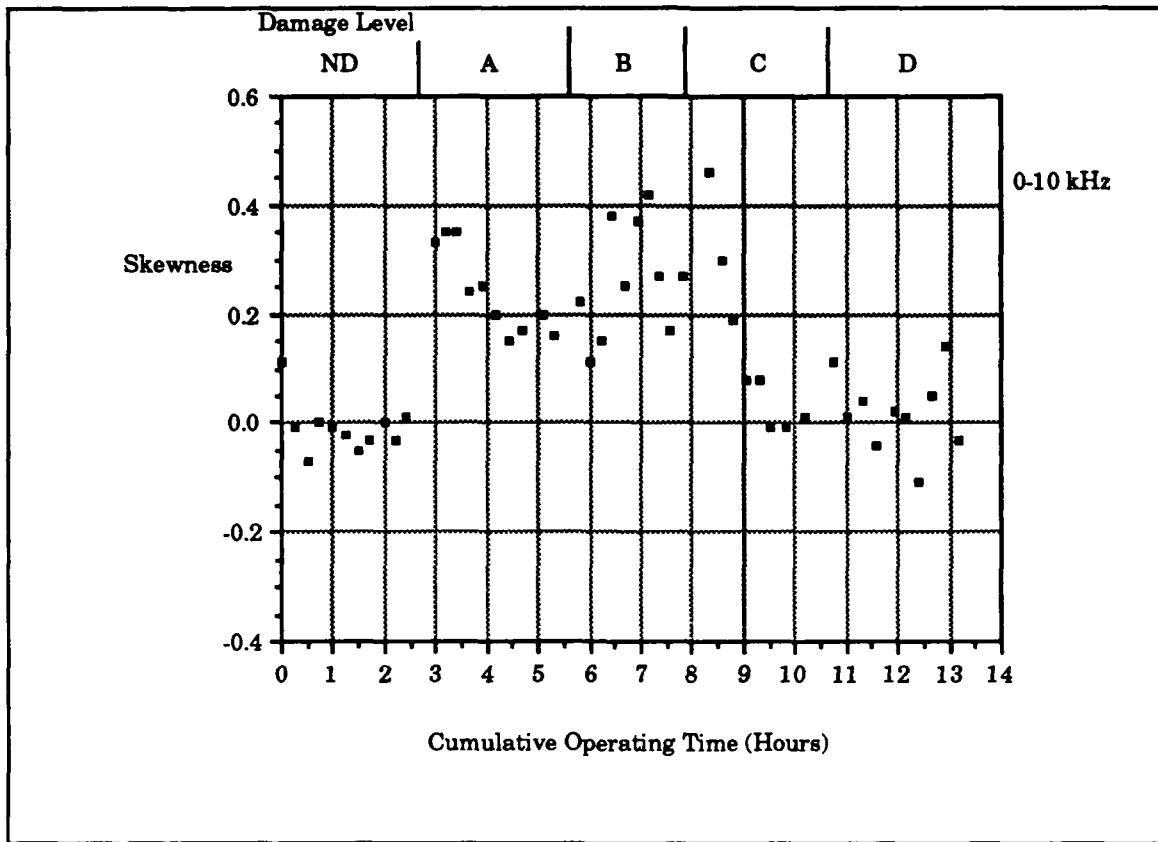
Figure 103. Skewness of the 0.0 to 10.0 kHz frequency span.

This figure shows a change in the skewness during damage level A. The level of the skewness parameter reaches the fault detection level at the start of damage level A, and although the level does fall it stays above the baseline level.

At the start of damage level B the skewness parameter again rises above 0.25 and maintains this level until midway through the damage level C portion of the run, at this point the skewness level falls back to the baseline level. This new level appears to have more scatter than the data then seen at the start of the run. Other frequency spans measured were of little use in detecting damage, having data with scatter and a magnitude near zero.

161

The skewness level for the 0.0 to 10.0 kHz frequency span has been very responsive to damage made on both pinions investigated. This responsiveness appears to be closely tied to the inclusion of the dc component of the monitored signal. Note that the accelerometer used in the investigation is not rated for use at the dc level, but it is capable of making measurements of the dc component. The coefficient of skewness is computed using equation (15).

$$\alpha_3 = \frac{m_3}{(\sigma^2)^{1.5}} \quad \text{(unitless)}$$

Skewness is computed using two quantities, the variance of the signal and the third moment about the mean. The variance of the measurements is essentially the same as the mean square value. The mean square value for the frequency range of 0.0 to 10.0 kHz was presented as Figure 99. Figure 103, shows the skewness value most responsive during damage levels A and B. The mean square value during damage levels A and B was fairly constant, Figure 99, this makes the denominator of equation (15) a constant value, indicating the change to the parameter was caused by an increase in the level of the third moment. The the third moment was also recorded in the measurements. The data measured is shown in Figure 104.
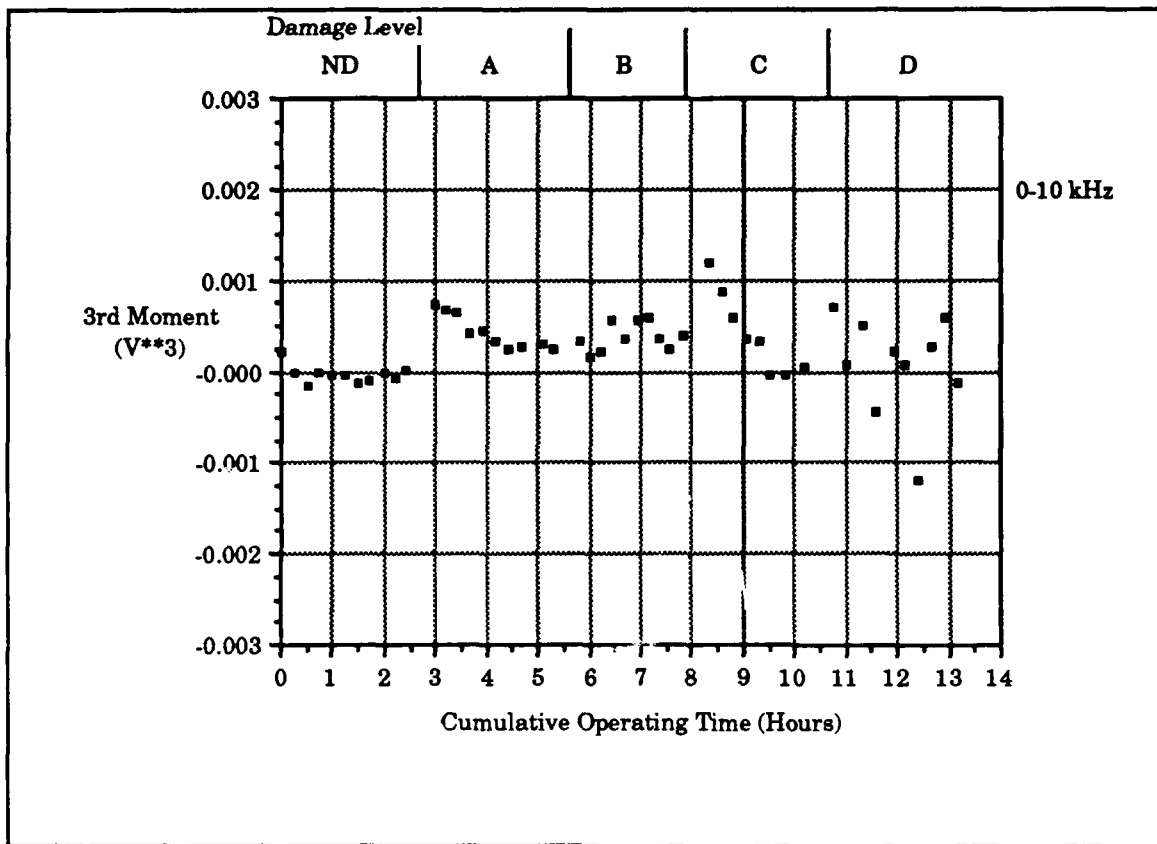
Figure 104. Third moment for 0.0 to 10.0 kHz span.

This data shows an increase in the magnitude of the third moment after the undamaged portion of the run. This increase from the baseline is maintained throughout the run, but is only reflected as an increase in the normalized skewness parameter when the mean square value is unresponsive. At the start of damage level C the third moment jumps and decreases rapidly, at the same time the mean square value is rising, this results in a decrease in the skewness. This response indicates that for this set of experiments the skewness of the signal is much more sensitive to the changes produced by the damage than the mean square value for early levels of damage . As damage

163

increases the skewness parameter becomes less sensitive because the mean square value starts to reflect the results of the damage.

Figure 105 can be used to make this explanation clearer. This figure shows the p.d.f. from a gear at two different states. The solid figure is an undamaged gear, while the dashed line is the p.d.f. of a damage gear.
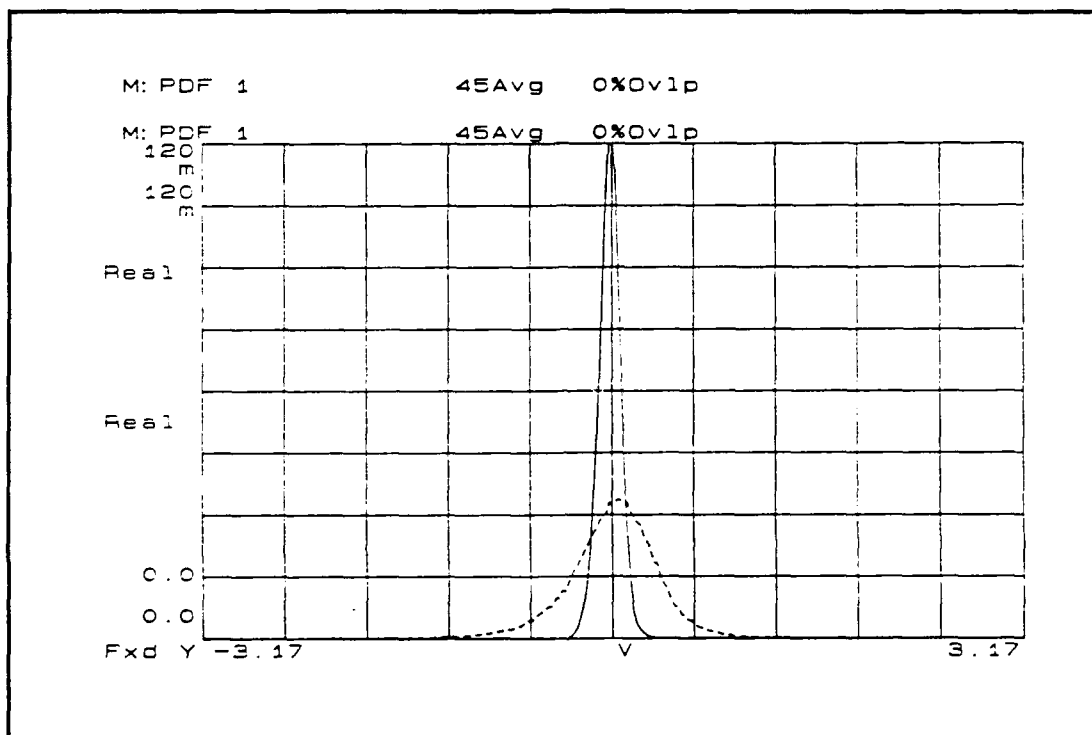
Figure 105 Effect of the mean square on skewness.

Skewness can be thought of as a comparison of the area to either side of the mean. In the figure, the p.d.f. of the undamaged gear is very tall when compared to the p.d.f. of the damaged gear. In the undamaged state the p.d.f. has a significant amount of area distributed in a small band near the mean, the tall narrow appearance of this area means that for small shifts in the symmetry of the p.d.f., the ratio of the areas can change dramatically.

164

For the damaged situation the p.d.f. has grown wider, this means that the area has been distributed away from the mean of the p.d.f. In this case a change in the symmetry of the p.d.f. will not affect the skewness as dramatically, because the area ratio cannot change significantly. This explanation also explains the significant shifts seen in the skewness during the early stages of the experiment, and the shifts in sign of the measurements. It also can be used to explain why the parameter tended to move back to the baseline level of zero.

4. Analysis of the Coefficient of Kurtosis

Analysis of the computed kurtosis levels from the damaged pinion two revealed that, the frequency spans containing higher frequency content were more responsive to the damage made to the gears.

a Kurtosis of the Frequency Span 0.0 to 10.0 kHz.

Figure 106 presents the results from the frequency span of 0.0 to 10.0 kHz.
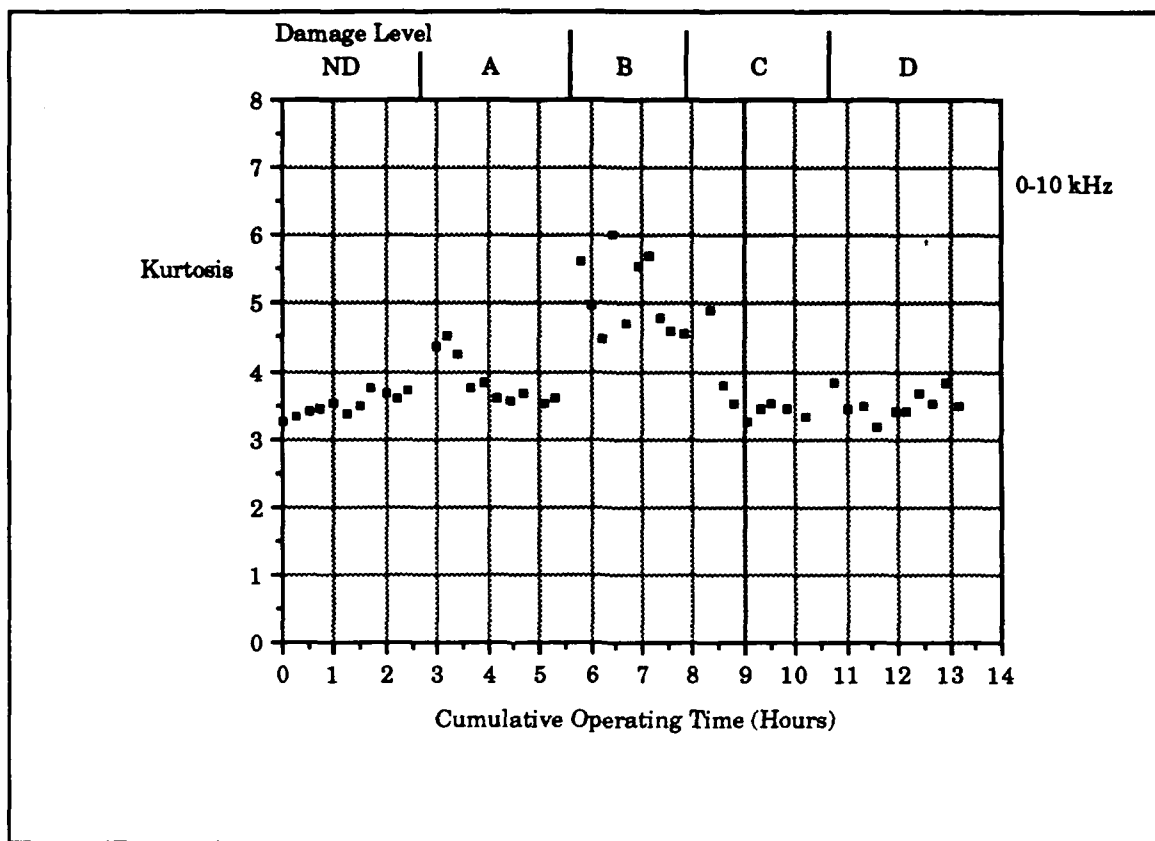
Figure 106. Kurtosis for frequency span 0.0 to 10.0 kHz

Fault detection criteria for the kurtosis level was at a level near 4.5. This figure shows a baseline level of the diagnostic machine at a level near 3.5. The cause of this high level is thought to be a result of damage accumulating on the 50 tooth gear from previous experiments. The response of the kurtosis level to the initial damage made to the gear is very good. In both damage levels A and B the kurtosis shows a rapid increase in level after the gear was damaged. During damage level A the kurtosis rises above 4.5 and remains at a high level, fault detection is considered to occur during this portion of the run.

The response of the parameter to the damage performed in damage level C and D is disappointing, but this is the region where the

mean square value begins to respond to damage, this increase results in a decrease to the Kurtosis level.

b. Kurtosis Levels for Low Frequency Spans.

Figure 107 presents the results of the kurtosis level measured over the frequency span of 0.27 to 1.53 kHz.
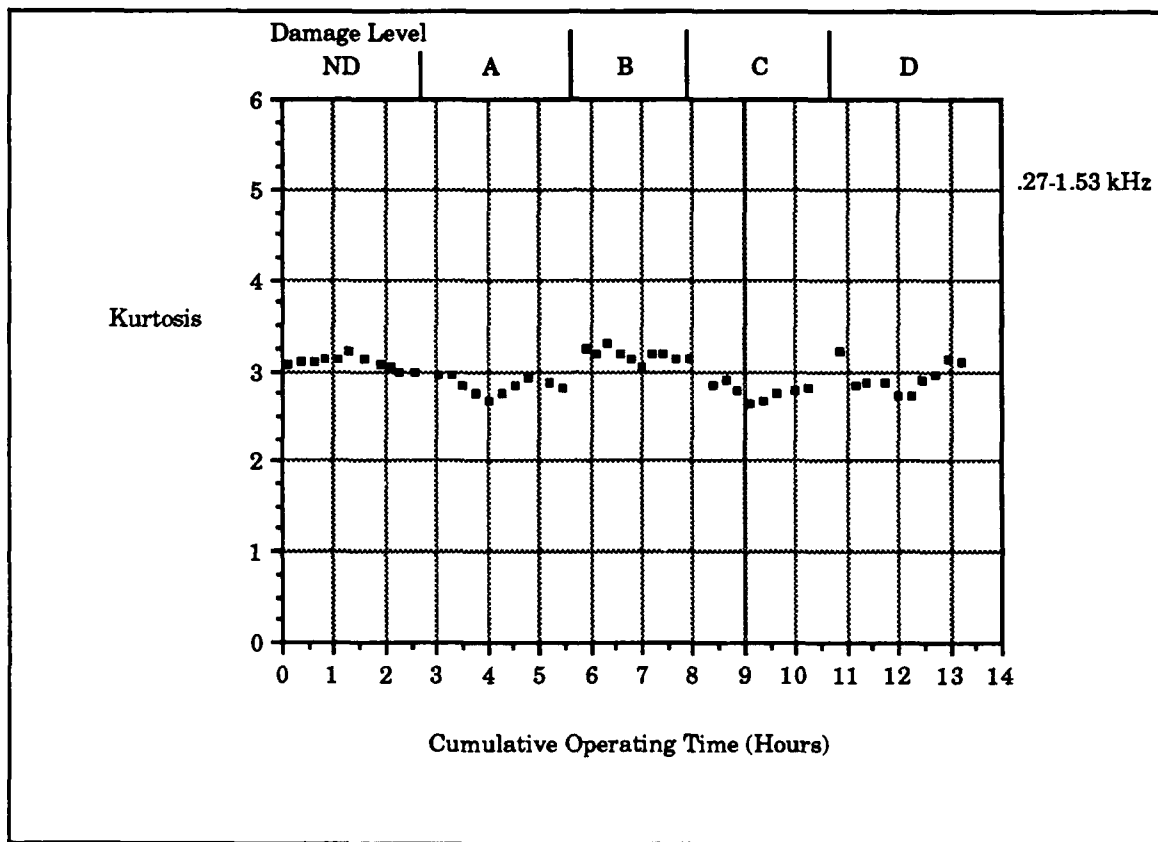
Figure 107. Kurtosis level of 0.27 to 1.53 kHz frequency span.

This figure shows little no response to damage. This aspect of the low frequency spans was seen in the analysis of pinion one and appears to be related to the high level of the mean square level in these frequency spans, and the filtering of the high frequencies. Figure 108 presents the results from the measurements made over the frequency span of 2.97 to 4.23 kHz.

167
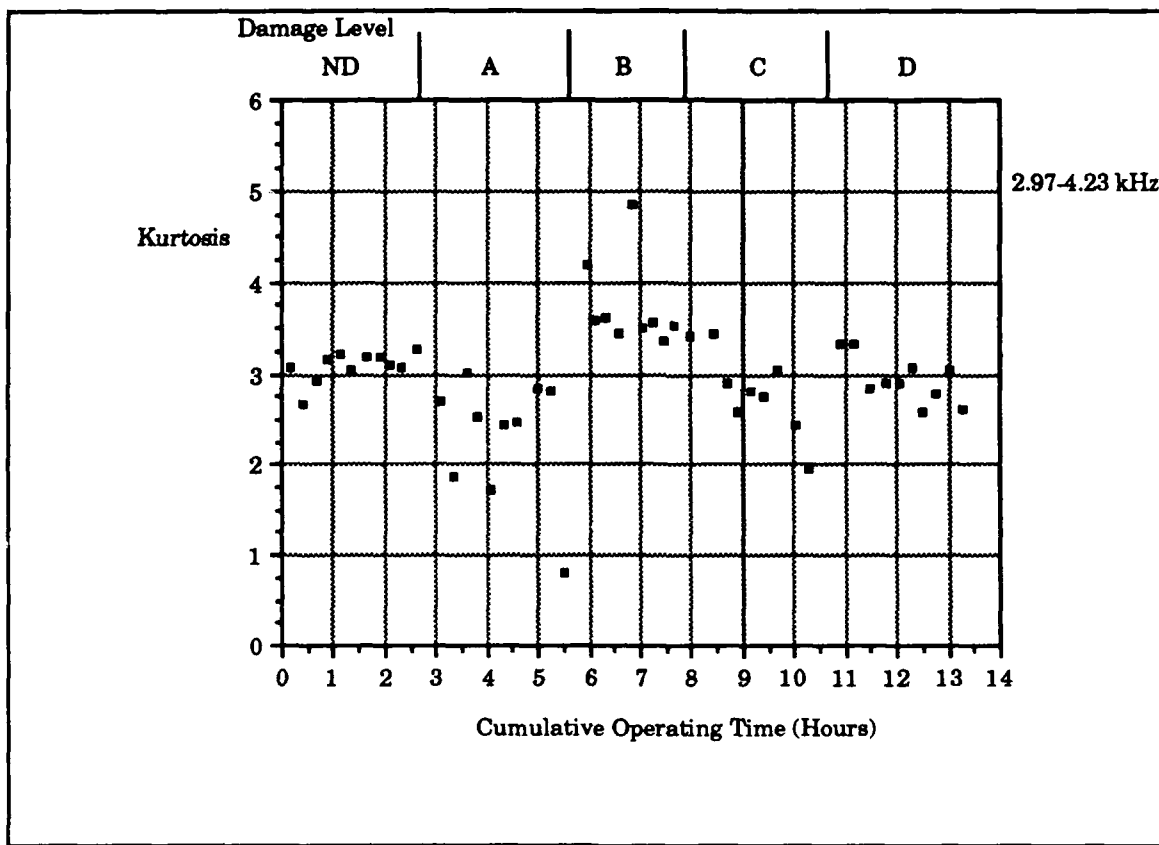
Figure 108. Kurtosis levels of 2.97 to 4.23 frequency span.

This figure shows the kurtosis level has more responsive to the damage, the kurtosis level shows an increase in level during damage level B, and indicates a fault detected.

c. Kurtosis Levels of High Frequency Spans.

Figure 109 shows the kurtosis parameter for the frequency span 4.32 to 5.58 kHz. This plot indicates a kurtosis level that is much more sensitive to the damage than the results seen previously.
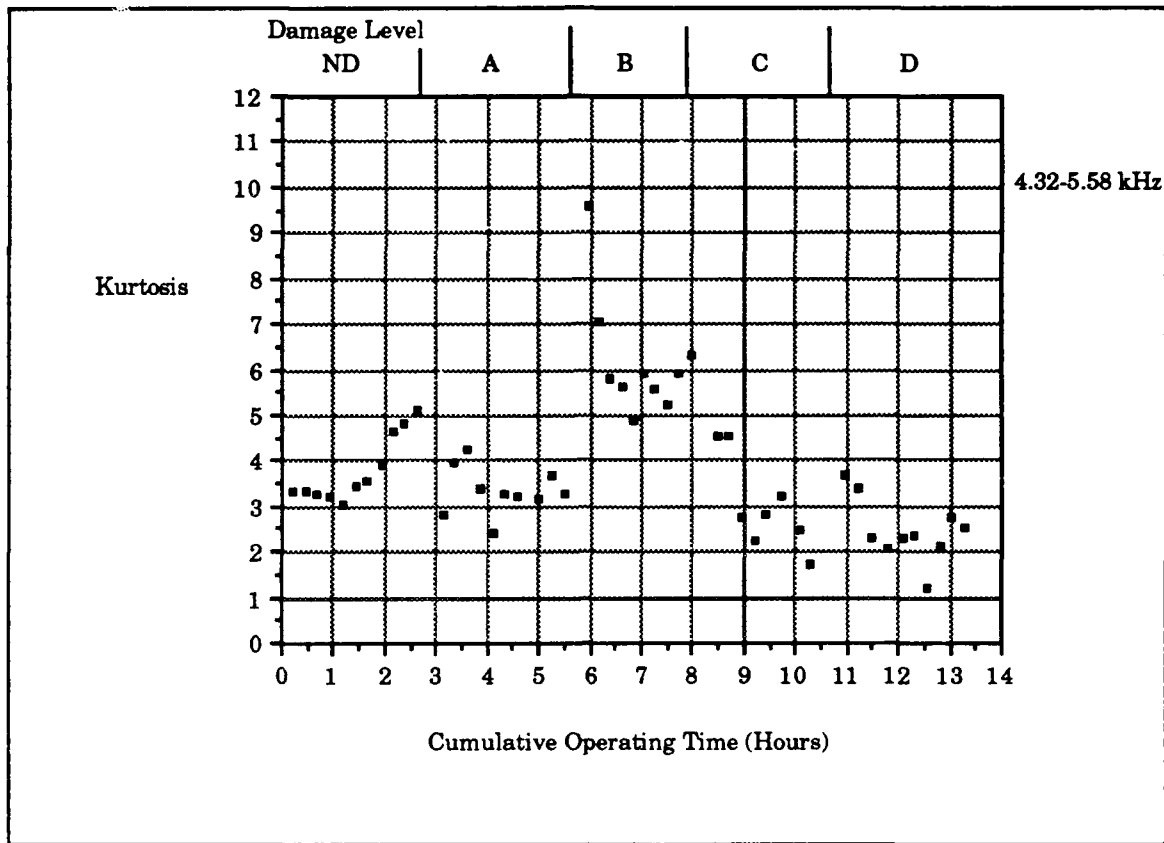
Figure 109. Kurtosis levels of the frequency span 4.32 to 5.58 kHz.

This figure shows an increase in kurtosis level during damage level A and B. The rise occurring in level A is large enough to indicate damage. The decrease in level after damage level B is not fully understood.

VIII. CONCLUSIONS AND RECOMMENDATIONS

A. CONCLUSIONS

This investigation focused on the use of statistical parameters as a method of fault detection. A diagnostics model configured as a speed reduction machine was used to investigate the changes in vibrations caused by damaging a gear in the model. Traditional frequency analysis techniques were used as a method of producing data with which the results from statistical parameters were compared to evaluate the effectiveness of the parameters in detecting faults.

Using statistical parameters, changes in the vibration signal produced by simulated faults were detected earlier than with frequency analysis. The use of a single statistical parameter was effective in detecting faults, however the parameters when used in combination were even more impressive.

The mean value was effective in reflecting a change in the vibration signal using a frequency span of 0.0 to 10.0 KHz. Other frequency spans measured were plagued by excessive scatter in the measured value. By its nature the magnitude of the mean value for a machine is fairly small. This small magnitude, combined with the scatter seen in the measurements make the mean value the least effective of the parameters measured for detecting change in the vibration signal.

The mean square value is a form of measurement traditionally used in vibration monitoring. This parameter was very effective in detecting faults in the middle and late stages of experiments, the major limitation of this parameter occurred when monitoring high frequencies. Figure

68 was developed from the data analysis showing that as the frequency content of the measurement increased the sensitivity of the parameter to damage decreased.

The analysis of the skewness was very surprising. Only measurement over a frequency span of 0.0 to 10.0 kHz was effective for detection of faults. By its nature skewness appears to be useful in detecting a fault in the early stages of development. Measurements made at other frequency spans were ineffective for fault detection due to filtering the dc component during measurements. Only one measurement included the dc component for this investigation, but other smaller frequency bands that include the dc component should be investigated to determine if improved results are achieved.

The coefficient of kurtosis, like the mean square value, was very effective in detecting changes in the vibration signal. The kurtosis value was more responsive to changes in the high frequency content of the signal. The frequency span of 5.0 to 10.0 KHz appeared to be the most responsive to damage with the least amount of scatter in this investigation, but a broader range could prove to be more effective.

Figure 110 illustrates the frequency spans where the individual parameters appeared most effective.
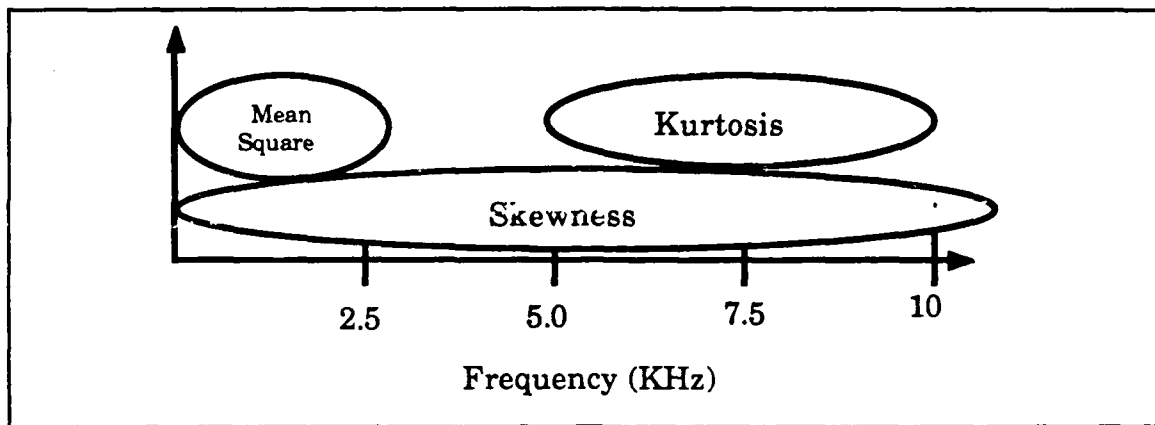
Figure 110. Effective regions of the statistical parameters.

These regions can be correlated with the frequency spectrum of the diagnostic model. Such a spectrum is provided in Figure 111.
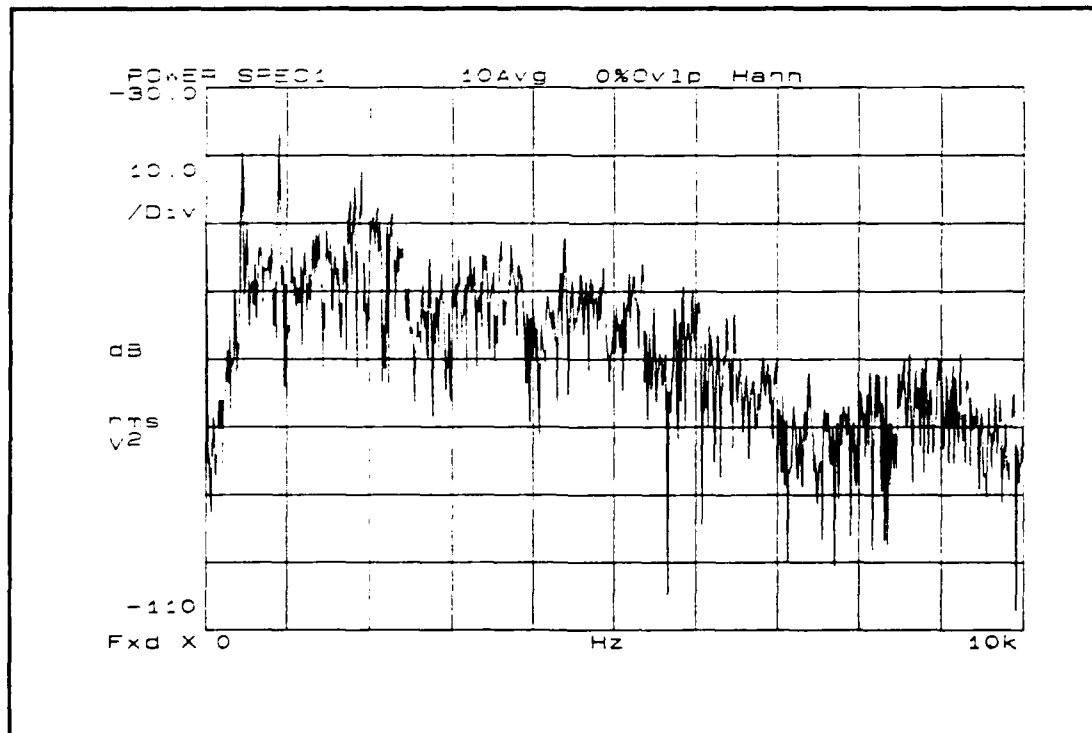
Figure 111. Frequency spectrum of the diagnostic model.

The effective frequency span of the mean square value covers much of the same range as the high amplitude components in the

172

spectrum, while the kurtosis level covers the smaller amplitude high frequency span. As was discussed, the skewness of the signal appears to be influenced by the dc component of the vibration signal, the optimum width of a monitoring band for skewness requires more investigation. Future study could investigate the relationship of the parameters with the spectrum and develop a method in which a frequency spectra could be used to quickly "set" the frequency limits used for the monitored parameters.

B. RECOMMENDATIONS

The results of this investigation indicate that further research into the use of statistical parameters for machinery fault detection would be justified.

Prior to any large scale investigation, additional basic research is needed to thoroughly investigate the response of the parameters to damage, the relationship of the parameters to frequency span monitored, and development of fault detection levels that ensure fault detection with minimum false alarms.

Another area of research needed is into the assumption that the monitored signal is stationary. Determine of the validity of this assumption needs to be made. During this investigation there was a minimum amount of time (about 1.5 hours) in which the diagnostics model had to be operated before statistical levels of the machinery stabilized, it is not unrealistic to expect actual machinery to have a similar limitation.

Research is required using of these parameters on actual machinery, and to investigate damage occurring to components other

than gears. This stage of investigation should include construction of a larger diagnostics model or/and use of actual machinery. The diagnostics model used in this investigation is limited because of its size and construction.

Development of hand held devices or automated electronics used to measure the statistical parameters and display results, or possibly evaluate results is an area ripe for investigation. In Reference [8], Stewart presents a block diagram of an analog circuit (included in Appendix D) which computes the kurtosis level of a input time signal. Using operational amplifiers this circuit can be constructed with little electronics background. Additional circuits using similar components can be designed to compute the other statistical parameters. More complex circuitry including analog to digital convertors and variable frequency spans could be justified by the results from research.

It is emphasized that use of these parameters is for detection purposes. Effective diagnostic techniques are available to trouble shoot faulty machinery, and although the analysis presented in the research attempted to explain changes in the parameters by relating them to events occurring in the machinery, the power of these methods is in the ability to screen out machinery that does not require attention and highlighting the machinery that does. Effective shipboard use by untrained maintenance personnel or development of cheap simple circuits which mindlessly compute probability distribution functions of electrical signals is a goal which can have significant returns.

APPENDIX A.

Specification sheet for model 302A06 accelerometer.

MODEL NO		302A05	302A06
RANGE (FOR ±5V OUTPUT)	±G	500	500
RESOLUTION	G	.01	.01
USEFUL OVERRANGE	G	1000	1000
SENSITIVITY (± 2%)	mV/G	10	10
RESONANT FREQUENCY (MTD)	kHz	30	30
FREQUENCY RANGE (±5%)	Hz	1-10000	1-10000
FREQUENCY RANGE (±10%)	Hz	-------	-------
DISCHARGE TIME CONSTANT 2	Sec	≥.5	≥.5
AMPLITUDE LINEARITY △1 % FS		1	1
POLARITY		POSITIVE	POSITIVE
OUTPUT IMPEDANCE	ohm	<100	<100
OUTPUT BIAS	- volt	8 to 14	8 to 14
OVERLOAD RECOVERY	μSec	10	10
TRANSVERSE SENSITIVITY	%	≤5	≤5
STRAIN SENSITIVITY	G/μin/in	.01	.01
TEMPERATURE RANGE	°F	-100 to +250	-100 to +250
TEMP COEFFICIENT	%/°F	≤.03	≤.03
VIBRATION (MAX)	±G's peak	2000	2000
SHOCK (MAX)	G	5000	5000
STRUCTURE		INVERTED	INVERTED
SIZE (HEX x HEIGHT)	inch	.50 x 1.3	.50 x 1.3
SEALING		EPOXY	EPOXY
CASE MATERIAL		ST STL	ST STL
WEIGHT	gm	25	25
CONNECTOR (micro)	coaxial	10-32	10-32
GROUND ISOLATION		NO	YES
EXCITATION	+ VDC/mA	24-27/2-20	24-27/2-20

△2 AT ROOM TEMPERATURE

△1 ZERO BASED BEST STRAIGHT LINE.
SUPPLIED ACCESSORIES:
SEE SHEET 1

APP'D			SPEC No.
ENGR			302-1010-80
SALES			

APPENDIX B.

Sample program used to collect data for this investigation.

```
10     !PROGRAM STATISTICAL DATA TAKER
20      !THIS PROGRAM TAKES THE PDF OF A MACHINE OVER VARIOUS FREQUENCY RANGES AND
THEN DETERMINES VARIOUS STATISTICAL PARAMETERS.
30      Dsa=720    !NAMES ADDR 720 THE DSA
40      PRINTER IS 701
50      PRINT "PROGRAM STATTAKER"
60      PRINT DATE$(TIMEDATE);"GEAR:___, DAMAGE LEVEL;LOAD:.70 AMPS;45 AVERAGES;SI
GNAL CONDITION ENDEVCO  UNIT #1"
70      !Freq=30                  !TROUBLE SHOOTING VARIABLE
80      FOR N=1 TO 100
90      !N IS A VARIABLE TO CONTROL THE NUMBER OF MEASUREMENT SERIES
100     GOSUB Hdr !PRINTS HEADER FOR DATA
110     !START OF CALIBRATION AND SPEED DETERMINATION
120     GOSUB Cal
130     OUTPUT Dsa;"IST"
140     ENTER Dsa;Is_b,te
150     !START OF FIRST MEASUREMENT
160     GOSUB Spd
170     PRINT Freq;"HZ"
180     GOSUB Setup
190     Fspan$="0-10"
200     OUTPUT Dsa;"ZST"
210     OUTPUT Dsa;"FRE10FHZ"
220     OUTPUT Dsa;"AJI"
230     WAIT 2.5
240     OUTPUT Dsa;"AUIU"
250     WAIT 3.5
260     OUTPUT Dsa;"STRT"
270     GOSUB Instrsts
280     T$=TIME$(TIMEDATE)
290     GOSUB Pdf
300     GOSUB Lfmt
310     !START OF 2ND MEASUREMENT
320     GOSUB Spd
330     PRINT Freq;"HZ"
340     GOSUB Setup
350     Fspan$="5-10"
360     OUTPUT Dsa;"SF5FHZ"
370     OUTPUT Dsa;"FRS5FHZ"
380     OUTPUT Dsa;"AUI"
390     WAIT 2.5
400     OUTPUT Dsa;"AUIU"
410     WAIT 3.5
420     OUTPUT Dsa;"STRT"
430     GOSUB Instrsts
440     T$=TIME$(TIMEDATE)
450     GOSUB Pdf
460     GOSUB Lfmt
470     !START OF 3RD MEASUREMENT
480     Fspan$="1-3H"
490     GOSUB Spd
500     PRINT Freq;"HZ"
```

176

```
510     GOSUB Setup
520     Fstrt=(1*15*Freq)-180
530     Fspn=(3*15*Freq)+180-Fstrt
540     OUTPUT Dsa;"SF";Fstrt;"HZ"
550     OUTPUT Dsa;"FRS";Fspn;"HZ"
560     OUTPUT Dsa;"AU1"
570     WAIT 2.5
580     OUTPUT Dsa;"AU1U"
590     WAIT 3.5
600     OUTPUT Dsa;"STRT"
610     GOSUB Instrsts
620     T$=TIME$(TIMEDATE)
630     GOSUB Pdf
640     GOSUB Lfmt
650     !START OF 4TH MEASUREMENT
660     Fspan$="4-6H"
670     GOSUB Spd
680     PRINT Freq;"HZ"
690     GOSUB Setup
700     Fstrt=(4*15*Freq)-180
710     Fspn=(6*15*Freq)+180-Fstrt
720     OUTPUT Dsa;"SF";Fstrt;"HZ"
730     OUTPUT Dsa;"FRS";Fspn;"HZ"
740     OUTPUT Dsa;"AU1"
750     WAIT 2.5
760     OUTPUT Dsa;"AU1U"
770     WAIT 3.5
780     OUTPUT Dsa;"STRT"
790     GOSUB Instrsts
800     T$=TIME$(TIMEDATE)
810     GOSUB Pdf
820     GOSUB Lfmt
830     !START OF 5TH MEASUREMENT
840     Fspan$="7-9H"
850     GOSUB Spd
860     PRINT Freq;"HZ"
870     GOSUB Setup
880     Fstrt=(7*15*Freq)-180
890     Fspn=(9*15*Freq)+180-Fstrt
900     OUTPUT Dsa;"SF";Fstrt;"HZ"
910     OUTPUT Dsa;"FRS";Fspn;"HZ"
920     OUTPUT Dsa;"AU1"
930     WAIT 2.5
940     OUTPUT Dsa;"AU1U"
950     WAIT 3.5
960     OUTPUT Dsa;"STRT"
970     GOSUB Instrsts
980     T$=TIME$(TIMEDATE)
990     GOSUB Pdf
1000    GOSUB Lfmt
```

```
1010   !START OF 6TH MEASUREMENT
1020   Fspan$="10-12H"
1030   GOSUB Spd
1040   PRINT Freq;"HZ"
1050   GOSUB Setup
1060   Fstrt=(10*15*Freq)-180
1070   Fspn=(12*15*Freq)+180-Fstrt
1080   OUTPUT Dsa;"SF";Fstrt;"HZ"
1090   OUTPUT Dsa;"FRS";Fspn;"HZ"
1100   OUTPUT Dsa;"AU1"
1110   WAIT 2.5
1120   OUTPUT Dsa;"AU1U"
1130   WAIT 3.5
1140   OUTPUT Dsa;"STRT"
1150   GOSUB Instrsts
1160   T$=TIME$(TIMEDATE)
1170   GOSUB Fdf
1180   GOSUB Lfmt
1190   PRINT
1200   PRINT
1210   NEXT N
1220   PRINTER IS 1
1230   STOP
1240   !THE REMAINDER OF THIS PROGRAM ARE THE CALLED SUBROUTINES
1250   !LINE FORMAT FOR DATA PRINT OUT
1260   Lfmt:Ttime=TIME(T$)
1270   PRINT USING "5D,1X,8A,1X,D.6D,1X,.8D,1X,.8D,1X,D.10D,1X,.10D,1X,2D.2D,1X,2
D.2D";Ttime,Fspan$,Mean,Msquare,Variance,Moment3,Moment4,Skewness,Kurtosis
1280   RETURN
1290 Hdr:PRINT "TIME   FS(KHZ)      M         MS         V          3          4
     S     K "
1300     RETURN
1310     !CALIBRATION ACCOMPLISHED AFTER EACH SERIES OF FREQS MEASURED
1320 Cal:OUTPUT Dsa;"AUTO 0"
1330     OUTPUT Dsa;"RST"
1340     OUTPUT Dsa;"SNGC"
1350     RETURN
1360     !!!!!!!!!!
1370     !SUBROUTINE MEASURES SPEED OF THE MODEL
1380     !!!!!!!!!!
1390 Spd:OUTPUT Dsa;"LNRS"
1400     OUTPUT Dsa;"PSPC"
1410     OUTPUT Dsa;"CH2"
1420     OUTPUT Dsa;"HANN"
1430     OUTPUT Dsa;"AVOF"
1440     OUTPUT Dsa;"ZST"
1450     OUTPUT Dsa;"FRS50HZ"
1460     OUTPUT Dsa;"SROF"
1470     OUTPUT Dsa;"AU2"
1480     OUTPUT Dsa;"C2AC1"
1490     OUTPUT Dsa;"FLT2"
1500     OUTPUT Dsa;"FREE"
```

```
1510      WAIT 3.0
1520      OUTPUT Dsa;"STRT"
1530      OUTPUT Dsa;"PSP2"
1540      WAIT 4.5
1550      OUTPUT Dsa;"PAUS"
1560      OUTPUT Dsa;"X"
1570      OUTPUT Dsa;"RDMK"
1580      ENTER Dsa;Freq,Y
1590      OUTPUT Dsa;"XOFF"
1600      !SPEED HAS TO LIE BETWEEN THESE FREQS OR ELSE THE PROGRAM GOES INTO A LO
OP WAITING FOR THE PROPER SPEED
1610      IF Freq<29.80 THEN GOTO 1520
1620      IF Freq>30.20 THEN GOTO 1520
1630      RETURN
1640      !!!!!!!!!!
1650      !SUBROUTINE SETS UP THE DSA TO MEASURE HISTOGRAM
1660      !!!!!!!!!!
1670 Setup: OUTPUT Dsa;"IS?"
1680        ENTER Dsa;Is_byte
1690        OUTPUT Dsa;"LNRS"
1700        OUTPUT Dsa;"CH1"
1710        OUTPUT Dsa;"HIST"
1720        OUTPUT Dsa;"ZST"
1730        OUTPUT Dsa;"FRS10KHZ"
1740        OUTPUT Dsa;"HANN"
1750        OUTPUT Dsa;"SROF"
1760        OUTPUT Dsa;"NAVG45ENT"
1770        OUTPUT Dsa;"OVRJ1"
1780        OUTPUT Dsa;"STBL"
1790        OUTPUT Dsa;"FLT1"
1800        OUTPUT Dsa;"C1AC"
1810        OUTPUT Dsa;"FREE"
1820        OUTPUT Dsa;"VLT1"
1830        OUTPUT Dsa;"AU1"      !AUTO RANGE UP
1840        !OUTPUT Dsa;"FSAV1"
1850        RETURN
1860        !!!!!!!!!!
1870        !SUBROUTINE COMPUTES THE STATISTICAL VALUES
1880        !!!!!!!!!!
1890 Pdf: !THIS ASSUMES THAT THE MEASUREMENT IS COMPLETE!
1900        OUTPUT Dsa;"B"
1910        OUTPUT Dsa;"PDF1"
1920        OUTPUT Dsa;"DIV TRCB"
1930        OUTPUT Dsa;"INGR"
1940        WAIT .1
1950        OUTPUT Dsa;"X"
1960        WAIT .3
1970        OUTPUT Dsa;"RDMK"
1980        ENTER Dsa;Xrg,Y
1990        OUTPUT Dsa;"X 0.0V"
2000        WAIT .2
```

179

```
2010        OUTPUT Dsa;"RDMK"
2020        ENTER Dsa;X,Y
2030        OUTPUT Dsa;"XOFF"
2040        OUTPUT Dsa;"SUB";Y
2050        WAIT .1
2060      !THIS PORTION CALCULATES THE MEAN OF THE SIGNAL
2070        OUTPUT Dsa;"A"   .
2080        OUTPUT Dsa;"PDF1"
2090        OUTPUT Dsa;"MPY TRCB"
2100        WAIT .1
2110        OUTPUT Dsa;"INGR"
2120        WAIT .1
2130        OUTPUT Dsa;"YASC"
2140        OUTPUT Dsa;"X";Xrg;"V"
2150        WAIT .2
2160        OUTPUT Dsa;"RDMK"
2170        ENTER Dsa;X,Mean
2180        OUTPUT Dsa;"XOFF"
2190      !THIS IS CALCULATION OF THE MEAN SQUARE
2200        OUTPUT Dsa;"A"
2210        OUTPUT Dsa;"PDF1"
2220        OUTPUT Dsa;"MPY TRCB"
2230        WAIT .1
2240        OUTPUT Dsa;"MPY TRCB"
2250        WAIT .1
2260        OUTPUT Dsa;"INGR"
2270        WAIT .1
2280        OUTPUT Dsa;"YASC"
2290        OUTPUT Dsa;"X"
2300        WAIT .1
2310        OUTPUT Dsa;"RDMK"
2320        ENTER Dsa;X,Msquare
2330        OUTPUT Dsa;"XOFF"
2340      !THIS PORTION CALCULATES THE VARIANCE
2350        Variance=Msquare-(Mean^2)
2360      !THIS PORTION CALCULATES THE 3RD MOMENT
2370        OUTPUT Dsa;"B"
2380        OUTPUT Dsa;"SUB";Mean
2390        WAIT .1
2400        OUTPUT Dsa;"A"
2410        OUTPUT Dsa;"PDF1"
2420        OUTPUT Dsa;"MPY TRCB"
2430        WAIT .1
2440        OUTPUT Dsa;"MPY TRCB"
2450        WAIT .1
2450        OUTPUT Dsa;"MPY TRCB"
2470        WAIT .1
2480        OUTPUT Dsa;"INGR"
2490        WAIT .1
2500        OUTPUT Dsa;"X";Xrg;"V"
```

```
2510      WAIT .2
2520      OUTPUT Dsa;"RDMK"
2530      ENTER Dsa;X,Moment3
2540      OUTPUT Dsa;"XOFF"
2550    !THIS PORTION CALCULATES THE 4TH MOMENT
2560      OUTPUT Dsa;"A"
2570      OUTPUT Dsa;"PDF1"
2580      OUTPUT Dsa;"MPY TRCP"
2590      WAIT .1
2600      OUTPUT Dsa;"MPY TRCB"
2610      WAIT .1
2620      OUTPUT Dsa;"MPY TRCB"
2630      WAIT .1
2640      OUTPUT Dsa;"MPY TRCB"
2650      WAIT .1
2660      OUTPUT Dsa;"INGR"
2670      WAIT .1
2680      OUTPUT Dsa;"X"
2690      OUTPUT Dsa;"RDMK"
2700      ENTER Dsa;X,Moment4
2710      OUTPUT Dsa;"XOFF"
2720    !THIS CALCULATES THE SKEWNESS AND KURTOSIS FOR THE JUST MEASURED SIGNAL
2730      Skewness=Moment3/(Variance^1.5)
2740      Kurtosis=Moment4/(Variance^2)
2750      RETURN
2760      !!!!!!!!!!!
2770      !SUBROUTINE WAITS FOR THE DSA TO SIGNAL MEASUREMENT COMPLETE
2780      !!!!!!!!!!!
2790 Instrsts:   OUTPUT Dsa;"IS?"
2800              WAIT 3
2810              ENTER Dsa;Is_byte
2820              IF BIT(Is_byte,2) THEN 2840
2830              GOTO Instrsts
2840              RETURN
2850  END
```

181

APPENDIX C.

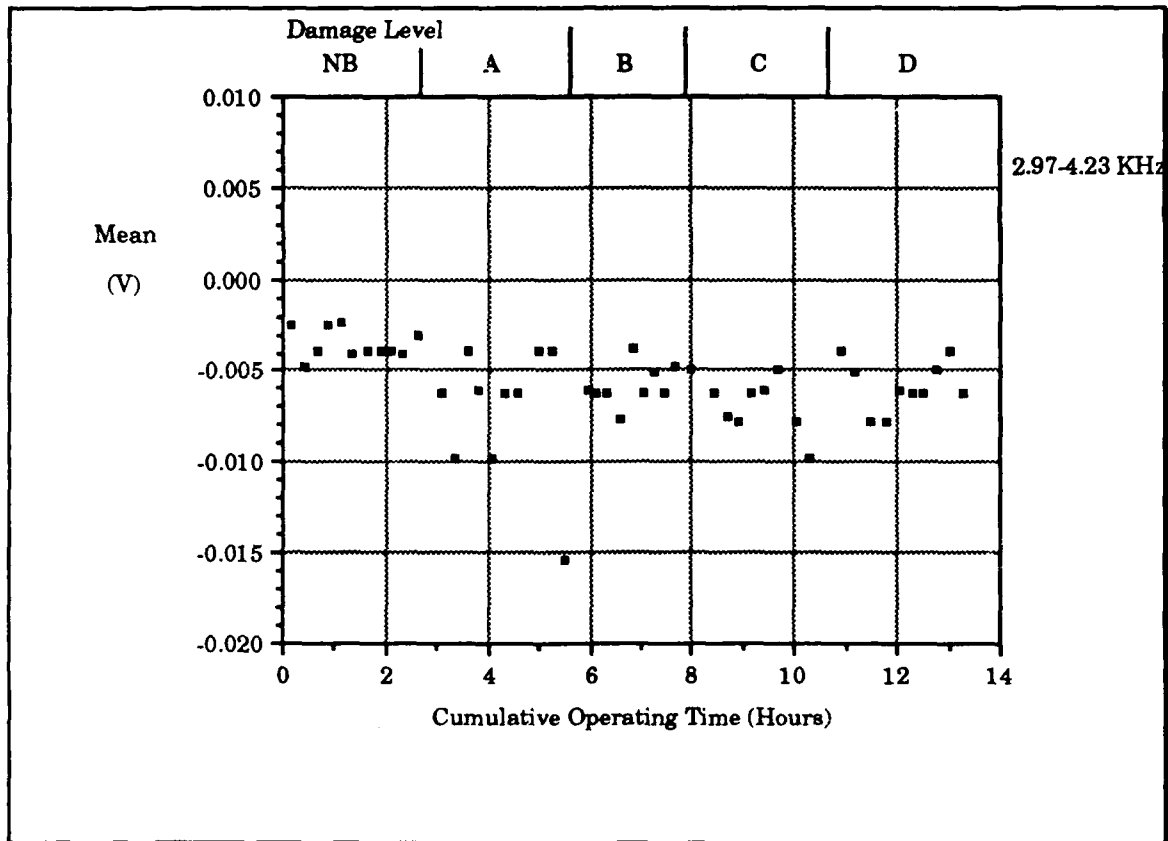Plots of pinion two data not presented in the main body.

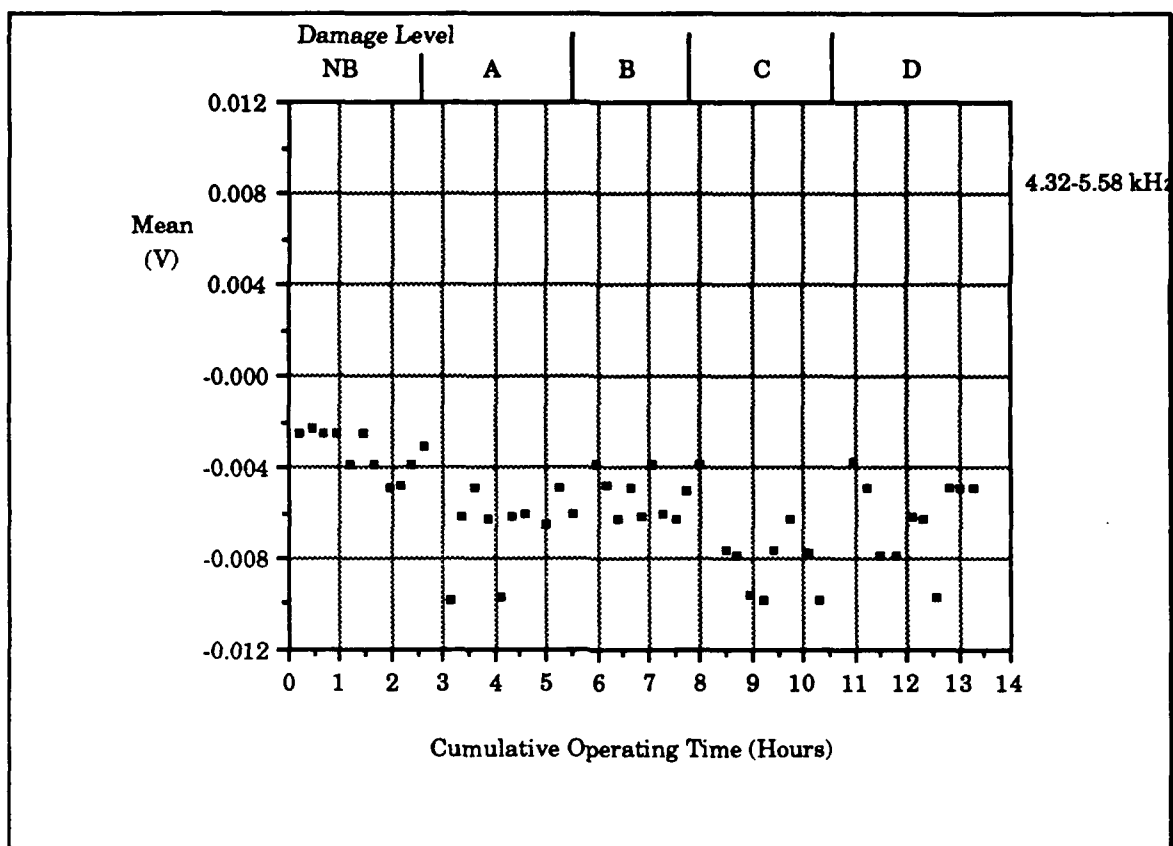Figure 112. Mean of 2.97 to 4.23 kHz frequency span.
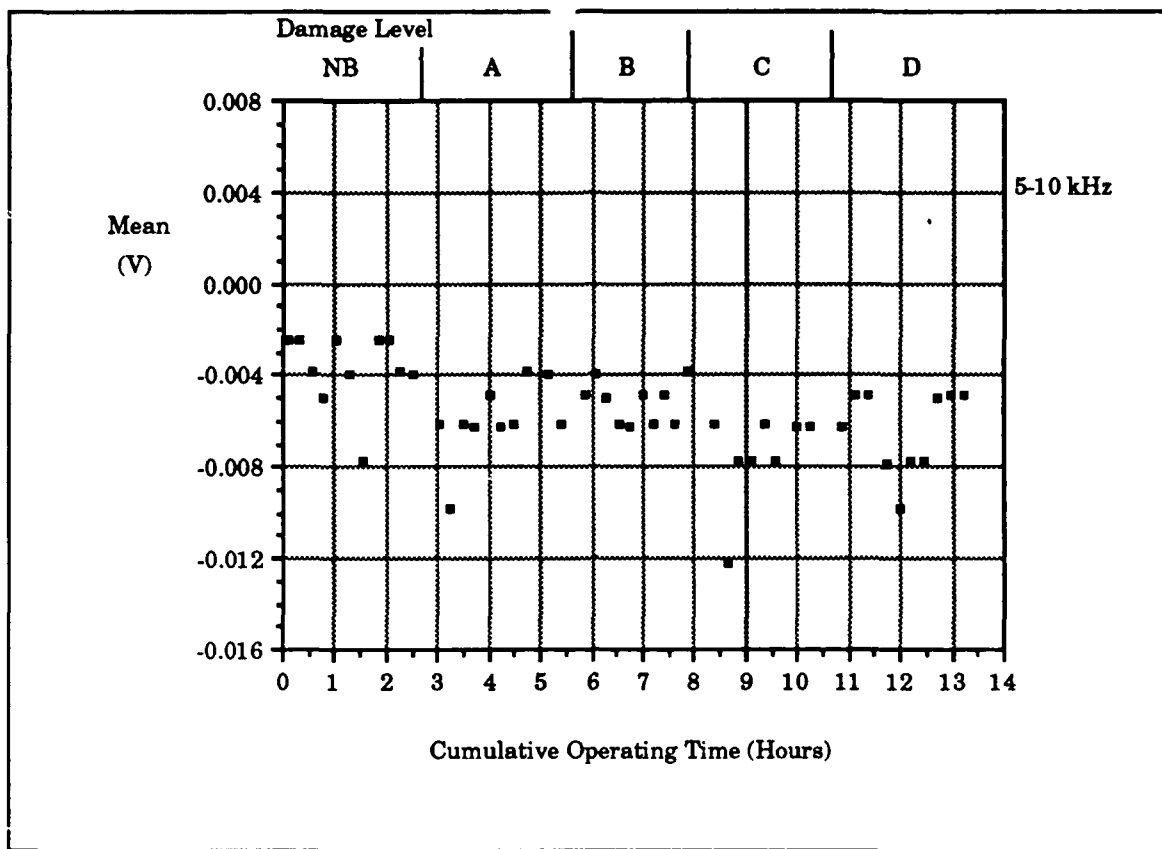
Figure 113. Mean of 4.32 to 5.58 kHz frequency span.

183

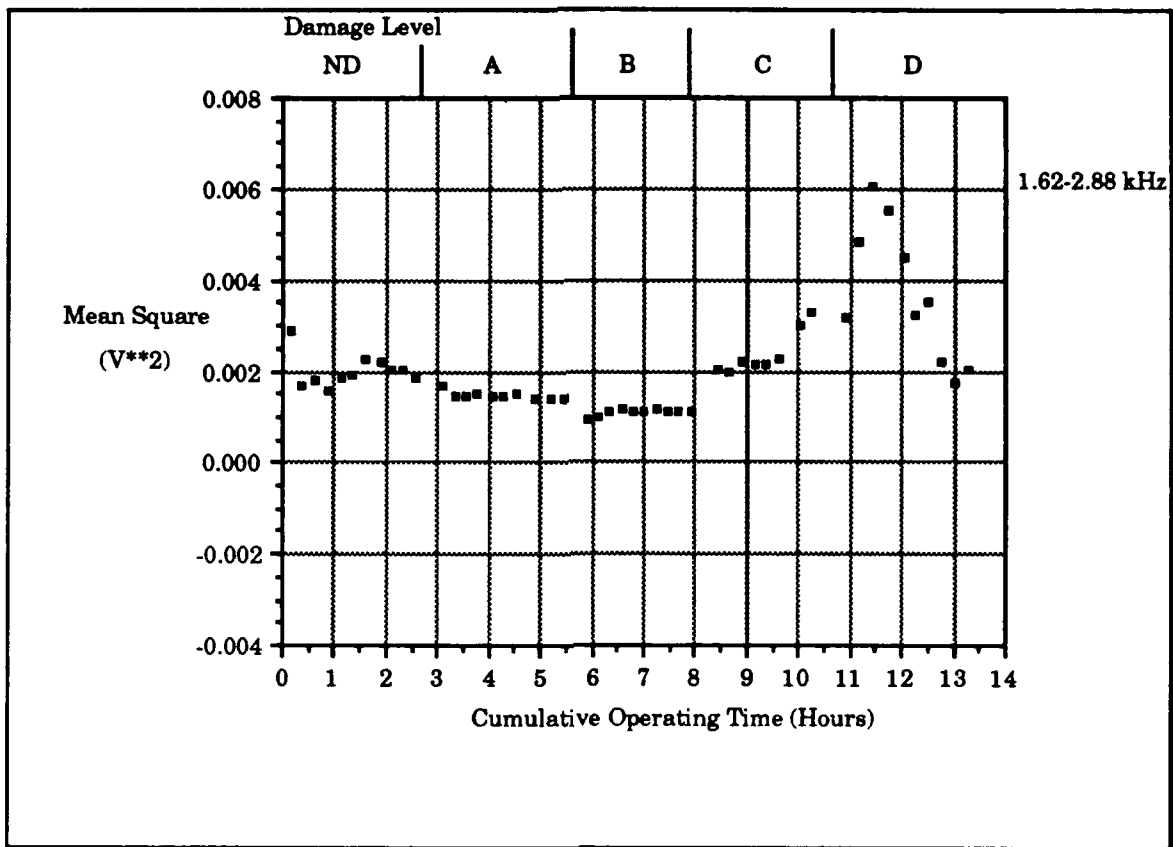**Figure 114. Mean of 5.0 to 10.0 kHz frequency span.**

184

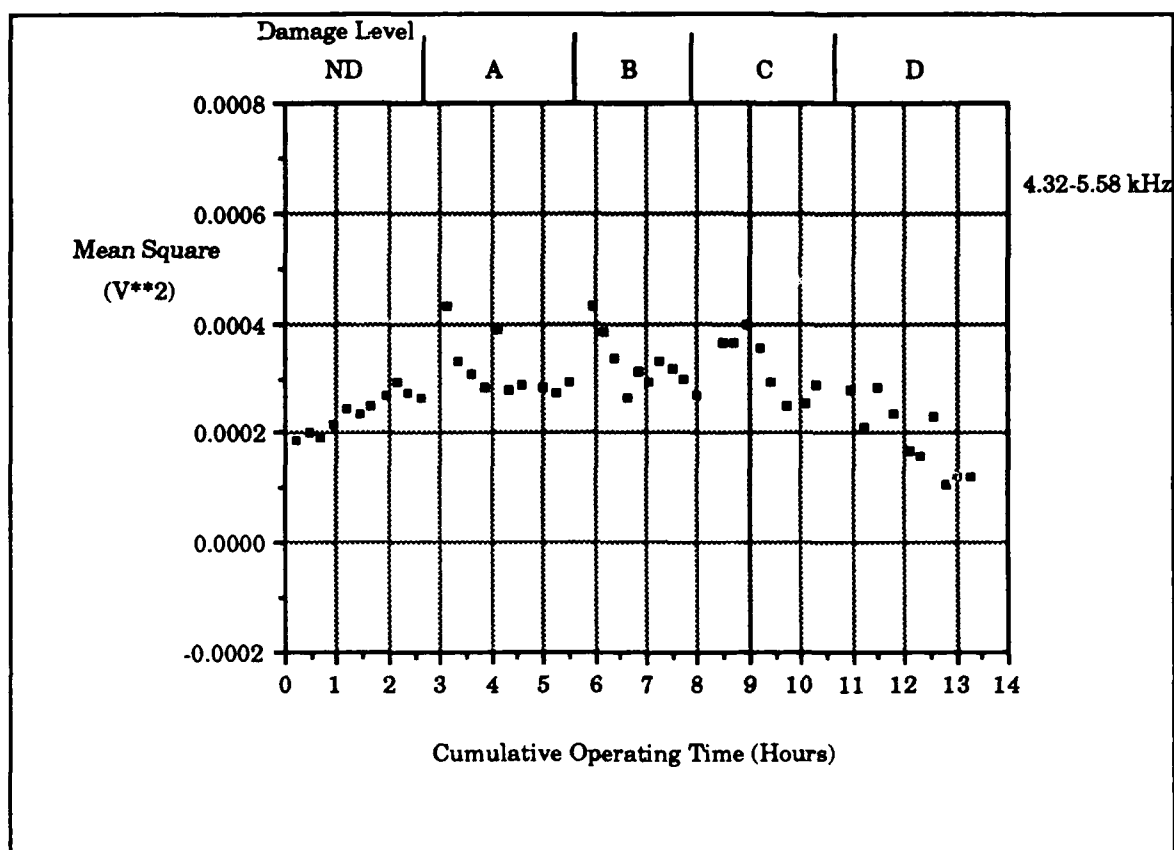Figure 115. Mean square of 1.62 to 2.88 kHz frequency span.

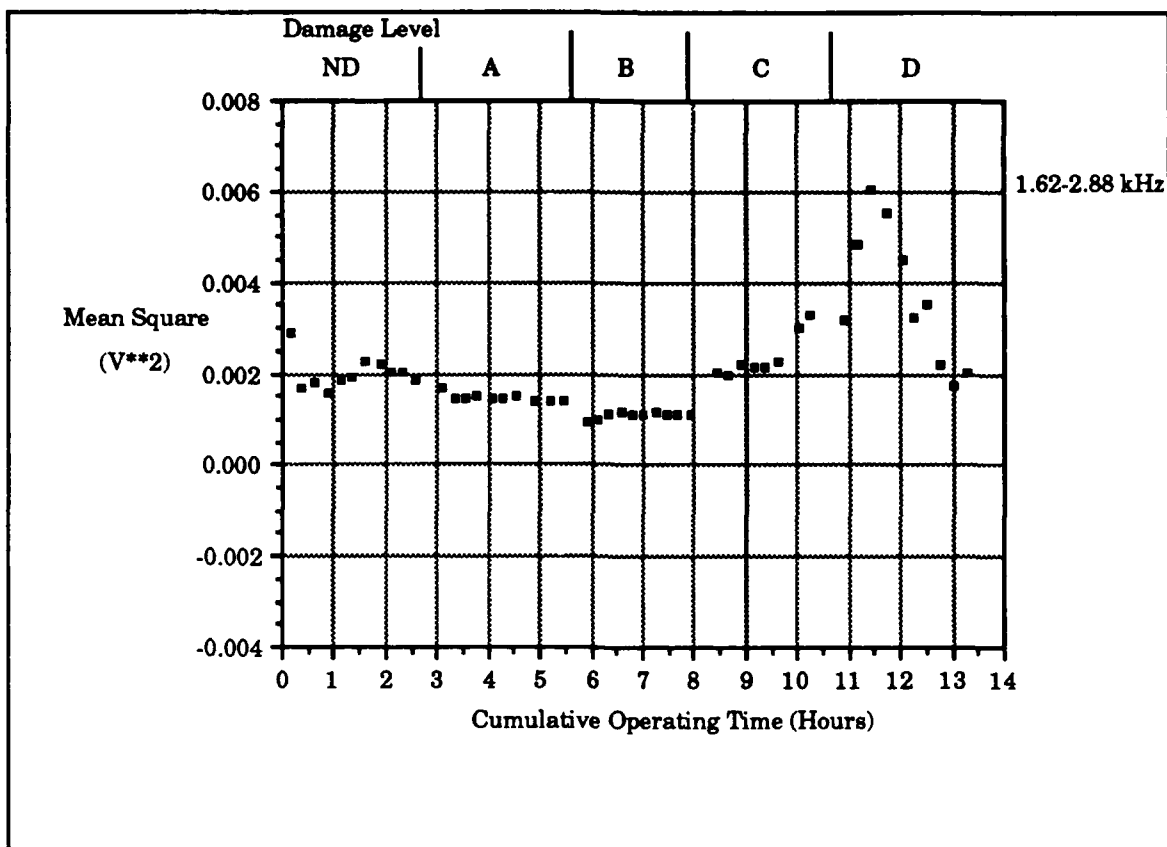Figure 116. Mean square of 4.32 to 5.58 kHz frequency span.

Figure 117. Kurtosis level for 1.62 to 2.88 kHz frequency span.
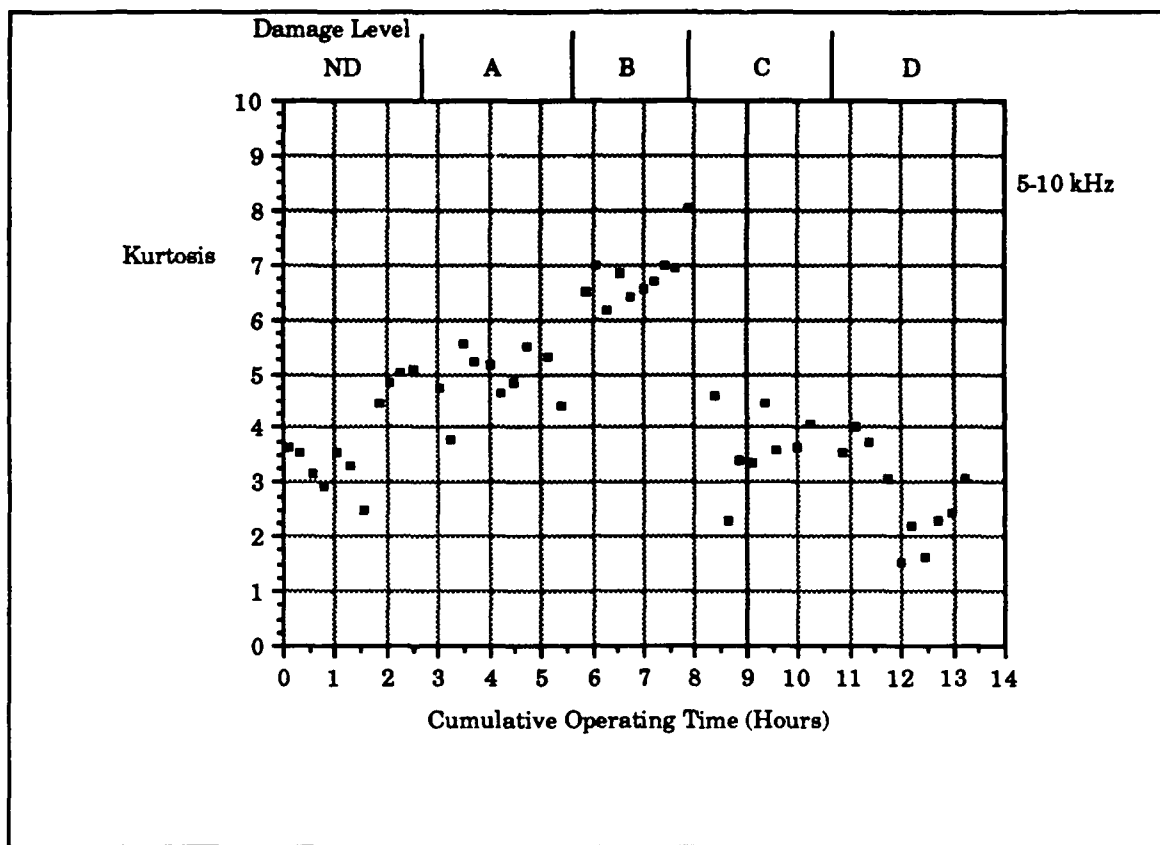
187

Figure 118. Kurtosis level for 5.0 to 10.0 kHz frequency span.

APPENDIX D.

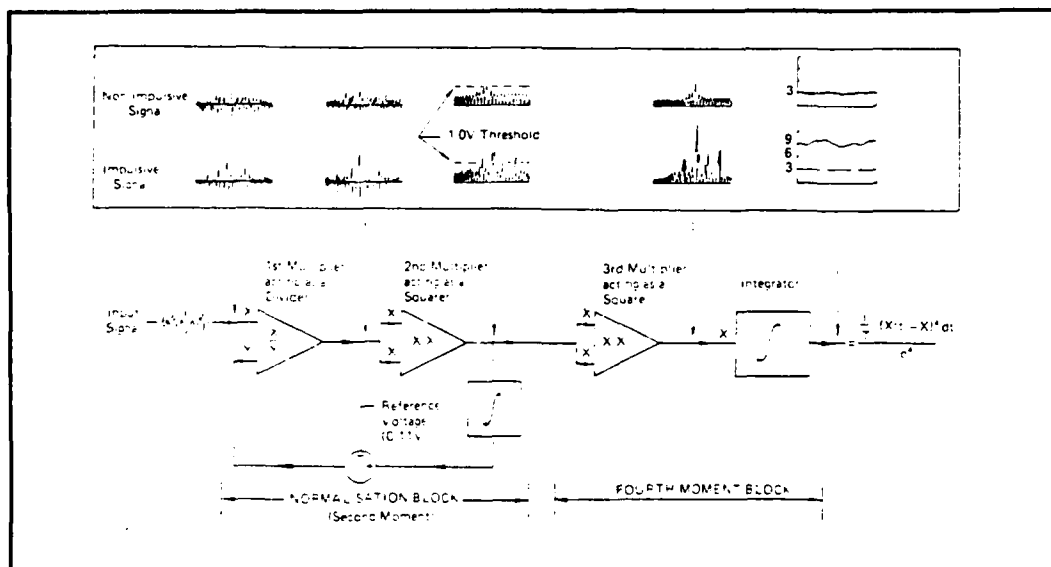Simple circuit from Reference [8] that can be used to measure a broad band kurtosis level.

Figure 119. Kurtosis monitoring circuit.

LIST OF REFERENCES

1. Strunk, William D.,"Considerations for the Establishment of a Machinery Monitoring and Analysis Program for Surface Ships of the U.S. Navy," <u>Proceedings of the 6th International Modal Analysis Conference</u>, January 1988, pp 914-920.

2. Stamm, J.A.,<u>Machinery Diagnostics Via Mechanical Vibration Analysis Using Spectral Analysis Techniques</u>, Master's Thesis,Naval Postgraduate School, Monterey, California, September 1988.

3. Mathew, J., "Machine Condition Monitoring Using Vibration Analyses," *Acoustics Australia*, v. 15, pp 7-13, April 1987.

4. Angelo, M., "Vibration Monitoring of Machines," *B & K Technical Review*, n. 1, pp 1-36, 1987.

5. Merritt, H.E., <u>Gears</u>. London: Sir Issaac Pitman And Sons, LTD, 1961.

6. Smith, J. D., <u>Gears and Their Vibrations</u>, New York: Marcel Dekker, Inc.,1983.

7. Mark,W. D., "Gear Noise Origins," AGARD Conference Proceedings, No. 369, pp 30-1- 30-14.

8. Stewart, R. M., "Application of Signal Processing Techniques to Machinery Health Monitoring," <u>Noise and Vibration</u>, edited by White, R.G., and Walker, J.G., New York,John Wiley & Sons, Chptr. 23, 1982.

9. Smith,J.D. "Transmission Error Measurement in Gearbox Development," <u>AGARD Conference Proceedings</u>, No. 369, pp 33-1 - 33-5.

10. Bruan, S.,ed., <u>Mechanical Signature Analysis</u>, Orlando, Fl., Academic Press Inc., 1986.

11. Bendat, J.S., and Piersol, A.G., <u>Engineering Applications of Correlation and Spectral Analysis,</u> New York, John Wiley & Sons, 1980.

12. Bendat, J.S., and Piersol, A.G., <u>Random Data Analysis and Measurement Procedures,</u> New York, John Wiley & Sons, 1986.

13. Newland, D.E., <u>An Introduction to Random Vibrations and Spectral Analysis</u>, Longman, 1975.

14. Randall, R.B., "Computer Aided Vibration Spectrum Trend Analysis for Condition Monitoring," *Maintenance International*, v. 5, 1985, pp. 185-167.

15. R. B. Randall, "A New Method of Modeling Gear Faults,"*Transactions of the ASME, Journal of Mechanical Design*, Vol. 104, pp 259-267, Apr. 1982.

16. C.M. Harris, ed., <u>Shock and Vibration Handbook,</u> New York: McGraw Hill Book Company, 1987.

17. McFadden, P.D., and Smith, J.D., "Effect of Transmission Path on Measured Gear Vibration," *Journal of Vibration, Acoustics, Stress, and Reliability in Design*, v. 108, n. 3, Jul 1986, pp.377-378.

18. Stronach, A., Johnston, A., and Cudworth, C.."Condition Monitoring of Rolling Element Bearings," Condition Monitoring '84, Proceedings of an International Conference on Condition Monitoring, Swansea, U.K.,10-13 April 1984, pp. 162-177.

19. Strunk, W. D.,"The Evaluation of Accelermeter Mount Transmissibility for U.S. Navy Applications," <u>Proceedings of the 6th International Modal Analysis Conference</u>, January 1988 , pp 1384-1389.

20. J. E. Shigley and L. D. Mitchell, <u>Mechanical Engineering Design,</u> New York: McGraw Hill Book Company, 1983.

21. Hewlett Packard, <u>Dynamic Signal Analyzer Applications, Effective Machinery Maintenance Using Vibration Analysis</u>, Application Note 243-1, Hewlett-Packard Company, 1983.

22. Hewlett Packard, 3562A-Dynamic Signal Analyzer Operating Manual, Oct. 1985.

INITIAL DISTRIBUTION LIST

		No. Copies
1.	Defense Technical Information Center Cameron Station Alexandria, Virginia 22304-6145	2
2.	Library, Code 0142 Naval Postgraduate School Monterey, California 93943-5004	2
3.	Dean of Science and Engineering, Code 06 Naval Postgraduate School Monterey, California 93943-5004	2
4.	Research Administrations Office, Code 012 Naval Postgraduate School Monterey, California 93943-5004	1
5.	Department Chairman, Code 69 Department of Mechanical Engineering Naval Postgraduate School Monterey, California 93943-5004	1
6.	Naval Engineering Curricular Office, Code 34 Department of Mechanical Engineering Naval Postgraduate School Monterey, California 93943-5004	1
7.	LCDR R.J. Martin Mechanical and Electrical Submarine Technology Program 1515 Wilson Blvd. Suite 705 Arlington, Virginia 22209	1
8	Professor Y. S. Shin, Code 69Sg Department of Mechanical Engineering Naval Postgraduate School Monterey, California 93943-5004	3

9. Professor J.F. Hamilton, Code 69Ha   1
   Department of Mechanical Engineering
   Naval Postgraduate School
   Monterey, California 93943-5004

10. Mr. G. Reid, Code 69Re   1
    Department of Mechanical Engineering
    Naval Postgraduate School
    Monterey, California 93943-5004

11. Mr. Alan Pride   1
    Submarine Maintenance and Support Office
    Naval Sea Systems Command, PMS 390
    Washington, DC 20362-5101

12. Mr. Don Bills   1
    Naval Sea Systems Command, 56W13
    Washington, DC 20362-5101

13. Ms. Debbie Cuomo   1
    Naval Sea Systems Command, PMS 390TC26
    Washington, DC 20362-5101

14. Mrs. Ruth Holtzman   1
    Naval Sea Systems Command, PMS 390TC25
    Washington, DC 20362-5101

15. Mr. John Crimmins   1
    Naval Sea Systems Command, PMS 390TC2
    Washington, DC 20362

16. Mr. Bruce R. Marshall   1
    Mr. Art Curtilli
    Naval Ship System Engineering Station
    Philadelphia, Pennsylvania 19112-5083

17. Dr. Kam Ng   1
    William Gianis
    Naval Underwater Systems Command
    Newport, Rhode Island 02841

18. Lt J.D. Robinson   1
    602 Waterman
    Texarkana, Texas 75501

19. Mr. Mardo Blanco, Code 69   1
    Department of Mechanical Engineering, Bldg 500
    Naval Postgraduate School
    Monterey, California 93943-5004